SUSTAINABLE SYNTHESIS OF POLYMERS

Ashwani Kumar

A thesis submitted for the degree of

Doctor of Philosophy

of The Australian National University

Research School of Chemistry

AUSTRALIAN NATIONAL UNIVERSITY

March 2023

Declaration

This doctoral thesis contains my own unique research for the degree of PhD and includes no previously reported or written material by anybody else except where explicit and due reference has been made in the text. All additional sources utilised have been properly acknowledged in the text. The thesis has less than 100,000 words, excluding footnotes, tables, figures, maps, bibliographies, supporting information, and appendices. This work has not been submitted for credit towards any other degree or certification at any other institution.

Ashwani Kumar

March 2023

Acknowledgements

It is a great honor for me to pursue my PhD with Professor Luke Connal at the Australian National University. I would like to express my gratitude to my supervisor, Dr. Luke Connal, for his exceptional support, guidance, and encouragement throughout my doctoral program. Working with him has given me the freedom to explore a diverse range of materials. Without his vision and guidance, this achievement would not have been possible.

I would also like to express my gratitude to Connal Group members. The Connal Group has made life at the Australian National University more joyful, and I am grateful to them for creating a pleasurable and productive workplace. Brett Pollard and I collaborated on several projects, and without his contributions, my work would have been far more challenging. I am fortunate to have collaborated with scientists from the Australian National University, the University of Queensland, and Monash University, and I would like to thank everyone involved.

Many thanks to my family for their support during my doctoral studies. First and foremost, I would like to thank Mum, Dad, Akshay, and Nikita for their unwavering love and support. Their support and companionship have been of great value to me and have helped me maintain perspective. I am really blessed to have parents like you, and I am extremely grateful for every bit of support you have given me. Many thanks to Akshay, my younger brother, for the support, good times, and laughs. And, gorgeous wife Nikita, my multi-coloured diamond, I cannot thank you enough for your love, encouragement, and patience.

Thanks to the Australian Research Council for your kind financial assistance.

Lastly, I would like to offer my thanks to God. God provided me with strength and support during the difficult phases of my doctoral program. I am grateful to God for his infinite, unconditional love.

Abstract

Traditional polymer development is dependent on petrochemicals, their fabrication includes the use of ecologically unfriendly chemicals, and their permanently crosslinked networks limit their recycling capabilities. This thesis focuses on improving the sustainability of both natural and synthetic polymer advancements in terms of simplified synthesis, recyclability, and circularity. **Chapter 1** discusses the concepts of artificial catalysts and dynamic thermosets, as well as their current challenges. In **Chapter 2**, an artificial catalytic triad inspired by the chemical structure of chymotrypsin was prepared using a simple synthetic strategy, yielding a remarkable turnover number (k_{cat}) of 3.3 s^{-1} and a rate acceleration (k_{cat}/k_{unc}) of 4.81 × 10^4-fold over the background reaction. **Chapter 3** outlines the transformation of a raspberry-ketone derived crosslinker into a dynamic thermoset elastomer. The thermoset networks incorporate catalyst-free bond exchange reactions in catalyst-dependent polyester networks by substituting oxime-esters for conventional ester linkages. The dynamic nature of thermosets allows them to demonstrate stress relaxation behavior and reprocessability. **Chapter 4** reports fully biomass-derived dynamic imine thermosets prepared using widely abundant cheap shrimp and cellulose waste materials. The dynamic nature of Schiff base bonds enables thermosets to exhibit fast stress relaxation behavior and reprocessability. At the "end of product life", thermosets can be degraded in a home compost within 4–5 days. **Chapter 5** outlines the development of a novel and entirely green dynamic thermoset composite using sustainably sourced spent coffee grounds and chia seed oil, which was epoxidized and crosslinked through esterification with kelp-derived alginic acid, without catalyst or solvent, at a mild reaction temperature (90–150 °C). The resultant suite of materials

has potential applications in industrial fields such as plant pots, thin film sheets, and beverage containers. At the “end of product life”, thermoset composites can be readily composted at home under natural conditions in 4-5 months. At last, **Chapter 6** concludes with a summary of this work and suggestions for potential future research directions.

Publications and Patent during candidature

Published

- **Kumar, A.**; Nothling, M. D.; Aitken, H. M.; Xiao, Z.; Lam, M.; Bell, C. A.; O'Mara, M. L.; Connal, L. A. Simple synthetic route to an enzyme-inspired transesterification catalyst. *Catal. Sci. Technol.* **2022**, *12*, 6655-6659.

- **Kumar, A.**; Connal, L. A. Bio-based Transesterification Vitrimers. *Macromol. Rapid Commun.* **2023**, 2200892.

- **Kumar, A.**; Gresil, M.; Connal, L. A. Dynamic Elastomers based on Bio-derived Crosslinker. *J. Polym. Sci.* 2023, 1.

- Shen, P.; Jiang, Z.; Viktorova, J.; Pollard, B.; **Kumar, A.**; Stachurski, Z.; Connal, L. A. Conductive and Self-Healing Carbon Nanotube–Polymer Composites for Mechanically Strong Smart Materials. *ACS Appl. Nano Mater.* **2023**, 6, 2, 986–994.

In Preparation

- **Kumar, A.**; Pollard, B.; Connal, L. A. Upcycling waste: Fully biomass-derived and backyard compostable imine thermosets.

- **Kumar, A.**[†]; Pollard, B.[†]; Connal, L. A. Pushing the limits of greenness: Fully Bio-based & Compostable dynamic thermosets.
  ([†]authors contributed equally)

Patent

- **Kumar, A.**; Pollard, B.; Connal, L. A. "Bio-based Polymers". *Australia Provisional Patent Application No.* 2022903603 — 28th Nov 2022.

Table of Contents

List of Figures and Tables

Chapter 1 Introduction

Chapter 2 Simple synthetic route to an enzyme-inspired transesterification catalyst

Chapter 3 Dynamic Elastomers based on Bio-derived Crosslinker

Chapter 4 Upcycling waste: Fully biomass-derived and backyard compostable imine thermosets

Chapter 5 Pushing the Limits of Greenness: Fully Bio-Based & Compostable Dynamic Thermoset Composites

Chapter 1 Introduction and Literature Review

Introduction

The plastics industry has expanded greatly with the discovery of several strategies for preparing polymers from petrochemical resources. Plastics are low-cost, resilient, lightweight, corrosion-resistant materials with excellent electrical and thermal insulating properties. The myriad of polymers and the customization of their properties are utilised to manufacture a large array of goods that contribute to energy savings, technological and medical advancements, and several other social advantages.[1] As a result, plastic output has expanded significantly over the last seven decades, from 2 million tonnes in 1950 to more than 400 million tonnes in 2019 (**Figure 1.1**).[2] The plastic sector in Europe alone generates a revenue of

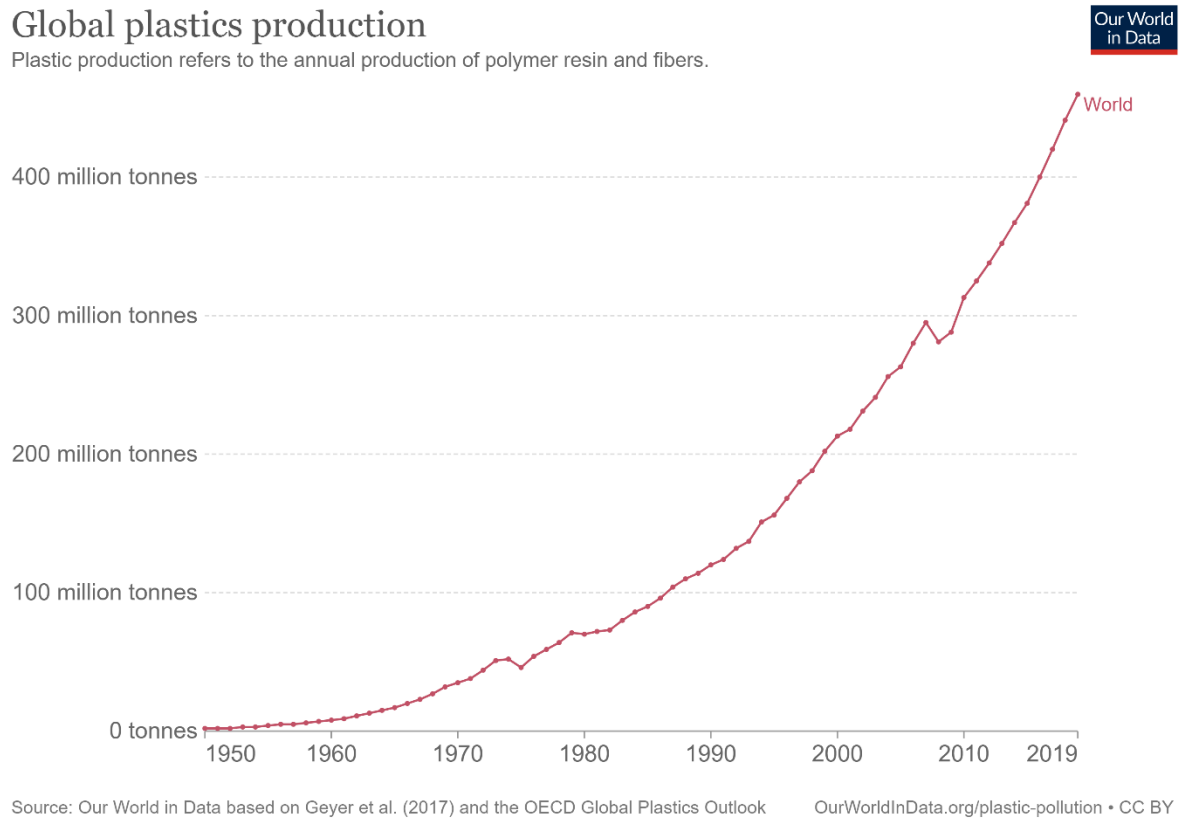

Figure 1.1: *The exponential growth of worldwide plastic manufacturing since 1950.*[2]

more than 350 billion euros and employs more than 1.5 million people.[3] Plastic is found in almost every element of modern life, that permit the distribution of a broad variety of food, beverages, and other commodities.

In the last few years, researchers have been intensively focusing on thermosetting polymeric materials for many applications. Thermoset polymers are comprised of permanent cross-linked networks, which provides them with superior stability, mechanical and thermal properties. These covalent crosslinks are difficult to break, and the polymer often decomposes prior to melting even at high temperatures. They become an infusible solid upon heating, which makes them non reprocessable (**Figure 1.2**). The inherent irreversible linkage in

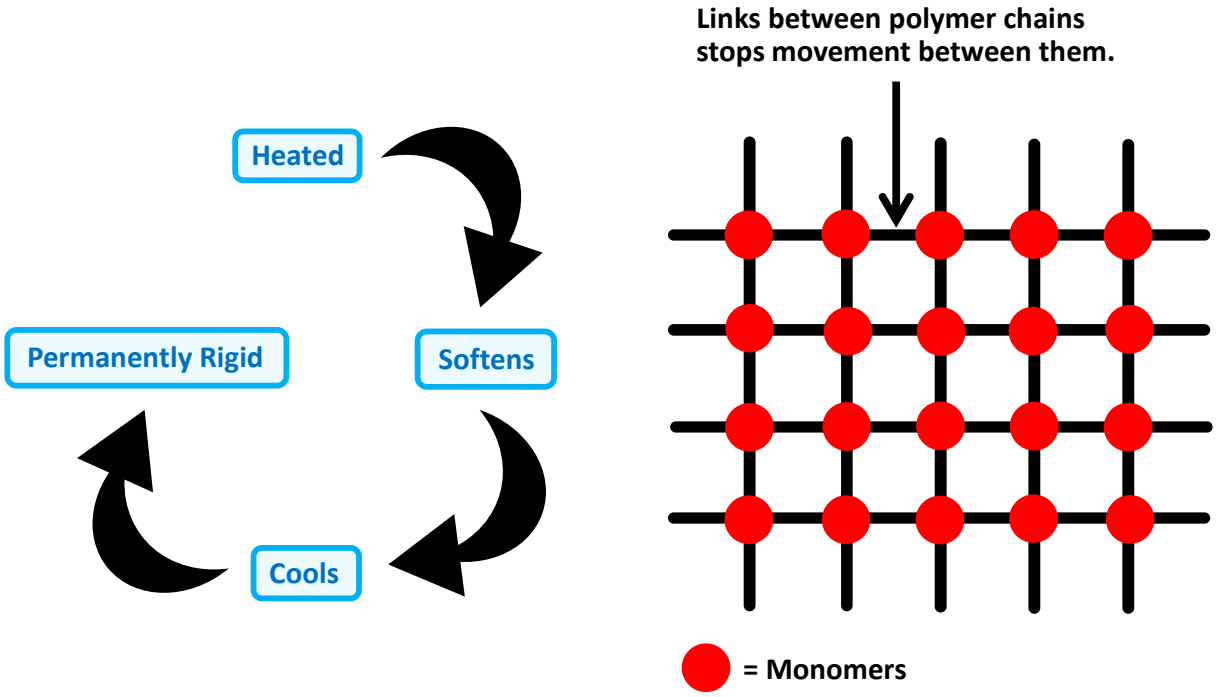

Figure 1.2: *The permanent crosslinked networks in thermosets.*

thermosets naturally limits flow, bond exchange and malleability, which are essential for reprocessing capabilites.[4-6] Traditional thermosetting materials are at risk of breakdown due to deterioration, leading to a substantial reduction in their durability and sustainability.[7, 8]

Consequently, there is a need for new types of plastics to be developed that have the strength and durability of thermosets but can be recycled once their useful life has ended.[2]

In the past few decades Lehn's invention of supramolecular macromolecules and dynamers has laid the foundation for the development of dynamic polymers.[9, 10] This idea gained depth when reversible covalent linkages were included in the network architecture.[11] Subsequently, Kloxin *et al.* introduced the term "Covalent Adaptable Networks" to describe the process of developing crosslinked polymer networks with reversible bonds.[12] Numerous studies have been conducted on this emerging category of polymers, which integrate the features of both thermosets and thermoplastics.[12-14] CANs are characterised by the existence of dynamic covalent bonds inside their networks, which can rearrange their network topology. CANs can be recycled, unlike traditional thermosets due to its dynamic crosslink network. CANs are classified into two categories according to their exchange mechanism. The first category of CANs is based on dissociative dynamic mechanism. In this category, the covalent crosslinks are first destroyed and then reconstructed at a different place in the network (**Figure 1.3a**). When network crosslinks are broken, the crosslink density decreases, which disrupt the polymer interconnections or possibly cause the network to depolymerize entirely. The two well-known examples of dissociative dynamic mechanism are Diels-Alder addition[15] and photo-triggered reactions.[16] The second category consists of associative dynamic mechanism. In this category the crosslink density remains constant by the concomitant formation of a new bond and the breaking of an existing bond (**Figure 1.3b**).[17, 18] Scott *et al.* reported the first example of associative dynamic mechanism in 2005.[19] This research area was expanded in 2011 with the advancement of associative CAN mechanism based on transesterification by Leibler and co-workers.[20] For the first time, the term ‘vitrimer’ was used to describe the

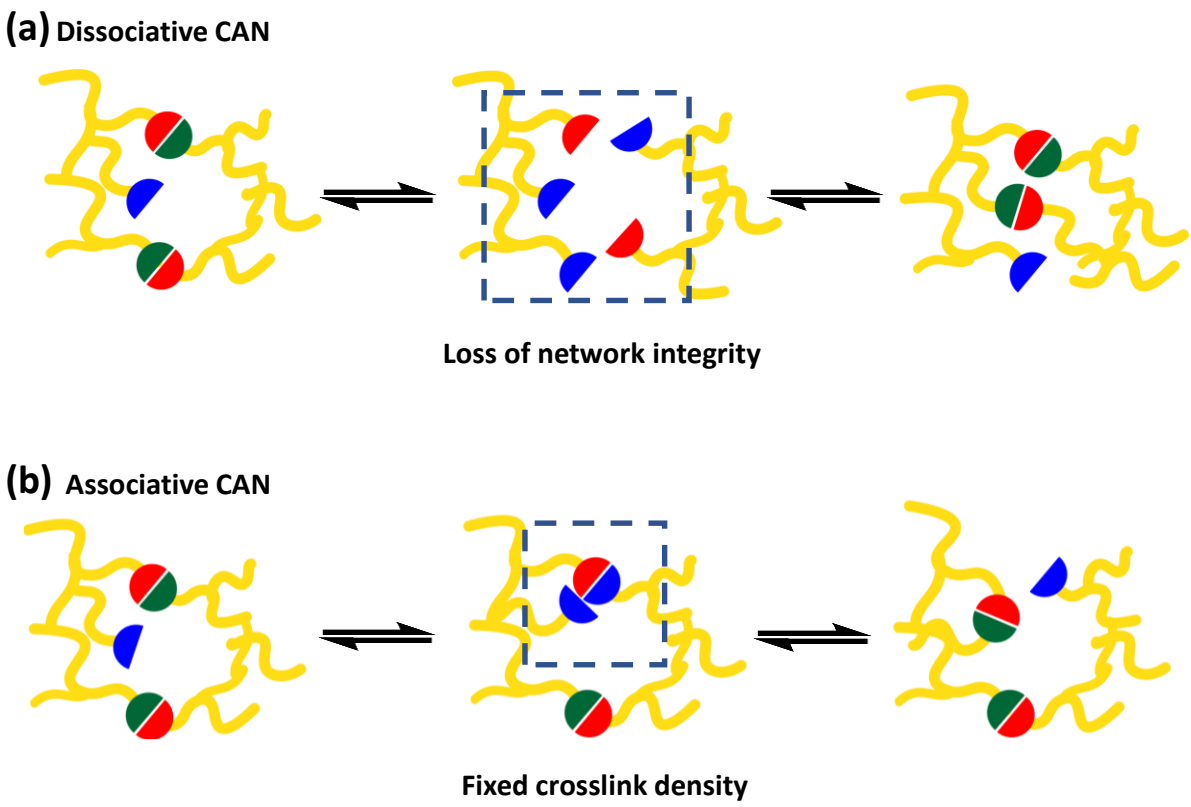

Figure 1.3: *Two types of CANs, (a) Dissociative CAN and (b) Associative CAN.*

closeness of some features of these organic networks to vitreous silica.[21] In contrast to dissociative CANs, the vitrimers have a fixed crosslink density. The network topology can change upon heating while the number of crosslinks remains constant due to the exchange process, resulting in a shift from (visco)elastic solid to viscoelastic liquid. This feature enables vitrimer networks to flow when heated, allowing the materials to be reshaped and recyclable without compromising network integrity. Several other vitrimeric polymers have been reported since Lieber's work by using different dynamic covalent bonds such as transesterification,[22-27] transcarbamoylation,[28-30] transesterification of oxime-esters,[31] imine metathesis,[21] transamination,[32] transalkylation,[33] siloxane equilibration reaction,[34-36]

transcarbamoylation of thiourethanes,[37, 38] transacetalation,[39] transimination,[40, 41] and transalkylation of sulfonium salts[42] (**Figure 1.4**).

The transesterification is a classic reaction in the field of organic chemistry and has found numerous applications across a wide range of substrates.[43, 44] The presence of free OH groups and high temperature are required for the transesterification exchange process in the presence or absence of catalyst. Transesterification is an equilibrium reaction and in order to achieve the high ester yields, the presence of an acidic or basic catalyst is required to accelerate and maintain equilibrium, but the alcohol must be used in surplus. A homogenous transesterification process catalysed by a strong base (NaOH or KOH) have limitations in product separation which leads to higher manufacturing costs. The most extensive research has been conducted on dynamic thermosets based on transesterification exchange process between ester bonds and –OH groups because: (1) the dynamic transesterification reaction mechanism can be employed to a broad variety of thermosetting polymers, particularly epoxy resins and (2) the high reaction temperature (>120 °C) of dynamic transesterification reaction enables the development of materials with a high service temperature. The majority of reported vitrimers rely on catalysts to induce the dynamic transesterification reaction. If the catalyst loading is insufficient or the catalyst is not effective, the dynamic transesterification reaction will not be fast enough to reform the crosslink networks. The most commonly employed catalysts for promoting dynamic transesterification reaction are zinc acetylacetonate and zinc acetate. Using 1 mol% of Zn catalyst based on epoxy, a bisphenol A (BPA) epoxy network cured with carboxylic acid (a combination of dimer and trimer acid) takes more than 10^5 s to relax at 150 °C. However, the relaxation time dropped to ≈10^4 s, when the Zn catalyst loading was raised to 5 mol%.[45] During catalysis, Zn^{2+} ions coordinate

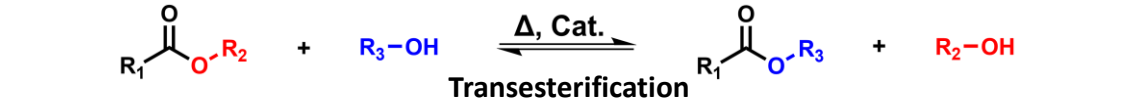

Transesterification

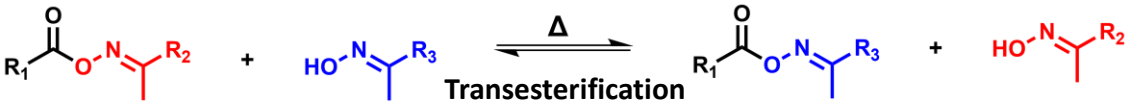

Transesterification of oxime esters

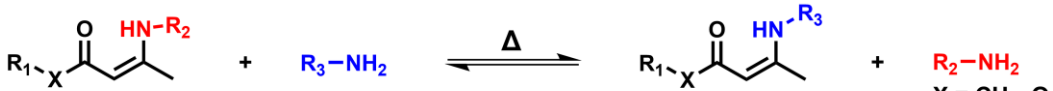

Transamination

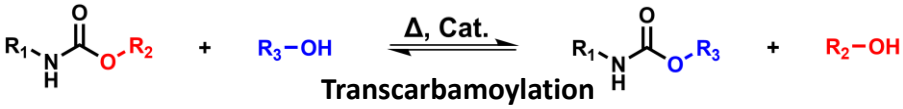

Transcarbamoylation

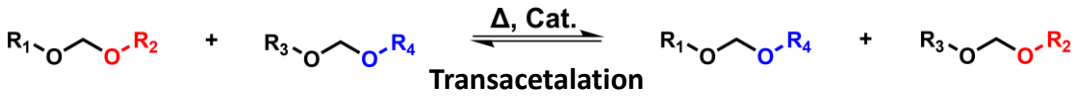

Transacetalation

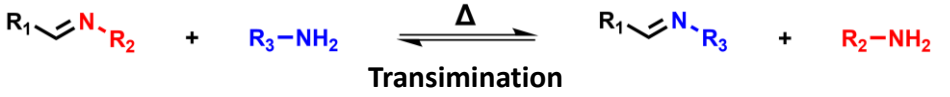

Transimination

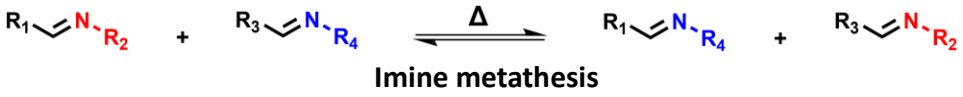

Imine metathesis

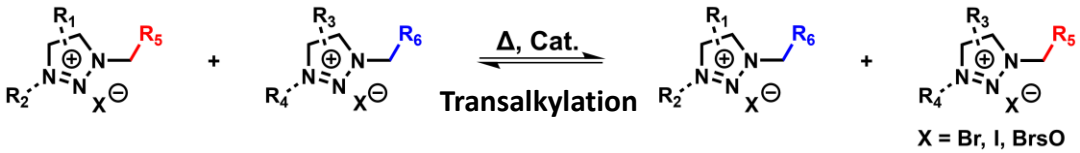

Transalkylation

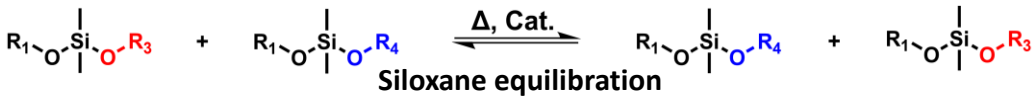

Siloxane equilibration

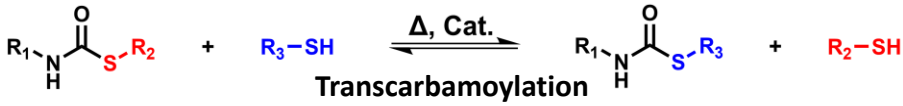

Transcarbamoylation of thiourethanes

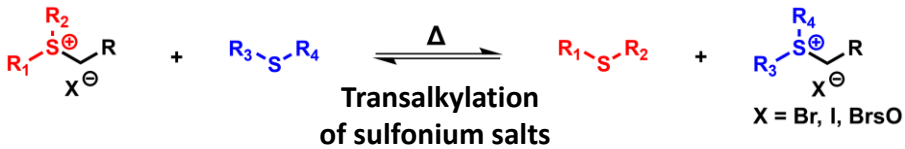

Transalkylation of sulfonium salts

Figure 1.4: *Different types of dynamic covalent bonds based on associative mechanism.*

and activate the ester carbonyl, stabilise the alkoxide group, and bring the alkoxide and ester carbonyl groups into close proximity with one another to facilitate transesterification process.[46, 47] Dynamic transesterification reaction has also been catalysed using triphenylphosphine (PPh_3) and triazabicyclodecene (TBD).[45, 48, 49] However, the inclusion of external catalysts has various disadvantages. In fact, strong bases,[50] and organic salts[22, 51] which are utilised as catalysts in epoxy vitrimers are often corrosives and toxic, and they may leach from the materials or deteriorate over time, limiting their practical application.[52] Additionally, the solubility of the catalyst in the polymer can be decreased at high loadings, resulting in heterogeneous systems.

Catalyst-free vitrimers have been developed to overcome the disadvantages brought by catalysts. The activation of exchange reactions can occur without external catalyst through two mechanisms: neighbouring group participation and internal catalysis. In first mechanism, neighbouring group participation involves substituent effects that stabilise the transition state by bonding to the reaction centre. Leibler's first vitrimers have already been subject to this neighbouring group participation effect owing to the existence of β-hydroxy ester linkages.[20] The second mechanism, generally incorrectly referred as internal catalysis, relates to the rate-enhancing effect resulting from electronic interactions. It has been reported that a group of β-activated ester-based vitrimers can be reprocessed at 150 °C under catalyst-free conditions.[53]

A further growing research field of transesterification is based on natural polymers *i.e.* enzymes. Natural enzymes are incredible biological catalysts. Because of their superior catalytic performance, they have found several applications in industry.[54, 55] Hassani *et al.*,

demonstrated that Pseudomonas stutzeri can enhance epoxy-acid addition and transesterification, which facilitates the formation of poly(hydroxyester) chemical networks.[56] Unfortunately, the catalytic efficacy natural enzymes is severely limited outside the tightly regulated biological conditions in which enzymes have evolved. Enzymes are capable of accelerating the chemical reactions, but their limited adaptation to abiotic reaction conditions and operations at a certain pH and temperature limits their application. The spectrum of enzyme activities can be broadened by developing enzyme inspired synthetic catalyst that is more robust and resistant to adverse condition. Synthetic enzymes or artificial enzymes or enzyme mimics are a family of catalysts that have garnered significant attention as potentially viable alternatives to native enzymes. Artificial enzymes offer catalysis based on characteristic feature of enzymes inspired by the ground-breaking work of Breslow,[57] Cram,[58, 59] Rebek[60] and their colleagues. The practical use of an artificial transesterification catalyst based on enzymes is significant for product target transformations and vitrimer development.

In addition to dynamic transesterification bonds, the reversible condensation of amines and aldehydes is also one of the earliest and most common reactions. Condensation products of the type $R_1R_2C=NR_3$, where R_1 and R_2 can be (i) a hydrogen atom with R_3 an aryl or alkyl group (ii) an aryl or alkyl group, or (iii) a mixture of these two, are commonly referred to as "Schiff's bases". This reaction was discovered in 1864 by the German chemist Hugo Schiff.[61] The formation of an imine bond between an amino and a carbonyl group is an effective reaction that results in the formation of C=N bond either inter- or intramolecularly. There are several extrinsic factors that can affect the equilibrium between an imine and its precursors such as but not limited to, concentration, temperature, solvent, and pH. The reversible nature of the imine bond enables the reaction to proceed either forwards or backwards. The dynamic

chemistry of imine bonds is another viable option for developing dynamic thermosets because it is capable of three dynamic reactions: imine condensation/hydrolysis, imine exchange, and imine metathesis (**Figure 1.5**).[41] There is no catalyst required for the dynamic imine

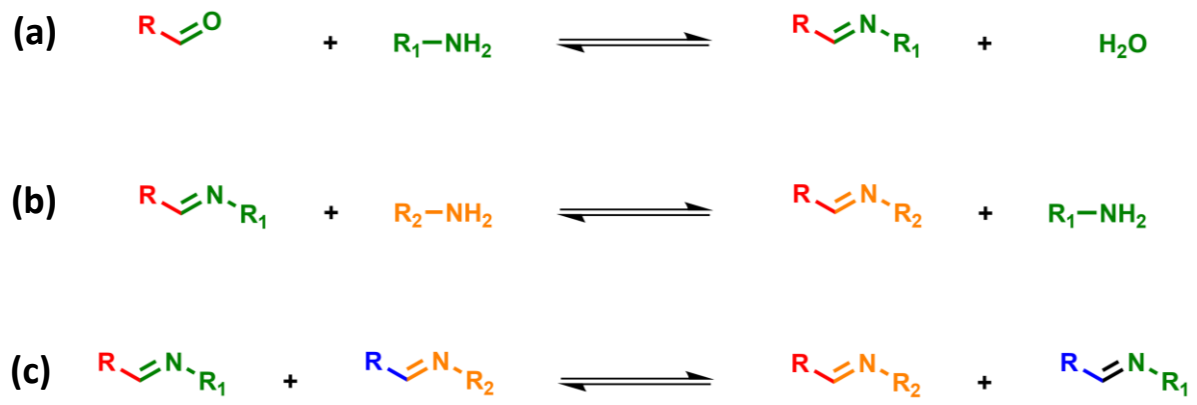

Figure 1.5: *Different types of dynamic imine reactions, (a) imine condensation, (b) exchange, and (c) metathesis.*

reactions in contrary to transesterification exchange process. The abundant availability of naturally occurring amines and aldehydes facilitates the development of a diverse array of dynamic imine thermosets.

A major trend in recent dynamic thermoset development is the transition towards biobased precursors. Currently, the majority of thermosets waste is treated by landfilling or incineration, resulting in significant negative environmental impacts. With this perspective, the development of biobased thermosets has appeared to be a viable alternative to fossil-based resources. In addition to minimising the use of fossil resources, the development of biobased thermosets reduces the carbon footprint by lowering CO_2 emissions into the atmosphere. Several types of biomass can serve as the starting point for creating biobased thermosets, for example, but not limited to, cellulose, vegetable oil, lignin, naturally occurring

carboxylic acids, and natural rubber (**Figure 1.6**). Vegetable oils are easily accessible, produced

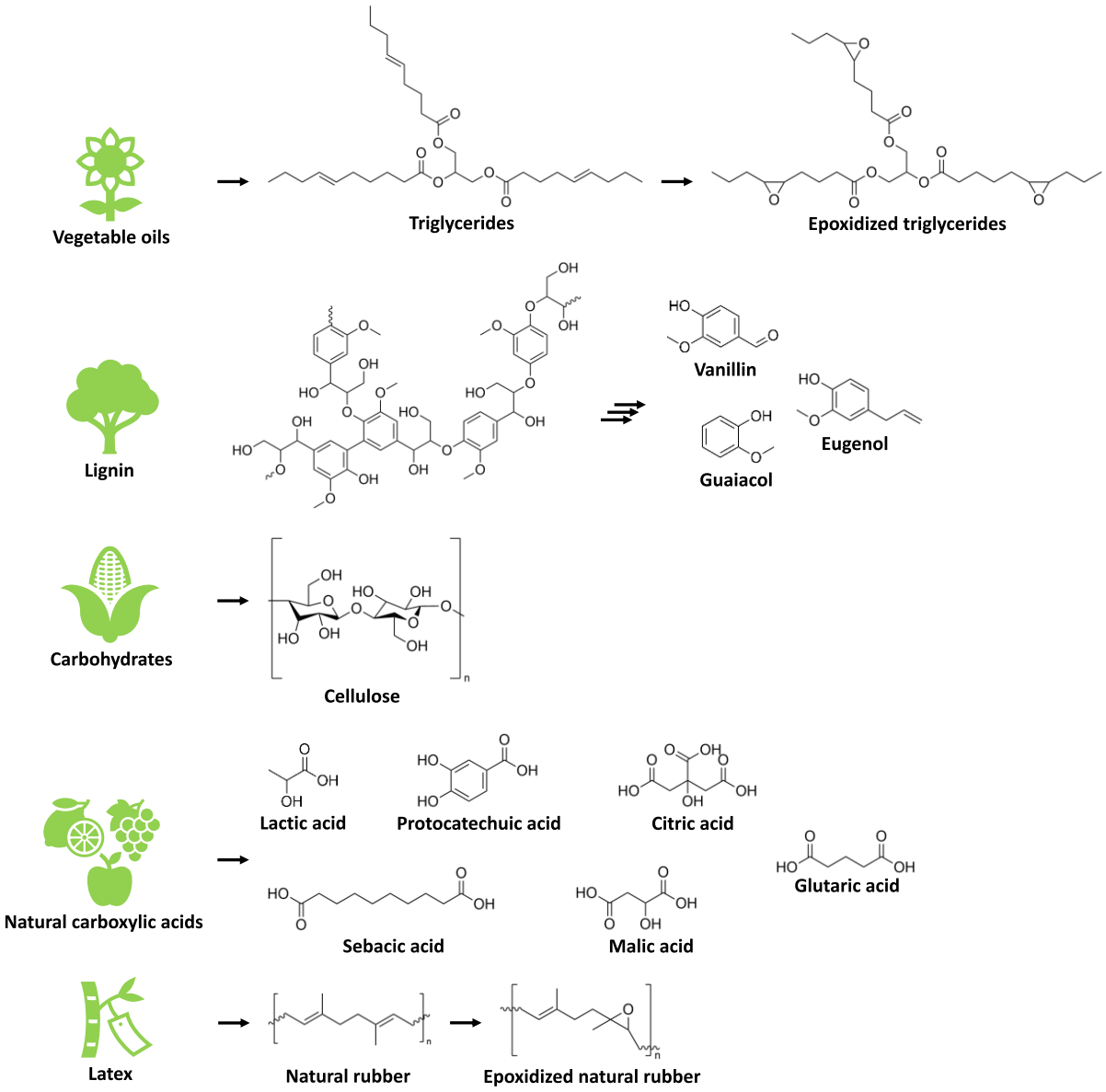

Figure 1.6: *Different biomasses and molecular structural diversity of widely used biobased building blocks for preparing dynamic thermosets.*[62]

on a large scale, and relatively inexpensive, making them ideal precursors for the synthesising polymers.[63, 64] The most abundant organic material on Earth is cellulose.[65]Around 35–50% of the total mass of lignocellulosic biomass is composed of cellulose.[66] Celluloid, a thermoplastic polymer comprised of cellulose nitrate and camphor and employed as a plasticiser, was the first thermoplastic material to be mass-produced.[67] Cellulose is used as a non-petroleum

renewable feedstock to produce important substrates such as 5-hydroxymethylfurfural and levoglucosenone.[68] Triglycerides can be transformed into fatty acids by hydrolysis, further separation, and purification.[69] Highly abundant carboxylic acids including lactic, citric, and many others[70, 71] are important raw materials for the synthesis of biodegradable polyesters.[71, 72] Integrating renewable feedstocks and dynamic bonds in the fabrication of conventional polymer networks outlines the path for the next generation of environmentally friendly thermoset materials.

This thesis has focused on developing sustainable thermosets based on dynamic transesterification and imine chemical bonds. Dynamic transesterification and imine chemistry are two promising avenues to explore in developing vitrimer type dynamic thermosets from readily available renewable feedstocks. In every instance, effort has been made to use simple and versatile synthetic methods. This thesis is comprised of four research chapters in the form of articles, out of which two have been published, one has been submitted, and one has been filed as provisional patent and is in preparation for publication.

In **Chapter 2**, I took inspiration from nature to develop an organocatalyst termed as artificial catalytic triad (ACT) for the transesterification chemical reaction. This ACT is inspired by the transesterification ability of native lipase enzyme. The ACT was prepared using a simple high yielding modular synthetic procedure without any protecting groups, incorporating three active site residues similar to chymotrypsin (histidine, aspartate, and serine), on a single trifunctional molecule. The ACT surfactant is comprised of a hydroxyl to act as a nucleophile, imidazole residue as a base, carboxylate group as an acid and the C-8 alkyl chain to address solubility in the non-aqueous environment. The three triads on ACT surfactant facilitates the transesterification reaction between vinyl trifluoroacetate (VTFA) and methanol.

Red raspberry (*Rubus idaeus*) is a prominent fruit, commonly cultivated in the northern temperate zones. 4(4-hydroxyphenyl)-2-butanone, often known as frambinone or raspberry ketone, is a unique phenolic molecule found in raspberries.[73]

In **Chapter 3**, I utilised raspberry ketone in developing dynamic thermoset elastomers based on oxime transesterification exchange process. The thermosets exhibits catalyst free transesterification exchange process which enabled them to exhibit stress relaxation, and reprocessability. After reprocessing the tensile strength of elastomers can be recovered up to 78.1 ± 10.9%.

Abundant cellulose and shrimp waste are inexpensive raw materials for the preparation of materials with superior properties. In **chapter 4**, a fully biomass-derived dynamic imine thermosets were readily prepared using chitosan and cellulose derived-levoglucosenone diketone. The imine thermosets showed high glass transition temperature (T_g) (171–176.1 °C), enhanced modulus (3.7–7.9 GPa), and tuneable mechanical properties (tensile strength, 12.5 ± 3.5—21.1 ± 3.1 MPa). The thermosets can be decomposed under natural conditions at home compost in 4-5 days.

In **Chapter 5**, the chemistry of transesterification is expanded in developing novel green dynamic thermoset composites from abundant biomasses (coffee waste, vegetable chia oil, and algae). The thermoset network comprises of β-hydroxyester linkages that can undergo catalyst free transesterification exchange process, enabling them to exhibit thermally induced stress relaxation and reprocessing capabilities. The thermoset composite can be easily composted at home under normal conditions in 4-5 months.

Chapter 6 provides a summary of the thesis and insights into future research. Though previous reports had shown progress toward mimicking certain aspects of enzyme activity using

multistep low yielding protecting group chemistry. While, in this thesis a simple modular, and protection group free synthetic approach were used for preparing artificial catalyst with high catalytic efficiency. I have presented dynamic bonding as a solution to the recycling issue of conventional thermosets. The advancements in dynamic covalent chemistry will allow the development of material to be optimised for exceptional reprocessability. Most importantly, I emphasised that most of these chemistries should be practised to renewable feedstocks which enables thermosetting polymers to decompose under normal conditions. The ultimate objective of this work is to create innovative green thermosets by substituting traditional precursors derived from fossil fuels with abundant sustainable feedstocks.

Literature Review

This comprehensive review outlines the advancement of research to date in the development of biomass derived vitrimers with a special focus on transesterification dynamic chemistry. The review begins with a brief overview of the key benefits and characteristics of dynamic thermosets, supplemented by a classification and examination of different types of biomass to harness their potential in the design of the next generation of environmentally friendly materials. The attention is on novel renewable resources, stressing the design concepts that must be addressed in the construction of high performance sustainable thermosets by researchers. How these key aspects have been evolved since the first discovery of vitrimers by Leibler, is the core purpose of this review.

This review targets three research questions: why is the development of dynamic thermosets important; how have past studies of vitrimers been applied in the development of more eco-friendly vitrimers; and what remains to be done to enhance the performance and lower down the production costs of vitrimers?

Bio-based transesterification vitrimers

Kumar, A.; Connal, L. A. Bio-based Transesterification Vitrimers. *Macromol. Rapid Commun.* **2023**, 2200892.

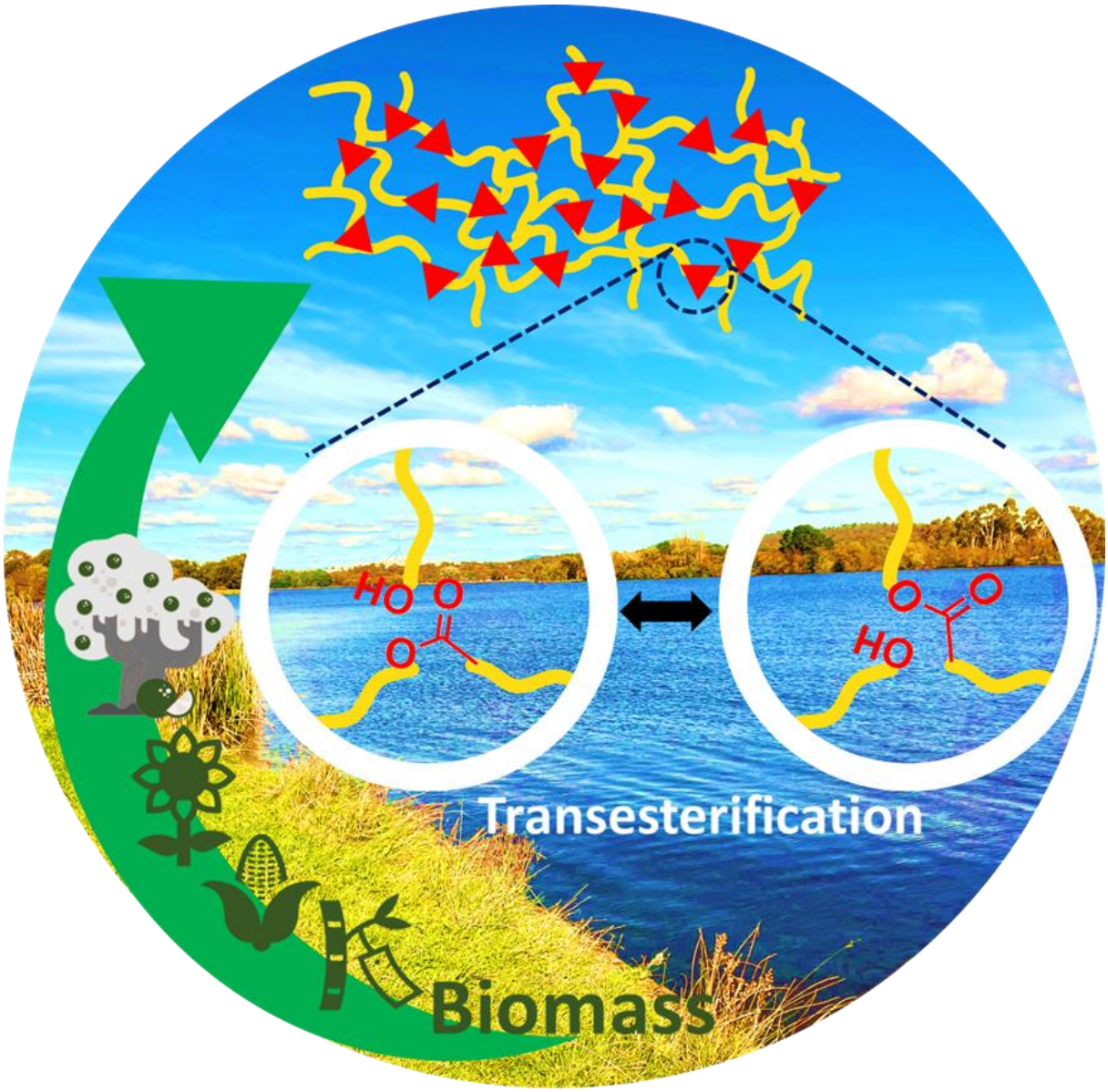

Introduction

Global population growth continues to increase the demand for energy, chemicals, and commodities on an ever increasing scale. Most chemicals and polymers are extracted from fossil fuels, including petroleum. The development of macromolecular materials made from renewable resources to substitute traditional fossil-based polymers is important to minimise their environmental impact, optimise waste disposal, and reduce the depletion of non-renewable resources.[74-77] In the 21st century, nonpetrochemical feedstock have become a societal paradigm because renewable raw materials have the ability to provide a wide array of monomers and polymers, potentially even more diverse than those now delivered by the petrochemical sector.[78, 79] The worldwide manufacturing capacity of biobased polymers grew from approximately 1.7 Mt year^{-1} in 2014 to 2.1 Mt yr^{-1} in 2020 and is anticipated to reach 2.9 Mt yr^{-1} by 2025.[80, 81] The majority of biobased polymers are industrially manufactured such as starch-based compounds, cellulose acetate, polybutylene succinate, various polyesters polylactic acid, poly (butylene adipate-co-terephthalate), and green polyolefins.[80, 82, 83] Thermosetting polymeric materials are possibly one of the most versatile engineered materials that find a wide variety of applications due to their excellent thermal stability, mechanical properties, resilience to environmental conditions, and chemical resistance.[84-87] The irreversible crosslinking of thermosets, on the other hand, inherently limits fluidity, bond exchange and malleability, both necessary for recycling, reprocessing or self-healing.[4-6] Traditional thermosetting materials are prone to collapse upon wear and tear, resulting in dramatic decline of their lifespan, safety, and sustainability.[7, 8] The quest for recyclable and healable thermosetting polymeric materials are immensely important since these materials would allow us to address not only the challenges associated with damage monitoring, but

also to incorporate suitable procedures to restore and recover the material's functionality.[88-91] In the hunt for alternatives, renewable feedstocks are worthy candidates owing to its renewability and structural variety.

Several biobased thermosets have been developed using a wide variety of biobased feedstocks, such as natural rubber (NR), tannin, vegetable oil, lignin or lignin derivatives, sugar, cardanol, and itaconic acid.[92, 93] Many outstanding reviews cover the design, synthesis, and properties of biobased thermosets such as unsaturated polyesters,[94, 95] epoxy resins,[96] and benzoxazines.[97] Significant advances have been made in this field, however the majority of reported biobased thermosets are not yet reprocessable. If these problems could be addressed, biobased thermosets would be much more environmentally friendly.

Transesterification is a classical organic chemistry reaction that has been used on many different substrates for various applications.[43, 44] It is a process in which the ester is transformed into another ester by the exchange of the alkoxy moiety. Transesterification has found great utility in polymer science.[52, 98, 99] It is well known that the reaction is catalysed by acids and bases.[43] Therefore, acid or base-catalysed reactions have been extensively studied,[43] and have been employed to dynamic chemistry in sustainable polymers.

In the past two decades, significant advances have been made in the area of vitrimers, with a stupendous diversity of polymers, and applications being reported.[17, 18, 100-102] In this review we will highlight sustainable approaches to create vitrimers. Previous review in this area are not specific and do not incorporate the most recent literatures.[103-105] We focus the review based on systems that use dynamic chemistry of transesterification reactions and the renewable feedstocks that can be used for this versatile reaction (**Figure 1.7**). We offer a

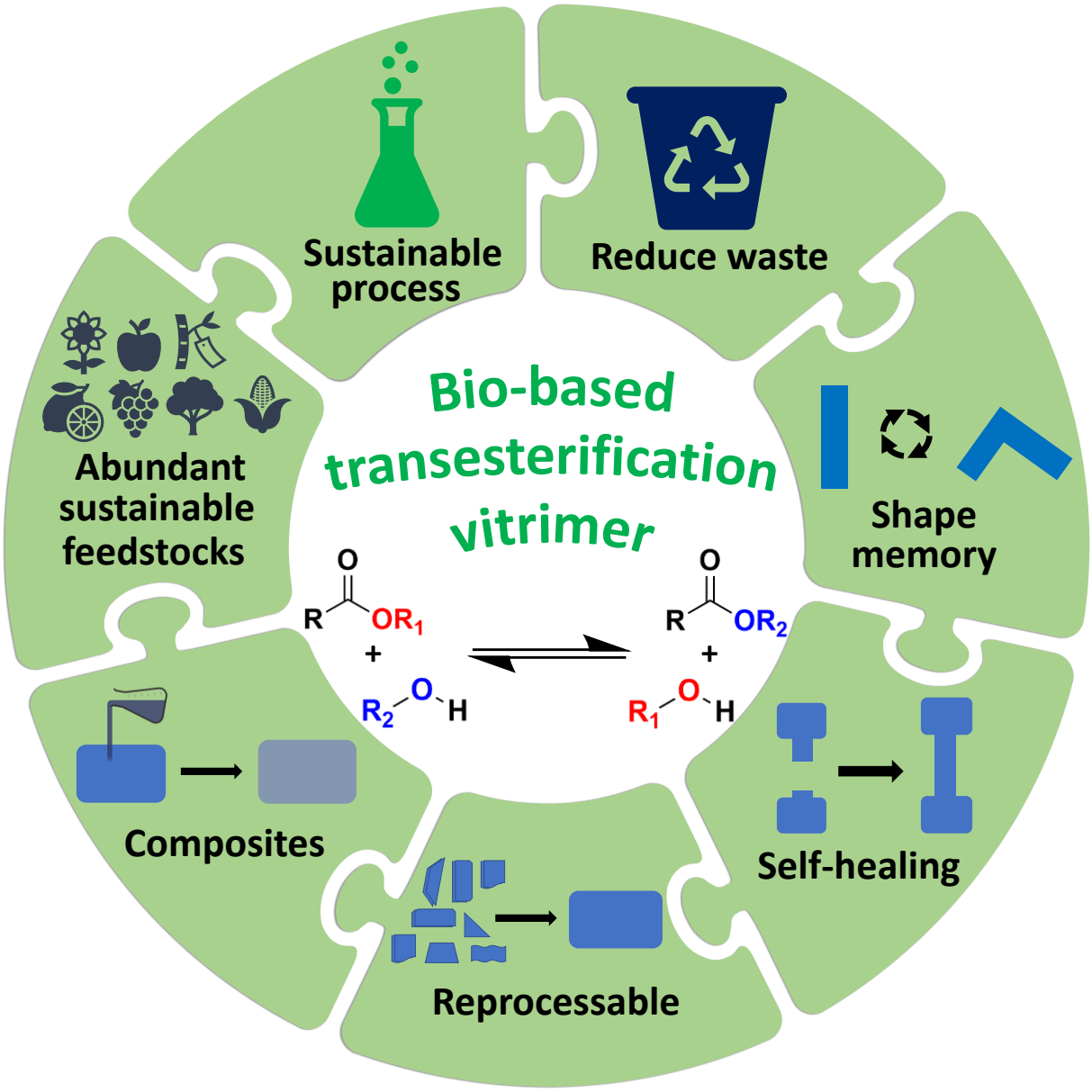

Figure 1.7: *Schematic illustration of dynamic transesterification bond in bio-based vitrimeric materials and their features.*

classification of biobased vitrimers based on their primary renewable component, which we perceive will contribute to the future categorisation and progress of this hot field of study.

Dynamic transesterification vitrimer

Vitrimers as described by the pioninering work of Montarnal *et al.* have creeated a new field in polymer science.[20] These materials undergo associative bond exchange reaction triggered by heat in the presence of Zn salts-based catalysts. The authors prepared an elastomeric epoxy resin using diglycidyl ether bisphenol A (DGEBA) and a mixture of dicarboxylic and tricarboxylic acids through the transesterification process catalyzed by a zinc acetate [$Zn(ac)_2$]. The authors also prepared materials which were hard at room temperature by employing DGEBA and glutaric anhydride in the presence of different concentrations of the zinc acetyl acetonate [$Zn(acac)_2$] catalyst. For both the hard and elastomeric networks, the resulting Arrhenius based energies of activation were 80 kJ mol^{-1} and 88 kJ mol^{-1} respectively.

Abundant sustainable feedstocks

Biobased transesterification vitrimers with a wide variety of thermomechanical properties could be made from aliphatic, aromatic, and cycloaliphatic structures found in nature. Vegetable oils are widely accessible, manufactured on a large scale, and at a reasonable cost, making them ideal building blocks for the synthesis of polymer materials.[63, 106] The molecular nature of fatty acids, particularly unsaturated fatty acids, permits many chemical modifications,[107, 108] making them a popular biobased resource for polymer synthesis.[106, 109-112] Lignins constitute the most significant renewable source of aromatic compounds on earth. They are abundant in wood (up to 30% by weight), but also in the stems of annual crops and nut shells.[113] Lignin has a high degree of functionality due to the presence of aliphatic and aromatic hydroxyl (OH) groups. Lignin also has a large number of aromatic and aliphatic hydroxyl (OH) groups. Numerous studies have been conducted over the past decades on the use of lignin in biobased thermoset polymers.[114-116] Cellulose is a significant component of

lignocellulosic biomass, accounting for *ca.* 35–50% of the total mass.[66] Cellulose is one of the most plentiful organic compounds on the planet, with an appealing array of unique features. Celluloid, a thermoplastic material composed of camphor and cellulose nitrate and as a plasticiser, is believed to be the first thermoplastic material to be made on a large scale.[117] Fatty acids can be obtained from triglycerides upon hydrolysis and subsequent separation and purification.[69] Additional transformations allow ricinoleic acid to be translated into an aliphatic diacid, sebacic acid, and linoleic acid can be dimerized into a blend of triacids and diacids known as Pripol.[118, 119] Abundant carboxylic acids such as lactic, citric as well as many others,[70, 71] are key raw ingredients for the synthesis of biodegradable polyesters.[71, 72] Another important sustainable resource is NR which has been a critical component of human civilisation.[120] NR is made from latex, a milky liquid found in latex ducts or in the cells of rubber-producing plants. Among rubber's numerous qualities are its great tensile strength and its ability to withstand repeated stretching without breaking. There has been great progress in the development of new materials from these feedstocks with control of their mechanical properties which we have analysed (**Table 1.1**).

Table 1.1: *Overview of the biobased transesterification vitrimers including T_g, T_v, E_a, mechanical properties, and reprocessing/repairing/self-healing conditions.*

Biobased monomers	Catalyst	T (°C)	E_a (kJ mol^{-1})	Mechanical Properties	Reprocessing[j] /Repairing[k]/Self-healing[l] conditions	Ref.
Hydroxylterminated 4-arm star-shaped poly((±)-lactide)	$Sn(Oct)_2$	50–57,[ae]55–65,[af] 57–63[b]	150 ± 3	49–50 MPa,[c] 1.5–1.8 GPa,[d]	140 °C,[j] 4 MPa[j]	22
Eugenol epoxy and succinic anhydride	$Zn(acac)_2$	42–47[ae]	-	≈25 MPa[c]	190 °C,[k] 200 °C[j]	121
Citric, sebacic and glutaric acid	1-methylimidazole	30–62,[ae] 45–78,[af] 105–117[b]	90–120	-	-	122

Triepoxy from vanillin and guaiacol	$Zn(acac)_2.H_2O$	157–187[af]	-	62.8–69.2 MPa,[c] 1.63–2.11 GPa,[d]	220 °C[k]	123
Ozonated lignin and sebacic acid-derived epoxy	$Zn(acac)_2$	95–133[af]	-	5.1–12.9 MPa,[c] 44.2–354.8 MPa,[d]	190 °C,[k] ≈0.14 MPa[k]	124
Cellulose nanofibrils	$Zn(Ac)_2$	-60[ae]	-	44–68 MPa,[c] 1.2–8.9[d] GPa	120 °C,[j] 3 bar[j]	125
Bisphenolic compound based on vanillyl alcohol and Pripol 1040	$Zn(acac)_2.H_2O$	11–23,[ae] 34–38[af]	24.3–59.5	0.18–25.1 MPa,[c]	120 °C,[k] 100 °C,[l]	126
Epoxy functionalized ethylenepropylene-diene rubber and decanedioic acid	$Zn(Ac)_2$	≈-30–-20[af]	≈74.16	19.4–22.7 MPa,[c] 2.4–4.5 MPa[d]	180 °C[j]	127
Epoxidized natural rubber and dodecanedioic acid	$Zn(Ac)_2$	-21.6–-6.3,[af] 180[b]	≈58.5	1.05–1.99 MPa[c]	200 °C[l]	128
Epoxidized natural rubber	$Zn(Ac)_2$	≈10–70,[af] >200[b]	51–144	5.9–38.9 MPa,[c] 1.7–415 MPa[d]	180 °C[k]	129
Epoxidized soybean oil and Fumaropimaric acid	$Zn(acac)_2$	65[af]	87.88	16.6 ± 0.4 MPa[c]	180 °C[l]	130
Epoxidized protocatechuic acid and maleic anhydride	$Zn(acac)_2$	148–157[af]	65.8	64.3 ± 4.5 MPa,[c] 2.13 ± 0.01 GPa[d]	230 °C, [j] 10 MPa[j]	131
Epoxidized soybean oil and glycyrrhizic acid	TBD	8–18,[ae] 39–64[af], 69[b]	112	3.1 MPa[c]	200 °C[j] [k]	132
Cellulose-functionalized halloysite nanotubes	Catalyst free	41.97–141.54[ag]	-	≈4.7–7.5 MPa[c]	-	133
sebacic acid	TBD	43.9,[af] 47.9,[af] 7.6,[b] 9.3[b]	71.61, 78.11	5.9 MPa,[c] 16.3 MPa,[c] 1230.7 MPa,[d] 1490.3 MPa,[d]	100 °C,[j] 10 MPa[j]	134
Epoxidized soyabean oil and citric acid	Catalyst free	≈10–38[af]	106	0.5 MPa[c]	160 °C[l]	23
Epoxidized natural rubber and citric acid modified bentonite	Catalyst free	-11.3,[af] >≈200[b]	-	0.8–4.5 MPa,[c] 1.5–16.8 MPa[d]	≈190 °C,[j] 150 °C[l]	135
Epoxidized natural rubber	Catalyst free	≈2–25,[af] >≈200[b]	166	≈10–22 MPa[c]	180 °C[j]	136
Epoxidized natural rubber and sodium alginate	$Zn(Ac)_2$ and 1,2-	≈5-≈40[af]	156.33	≈10 MPa - 26.5 MPa[c]	180 °C[j]	137

	Dimethylimidazole					
Vegetable oil derived hydrogenated dimer acid	Catalyst free	−10.6–24.6[ae]	74.4, 74, and 75.6	2.3–21.7 MPa,[c] 2.9–36.9 MPa[d]	200 °C,[k] ≈0.375 MPa[k]	138
Palm oil-based epoxy and citric acid	Catalyst free	35.1–65.2[af]	-	1.2–28.9 MPa[c]	170 °C,[j] 10 MPa[j]	139
Diethyl malonate	Catalyst free	120–130[af]	106.3–108.1	11.3–33 MPa,[c] 317–1112 MPa[d]	150 °C,[j] [l] 40 kg,[j] 10 kg[l]	53
Epoxidized linseed, soybean, karanja, castor, St John's Wort, peanut, rapeseed, rose hip seed, safflower, grapeseed, camelina, hemp and perilla oil	Catalyst free	17–91,[ae] 34–111[af]	-	-	120–170 °C,[k] 0.3–0.7 tons[k]	140
Methacrylated oleic, lauric acids and acrylated epoxidized soybean oil	Catalyst free	10–75[af]	99.5–139.7	≈8–60 N,[h] ≈1–2.3 mm[i]	180 °C[k]	141
Malic acid	Catalyst free	115–131.1[af]	131.35	88–117.7 MPa,[c] 2.6–3.6 GPa[d]	160 °C,[k] 180 °C[l]	142
Aminated epoxidized soybean oil and epoxidized maleopimaric anhydride	Catalyst free	40.5–82.0[af]	90.21	2.3–29.1 MPa[c]	180 °C, [j] [k] [l] 15 MPa[j] [k]	143
Fractionated lignin and sebacic acid	$Zn(acac)_2$	40.4–66.8[af]	-	20.79–39.82 MPa,[c] 1.03–1,89 GPa[d]	160 °C,[j] [l] 5 MPa[j]	144
Adipic acid	$Zn(OAc)_2$	-	-	49.9–51.5 MPa,[c] 2.9–3.5 GPa,[d]	190 °C[l]	145
Tung oil	Zinc (II) acetylacetonate	38.60–77.36[af]	89.97	1.05 ± 0.90–45.97 ± 1.07 MPa,[c] 198.64–1922.28 MPa[d]	180 °C[l]	146
Fumaropimaric acid	Hydroxy-terminated hyperbranched polyesters	75.6–90.5[af]	101.68	36.3 ± 3.2–57.2 ± 4.3 MPa[c]	200 °C,[j]15 MPa,[j] 180 °C[l]	147
Menthane diamine and adipic acid	Catalyst free	72.1–86.4[af]	105.8	75.5–57.4 MPa[c]	180 °C[l]	148
Ferulic acid	Catalyst free	57–60,[ae] 93–97[af]	58–98	111.0 ± 3.2–126.4 ± 1.5 MPa[c]	140 °C,[l][j] 5 MPa[j]	149

Itaconic acid	TBD	61 ± 15–123 ± 5,[b]	54 ± 10–94 ± 10	21 ± 4–90 ± 20 kPa,[c] 150 ± 50–990 ± 60 kPa[d]	140–180 °C,[j] 5–7 bar[j]	150
Epoxidized natural rubber and oxidized starch	Catalyst free	-23.4–-29.9,[ae] -9.4–-19.1[af]	80.3	3–9 MPa[c]	140 °C,[j] 15 MPa[j]	151
Epoxidized soyabean oil, succinic and sebacic acid	Catalyst free	0.4,[af] 8.4[af]	78.06 ± 3.11, 103.51 ± 9.84	442 kPa,[c] 980 kPa,[c] 1000 kPa,[d] 2267 kPa[d]	160 °C,[j][k] 10 MPa[j]	152

[ae] T_g calculated from DSC. [af] T_g calculated from DMA. [ag] T_g calculated from calorimetry. [b] T_v. [c] tensile strength. [d] Young's modulus. [h] force at break. [i] displacement. [j] reprocessing. [k] repairing. [l] self-healing

Vegetable oil based-vitrimers

Plant oils are excellent renewable raw materials because of their plentiful supply.[110, 153] Additionally, various chemical modifications can be carried out on vegetable oils to produce functionalized vegetable oils that can be utilised to make a variety of materials. Sun and Wool outlined the chemical transformations that could be made to vegetable oils in attempt to develop various functionalized vegetable oils, several of which have significant industrial uses.[154] The primary difference in the chemical structures of vegetable oils derived from various oilseeds is the fatty acid distribution which governs the number of double bonds per triglyceride. Soybean oil has a high proportion of linoleic (~53%) and oleic (~23%) acids with two and one unsaturation's, respectively, offering around 4.6 double bonds per triglyceride.[154] Epoxidized soybean oil (ESO) a popular soybean oil derivative, is a low-cost and widely accessible monomer.[111, 155] Due to the abundance of epoxy groups in ESO, it reacts readily with other compounds containing amines[156] and anhydride groups.[157, 158] Traditional crosslinking agents, on the other hand, are made from petroleum-derived molecules. Aspergillus niger, a filamentous fungus, produces citric acid, a tricarboxylic acid, on a large industrial scale[159] which when reacted with epoxides forms β-hydroxyester linkages. Under

suitable conditions and in the presence of catalysts, the β-hydroxyester linkages produced by the epoxy–acid reaction may engage in transesterification processes.[20, 21, 45] However, the mutual insolubility of ESO and citric acid is a major hurdle in the development of polymeric networks. Entirely green and homogeneous ESO–citric acid vitrimeric networks were developed by Altuna *et al.*, employing the protons released during the deprotonation of citric acid as a catalyst for the ESO-citric acid reaction.[23] In this process, the interaction of ESO with the carboxylate anion results in the formation of a β-hydroxyester. The relaxation rate accelerated at 160 °C upon decrease in the carboxylic acid equivalents per epoxy acid could be attributed to either the reduction in crosslink density or an increase in residual OH concentration.[21] While an increase in transesterification rates was observed with elevated temperatures. The relaxation rates are comparable to those observed for Zn^{+2} catalysed systems. The relaxation times were fitted to theArrhenius equation which gave activation energy (E_a) with an average value of *ca*. 104 kJ mol^{-1}. This value is somewhat higher than that reported by Leibler and coworkers[45] for Zn^{2+} salt-catalysed transesterification processes.

The preparation of vitrimers based on plant oils with high glass transition temperature (T_g) and strength continues to be a challenge. Yang *et al.*, developed a 'green' ESO-based vitrimer by incorporating fumaropimaric acid as a curing agent and employing zinc acetylacetonate $Zn(acac)_2$ (10 mol% of fumaropimaric acid) as a transesterification catalyst.[130] The T_g, modulus, and tensile strength of the ESO-fumaropimaric acid vitrimers increased as the fumaropimaric acid loading in the polymer networks increased, due to the stiff hydrogenated phenanthrene ring structure present in fumaropimaric acid and numerous reactive groups. The high fumaropimaric acid contents increases the abundance of carboxyl groups and hence extra ester groups are generated, causing faster stress relaxation. The relaxation rate of ESO-

fumaropimaric $acid_{1.0}$ rose as the temperature increased due to increase in the transesterification rate. The computed E_a values was 87.88 kJ mol^{-1} (G/G_0 = 0.63). The dynamic transesterification with methanol was used to degrade ESO-fumaropimaric acid networks at 140 °C and subsequently reprocessed into new vitrimers at 180 °C.

Glycyrrhizic acid is a naturally occurring triterpene saponin found mostly in licorice roots. It has been extensively used as a sweetener in food and as a medicinal component.[160-163] Glycyrrhizic acid includes numerous hydroxyl groups which aid in the transesterification of epoxy/acid vitrimer networks.[26] The thermal stability and mechanical properties both benefit from the distinctive rigid structure of glycyrrhizic acid. Wu *et al.*, utilised ESO and glycyrrhizic acid to develop entirely biobased vitrimers in the presence of a 1,5,7-triazabicyclo[4.4.0]dec-5-ene (TBD) catalyst (5% molar ratio to carboxylic acid) (**Figure 1.8a**).[132] The relaxation rate of the networks rose as the temperature is increased (**Figure 1.8b**). The decrease in relaxation time was attributed to the accelerated transesterification that occurs at elevated temperatures. The E_a and topology freezing transition temperature (T_v), was reported to be 112 kJ mol^{-1} and 69 °C respectively for R = 0.5 ESO/glycyrrhizic acid networks. ESO/glycyrrhizic acid networks with R = 0.5 could be welded at 200 °C for 15 mins without any external pressure (**Figure 1.8c, left**). The material showed excellent weldability because of the topological network rearrangement as it can withstand almost 300 times its own weight (**Figure 1.8c, right**). The majority of elastomeric materials derived from vegetable oil derivatives display poor mechanical properties and lack reparability and recyclability due to the irreversible nature of the crosslink networks. A tetra functional epoxide (N,N,N',N'-tetraglycidyl-4,4'-

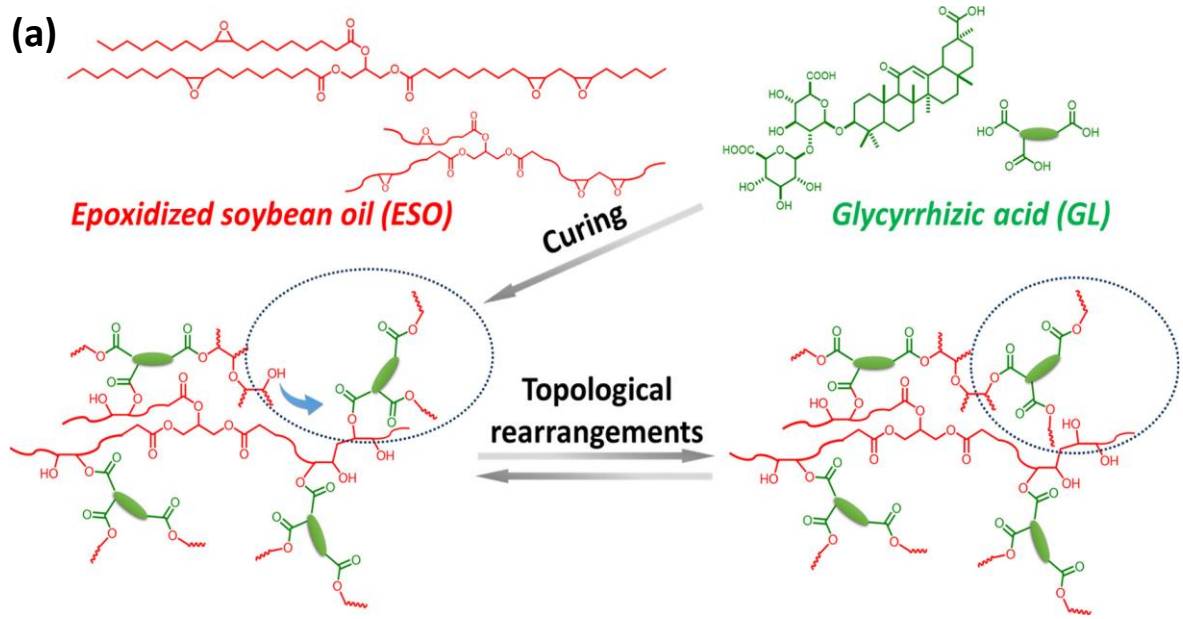
(a)
Epoxidized soybean oil (ESO)
Glycyrrhizic acid (GL)
Curing
Topological
rearrangements

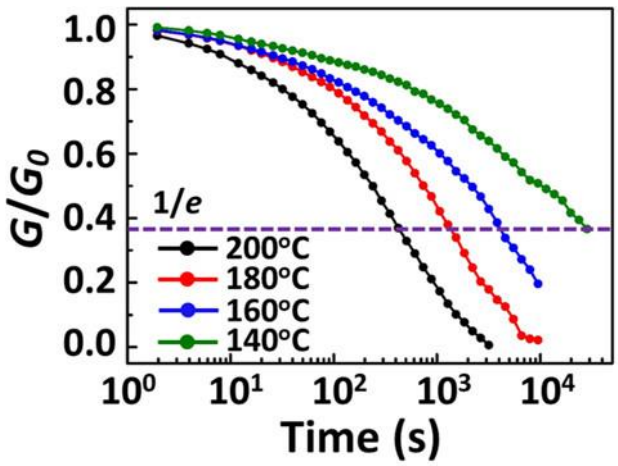
(b)
G/G0
1/e
200°C
180°C
160°C
140°C
Time (s)

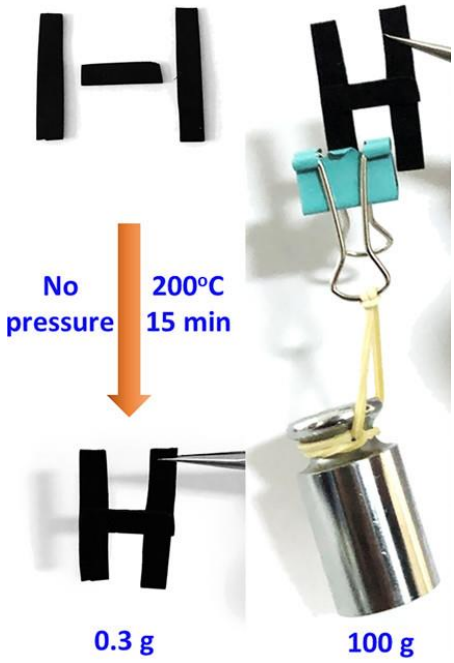
(c)
No
pressure
200°C
15 min
0.3 g
100 g

Figure 1.8: *Vitrimeric networks from epoxidized soyabean oil (ESO) and glycyrrhizic acid (GL), (a) synthetic strategy of ESO/GL vitrimeric networks. Topological network rearrangements in ESO/GL, (b) stress relaxation of R = 0.5 ESO/GL networks at different temperatures and (c) welding of R = 0.5 ESO/GL (left) and after welding the material could withstand 300 times heavier than its own weight (right). Reprinted (adapted) with permission from Ref, Copyright 2020, American Chemical Society.*[132]

diaminodiphenylmethane,TGDDM) is extensively used in aerospace materials because of its high temperature resistance, high reactivity, and outstanding mechanical properties.[164] Li *et al.*, developed catalyst free elastomers by curing of a vegetable oil-derived dimer acid and TGDDM.[138] Dynamic transesterification reactions (DTER) were possible due to the abundance of tertiary amine groups in the network structure, which acted as an internal catalyst for transesterification at temperatures over 190 °C. As TGDDM has more rigid structure and higher functionality than dimer acid, the increasing amount of TGDDM tends to raise the T_g. Elastomer-1/0.8 has the highest tensile properties with a tensile stress of 21.7 MPa and elongation of break 210.8%. The higher tensile properties observed at higher loadings of TGDDM could be due to more uniform network topology and a higher crosslink density. The elastomer was fully degraded in water at 190 °C in 5 h. The hydrolysis process was expedited because of the presence of tertiary amines in network which acts as internal catalysts to facilitate hydrolysis. Additionally, the degraded product is polymerizable to a new crosslinked elastomer, because of DTER catalysed by the internal tertiary amines.

Palm oil is one of the most appealing renewable alternatives.[165] Mu *et al.*, developed palm oil-based programmable shape memory epoxy resins which are mechanically tough and recyclable.[139] The authors employed citric acid as a catalyst-free curing agent for palm oil-

based methyl methacrylate epoxide resin to introduce β-hydroxyl ester groups in the network (**Figure 1.9a**). The ultimate tensile strength improves from 1.2 to 28.9 MPa as citric acid content increases due to the increase in crosslinking density, whereas the ultimate tensile strain decreases from 109 to 12%. Epoxy resins-40 films were recycled at 170 °C under 10 MPa pressure for 10 min (**Figure 1.9b**). After reprocessing (three times), there was no change in the chemical functionality and the mechanical properties could be restored to the pristine sample. With an increase of temperature from 150 to 160 °C the relaxation rate increases due to faster transesterification at elevated temperature. Topological networks could undergo DTER at high temperature due to the abundance of the β-hydroxyl ester groups which enables the epoxy resins to possess shape memory properties (**Figure 1.9c**). An initial heart-shaped sample (permanent shape 1) was heated to 150 °C, reshaped into a spiral shape and held for 2 h to achieve permanent shape 2. Other permanent shapes, such as "S" shape (permanent shape 3), could be prepared by repeating the shape editing procedure. Temporary "S" shape was prepared at 120 °C and cooled to room temperature to lock-in the shape. Upon reheating the "S"-shape to 120 °C, it demonstrated complete shape recovery within 30 seconds (**Figure 1.9c**).

An exciting new area of research in vitrimer development which aims to build networks *via* dual dynamic bonds is emerging. Mauro *et al.*, studied repairability, recyclability, and reshapability and shape memory behavior of the vitrimers prepared by copolymerizing various epoxidized oils with 2,2'-dithiodibenzoic acid as hardener.[140] The topological network provides recycling abilities by combining two recycling mechanisms: disulphide exchange and transesterification. Thermosets from epoxidized vegetable oils with lower epoxy content required milder recycling conditions owing to less crosslinking density, which correspond to

lower T_g. Epoxidized vegetable oils with high-epoxy contents are more difficult to recycle

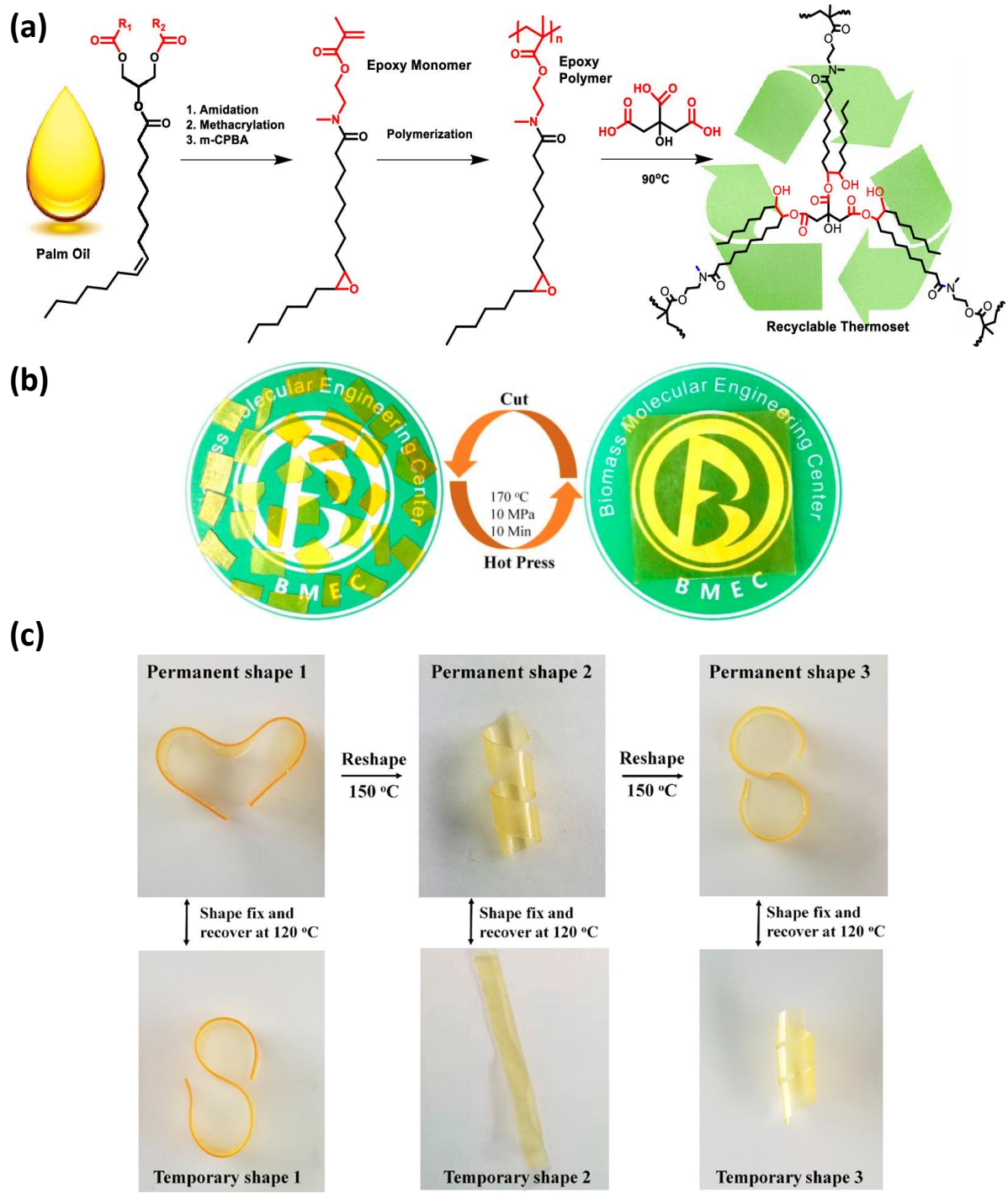

Figure 1.9: *Palm oil-based transesterification resins, (a) synthesis of epoxy resins, (b) reprocessing of epoxy resins-40 and (c) programmable shape–memory properties. Reprinted (adapted) with permission from Ref, Copyright 2020, American Chemical Society.*[139]

because they have a high crosslink density resulting in a higher T_g. Thermosets prepared from epoxidized karanja oil and epoxidized St John's Wort oil were repaired and reshaped respectively on a hot press in 5 min at a temperature of 150 °C. The combination of disulphide exchange and transesterification reaction ensured complete mechanical recycling of all thermosets.

Commercially available acrylated epoxidized soybean oil is derived by the epoxidation of soybean oil followed by ring-opening of epoxide using acrylic acid. Acrylated epoxidized soybean oil and other functionalized vegetable oils were used as green monomers to produce highly crosslinked thermosets.[166-168] Acrylated epoxidized soybean oil is a multifunctional reactive oil which is more reactive than soybean oil due to the ability of acrylate groups to self-react at high temperatures in the presence of air without the addition of a radical comonomer or initiator.[166] Capiel *et al.*, prepared catalyst free vitrimers using radical polymerization of functionalized fatty acids with styrene or acrylated ESO.[141] The short chain length of polymer formed from lauric acid has less plasticizing effect resulting slow physical relaxation compared to the polymer formed using oleic acid. This plasticizing effect was more dominant compared to the transesterification rate, therefore polymers formed from oleic acid relax faster than those with lauric acid. The copolymer with the styrene showed enhanced mechanical properties due to the presence of rigid aromatic rings in the polymer molecular structure and the highly reactive C=C groups of styrene offer a long linear chain between crosslinking sites.

The incorporation of amine groups in polymers not only acts as catalysts, but can also form H-bonds between groups, enhancing the self-healing, adhesive, and mechanical properties. Xu *et al.*, prepared catalyst-free self-healing bio-based polymers using aminated epoxidized

soybean oil and epoxidized maleopimaric anhydride consisting of dual dynamic networks comprising of numerous hydrogen bonds and ester bonds.[143] As the epoxidized maleopimaric anhydride content increases, the T_g increases for the polymer. This was ascribed to two reasons, firstly, the increase of epoxy groups available to react with amino groups in aminated epoxidized soybean oil thus increasing the crosslink density and restricting the mobility. Secondly, epoxidized maleopimaric anhydride contains a hydrogen phenanthrene structure that functions as a hard phase in the polymer and substantially increases the storage modulus and T_g.[130, 169, 170] The rate of stress relaxation in polymers increases in direct proportion to the amount of epoxidized maleopimaric anhydride present, as increased epoxidized maleopimaric anhydride content results in the introduction of numerous β-hydroxyl groups which promotes DTER. The E_a value of $polymer_{0.8}$ was observed to be 90.21 kJ mol^{-1}, which is comparable to the E_a value of 87.9 kJ mol^{-1} previously reported for a vitrimer system catalysed by $Zn(acac)_2$.[130] The self-healing properties of polymers increases as the epoxidized maleopimaric anhydride content is increased.

The increasing demand for carbon-fiber-reinforced materials leads to an enormous consumption of petroleum products and adds difficult post-processing steps. Therefore, the development of a degradable epoxy vitrimer matrix is a viable and accessible method.[171] Li *et al.*, prepared a tung oil-based epoxy vitrimer matrix and carbon-fiber-reinforced materials with high mechanical and excellent thermostability properties.[146] DTERs are promoted at high temperatures by the zinc (II) acetylacetonate-catalyst, which accounts for the material's impressive self-healing, shape-changing, and recycling characteristics. The epoxy vitrimer matrix and carbon-fiber-reinforced materials can be fully degraded in ethanol and NaOH solution.

Li *et al.*, prepared ESO, succinic and sebacic acid based vitrimers.[152] The vitrimers exhibited low T_g. The compressive remoulding at 160 °C and 10 MPa revealed that the vitrimers were able to cure apparent flaws in 30 min. After 3 mechanical recycling, the thermal stability and mechanical strength of vitrimers were well preserved.

All of the aforementioned literature depends on the epoxidation of vegetable oil. In contrast, the vitrimers could be prepared using an epoxide-free method. For example, free radical polymerization of C=C unsaturation could be used to crosslink monomers derived from renewable resources that contain ester and hydroxyl functional groups.

Lignin based-vitrimers

Lignin is the second most abundant natural polymer and is present in many plant species. Lignin has been widely utilised as a building block in thermosetting materials like epoxy and phenol-formaldehyde resins.[172, 173] Unfortunately, because of its highly ramified aromatic structure and large molecular weight, lignin is frequently not consistent with other components and so limits its use. Therefore, lignin must be chemically modified before it can be used for any application. A green technique of bleaching pulp is ozonation. It breaks down lignin's benzene rings and introduces carboxylic acid groups, improving the degraded lignin's solubility and allowing it to be easily washed away.[174, 175] Zhang *et al.*, developed lignin-based vitrimers by reacting ozonated lignin with sebaceous acid-derived with 10 mol% zinc catalyst, $Zn(acac)_2$, this undergoes a bond exchange process under thermal conditions.[124] The tensile strength, modulus and T_g increased the ratio of lignin loading. External pressure deforms the sample, whilst the transesterification reactions promote rapid rebuilding of the crosslinked structure. The scratch width of all vitrimers decreased by more than 70% in just 5 mins.

It remains a challenge to develop high T_g epoxy-based vitrimers with good repairability.[176] To overcome these limitations, Liu *et al.*, developed a triepoxy vitrimeric materials based on sustainable feedstocks such as guaiacol and vanillin, following curing with 4-methylcyclohexane-1,2-dicarboxylic anhydride in the presence of 10 mol% $Zn(acac)_2$ catalyst.[123] The triepoxy vitrimer films could be repaired at 220 °C such that crack was healed up to 90% in 5 mins. The materials demonstrated remarkable reparability (crack decreased over 70% in just 5 min) among all triepoxy vitrimers.

Tang *et al.*, prepared lignin-based epoxy vitrimers from fractionated lignin and sebacic acid.[144] The fractionated lignin was then epoxy-modified using epichlorohydrin to produce glycidyl ethers of lignin which was subsequently reacted with sebacic acid. The epoxy vitrimers had a Young's modulus above 1 GPa. In terms of reprocessing, ethanol-soluble epoxy vitrimers achieved the best properties, whereas ethyl acetate-soluble epoxy vitrimers had a somewhat lower value. Reprocessing efficiency of fractionated lignin declined to 31.02% as its molecular weight increased, perhaps because of poor reactivity of glycidyl ethers of lignin extracted in acetone, the high level of steric hindrance, and the inflexible structure of lignin.[177]

Liu *et al.*, prepared crosslinked polymer networks by reacting succinic anhydride and eugenol-derived epoxy in the presence of ($Zn(acac)_2$) catalyst (**Figure 1.10**).[121] At low temperatures, transesterification reactions are slow and the topology structure is frozen, which results in a slow relaxation rate. Transesterification reactions are rapid at high temperatures owing to the faster topological rearrangement, which results in a fast relaxation rate. The vitrimers could be reprocessed and degraded at 160 °C (**Figure 1.10b, c**).

The exploration for innovative epoxy vitrimers, particularly with customizable properties are generally overlooked. This is reflected in the notion that the petroleum-based diglycidyl ether

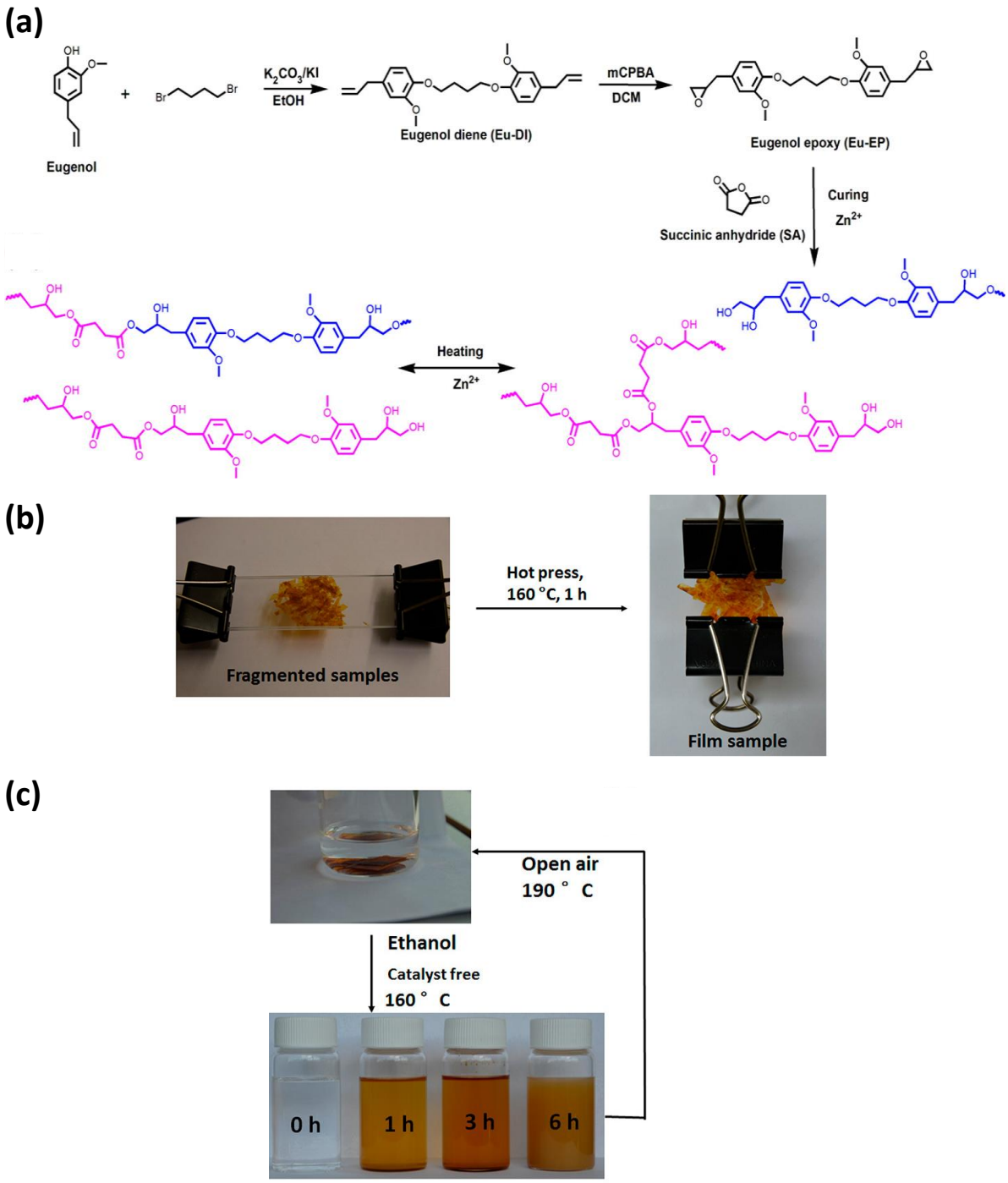

Figure 1.10: *Vitrimer prepared from succinic anhydride (SA) and eugenol-derived epoxy (Eu-EP), (a) synthetic strategy (top), topological rearrangement in the presence of* Zn^{2+} *under thermal conditions (bottom), (b) reprocessing of vitrimer with R = 1: 0.5 and (c) chemical recycling of cured vitrimer with R = 1: 0.5. Reprinted (adapted) with permission from Ref, Copyright 2017, American Chemical Society.*[121]

is being used primarily in vitrimers synthesis.[178-183] Zhao *et al.*, reported a range of epoxy prepolymers whose attributes can be tailored by utilising the same initial phenol in a single epoxidation process.[126] Vitrimers were prepared by treating epoxy prepolymers with Pripol 1040 having a combination of dicarboxylic (23 wt%) and tricarboxylic (77 wt%) fatty acids with a $Zn(acac)_2$ catalyst (5 mol%). When the triepoxide content of a vitrimer is increased in comparison to the monoepoxide content, it offers a larger number of dangling OH groups, it also results in an increased crosslink density, which reduces chain mobility, causing an incremental increase in T_g values from 16 to 23 °C. The relaxation time was lengthened when the crosslink density was increased while for the sample having 60% monoepoxide content, lower E_a were observed, which can be a result of its lower crosslink density and a greater proportion of dangling hydroxyl groups.

Numerous techniques were employed to extract the necessary chemicals from lignin, however they have some limitations. One of the issues during the pretreatment of lignin material is the use of potentially hazardous chemicals and the production of a substantial volume of toxic chemical waste. As a result, the concept of Green Chemistry has gained traction as a way forward in the designing of innovative technologies, with the overarching goal of reducing waste and the use of harmful or hazardous substances wherever possible. Raw material has additional challenges, such as complexity and inconsistency.

Carbohydrate based-vitrimers

Cellulose is the highest abundant organic substance in the world. Cellulose-based nanofibrils have become an ecofriendly class of materials with excellent performance. Lossada *et al.*, prepared a vitrimer-based nanocomposite[184] by the incorporation of poly(dimethylsiloxane) vitrimer nanoparticles in a cellulose nanofibril network (**Figure 1.11a**).[125] The vitrimeric system

was based on epoxy/acid condensation reaction leading to the formation of β-hydroxyester bonds which undergoes transesterification reaction at 120 °C in the presence of 5 mol% $Zn(acac_2)$ catalyst. The cellulose nanofibril softened and become more ductile after inclusion of the vitrimer. Furthermore, the addition of hydrophobic poly(dimethylsiloxane) in the cellulose nanofibril networks, minimising water intake while substantially improves the mechanical resistance by retaining significant tensile strength (20−35 MPa) and stiffness (Youngs modulus = 0.20−0.30 GPa) when immersed in water for 4 h. Vitrimer nanocomposite containing 65 wt% cellulose nanofibrils and 35 wt% vitrimer nanoparticles were welded by hot-pressing two films together at pressure of 3 bar, for 24 h at 120 °C (**Figure 1.11b**). The welded nanocomposite exhibits a force at break of *ca*. 1 N, while a pristine sample offers a force at break of *ca*. 3 N (**Figure 1.11c**).

Halloysite nanotubes are a kind of natural, odourless, biocompatible, and economically viable clay mineral that belongs to the kaolinite group, well-known for their good mechanical and thermal properties.[185-188] Aluminosilicate-based nanoscale lumens are well-known for their low hydroxyl group density and high aspect ratio, culminating a multilayered structure suitable for a variety of applications.[189] Researchers have often encountered difficulties in incorporating these into an epoxy resin because of the poor interfacial interaction and load transfer between epoxy molecules and halloysite nanotubes. Jouyandeh *et al.*, developed silane-coupled cellulose-functionalized halloysite nanotubes/bifunctional epoxy resins with vitrimer-like properties.[133] Transesterification reactions of β-hydroxyl ester bonds imparted self-healing properties to epoxy halloysite nanotubes-cellulose microcrystals at higher temperatures**.**

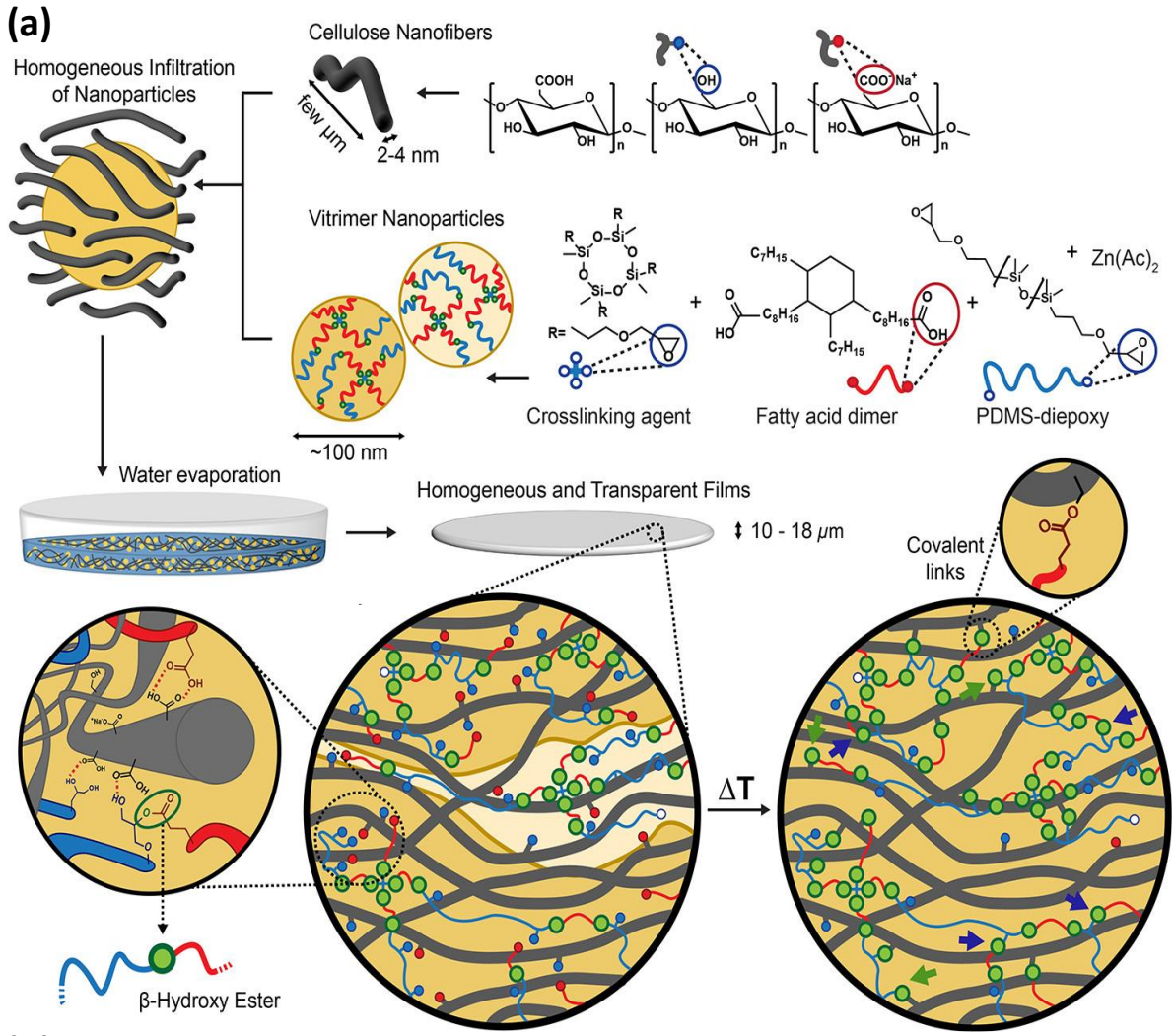
(a)
Homogeneous Infiltration of Nanoparticles
Cellulose Nanofibers
few μm
2-4 nm
Vitrimer Nanoparticles
~100 nm
Crosslinking agent
Fatty acid dimer
PDMS-diepoxy
Zn(Ac)2
Water evaporation
Homogeneous and Transparent Films
10 - 18 μm
Covalent links
ΔT
β-Hydroxy Ester

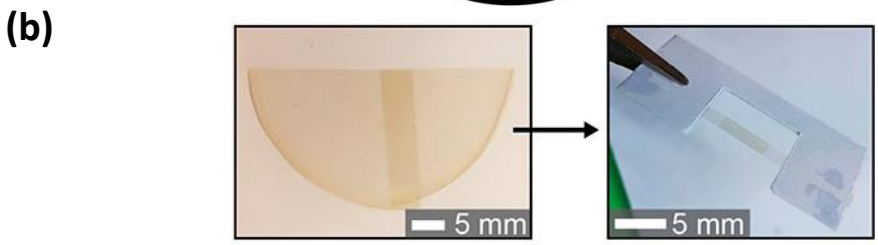
(b)
5 mm
5 mm

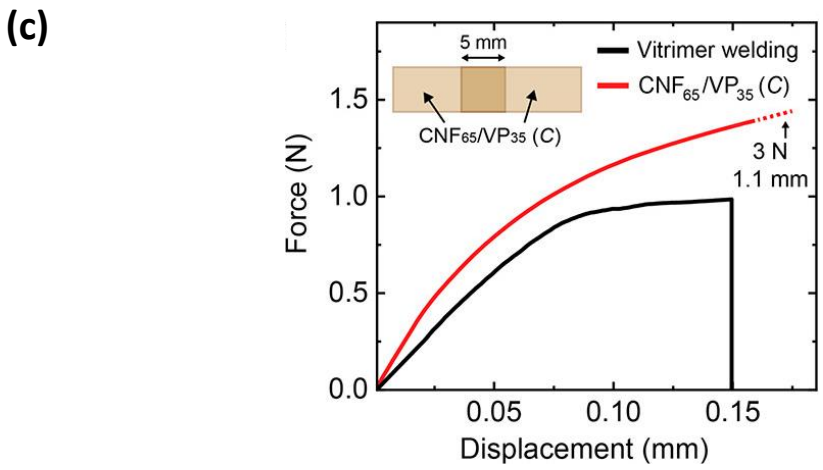
(c)
5 mm
Vitrimer welding
CNF65/VP35 (C)
CNF65/VP35 (C)
3 N
1.1 mm
Force (N)
1.5
1.0
0.5
0.0
0.05
0.10
0.15
Displacement (mm)

Figure 1.11: *Cellulose nanofiber based vitrimers, (a) synthetic strategy of cellulose vitrimer nanocomposites by aqueous mixing of poly(dimethylsiloxane) (PDMS) vitrimer nanoparticles with cellulose nanofibrils. Additional heating enhances the completion of crosslinking processes, leading to the formation of homogenous films, (b) welding of vitrimer nanocomposite containing 65 wt% cellulose nanofibrils and 35 wt% vitrimer nanoparticles (CNF_{65}/VP_{35}) nanocomposite films at pressure of 3 bar, for 24 h at 120 °C and (c) Tensile curves of welded CNF_{65}/VP_{35} films. Reprinted (adapted) with permission from Ref, Copyright 2019, American Chemical Society.*[125]

There are some limitations that will need to be overcome in the coming years before cellulose derived polymers can fully replace their petroleum-based counterparts. These limitations include developing simple, inexpensive, and less time-consuming procedures for all phases of polymer synthesis, including cellulose separation from lignocelluloses, synthesis of suitable forms of cellulose, and polymerization.

Naturally occurring carboxylic acid based-vitrimers

Lactic acid can be synthesized either by microbial fermentation or chemical processes. Lactic acid is a building block for the creation of poly(lactide), a widely used polymer in the production of packaging material and containers.[190] Poly(lactide), perhaps the most extensively researched bio-based thermoplastic, has high modulus and strength making it a viable alternative for petrochemical polymers like poly(ethylene terephthalate) and poly(styrene).[191, 192] In 2014, Brutman *et al.*, produced poly(lactide) vitrimers that could be readily processed and reprocessed or repaired after usage or breakage.[22] The authors used stannous (II) octoate [$Sn(Oct)_2$] as a transesterification catalyst in crosslinking methylene diphenyl diisocyanate and hydroxyl terminated 4-arm star-shaped poly((±)-lactide)

monomers. In this system T_v was within a few degrees of T_g, suggesting that the material could undergoe transesterification and flow once it reaches the rubbery state. The Arrhenius relationship yielded E_a, of 150 ± 3 kJ mol^{-1}. The poly(lactide) vitrimers were healed *via* compression molding at 140 °C and pressure of 4 MPa for 30 min. Poly(lactide) vitrimers with lower isocyanate: hydroxyl ratios and high catalyst loadings resulted in a better recovery of tensile properties. This is attributed to the rapid transesterification at higher catalyst loading. While at lower isocyanate: hydroxyl ratio the fast transesterification were most likely caused by an increase in the amount of unreacted hydroxyl groups.

Altuna *et al.*, developed shape memory epoxy vitrimers based on DGEBA, citric, sebacic and glutaric acids with a T_g at temperatures high enough to establish the temporary shape at 20 °C.[122] The transesterification was catalysed by 1-methylimidazole. The accelerated polymer network rearrangement made it possible to permanently alter the material shape within an acceptable timescale. The vitrimer showed excellent shape memory properties with shape fixity ratio and recovery ratio greater than 99%. The vitrimer system has a T_v in the range of 105–117 °C while the E_a, is about 90–120 kJ mol^{-1}.

The natural trifunctional chemical protocatechuic acid is derived by biological fermentation from lignin.[193] Tao *et al.*, had developed epoxy vitrimers made from protocatechuic acid and maleic anhydride in the presence of transesterification catalyst ($Zn(acac)_2$), and compared their properties to those of a commercial DGEBA.[131] All epoxy vitrimers produced from protocatechuic acid have a T_g greater than DGEBA, implying that bio-based epoxy vitrimers are more thermally stable than commercial epoxy resins. The tensile modulus of this bio-based vitrimer was found to be 2.13 GPa, which is 2.5 times higher than the value found in DGEBA. The E_a of bio-based vitrimer with 2: 1 (epoxy: anhydride) was determined to be 65.8

kJ mol^{-1}. The vitrimer could be reprocessed in a hot press machine at 230 °C for 2 h under a pressure of 10 MPa.

Malonic acid is an important chemical present in lucerne[194] and wheat leaves.[195] Diethyl malonate is a low-cost, β,β'-diester found in fruit juices such as guava, blackberry pineapple bilberry, Cape and gooseberries. Vitrimers based on β-activated ester are a relatively unexplored field. Debnath *et al.*, prepared catalyst free polyester networks using poly-hydroxyethyl methacrylate as the hydroxyl precursor and diethyl malonate as the crosslinking agent, which could undergo ester bond exchange reaction under thermal conditions.[53] Diethyl malonate is a promising candidate for β-activated ester due to the presence of C=O groups in two ester groups at the β position. Transesterification of β-activated esters occurs rapidly at 150 °C. The E_a values range from 108.1–106.3 kJ mol^{-1}. The vitrimers were reprocessed at 150 °C for 5 h under compression load of 40 kg resulting in formation of crack free film. Reprocessed films regained up to 90% of the original ultimate tensile strength value.

Malic acid is found in apples and a wide variety of plants and animals. Wang *et al.*, prepared bio-based, catalyst free, vitrimer using malic acid with glycidyl methacrylate.[142] The authors used malic acid because the position of hydroxyl group relative to carbonyl is advantageous in forming intramolecular six-membered ring hydrogen bonds (O---HO=C) in crosslinked networks. These are connected by both covalent and hydrogen bonds. This includes the hydrogen bond between the hydroxyl and carbonyl group in the chain and additional intramolecular hydrogen bonds between the six-membered ring hydrogen-bonded O-H⋯O=C, which raises the molecular rigidity, thus causing higher strength, modulus, and T_g.[196, 197] The formation of intramolecular hydrogen bonds raises the electropositivity of the carbonyl carbon atom in ester units, resulting in a faster transesterification reaction. The

stress relaxation rate of cured malic acid-glycidyl methacrylate increases with an increase in temperature ascribed to the increased chain mobility and accelerated transesterification reaction. The E_a of the transesterification process of cured malic acid-glycidyl methacrylate is determined to be 131.35 kJ mol $^{-1}$. The cured malic acid-glycidyl methacrylate samples were repaired at 160 °C for 1 h. The welded and repaired samples recovered 93.4% and 93.5% strength of the original cured samples, respectively.

Sebacic acid, a saturated dicarboxylic acid, is one of the most widely used castor oil derivatives on a global scale. Sebacic acid is used in the production of many oleochemical derivatives, including polyesters, lubricants, Nylon 6–10, polyols, and hydrogels.[119, 198] Guo *et al.*, developed a unique kind of electrically conductive epoxy vitrimer composites using sebacic acid and multi wall carbon nanotubes having double dynamic covalent bonds (carboxylate and disulphide bonds) (**Figure 1.12a**).[134] The epoxy resin matrix was synthesised, through ring-opening reaction of epoxy group in the presence of a TBD catalyst from bis (4-glycidyloxyphenyl) disulfide and sebacic acid. The epoxy groups would react with the carboxylic acid to generate hydroxyl groups, and they would then react with additional carboxyl and epoxy groups to build the crosslinked network with two kinds of dynamic covalent bonds (**Figure 1.12a**). The bis (4-glycidyloxyphenyl) disulfide is used to inject dynamic disulphide bonds into the network, whereas TBD introduces dynamic ester bonds in the network. The relaxation time decreases with increasing temperature. This decrease in relaxation time is attributed to the rapid transesterification and disulphide exchange process at higher temperatures. The E_a for epoxy vitrimer composites containing 5 wt% and 0 wt% multi wall carbon nanotubes was found to be 78.11 kJ mol^{-1} and 71.61 kJ mol^{-1} respectively. Epoxy vitrimer composites containing 5 wt% multi wall carbon nanotubes could be effectively

reprocessed at 100 °C, 10 MPa for 1 hr owing to the simultaneous exchange reaction of carboxylate and disulphide bonds in the network. In addition, epoxy vitrimer composites containing 5 wt% multi wall carbon nanotubes display no significant drop in tensile strength after three processing cycles, which proves that the incorporation of double dynamic bonds considerably improved the reprocessing efficiency. Multi wall carbon nanotubes can convert near-infrared light to heat in situ and have a high energy conversion rate.[199] The good dispersion of multi wall carbon nanotubes in the matrix provides the material with outstanding photothermal properties, allowing near-infrared light welding in the presence of thiols. The repaired epoxy vitrimer composites containing 5 wt% multi wall carbon nanotubes retain its electrical conductivity (**Figure 1.12b**) and mechanical properties, also demonstrating superior photo-welding capability at room temperature. These might find use as a flexible wearable device for skin sensors (**Figure 1.12c**). These studies help pave the way for more widespread usage of multifunctional epoxy resins in everyday life.

Wu *et al.*, synthesised an epoxy vitrimer composite, by combining DGEBA epoxy resin, adipic acid, a primary amine curing agent with amino-functionalized CNTs.[145] The amine curing agent generates sufficient hydroxyl groups that promote transesterification exchange processes, which results in self-healing abilities of the composites.

Xu *et al.*, prepared bio-based vitrimer using hydroxy-terminated hyperbranched polyesters, fumaropimaric acid, and glycerol triglycidyl ether.[147] The T_g and tensile strength of the vitrimer are 90.5 °C and 57.2 ± 4.3 MPa, respectively. These are due to the presence of a rigid hydrogenated phenanthrene ring structure and hyperbranched polyesters with numerous

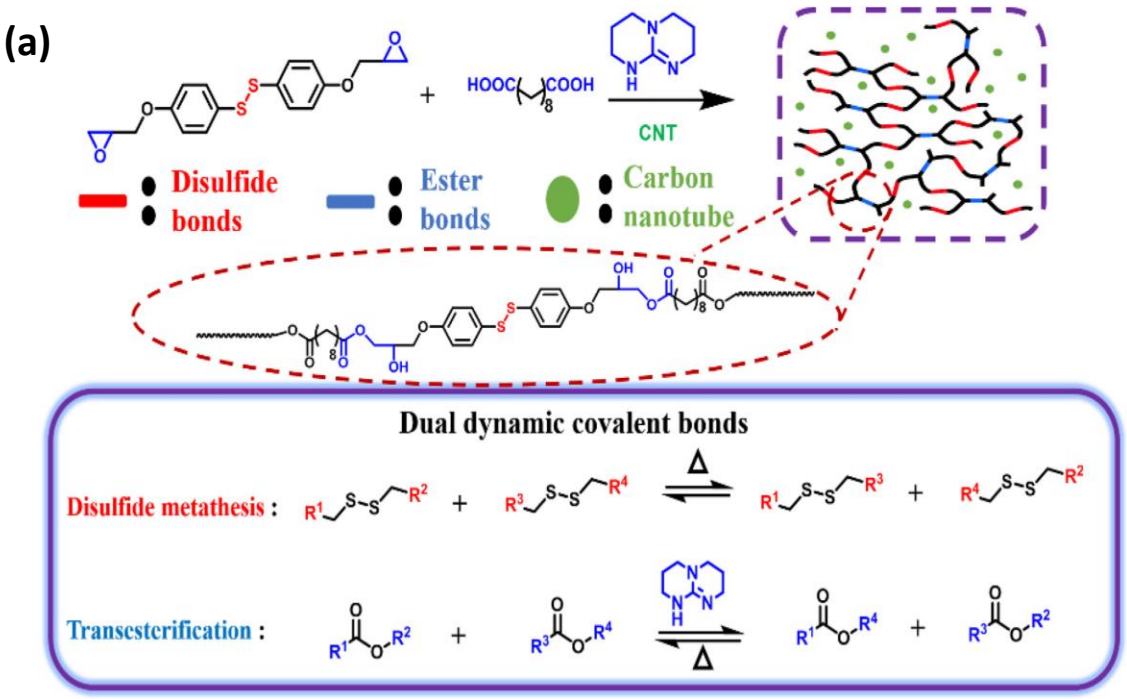
(a)
HOOC
COOH
CNT
Disulfide bonds
Ester bonds
Carbon nanotube
Dual dynamic covalent bonds
Disulfide metathesis :
Transesterification :

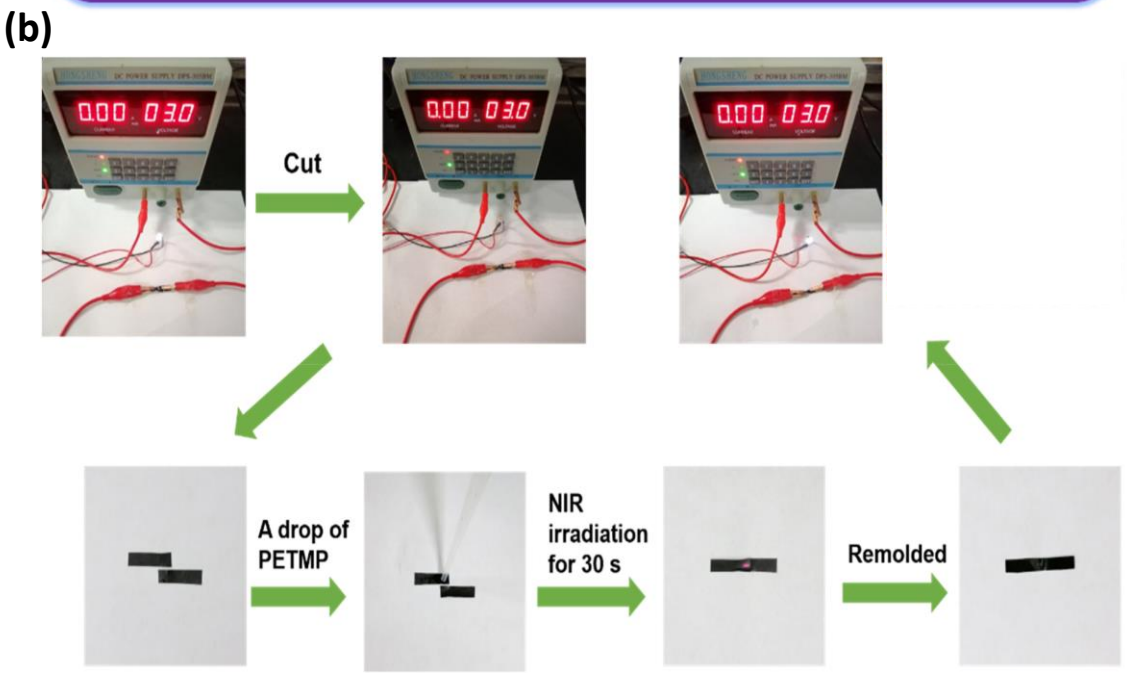
(b)
Cut
A drop of PETMP
NIR irradiation for 30 s
Remolded

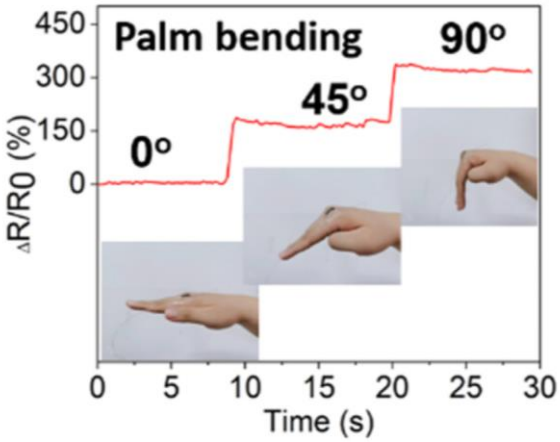
(c)
Palm bending
90°
45°
0°
ΔR/R0 (%)
Time (s)

Figure 1.12: *Epoxy vitrimer composites using multi wall carbon nanotubes, (a) preparation of electrically conductive epoxy vitrimer composites using carbon nanotube (CNT) and TBD. The epoxy vitrimer composites undergoes dual dynamic bond shuffling under thermal conditions, (b) Near-infrared light induced welding of epoxy vitrimer composites containing 5 wt% multi wall carbon nanotubes by applying a drop of pentaerythritol tetrakis (2-mercaptoacetate) (PETMP) between two pieces of vitrimer composites. Repaired epoxy vitrimer composites shows good electrical conductivity (led turns on) and (c) epoxy vitrimer composites containing 5 wt% multi wall carbon nanotubes is employed as skin sensor which is used to track human movements. Reprinted (adapted) with permission from Ref, Copyright 2021, Elsevier.*[134]

hydroxyl groups. The DTER was catalysed by hydroxy-terminated hyperbranched polyesters, resulting in self-healing and physical recycling without an additional catalyst.

Xu *et al.*, prepared catalyst-free bio-based vitrimer using adipic acid and epoxidized menthane diamine.[148] The turpentine derivative menthane diamine is a rigid six-membered ring that can be employed as a rigid component in polymers.[200, 201] The vitrimer exhibits high mechanical properties owing to the rigid structure of the epoxidized menthane diamine. The vitrimer exhibited effective topological network rearrangement based on DTER, due to the presence of tertiary amines, which are derived from epoxidized menthane diamine.

Ferulic acid is present in vegetables, fruits, some drinks (such as coffee, beer, etc.), and several Chinese medicinal plants, including *Angelica sinensis*, *Cimicifuga racemosa*, and *Ligusticum chuangxiong*.[202] Zhong *et al.*, synthesised fully bio-based catalyst-free epoxy vitrimers from ferulic acid-based hyperbranched epoxy resin.[149] The vitrimers showed dynamic transesterification exchanges owing to the hydroxyl groups and hyperbranched topological structure of ferulic acid-based epoxy resins. The vitrimers can be depolymerized using NaOH

and reused again to prepare vitrimers, enabling a closed-loop recycling system. The recycled vitrimers preserved the original vitrimers thermal stability, chemical resistance, and mechanical properties.

Itaconic acid is produced by thermal decomposition of citric acid.[203] Kolsch *et al.*, synthesised vitrimers using itaconic acid vinyl monomer, diethyl succinate, and (4,4'-bioxepane)-7,7'-dion in the presence of TBD as a transesterification catalyst.[150] The vitrimer showed faster relaxation times at higher amount of the catalyst owing to the faster transesterification exchange process. Vitrimers could be reprocessed in 1 h at 140–180 °C and 5–7 bar due to thermally activated transesterification reactions.

Natural rubber based-vitrimers

Traditional vulcanised rubbers have good mechanical properties because of the formation of a stable three dimensional covalently crosslinked network. Because of the irreversibility of their crosslinked networks, covalently crosslinked rubbers are intrinsically difficult to reshape and recycle, causing significant resource waste and environmental concerns.[204, 205] Covalent linkages in rubber networks that are stronger and more reversible could lead to improved mechanical performance.[10, 14] Such networks can be reconfigured in response to external stimuli, such as temperature, which allows rubbers to reshape and mend themselves.[206-214] For rubber to have the capability for reprocessing and recycling as well as self-repair, the introduction of vitrimer-like concepts into rubber networks is clearly a viable option. Bentonite, a naturally occurring substance, can be used to substitute petroleum-based rubber reinforcing agents such as carbon nanotube, carbon nanodot and carbon black and many others.[129] A special sort of elastomer, known as epoxidized NR (ENR) is obtained when NR is epoxidized. Xu *et al.*, prepared an ENR composite that is crosslinked through β-hydroxyl ester

linkages using citric acid-modified bentonite without use of any catalyst.[135] Citric acid-modified bentonite with many carboxyl groups on the surface were used as a crosslinker to crosslink ENR. Due to citric acid modified bentonite's filler-reinforcement towards ENR and the development of an elastic hybrid rubber network, both strength and elongation were increased simultaneously. At room temperature, the stress relaxation behavior of a 20% ENR/citric acid-modified bentonite composite was severely restricted owing to the frozen topology of the hybrid rubber network. The stress relaxation rate increases with increased temperature because of higher transesterification rates. When the sample was heated to 200°C, it displayed a larger stress relaxation which indicates that the hybrid ENR network could flow at this temperature. The gluey feature of the ENR matrix, as well as the transesterification processes, assist in the self-healing of the ENR/citric acid-modified bentonite composites. After 3 h of healing at 80 °C, the tensile strength and elongation recovered to 60% and 68%, respectively. This high healing rate at 80 °C was mostly due to gluey nature of ENR matrix.[215]

Carbon black is the most important rubber reinforcer in the tyre business because it gives rubber its outstanding abrasion resistance, mechanical properties, and durability.[216, 217] As a result, carbon black-reinforced rubber composites that are crosslinked using sulfur-based curing chemicals cannot be reprocessed or moulded because of the irreversibility of the permanent network. Qiu *et al.*, employed exchangeable interface design to develop recyclable and durable elastomeric vitrimer composites out of the most widely used rubber raw materials (NR and carbon black).[136] Diazonium-based chemistry was used to attach carboxyl groups to 35-nm-diameter commercial carbon black. The NR network was functionalized with epoxide groups to prepare epoxidized version of NR (ENR).[218, 219] The interfacial β-hydroxyl ester bonds were formed between carboxyl-functionalized carbon black and ENR which leads

to topological rearrangement *via* the transesterification exchange process. ENR composites with different parts per hundred of rubber (phr) carboxyl-functionalized carbon black, show a significant increase in relaxation rates with increasing temperature owing to the faster transesterification process. The E_a of ENR composites with 20 phr carboxyl-functionalized carbon black is reported to be 166 kJ mol^{-1}. Since the ENR composites with different phr carboxyl-functionalized carbon black display a gradual decrease in viscosity in accordance with the Arrhenius equation, they may be shaped into complicated artefacts (such as elastomer fusilli) by simply bending or twisting at 180 °C. The ENR composites with 20 phr carboxyl-functionalized carbon black sample is hot-pressed at 180 °C with no reduction in size. The mechanical properties of all the recycled samples have recovered to their original state. Incredibly, all recycled samples show a remarkable recovery to their original mechanical properties. The interfacial regulation technique provided in this study may bring new insights into the design of future sustainable vitrimers.

The sulphur and peroxide curing systems, which are the two most often utilised curing processes, have environmental issues in the rubber business. Additionally, when curing chemicals are heated, hazardous volatile organic compounds are released during the curing process. Due to the presence of amines and sulfur-containing organic molecules in volatile organic compounds, they emit an unpalatable odour (with very low odour thresholds).[220] To address the aforementioned severe problems, it is essential to conduct research into environmentally friendly and efficient rubber curing methods. Zhang *et al.*, provide a straightforward and ecologically acceptable approach for curing elastomeric vitrimer composites made from commercial ethylene-propylene-diene monomers.[127] The epoxy groups were inserted into ethylene-propylene-diene monomer chains *via* the use of in situ

epoxidation, which act as crosslinking sites. After that, biobased decanedioic acid were used to crosslink the epoxy-functionalized ethylene-propylene-diene monomer, forming exchangeable β-hydroxyl ester linkages. To enhance the superior mechanical performance, epoxy-functionalized ethylene-propylene-diene monomer was reinforced with carbon black in a simple and cost-effective manner with filler amounts up to 80 phr. At high temperatures (180–200 °C), the covalent crosslinking networks containing exchangeable β-hydroxyl ester groups can undergo network rearrangements through transesterification processes in the presence of 20 mol% zinc acetate catalyst. As the carbon black loading increased from 50 phr to 80 phr, the modulus of epoxy-functionalized ethylene-propylene-diene monomer/carbon black composites improves significantly from 2.4 to 4.5 ± 0.1 MPa, which could be ascribed to the hydrodynamic impact of CB and the increased constraint on chain mobility.

Tang *et al.*, reported covalently crosslinked but recyclable and mechanically robust elastomeric vitrimers by introducing carboxyl group-functionalized carbon nanodots into ENR to construct exchangeable β-hydroxyl ester linkages links into the ENR- carbon nanodots interface.[129] The prepared carbon nanodots crosslinked ENR have adjustable T_g values in the range of 10 to 50 °C and tensile strength in the range of 8.7 ± 0.8 to 38.9 ± 1.0 MPa. At elevated temperatures, the interface can undergo dynamic shuffling through transesterification processes, allowing the materials to be recycled, reshaped, and welded. Whilst the preferred breaking of the comparatively short rubber chains between adjacent carbon nanodot acts as an efficient energy dissipation mechanism that reinforces ENR. Furthermore, carbon nanodots crosslinked ENR samples can access reconfigurable/multiple shape memory rubbers capable of unrestricted programming of both permanent and temporary shapes.

Numerous photothermal moieties have been introduced into vitrimers to provide them with functional capabilities in order to confer the vitrimer with a photothermal effect.[221-223] Feng *et al.*, reported a vitrimer which is covalently crosslinked using ENR and dodecanedioic acid, that is self-healable, recyclable, and sensitive to pH and light by incorporating a small amount of aniline trimer.[128] High-temperature transesterification processes using $Zn(Ac)_2$ enable these ENR- dodecanedioic acid-aniline trimer vitrimers to relax stress through topological network rearrangements. The T_g values of the ENR- dodecanedioic acid-aniline trimer's ranged from -21.6 to -6.3 °C and rose with increasing crosslinking density. ENR-dodecanedioic acid-aniline trimer vitrimer could be recycled using thermal pressing at a pressure of 15 MPa for 20 min at 200 °C. After three cycles of recycling, the recycled samples preserved 88% of their pristine mechanical properties. While, incorporating aniline trimer into the vitrimer makes it photoresponsive as well as pH-responsive, allowing the vitrimer to self-heal under illumination. Furthermore, aniline trimer may speed up self-healing process by catalysing the transesterification reaction. The ENR-dodecanedioic acid-aniline trimer vitrimer could be employed as reconfigurable shape memory materials by heating at 200 °C which was above the T_v temperature, with a shape recovery and shape fixing ratio of over 95% during the reconfiguration process. The inclusion of aniline trimer causes the vitrimer to display light-induced multistage shape memory characteristics, which may pave the way for a broader use of ENR in the actuator area.

TER-based vitrimers need external catalysts to catalyse the curing and bond-exchanging processes, like most other vitrimers. There are several negative consequences of using catalysts, such as the toxicity of catalysts and the deterioration of recyclability due to leaching catalysts and the increased thermal degradation.[22, 45, 224] Sodium alginate is a nontoxic and

renewable natural polysaccharide obtained from sea algae. Sodium alginate has an abundance of carboxyl groups, which makes it a perfect multifunctional curing agent for ENR. Zhu *et al.*, employed sodium alginate and ENR to prepare a class of catalyst-free, strong, defect-tolerant, and tough elastomeric vitrimers with sodium alginate content ranging from 0 phr to 20 phr using an incredibly easy and eco-friendly latex assembly method (**Figure 1.13a**).[137] Throughout this process, the rubber chains diffuse between rubber particles and eventually unite to form a continuous matrix, while the sodium alginate molecules are more extruded to form the three-dimensional interconnected and segregated structure. Finally, the hybrid material exhibits a distinct microstructure that is composed of a segregated rigid phase of sodium alginate and a continuous soft phase of ENR. The vitrimers have a unique microscopic 3D segregated structure of sodium alginate in ENR matrix obtained by the evaporation-induced phase segregation. The segregated sodium alginate phase act as a reacting moiety for the esterification reactions between its carboxyl groups and the epoxy groups of ENR to form exchangeable β-hydroxyl ester bonds at the ENR-sodium alginate interface. It also provides an internal catalyst to activate both the esterification reactions and the transesterification reactions at elevated temperatures with the abundance of free hydroxyl groups on the backbone of sodium alginate molecules. Stress relaxation measurements indicate that increasing the sodium alginate loading slows down the relaxing rate, since greater sodium alginate loadings lead to increased crosslinking density, which required more exchanges for the topological rearrangement. The relaxation rate of the vitrimers significantly rises with temperature since the transesterification rate increases at higher temperatures. The E_a is determined to be 156.33 kJ mol^{-1} which is more than that reported by Leibler and coworkers[20, 45] (80 kJ mol^{-1}). This higher activation energy is due to

the high molecular weight of sodium

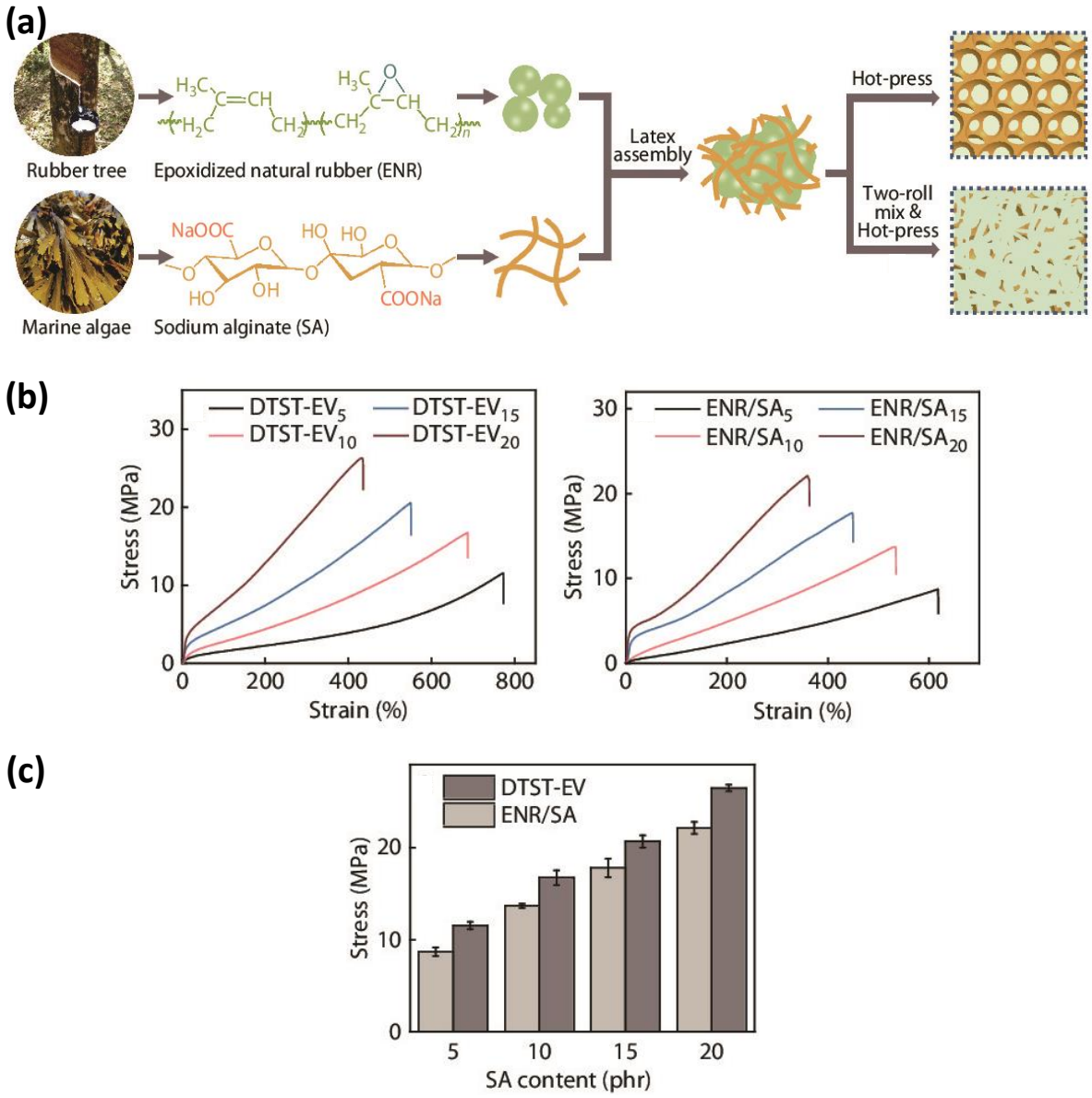

Figure 1.13: *Sodium alginate and ENR based elastomeric vitrimers, (a) vitrimer fabrication using ecologically friendly latex assembly method, (b) Stress-strain curves of vitrimers (DTST-EV$_x$ where x is the sodium alginate (SA) content ranging from 0 phr to 20 phr) and ENR/sodium alginate$_{10}$ (ENR/SA$_{10}$, containing 10 phr sodium alginate) with various sodium alginate contents and (c) ultimate strength between vitrimers (DTST-EV) and ENR/sodium alginate with*

increasing sodium alginate content. Reprinted (adapted) with permission from Ref, Copyright 2020, Springer Nature.[137]

alginate and the glycoside structures in its backbone, which causes steric hindrance resulting barrier raising to transesterification. Furthermore, the large E_a may also be due to the absence of an external catalyst.[127, 225-228] The tensile modulus and strength of vitrimers and ENR/sodium alginate improve considerably as the sodium alginate loading increases because the embedded sodium alginate acts as both a crosslinker and a reinforcer (**figure 1.13b**). The mechanical properties of vitrimers were superior to ENR/sodium alginate counterparts (**Figure 1.13c**), demonstrating that the microstructure also contributes significantly to the reinforcing effect.

Tong *et al.*, prepared vitrimers using ENR and oxidized starch with 57% carboxyl content as a crosslinker.[151] The dynamic β-hydroxyl ester bonds enhance the tensile strength, elongation at break, and enable reprocessing and shape memory abilities. α-amylase was used for rapidly degrading composite of 30 phr of oxidized starch with 57% carboxyl content in 100 phr of ENR to low-molecular-weight polysaccharide.

Conclusion and Prospects

The development of sustainable feedstocks for thermoset materials is critical for the environment. While the use of bio-based feedstocks is not a unique idea in the chemical industry, more needs to be done. The main aim of this review is to highlight the literature focussed on current developments in renewable-based transesterification vitrimers. The study of vitrimers has advanced significantly since the ground-breaking work of Leibler's team a decade ago. Preliminary findings from this review showed that vegetable oil and natural rubber have the highest potential as biobased feedstocks for vitrimers. Vegetable oils and

their derivatives, such as dimers of fatty acids, have already garnered considerable attention due to their widespread availability and low cost, as well as their diverse chemical structures, which allow for easy chemical modification to develop a range of multifunctional building blocks. Additionally, several readily accessible biobased materials, such as lignin, carbohydrates (e.g., starch, cellulose etc.) or furan derivatives, have been explored sparingly in the design of vitrimers, leaving much room for future advancements.

Challenges that need to be addressed in the future include the performance of biobased vitrimeric materials, management of raw ingredients and their production costs. A major challenge will be economy of scale for the manufacture of bio-based monomers and vitrimers from renewable resources. Transesterification vitrimers with a high T_g are as rare as their petroleum-based equivalents. Utilizing aromatic biomass, primarily lignin or lignin derivatives, is a technique for achieving T_g values greater than 100 °C, which is typical for thermosets but creates processability challenges. Thermal stability of biobased vitrimers also require that no secondary reaction occurs during the high-temperature exchange process. Research into the applications of transesterification exchange reactions in vitrimeric materials warrants the attention of chemists from diverse backgrounds. The development of high-specification engineering-grade biobased vitrimers will expedite further research into the area, which have previously been described at the lab scale. Building large-scale facilities can be challenging owing to a lack of prior experience with new technology and an inability to accurately predict the supply/demand relationship. To make transesterification vitrimeric technology commercially feasible, it is essential to create supply chain for biomass feedstocks, new synthetic routes by substituting current processes with high yields and efficient downstream processing procedures for the recovery of bio-based products. In particular, fully bio-based

vitrimers are very important. While we have highlighted many examples that utilise feedstocks partly sourced from sustainable approaches, it is very rare for all the feedstocks to be biobased/sustainable, without this approach there will still be a reliance on fossil fuel input.

Many additive-based chemical techniques have been developed to enhance the processing and performance of fossil fuel-based polymers, and these techniques can be used to create novel additive chemistry for bio-based transesterification vitrimers.[229] To increase the performance of biobased polymers such as PLA and PHA, additives are being produced by blending them with other polymers or creating new copolymers. But, the additive market for bio-based polymers is currently quite limited, making it more challenging to warrant substantial research efforts according to several big additive suppliers.

Fossil fuel-based polymers have traditionally used nanoparticle additions to improve their performance. Developing bio-based transesterification vitrimers in conjunction with nanofillers such as graphene, carbon nanotubes, cellulose nanowhiskers, 2-D layered materials and nanoclays could improve a variety of physical properties, including solvent absorption, thermal stability, barrier, flame resistance and biodegradation rate. Usually, these modifications are attained at low filler content, and this nano-reinforcement technique is a highly appealing way to develop novel functional biomaterials for wide applications.

In near future, these innovative and sustainable materials could be employed in conjunction with various microfabrication techniques, such as 3D/4D printing, as well as for demanding applications in the healthcare and energy industries. The development of biobased architectural components paves the way for the development of crosslinked biobased materials that exhibit thermoset-like properties at their operating temperature that can be easily molded, self-healed, and thermally or chemically recycled. Bio-based polymers are now

closer than ever to replacing conventional polymers. This is a huge step forward in the creation of high-performance materials with low environmental impact. As a result of these perspectives, transesterification vitrimer is seen as a key contributor for the future generation of polymeric materials. Consequently, the incorporation of renewable feedstocks for their synthesis is a crucial part to this transformation.

References

(1) Andrady, A. L.; Neal, M. A. Applications and societal benefits of plastics. *Philosophical Transactions of the Royal Society B: Biological Sciences* **2009**, *364*, 1977-1984.
(2) "Plastics use in 2019"; https://www.oecd-ilibrary.org/content/data/efff24eb-en (accessed: February 2023).
(3) "Plastics Europe 2020"; https://issuu.com/plasticseuropeebook/docs/plastics_the_facts-web-dec2020 (accessed: February 2023).
(4) Campanella, A.; Döhler, D.; Binder, W. H. Self-Healing in Supramolecular Polymers. *Macromolecular Rapid Communications* **2018**, *39*, 1700739.
(5) Herbst, F.; Döhler, D.; Michael, P.; Binder, W. H. Self-Healing Polymers via Supramolecular Forces. *Macromolecular Rapid Communications* **2013**, *34*, 203-220.
(6) Döhler, D.; Michael, P.; Binder, W. H. CuAAC-Based Click Chemistry in Self-Healing Polymers. *Accounts of Chemical Research* **2017**, *50*, 2610-2620.
(7) Supian, A. B. M.; Sapuan, S. M.; Zuhri, M. Y. M.; Zainudin, E. S.; Ya, H. H. Hybrid reinforced thermoset polymer composite in energy absorption tube application: A review. *Defence Technology* **2018**, *14*, 291-305.
(8) Soutis, C. Fibre reinforced composites in aircraft construction. *Progress in Aerospace Sciences* **2005**, *41*, 143-151.
(9) Lehn, J.-M. Dynamers: dynamic molecular and supramolecular polymers. *Progress in Polymer Science* **2005**, *30*, 814-831.
(10) Roy, N.; Bruchmann, B.; Lehn, J.-M. DYNAMERS: dynamic polymers as self-healing materials. *Chemical Society Reviews* **2015**, *44*, 3786-3807.
(11) Chen, X.; Dam, M. A.; Ono, K.; Mal, A.; Shen, H.; Nutt, S. R.; Sheran, K.; Wudl, F. A Thermally Re-mendable Cross-Linked Polymeric Material. *Science* **2002**, *295*, 1698-1702.
(12) Kloxin, C. J.; Scott, T. F.; Adzima, B. J.; Bowman, C. N. Covalent Adaptable Networks (CANs): A Unique Paradigm in Cross-Linked Polymers. *Macromolecules* **2010**, *43*, 2643-2653.
(13) Bowman, C. N.; Kloxin, C. J. Covalent Adaptable Networks: Reversible Bond Structures Incorporated in Polymer Networks. *Angewandte Chemie International Edition* **2012**, *51*, 4272-4274.
(14) Kloxin, C. J.; Bowman, C. N. Covalent adaptable networks: smart, reconfigurable and responsive network systems. *Chemical Society Reviews* **2013**, *42*, 7161-7173.
(15) Gandini, A. The furan/maleimide Diels–Alder reaction: A versatile click–unclick tool in macromolecular synthesis. *Progress in Polymer Science* **2013**, *38*, 1-29.

(16) Kaur, G.; Johnston, P.; Saito, K. Photo-reversible dimerisation reactions and their applications in polymeric systems. *Polymer Chemistry* **2014**, *5*, 2171-2186.
(17) Van Zee, N. J.; Nicolaÿ, R. Vitrimers: Permanently crosslinked polymers with dynamic network topology. *Progress in Polymer Science* **2020**, *104*, 101233.
(18) Denissen, W.; Winne, J. M.; Du Prez, F. E. Vitrimers: permanent organic networks with glass-like fluidity. *Chemical Science* **2016**, *7*, 30-38.
(19) Scott, T. F.; Schneider, A. D.; Cook, W. D.; Bowman, C. N. Photoinduced Plasticity in Cross-Linked Polymers. *Science* **2005**, *308*, 1615-1617.
(20) Montarnal, D.; Capelot, M.; Tournilhac, F.; Leibler, L. Silica-Like Malleable Materials from Permanent Organic Networks. *Science* **2011**, *334*, 965-968.
(21) Capelot, M.; Montarnal, D.; Tournilhac, F.; Leibler, L. Metal-Catalyzed Transesterification for Healing and Assembling of Thermosets. *Journal of the American Chemical Society* **2012**, *134*, 7664-7667.
(22) Brutman, J. P.; Delgado, P. A.; Hillmyer, M. A. Polylactide Vitrimers. *ACS Macro Letters* **2014**, *3*, 607-610.
(23) Altuna, F. I.; Pettarin, V.; Williams, R. J. J. Self-healable polymer networks based on the cross-linking of epoxidised soybean oil by an aqueous citric acid solution. *Green Chemistry* **2013**, *15*, 3360-3366.
(24) Pei, Z.; Yang, Y.; Chen, Q.; Terentjev, E. M.; Wei, Y.; Ji, Y. Mouldable liquid-crystalline elastomer actuators with exchangeable covalent bonds. *Nature Materials* **2014**, *13*, 36-41.
(25) Zhou, Y.; Goossens, J. G. P.; Sijbesma, R. P.; Heuts, J. P. A. Poly(butylene terephthalate)/Glycerol-based Vitrimers via Solid-State Polymerization. *Macromolecules* **2017**, *50*, 6742-6751.
(26) Han, J.; Liu, T.; Hao, C.; Zhang, S.; Guo, B.; Zhang, J. A Catalyst-Free Epoxy Vitrimer System Based on Multifunctional Hyperbranched Polymer. *Macromolecules* **2018**, *51*, 6789-6799.
(27) Ube, T.; Kawasaki, K.; Ikeda, T. Photomobile Liquid-Crystalline Elastomers with Rearrangeable Networks. *Advanced Materials* **2016**, *28*, 8212-8217.
(28) Fortman, D. J.; Brutman, J. P.; Cramer, C. J.; Hillmyer, M. A.; Dichtel, W. R. Mechanically Activated, Catalyst-Free Polyhydroxyurethane Vitrimers. *Journal of the American Chemical Society* **2015**, *137*, 14019-14022.
(29) Zheng, N.; Fang, Z.; Zou, W.; Zhao, Q.; Xie, T. Thermoset Shape-Memory Polyurethane with Intrinsic Plasticity Enabled by Transcarbamoylation. *Angewandte Chemie International Edition* **2016**, *55*, 11421-11425.
(30) Chen, X.; Li, L.; Jin, K.; Torkelson, J. M. Reprocessable polyhydroxyurethane networks exhibiting full property recovery and concurrent associative and dissociative dynamic chemistry via transcarbamoylation and reversible cyclic carbonate aminolysis. *Polymer Chemistry* **2017**, *8*, 6349-6355.
(31) He, C.; Shi, S.; Wang, D.; Helms, B. A.; Russell, T. P. Poly(oxime–ester) Vitrimers with Catalyst-Free Bond Exchange. *Journal of the American Chemical Society* **2019**, *141*, 13753-13757.
(32) Denissen, W.; Rivero, G.; Nicolaÿ, R.; Leibler, L.; Winne, J. M.; Du Prez, F. E. Vinylogous Urethane Vitrimers. *Advanced Functional Materials* **2015**, *25*, 2451-2457.
(33) Obadia, M. M.; Mudraboyina, B. P.; Serghei, A.; Montarnal, D.; Drockenmuller, E. Reprocessing and Recycling of Highly Cross-Linked Ion-Conducting Networks through Transalkylation Exchanges of C–N Bonds. *Journal of the American Chemical Society* **2015**, *137*, 6078-6083.

(34) Zheng, P.; McCarthy, T. J. A Surprise from 1954: Siloxane Equilibration Is a Simple, Robust, and Obvious Polymer Self-Healing Mechanism. *Journal of the American Chemical Society* **2012**, *134*, 2024-2027.
(35) Nishimura, Y.; Chung, J.; Muradyan, H.; Guan, Z. Silyl Ether as a Robust and Thermally Stable Dynamic Covalent Motif for Malleable Polymer Design. *Journal of the American Chemical Society* **2017**, *139*, 14881-14884.
(36) Stukenbroeker, T.; Wang, W.; Winne, J. M.; Du Prez, F. E.; Nicolaÿ, R.; Leibler, L. Polydimethylsiloxane quenchable vitrimers. *Polymer Chemistry* **2017**, *8*, 6590-6593.
(37) Li, L.; Chen, X.; Torkelson, J. M. Reprocessable Polymer Networks via Thiourethane Dynamic Chemistry: Recovery of Cross-link Density after Recycling and Proof-of-Principle Solvolysis Leading to Monomer Recovery. *Macromolecules* **2019**, *52*, 8207-8216.
(38) Fan, C.-J.; Wen, Z.-B.; Xu, Z.-Y.; Xiao, Y.; Wu, D.; Yang, K.-K.; Wang, Y.-Z. Adaptable Strategy to Fabricate Self-Healable and Reprocessable Poly(thiourethane-urethane) Elastomers via Reversible Thiol–Isocyanate Click Chemistry. *Macromolecules* **2020**, *53*, 4284-4293.
(39) Cacciapaglia, R.; Di Stefano, S.; Mandolini, L. Metathesis Reaction of Formaldehyde Acetals: An Easy Entry into the Dynamic Covalent Chemistry of Cyclophane Formation. *Journal of the American Chemical Society* **2005**, *127*, 13666-13671.
(40) Belowich, M. E.; Stoddart, J. F. Dynamic imine chemistry. *Chemical Society Reviews* **2012**, *41*, 2003-2024.
(41) Chao, A.; Negulescu, I.; Zhang, D. Dynamic Covalent Polymer Networks Based on Degenerative Imine Bond Exchange: Tuning the Malleability and Self-Healing Properties by Solvent. *Macromolecules* **2016**, *49*, 6277-6284.
(42) Hendriks, B.; Waelkens, J.; Winne, J. M.; Du Prez, F. E. Poly(thioether) Vitrimers via Transalkylation of Trialkylsulfonium Salts. *ACS Macro Letters* **2017**, *6*, 930-934.
(43) Otera, J. Transesterification. *Chemical Reviews* **1993**, *93*, 1449-1470.
(44) Fukuda, H.; Kondo, A.; Noda, H. Biodiesel fuel production by transesterification of oils. *Journal of Bioscience and Bioengineering* **2001**, *92*, 405-416.
(45) Capelot, M.; Unterlass, M. M.; Tournilhac, F.; Leibler, L. Catalytic control of the vitrimer glass transition. *ACS Macro Letters* **2012**, *1*, 789-792.
(46) Niu, X.; Wang, F.; Li, X.; Zhang, R.; Wu, Q.; Sun, P. Using Zn2+ Ionomer To Catalyze Transesterification Reaction in Epoxy Vitrimer. *Industrial & Engineering Chemistry Research* **2019**, *58*, 5698-5706.
(47) Demongeot, A.; Mougnier, S. J.; Okada, S.; Soulié-Ziakovic, C.; Tournilhac, F. Coordination and catalysis of Zn^{2+} in epoxy-based vitrimers. *Polymer Chemistry* **2016**, *7*, 4486-4493.
(48) Chen, J. H.; An, X. P.; Li, Y. D.; Wang, M.; Zeng, J. B. Reprocessible Epoxy Networks with Tunable Physical Properties: Synthesis, Stress Relaxation and Recyclability. *Chinese Journal of Polymer Science (English Edition)* **2018**, *36*, 641-648.
(49) Liu, Y.; Tang, Z.; Chen, Y.; Zhang, C.; Guo, B. Engineering of β-Hydroxyl Esters into Elastomer–Nanoparticle Interface toward Malleable, Robust, and Reprocessable Vitrimer Composites. *ACS Applied Materials & Interfaces* **2018**, *10*, 2992-3001.
(50) Yang, Z.; Wang, Q.; Wang, T. Dual-Triggered and Thermally Reconfigurable Shape Memory Graphene-Vitrimer Composites. *ACS Applied Materials & Interfaces* **2016**, *8*, 21691-21699.
(51) Yu, K.; Taynton, P.; Zhang, W.; Dunn, M. L.; Qi, H. J. Reprocessing and recycling of thermosetting polymers based on bond exchange reactions. *RSC Advances* **2014**, *4*, 10108-10117.

(52) Liu, T.; Zhao, B.; Zhang, J. Recent development of repairable, malleable and recyclable thermosetting polymers through dynamic transesterification. *Polymer* **2020**, *194*, 122392.
(53) Debnath, S.; Kaushal, S.; Ojha, U. Catalyst-Free Partially Bio-Based Polyester Vitrimers. *ACS Applied Polymer Materials* **2020**, *2*, 1006-1013.
(54) Whitcomb, D. C.; Lowe, M. E. Human Pancreatic Digestive Enzymes. *Digestive Diseases and Sciences* **2007**, *52*, 1-17.
(55) Kirby, A. J. Enzyme Mechanisms, Models, and Mimics. *Angewandte Chemie International Edition in English* **1996**, *35*, 706-724.
(56) Bakkali-Hassani, C.; Poutrel, Q.-A.; Langenbach, J.; Chappuis, S.; Blaker, J. J.; Gresil, M.; Tournilhac, F. Lipase-Catalyzed Epoxy–Acid Addition and Transesterification: from Model Molecule Studies to Network Build-Up. *Biomacromolecules* **2021**, *22*, 4544-4551.
(57) Breslow, R. Biomimetic Chemistry and Artificial Enzymes - Catalysis by Design. *Accounts of Chemical Research* **1995**, *28*, 146-153.
(58) Cram, D. J.; Katz, H. E.; Dicker, I. B. Host Guest Complexation .31. A Transacylase Partial Mimic. *Journal of the American Chemical Society* **1984**, *106*, 4987-5000.
(59) Cram, D. J.; Cram, J. M. *Container Molecules and Their Guests*; 1994.
(60) Lücking, U.; Tucci, F. C.; Rudkevich, D. M.; Rebek, J. Self-Folding Cavitands of Nanoscale Dimensions. *Journal of the American Chemical Society* **2000**, *122*, 8880-8889.
(61) Schiff, H. Mittheilungen aus dem Universitätslaboratorium in Pisa: Eine neue Reihe organischer Basen. *Justus Liebigs Annalen der Chemie* **1864**, *131*, 118-119.
(62) Kumar, A.; Connal, L. A. Biobased Transesterification Vitrimers. *Macromolecular Rapid Communications* 2200892.
(63) Tremblay-Parrado, K.-K.; García-Astrain, C.; Avérous, L. Click chemistry for the synthesis of biobased polymers and networks derived from vegetable oils. *Green Chemistry* **2021**, *23*, 4296-4327.
(64) Biermann, U.; Bornscheuer, U.; Meier, M. A.; Metzger, J. O.; Schäfer, H. J. Oils and fats as renewable raw materials in chemistry. *Angewandte Chemie International Edition* **2011**, *50*, 3854-3871.
(65) Van de Vyver, S.; Geboers, J.; Jacobs, P. A.; Sels, B. F. Recent Advances in the Catalytic Conversion of Cellulose. *ChemCatChem* **2011**, *3*, 82-94.
(66) Rinaldi, R.; Schüth, F. Design of solid catalysts for the conversion of biomass. *Energy & Environmental Science* **2009**, *2*, 610-626.
(67) Painter, P. C.; Coleman, M. M. *Essentials of polymer science and engineering*; DEStech Publications, Inc, 2008.
(68) Comba, M. B.; Tsai, Y.-h.; Sarotti, A. M.; Mangione, M. I.; Suárez, A. G.; Spanevello, R. A. Levoglucosenone and Its New Applications: Valorization of Cellulose Residues. *European Journal of Organic Chemistry* **2018**, *2018*, 590-604.
(69) Savaliya, M. L.; Dhorajiya, B. D.; Dholakiya, B. Z. Current Trends in Separation and Purification of Fatty Acid Methyl Ester. *Separation & Purification Reviews* **2015**, *44*, 28-40.
(70) Amass, W.; Amass, A.; Tighe, B. A review of biodegradable polymers: uses, current developments in the synthesis and characterization of biodegradable polyesters, blends of biodegradable polymers and recent advances in biodegradation studies. *Polymer International* **1998**, *47* , 89-144.
(71) Williams, C. K. Synthesis of functionalized biodegradable polyesters. *Chemical Society Reviews* **2007**, *36*, 1573-1580.

(72) Yang, J.; Webb, A. R.; Ameer, G. A. Novel Citric Acid-Based Biodegradable Elastomers for Tissue Engineering. *Advanced Materials* **2004**, *16*, 511-516.
(73) Borejsza-Wysocki, W.; Hrazdina, G. Biosynthesis of p-hydroxyphenylbutan-2-one in raspberry fruits and tissue cultures. *Phytochemistry* **1994**, *35*, 623-628.
(74) Belgacem, M. N.; Gandini, A. *Monomers, Polymers and Composites from Renewable Resources*; Elsevier Science & Technology, 2008.
(75) Gandini, A. The irruption of polymers from renewable resources on the scene of macromolecular science and technology. *Green Chemistry* **2011**, *13*, 1061-1083.
(76) Mathers, R. T. How well can renewable resources mimic commodity monomers and polymers. *Journal of Polymer Science Part A: Polymer Chemistry* **2012**, *50*, 1-15.
(77) Wilbon, P. A.; Chu, F.; Tang, C. Progress in Renewable Polymers from Natural Terpenes, Terpenoids, and Rosin. *Macromolecular Rapid Communications* **2013**, *34*, 8-37.
(78) Ragauskas, A. J.; Williams, C. K.; Davison, B. H.; Britovsek, G.; Cairney, J.; Eckert, C. A.; Frederick, W. J.; Hallett, J. P.; Leak, D. J.; Liotta, C. L.; et al. The Path Forward for Biofuels and Biomaterials. *Science* **2006**, *311*, 484-489.
(79) Dodds, D. R.; Gross, R. A. Chemicals from Biomass. *Science* **2007**, *318*, 1250-1251.
(80) Biobased Building Blocks and Polymers—Global Capacities, Production and Trends, 2018–2023. *Industrial Biotechnology* **2019**, *15*, 237-241.
(81) *"European Bioplastics. Bioplastics - informations", 2016 https://www.european-bioplastics.org/marketdata-update-2016/ (accessed: March 2022).*
(82) Mohanty, A.; Misra, M. a.; Hinrichsen, G. Biofibres, biodegradable polymers and biocomposites: An overview. *Macromolecular materials and Engineering* **2000**, *276*, 1-24.
(83) Vink, E. T. H.; Rábago, K. R.; Glassner, D. A.; Springs, B.; O'Connor, R. P.; Kolstad, J.; Gruber, P. R. The Sustainability of NatureWorks™ Polylactide Polymers and Ingeo™ Polylactide Fibers: an Update of the Future. *Macromolecular Bioscience* **2004**, *4*, 551-564.
(84) Shiota, A.; Ober, C. K. Rigid rod and liquid crystalline thermosets. *Progress in Polymer Science* **1997**, *22*, 975-1000.
(85) Raquez, J. M.; Deléglise, M.; Lacrampe, M. F.; Krawczak, P. Thermosetting (bio)materials derived from renewable resources: A critical review. *Progress in Polymer Science* **2010**, *35*, 487-509.
(86) Rutz, B. H.; Berg, J. C. A review of the feasibility of lightening structural polymeric composites with voids without compromising mechanical properties. *Advances in Colloid and Interface Science* **2010**, *160*, 56-75.
(87) Kaiser, T. Highly crosslinked polymers. *Progress in Polymer Science* **1989**, *14*, 373-450.
(88) Tsangouri, E.; Aggelis, D.; Van Hemelrijck, D. Quantifying thermoset polymers healing efficiency: A systematic review of mechanical testing. *Progress in Polymer Science* **2015**, *49-50*, 154-174.
(89) Urdl, K.; Kandelbauer, A.; Kern, W.; Müller, U.; Thebault, M.; Zikulnig-Rusch, E. Self-healing of densely crosslinked thermoset polymers—a critical review. *Progress in Organic Coatings* **2017**, *104*, 232-249.
(90) Azcune, I.; Odriozola, I. Aromatic disulfide crosslinks in polymer systems: Self-healing, reprocessability, recyclability and more. *European Polymer Journal* **2016**, *84*, 147-160.
(91) Zhang, P.; Li, G. Advances in healing-on-demand polymers and polymer composites. *Progress in Polymer Science.* **2016**, *57*, 32-63.
(92) Kumar, S.; Samal, S. K.; Mohanty, S.; Nayak, S. K. Recent Development of Biobased Epoxy Resins: A Review. *Polymer-Plastics Technology and Engineering* **2018**, *57*, 133-155.

(93) Veith, C.; Diot-Néant, F.; Miller, S. A.; Allais, F. Synthesis and polymerization of bio-based acrylates: a review. *Polymer Chemistry* **2020**, *11*, 7452-7470.
(94) Ma, S.; Li, T.; Liu, X.; Zhu, J. Research progress on bio-based thermosetting resins. *Polymer International* **2016**, *65*, 164-173.
(95) Li, Q.; Ma, S.; Xu, X.; Zhu, J. Chapter 20 - Bio-based Unsaturated Polyesters. In *Unsaturated Polyester Resins*, Thomas, S., Hosur, M., Chirayil, C. J. Eds.; Elsevier, 2019; pp 515-555.
(96) Gonçalves, F. A. M. M.; Santos, M.; Cernadas, T.; Ferreira, P.; Alves, P. Advances in the development of biobased epoxy resins: insight into more sustainable materials and future applications. *International Materials Reviews* **2022**, *67*, 119-149.
(97) Lyu, Y.; Ishida, H. Natural-sourced benzoxazine resins, homopolymers, blends and composites: A review of their synthesis, manufacturing and applications. *Progress in Polymer Science* **2019**, *99*, 101168.
(98) Ilia, G.; Simulescu, V.; Mak, C. A.; Crasmareanu, E. The Use of Transesterification Method for Obtaining Phosphorus-Containing Polymers. *Advances in Polymer Technology* **2014**, *33*.
(99) Ganguly, A.; Channe, P.; Jha, R.; Mitra, S.; Saha, S. Review on transesterification in polycarbonate–poly(butylene terephthalate) blend. *Polymer Engineering & Science* **2021**, *61*, 650-661.
(100) Guerre, M.; Taplan, C.; Winne, J. M.; Du Prez, F. E. Vitrimers: directing chemical reactivity to control material properties. *Chemical Science* **2020**, *11*, 4855-4870.
(101) Zheng, J.; Png, Z. M.; Ng, S. H.; Tham, G. X.; Ye, E.; Goh, S. S.; Loh, X. J.; Li, Z. Vitrimers: Current research trends and their emerging applications. *Materials Today* **2021**, *51*, 586-625.
(102) Schenk, V.; Labastie, K.; Destarac, M.; Olivier, P.; Guerre, M. Vitrimer composites: current status and future challenges. *Materials Advances* **2022**, *3*, 8012-8029.
(103) Lucherelli, M. A.; Duval, A.; Avérous, L. Biobased vitrimers: Towards sustainable and adaptable performing polymer materials. *Progress in Polymer Science* **2022**, *127*, 101515.
(104) Rana, S.; Solanki, M.; Sahoo, N. G.; Krishnakumar, B. Bio-Vitrimers for Sustainable Circular Bio-Economy. *Polymers* **2022**, *14*, 4338.
(105) Vidil, T.; Llevot, A. Fully Biobased Vitrimers: Future Direction toward Sustainable Cross-Linked Polymers. *Macromolecular Chemistry and Physics* **2022**, *223*, 2100494.
(106) Biermann, U.; Bornscheuer, U.; Meier, M. A. R.; Metzger, J. O.; Schäfer, H. J. Oils and Fats as Renewable Raw Materials in Chemistry. *Angewandte Chemie International Edition* **2011**, *50*, 3854-3871.
(107) Biermann, U.; Friedt, W.; Lang, S.; Lühs, W.; Machmüller, G.; Metzger, J. O.; Rüsch gen. Klaas, M.; Schäfer, H. J.; Schneider, M. P. New syntheses with oils and fats as renewable raw materials for the chemical industry. *Angewandte Chemie International Edition* **2000**, *39*, 2206-2224.
(108) Biermann, U.; Butte, W.; Eren, T.; Haase, D.; Metzger, J. O. Regio- and Stereoselective Diels–Alder Additions of Maleic Anhydride to Conjugated Triene Fatty Acid Methyl Esters. *European Journal of Organic Chemistry* **2007**, *2007*, 3859-3862.
(109) Ding, C.; Matharu, A. S. Recent Developments on Biobased Curing Agents: A Review of Their Preparation and Use. *ACS Sustainable Chemistry & Engineering* **2014**, *2*, 2217-2236.
(110) Gandini, A.; Lacerda, T. M.; Carvalho, A. J. F.; Trovatti, E. Progress of Polymers from Renewable Resources: Furans, Vegetable Oils, and Polysaccharides. *Chemical Reviews* **2016**, *116*, 1637-1669.

(111) Mustapha, R.; Rahmat, A. R.; Abdul Majid, R.; Mustapha, S. N. H. Vegetable oil-based epoxy resins and their composites with bio-based hardener: a short review. *Polymer-Plastics Technology and Materials* **2019**, *58*, 1311-1326.
(112) Meier, M. A. R.; Metzger, J. O.; Schubert, U. S. Plant oil renewable resources as green alternatives in polymer science. *Chemical Society Reviews.* **2007**, *36*, 1788-1802.
(113) Novaes, E.; Kirst, M.; Chiang, V.; Winter-Sederoff, H.; Sederoff, R. Lignin and biomass: a negative correlation for wood formation and lignin content in trees. *Plant Physiol* **2010**, *154*, 555-561.
(114) Laurichesse, S.; Avérous, L. Chemical modification of lignins: Towards biobased polymers. *Progress in Polymer Science* **2014**, *39*, 1266-1290.
(115) Duval, A.; Lawoko, M. A review on lignin-based polymeric, micro- and nano-structured materials. *Reactive and Functional Polymers* **2014**, *85*, 78-96.
(116) Upton, B. M.; Kasko, A. M. Strategies for the Conversion of Lignin to High-Value Polymeric Materials: Review and Perspective. *Chemical Reviews* **2016**, *116*, 2275-2306.
(117) Painter, P. C.; Coleman, M. M. *Essentials of Polymer Science and Engineering*; DEStech Publications, 2008.
(118) El Fray, M.; Skrobot, J.; Bolikal, D.; Kohn, J. Synthesis and characterization of telechelic macromers containing fatty acid derivatives. *Reactive and Functional Polymers* **2012**, *72*, 781-790.
(119) Ogunniyi, D. S. Castor oil: A vital industrial raw material. *Bioresource Technology* **2006**, *97*, 1086-1091.
(120) Sarkar, P.; Bhowmick, A. K. Sustainable rubbers and rubber additives. *Journal of Applied Polymer Science* **2018**, *135*, 45701.
(121) Liu, T.; Hao, C.; Wang, L.; Li, Y.; Liu, W.; Xin, J.; Zhang, J. Eugenol-Derived Biobased Epoxy: Shape Memory, Repairing, and Recyclability. *Macromolecules* **2017**, *50*, 8588-8597.
(122) Altuna, F. I.; Hoppe, C. E.; Williams, R. J. J. Shape memory epoxy vitrimers based on DGEBA crosslinked with dicarboxylic acids and their blends with citric acid. *RSC Advances* **2016**, *6*, 88647-88655.
(123) Liu, T.; Hao, C.; Zhang, S.; Yang, X.; Wang, L.; Han, J.; Li, Y.; Xin, J.; Zhang, J. A Self-Healable High Glass Transition Temperature Bioepoxy Material Based on Vitrimer Chemistry. *Macromolecules* **2018**, *51*, 5577-5585.
(124) Zhang, S.; Liu, T.; Hao, C.; Wang, L.; Han, J.; Liu, H.; Zhang, J. Preparation of a lignin-based vitrimer material and its potential use for recoverable adhesives. *Green Chemistry* **2018**, *20*, 2995-3000.
(125) Lossada, F.; Guo, J.; Jiao, D.; Groeer, S.; Bourgeat-Lami, E.; Montarnal, D.; Walther, A. Vitrimer Chemistry Meets Cellulose Nanofibrils: Bioinspired Nanopapers with High Water Resistance and Strong Adhesion. *Biomacromolecules* **2019**, *20*, 1045-1055.
(126) Zhao, S.; Abu-Omar, M. M. Catechol-Mediated Glycidylation toward Epoxy Vitrimers/Polymers with Tunable Properties. *Macromolecules* **2019**, *52*, 3646-3654.
(127) Zhang, G.; Zhou, X.; Liang, K.; Guo, B.; Li, X.; Wang, Z.; Zhang, L. Mechanically Robust and Recyclable EPDM Rubber Composites by a Green Cross-Linking Strategy. *ACS Sustainable Chemistry & Engineering* **2019**, *7*, 11712-11720.
(128) Feng, Z.; Hu, J.; Zuo, H.; Ning, N.; Zhang, L.; Yu, B.; Tian, M. Photothermal-Induced Self-Healable and Reconfigurable Shape Memory Bio-Based Elastomer with Recyclable Ability. *ACS Applied Materials & Interfaces* **2019**, *11*, 1469-1479.

(129) Tang, Z.; Liu, Y.; Guo, B.; Zhang, L. Malleable, Mechanically Strong, and Adaptive Elastomers Enabled by Interfacial Exchangeable Bonds. *Macromolecules* **2017**, *50*, 7584-7592.
(130) Yang, X.; Guo, L.; Xu, X.; Shang, S.; Liu, H. A fully bio-based epoxy vitrimer: Self-healing, triple-shape memory and reprocessing triggered by dynamic covalent bond exchange. *Materials & Design* **2020**, *186*, 108248.
(131) Tao, Y.; Fang, L.; Dai, M.; Wang, C.; Sun, J.; Fang, Q. Sustainable alternative to bisphenol A epoxy resin: high-performance recyclable epoxy vitrimers derived from protocatechuic acid. *Polymer Chemistry* **2020**, *11*, 4500-4506.
(132) Wu, J.; Yu, X.; Zhang, H.; Guo, J.; Hu, J.; Li, M.-H. Fully Biobased Vitrimers from Glycyrrhizic Acid and Soybean Oil for Self-Healing, Shape Memory, Weldable, and Recyclable Materials. *ACS Sustainable Chemistry & Engineering* **2020**, *8*, 6479-6487.
(133) Jouyandeh, M.; Tikhani, F.; Hampp, N.; Akbarzadeh Yazdi, D.; Zarrintaj, P.; Reza Ganjali, M.; Reza Saeb, M. Highly curable self-healing vitrimer-like cellulose-modified halloysite nanotube/epoxy nanocomposite coatings. *Chemical Engineering Journal* **2020**, *396*, 125196.
(134) Guo, Z.; Wang, W.; Liu, Z.; Xue, Y.; Zheng, H.; Majeed, K.; Zhang, B.; Zhou, F.; Zhang, Q. Preparation of carbon nanotube-vitrimer composites based on double dynamic covalent bonds: Electrical conductivity, reprocessability, degradability and photo-welding. *Polymer* **2021**, *235*, 124280.
(135) Xu, C.; Cui, R.; Fu, L.; Lin, B. Recyclable and heat-healable epoxidized natural rubber/bentonite composites. *Composites Science and Technology* **2018**, *167*, 421-430.
(136) Qiu, M.; Wu, S.; Fang, S.; Tang, Z.; Guo, B. Sustainable, recyclable and robust elastomers enabled by exchangeable interfacial cross-linking. *Journal of Materials Chemistry A* **2018**, *6*, 13607-13612.
(137) Zhu, Y.; Gao, J.-L.; Zhang, L.-J.; Peng, Y.; Wang, H.; Ling, F.-W.; Huang, G.-S.; Wu, J.-R. An Interfacial Dynamic Crosslinking Approach toward Catalyst-free and Mechanically Robust Elastomeric Vitrimer with a Segregated Structure. *Chinese Journal of Polymer Science* **2021**, *39*, 201-210.
(138) Li, Y.; Liu, T.; Zhang, S.; Shao, L.; Fei, M.; Yu, H.; Zhang, J. Catalyst-free vitrimer elastomers based on a dimer acid: robust mechanical performance, adaptability and hydrothermal recyclability. *Green Chemistry* **2020**, *22*, 870-881.
(139) Mu, S.; Zhang, Y.; Zhou, J.; Wang, B.; Wang, Z. Recyclable and Mechanically Robust Palm Oil-Derived Epoxy Resins with Reconfigurable Shape-Memory Properties. *ACS Sustainable Chemistry & Engineering* **2020**, *8*, 5296-5304.
(140) Di Mauro, C.; Malburet, S.; Graillot, A.; Mija, A. Recyclable, Repairable, and Reshapable (3R) Thermoset Materials with Shape Memory Properties from Bio-Based Epoxidized Vegetable Oils. *ACS Applied Bio Materials* **2020**, *3*, 8094-8104.
(141) Capiel, G.; Hernández, E.; Marcovich, N. E.; Mosiewicki, M. A. Stress relaxation behavior of weldable crosslinked polymers based on methacrylated oleic and lauric acids. *European Polymer Journal* **2020**, *132*, 109740.
(142) Wang, S.; Teng, N.; Dai, J.; Liu, J.; Cao, L.; Zhao, W.; Liu, X. Taking advantages of intramolecular hydrogen bonding to prepare mechanically robust and catalyst-free vitrimer. *Polymer* **2020**, *210*, 123004.
(143) Xu, Y.; Dai, S.; Bi, L.; Jiang, J.; Zhang, H.; Chen, Y. Catalyst-Free Self-Healing Bio-Based Polymers: Robust Mechanical Properties, Shape Memory, and Recyclability. *Journal of Agricultural and Food Chemistry* **2021**, *69*, 9338-9349.

(144) Tang, R.; Xue, B.; Tan, J.; Guan, Y.; Wen, J.; Li, X.; Zhao, W. Regulating Lignin-Based Epoxy Vitrimer Performance by Fine-Tuning the Lignin Structure. *ACS Applied Polymer Materials* **2022**, *4*, 1117-1125.
(145) Wu, P.; Liu, L.; Wu, Z. A transesterification-based epoxy vitrimer synthesis enabled high crack self-healing efficiency to fibrous composites. *Composites Part A: Applied Science and Manufacturing* **2022**, *162*, 107170.
(146) Li, W.; Xiao, L.; Huang, J.; Wang, Y.; Nie, X.; Chen, J. Bio-based epoxy vitrimer for recyclable and carbon fiber reinforced materials: Synthesis and structure-property relationship. *Composites Science and Technology* **2022**, *227*, 109575.
(147) Xu, Y.; Zhang, H.; Dai, S.; Xu, S.; Wang, J.; Bi, L.; Jiang, J.; Chen, Y. Hyperbranched polyester catalyzed self-healing bio-based vitrimer for closed-loop recyclable carbon fiber-reinforced polymers. *Composites Science and Technology* **2022**, *228*, 109676.
(148) Xu, Y.; Dai, S.; Bi, L.; Jiang, J.; Zhang, H.; Chen, Y. Catalyst-free self-healing bio-based vitrimer for a recyclable, reprocessable, and self-adhered carbon fiber reinforced composite. *Chemical Engineering Journal* **2022**, *429*, 132518.
(149) Zhong, L.; Hao, Y.; Zhang, J.; Wei, F.; Li, T.; Miao, M.; Zhang, D. Closed-Loop Recyclable Fully Bio-Based Epoxy Vitrimers from Ferulic Acid-Derived Hyperbranched Epoxy Resin. *Macromolecules* **2022**, *55*, 595-607.
(150) Kölsch, J. C.; Berač, C. M.; Lossada, F.; Stach, O. S.; Seiffert, S.; Walther, A.; Besenius, P. Recyclable Vitrimers from Biogenic Poly(itaconate) Elastomers. *Macromolecules* **2022**.
(151) Tong, H.; Chen, Y.; Weng, Y.; Zhang, S. Biodegradable-Renewable Vitrimer Fabrication by Epoxidized Natural Rubber and Oxidized Starch with Robust Ductility and Elastic Recovery. *ACS Sustainable Chemistry & Engineering* **2022**, *10*, 7942-7953.
(152) Li, J.; Zhang, S.; Ju, B. Soft, fully bio-based poly-hydroxyl thermosets based on catalyst-free transesterification with decent re-processability. *Journal of Applied Polymer Science* **2022**, *139*, e52676.
(153) Auvergne, R.; Caillol, S.; David, G.; Boutevin, B.; Pascault, J.-P. Biobased Thermosetting Epoxy: Present and Future. *Chemical Reviews* **2014**, *114*, 1082-1115.
(154) Wool, R.; Sun, X. S.; Sun, X. S.; Books24x, I. *Bio-Based Polymers and Composites*; Elsevier Science & Technology, 2005.
(155) Huang, X.; Liu, H.; Shang, S.; Rao, X.; Song, J. Preparation and Characterization of Polymeric Surfactants Based on Epoxidized Soybean Oil Grafted Hydroxyethyl Cellulose. *Journal of Agricultural and Food Chemistry* **2015**, *63*, 9062-9068.
(156) Ratna, D. Mechanical properties and morphology of epoxidized soyabean-oil-modified epoxy resin. *Polymer International* **2001**, *50*, 179-184.
(157) Boquillon, N.; Fringant, C. Polymer networks derived from curing of epoxidised linseed oil: influence of different catalysts and anhydride hardeners. *Polymer* **2000**, *41*, 8603-8613.
(158) Miyagawa, H.; Mohanty, A. K.; Misra, M.; Drzal, L. T. Thermo-Physical and Impact Properties of Epoxy Containing Epoxidized Linseed Oil, *Macromolecular Materials and Engineering* **2004**, *289*, 629-635.
(159) Papagianni, M. Advances in citric acid fermentation by Aspergillus niger: Biochemical aspects, membrane transport and modeling. *Biotechnology Advances* **2007**, *25*, 244-263.
(160) Ploeger, B.; Mensinga, T.; Sips, A.; Seinen, W.; Meulenbelt, J.; DeJongh, J. The pharmacokinetics of glycyrrhizic acid evaluated by physiologically based pharmacokinetic modelling. *Drug Metabolism Reviews* **2001**, *33*, 125-147.

(161) Kornievskaya, V. S.; Kruppa, A. I.; Leshina, T. V. NMR and photo-CIDNP investigations of the glycyrrhizinic acid micelles influence on solubilized molecules. *Journal of Inclusion Phenomena and Macrocyclic Chemistry* **2008**, *60*, 123-130.
(162) Tykarska, E.; Sobiak, S.; Gdaniec, M. Supramolecular Organization of Neutral and Ionic Forms of Pharmaceutically Relevant Glycyrrhizic Acid—Amphiphile Self-Assembly and Inclusion of Small Drug Molecules. *Crystal Growth & Design* **2012**, *12*, 2133-2137.
(163) Han, S.; Sun, L.; He, F.; Che, H. Anti-allergic activity of glycyrrhizic acid on IgE-mediated allergic reaction by regulation of allergy-related immune cells. *Scientific Reports* **2017**, *7*, 7222.
(164) Shree Meenakshi, K.; Pradeep Jaya Sudhan, E. Development of novel TGDDM epoxy nanocomposites for aerospace and high performance applications – Study of their thermal and electrical behavior. *Arabian Journal of Chemistry* **2016**, *9*, 79-85.
(165) Hassan, N.; Idris, A.; Akhtar, J. Overview on bio-refinery concept in Malaysia: Potential high value-added products from palm oil biomass. *Jurnal Kejuruteraan* **2019**, *2*, 113-124.
(166) Mauck, S. C.; Wang, S.; Ding, W.; Rohde, B. J.; Fortune, C. K.; Yang, G.; Ahn, S.-K.; Robertson, M. L. Biorenewable tough blends of polylactide and acrylated epoxidized soybean oil compatibilized by a polylactide star polymer. *Macromolecules* **2016**, *49*, 1605-1615.
(167) Fu, L.; Yang, L.; Dai, C.; Zhao, C.; Ma, L. Thermal and mechanical properties of acrylated expoxidized-soybean oil-based thermosets. *Journal of Applied Polymer Science* **2010**, *117*, 2220-2225.
(168) Zhang, C.; Yan, M.; Cochran, E. W.; Kessler, M. R. Biorenewable polymers based on acrylated epoxidized soybean oil and methacrylated vanillin. *Materials Today Communications* **2015**, *5*, 18-22.
(169) Li, Q.; Huang, X.; Liu, H.; Shang, S.; Song, Z.; Song, J. Properties enhancement of room temperature vulcanized silicone rubber by rosin modified aminopropyltriethoxysilane as a cross-linking agent. *ACS Sustainable Chemistry & Engineering* **2017**, *5*, 10002-10010.
(170) Zhang, L.; Jiang, Y.; Xiong, Z.; Liu, X.; Na, H.; Zhang, R.; Zhu, J. Highly recoverable rosin-based shape memory polyurethanes. *Journal of Materials Chemistry A* **2013**, *1*, 3263-3267.
(171) Wang, B.; Ma, S.; Yan, S.; Zhu, J. Readily recyclable carbon fiber reinforced composites based on degradable thermosets: a review. *Green Chemistry* **2019**, *21*, 5781-5796.
(172) Xin, J.; Li, M.; Li, R.; Wolcott, M. P.; Zhang, J. Green Epoxy Resin System Based on Lignin and Tung Oil and Its Application in Epoxy Asphalt. *ACS Sustainable Chemistry & Engineering* **2016**, *4*, 2754-2761.
(173) Zhang, W.; Ma, Y.; Wang, C.; Li, S.; Zhang, M.; Chu, F. Preparation and properties of lignin–phenol–formaldehyde resins based on different biorefinery residues of agricultural biomass. *Industrial Crops and Products* **2013**, *43*, 326-333.
(174) Ma, R.; Xu, Y.; Zhang, X. Catalytic Oxidation of Biorefinery Lignin to Value-added Chemicals to Support Sustainable Biofuel Production. *ChemSusChem* **2015**, *8*, 24-51.
(175) Rounsaville, J.; Rice, R. G. Evolution of ozone for the bleaching of paper pulps. *Ozone: Science & Engineering* **1996**, *18*, 549-566.
(176) Yang, Y.; Urban, M. W. Self-healing polymeric materials. *Chemical Society Reviews* **2013**, *42*, 7446-7467.
(177) Liu, W.; Fang, C.; Chen, F.; Qiu, X. Strong, Reusable, and Self-Healing Lignin-Containing Polyurea Adhesives. *ChemSusChem* **2020**, *13*, 4691-4701.
(178) Zhao, S.; Abu-Omar, M. M. Materials Based on Technical Bulk Lignin. *ACS Sustainable Chemistry & Engineering* **2021**, *9*, 1477-1493.

(179) Yue, L.; Amirkhosravi, M.; Gong, X.; Gray, T. G.; Manas-Zloczower, I. Recycling Epoxy by Vitrimerization: Influence of an Initial Thermoset Chemical Structure. *ACS Sustainable Chemistry & Engineering* **2020**, *8*, 12706-12712.
(180) Hayashi, M.; Katayama, A. Preparation of Colorless, Highly Transparent, Epoxy-Based Vitrimers by the Thiol-Epoxy Click Reaction and Evaluation of Their Shape-Memory Properties. *ACS Applied Polymer Materials* **2020**, *2*, 2452-2457.
(181) Hajj, R.; Duval, A.; Dhers, S.; Avérous, L. Network Design to Control Polyimine Vitrimer Properties: Physical Versus Chemical Approach. *Macromolecules* **2020**, *53*, 3796-3805.
(182) Ricarte, R. G.; Tournilhac, F.; Cloître, M.; Leibler, L. Linear Viscoelasticity and Flow of Self-Assembled Vitrimers: The Case of a Polyethylene/Dioxaborolane System. *Macromolecules* **2020**, *53*, 1852-1866.
(183) Chakma, P.; Morley, C. N.; Sparks, J. L.; Konkolewicz, D. Exploring How Vitrimer-like Properties Can Be Achieved from Dissociative Exchange in Anilinium Salts. *Macromolecules* **2020**, *53*, 1233-1244.
(184) Tran, T. N.; Rawstron, E.; Bourgeat-Lami, E.; Montarnal, D. Formation of Cross-Linked Films from Immiscible Precursors through Sintering of Vitrimer Nanoparticles. *ACS Macro Letters* **2018**, *7*, 376-380.
(185) Du, M.; Guo, B.; Jia, D. Newly emerging applications of halloysite nanotubes: a review. *Polymer International* **2010**, *59*, 574-582.
(186) Saif, M. J.; Asif, M.; Naveed, M.; Zia, K. M.; Uz-Zaman, W.; Khosa, M. K.; Jamal, M. A. Halloysite reinforced epoxy composites with improved mechanical properties. *Polish Journal of Chemical Technology* **2016**, *18*.
(187) Jouyandeh, M.; Karami, Z.; Jazani, O. M.; Formela, K.; Paran, S. M. R.; Jannesari, A.; Saeb, M. R. Curing epoxy resin with anhydride in the presence of halloysite nanotubes: The contradictory effects of filler concentration. *Progress in Organic Coatings* **2019**, *126*, 129-135.
(188) Servatan, M.; Ghadiri, M.; Damanabi, A. T.; Bahadori, F.; Zarrintaj, P.; Ahmadi, Z.; Vahabi, H.; Saeb, M. R. Zeolite-based catalysts for exergy efficiency enhancement: the insights gained from nanotechnology. *Materials Today: Proceedings* **2018**, *5*, 15868-15876.
(189) Prashantha, K.; Lacrampe, M.-F.; Krawczak, P. Processing and characterization of halloysite nanotubes filled polypropylene nanocomposites based on a masterbatch route: effect of halloysites treatment on structural and mechanical properties. *Express Polymer Letters* **2011**, *5,*295-307.
(190) Auras, R.; Harte, B.; Selke, S. An Overview of Polylactides as Packaging Materials. *Macromolecular Bioscience* **2004**, *4*, 835-864.
(191) Liu, H.; Zhang, J. Research progress in toughening modification of poly(lactic acid). *Journal of Polymer Science Part B: Polymer Physics* **2011**, *49*, 1051-1083.
(192) R. A. Auras, L.-T. L., S. E. Selke, H. Tsuji. *Poly (lactic acid): synthesis, structures, properties, processing, and applications*; John Wiley & Sons, 2011.
(193) Okamura-Abe, Y.; Abe, T.; Nishimura, K.; Kawata, Y.; Sato-Izawa, K.; Otsuka, Y.; Nakamura, M.; Kajita, S.; Masai, E.; Sonoki, T.; et al. Beta-ketoadipic acid and muconolactone production from a lignin-related aromatic compound through the protocatechuate 3,4-metabolic pathway. *Journal of Bioscience and Bioengineering* **2016**, *121*, 652-658.
(194) Turner, W. A.; Hartman, A. M. The non-volatile organic acids of alfalfa. *Journal of the American Chemical Society* **1925**, *47*, 2044-2047.
(195) Nelson, E.; Hasselbring, H. Some organic acids of wheat plants. *Journal of the American Chemical Society* **1931**, *53*, 1040-1043.

(196) Chen, J.; Liu, P.; Sun, D.; Zhang, D.; Miao, B.; Chen, J. Riverine Sediment Geochemistry as Provenance Fingerprints along the Eastern Coast of China: Constraint, Approach, and Application. *Minerals* **2020**, *10*, 29.
(197) Jabłoński, M.; Kaczmarek, A.; Sadlej, A. J. Estimates of the Energy of Intramolecular Hydrogen Bonds. *The Journal of Physical Chemistry A* **2006**, *110*, 10890-10898.
(198) Tang, J.; Zhang, Z.; Song, Z.; Chen, L.; Hou, X.; Yao, K. Synthesis and characterization of elastic aliphatic polyesters from sebacic acid, glycol and glycerol. *European Polymer Journal* **2006**, *42*, 3360-3366.
(199) Chen, Q.; Yu, X.; Pei, Z.; Yang, Y.; Wei, Y.; Ji, Y. Multi-stimuli responsive and multi-functional oligoaniline-modified vitrimers. *Chemical Science* **2017**, *8*, 724-733.
(200) Liu, X.; Yang, X.; Wang, S.; Wang, S.; Wang, Z.; Liu, S.; Xu, X.; Liu, H.; Song, Z. Fully bio-based polyhydroxyurethanes with a dynamic network from a terpene derivative and cyclic carbonate functional soybean oil. *ACS Sustainable Chemistry & Engineering* **2021**, *9*, 4175-4184.
(201) Zhu, S.; Xu, S.; Yi, X.; Wang, J.; Zhao, Z.; Jiang, J. High value-added application of turpentine as a potential renewable source for the synthesis of heterocyclic Schiff base derivatives of cis-1, 8-p-menthane-diamine serving as botanical herbicides. *Industrial Crops and Products* **2018**, *115*, 111-116.
(202) Mancuso, C.; Santangelo, R. Ferulic acid: pharmacological and toxicological aspects. *Food and Chemical Toxicology* **2014**, *65*, 185-195.
(203) Baup, S. Ueber eine neue Pyrogen-Citronensäure, und über Benennung der Pyrogen-Säuren überhaupt. *Annalen der Pharmacie* **1836**, *19*, 29-38.
(204) Shou, T.; Hu, S.; Wu, Y.; Tang, X.; Fu, G.; Zhao, X.; Zhang, L. Biobased and Recyclable Polyurethane for Room-Temperature Damping and Three-Dimensional Printing. *ACS Omega* **2021**, *6*, 30003-30011.
(205) Si, G.; Qi, M.; Tan, C.; Chen, C. Tandem Catalysts Combining Polymer Synthesis, Postpolymerization Modification, and Vitrimer Formation. *Macromolecules* **2021**, *54*, 6153-6160.
(206) Bai, J.; Li, H.; Shi, Z.; Yin, J. An Eco-Friendly Scheme for the Cross-Linked Polybutadiene Elastomer via Thiol–Ene and Diels–Alder Click Chemistry. *Macromolecules* **2015**, *48*, 3539-3546.
(207) An, S. Y.; Noh, S. M.; Oh, J. K. Multiblock Copolymer-Based Dual Dynamic Disulfide and Supramolecular Crosslinked Self-Healing Networks. *Macromolecular Rapid Communications* **2017**, *38*, 1600777.
(208) Cash, J. J.; Kubo, T.; Bapat, A. P.; Sumerlin, B. S. Room-Temperature Self-Healing Polymers Based on Dynamic-Covalent Boronic Esters. *Macromolecules* **2015**, *48*, 2098-2106.
(209) Zhang, Z. P.; Rong, M. Z.; Zhang, M. Q. Polymer engineering based on reversible covalent chemistry: A promising innovative pathway towards new materials and new functionalities. *Progress in Polymer Science* **2018**, *80*, 39-93.
(210) Hernández, M.; Grande, A. M.; Dierkes, W.; Bijleveld, J.; van der Zwaag, S.; García, S. J. Turning Vulcanized Natural Rubber into a Self-Healing Polymer: Effect of the Disulfide/Polysulfide Ratio. *ACS Sustainable Chemistry & Engineering* **2016**, *4*, 5776-5784.
(211) Pepels, M.; Filot, I.; Klumperman, B.; Goossens, H. Self-healing systems based on disulfide–thiol exchange reactions. *Polymer Chemistry* **2013**, *4*, 4955-4965.
(212) Yang, X.; Guo, Y.; Luo, X.; Zheng, N.; Ma, T.; Tan, J.; Li, C.; Zhang, Q.; Gu, J. Self-healing, recoverable epoxy elastomers and their composites with desirable thermal conductivities by

incorporating BN fillers via in-situ polymerization. *Composites Science and Technology* **2018**, *164*, 59-64.
(213) Lei, Z. Q.; Xie, P.; Rong, M. Z.; Zhang, M. Q. Catalyst-free dynamic exchange of aromatic Schiff base bonds and its application to self-healing and remolding of crosslinked polymers. *Journal of Materials Chemistry A* **2015**, *3*, 19662-19668.
(214) Kuang, X.; Liu, G.; Dong, X.; Liu, X.; Xu, J.; Wang, D. Facile fabrication of fast recyclable and multiple self-healing epoxy materials through diels-alder adduct cross-linker. *Journal of Polymer Science Part A: Polymer Chemistry* **2015**, *53*, 2094-2103.
(215) Rahman, M. A.; Sartore, L.; Bignotti, F.; Di Landro, L. Autonomic Self-Healing in Epoxidized Natural Rubber. *ACS Applied Materials & Interfaces* **2013**, *5*, 1494-1502.
(216) Mokhtari, M.; Schipper, D. J.; Tolpekina, T. V. On the Friction of Carbon Black- and Silica-Reinforced BR and S-SBR Elastomers. *Tribology Letters* **2014**, *54*, 297-308.
(217) Rigbi, Z. Reinforcement of rubber by carbon black. Berlin, Heidelberg, 1980; Springer Berlin Heidelberg: pp 21-68.
(218) Yu, Z. W.; Liu, Y. Combination of DSC and X-ray Diffraction in the Study of the Phase Behavior of Lipids: Mini-review. *Journal of Thermal Analysis and Calorimetry* **1999**, *58*, 363-368.
(219) Jeerupun, J.; Wootthikanokkhan, J.; Phinyocheep, P. Effects of Epoxidation Content of ENR on Morphology and Mechanical Properties of Natural Rubber Blended PVC. *Macromolecular Symposia* **2004**, *216*, 281-292.
(220) Liang, K.; Zhang, G.; Zhao, J.; Shi, L.; Cheng, J.; Zhang, J. Malleable, Recyclable, and Robust Poly(amide–imine) Vitrimers Prepared through a Green Polymerization Process. *ACS Sustainable Chemistry & Engineering* **2021**, *9*, 5673-5683.
(221) Reisinger, D.; Kaiser, S.; Rossegger, E.; Alabiso, W.; Rieger, B.; Schlögl, S. Introduction of Photolatent Bases for Locally Controlling Dynamic Exchange Reactions in Thermo-Activated Vitrimers. *Angewandte Chemie International Edition* **2021**, *60*, 14302-14306.
(222) Wang, S.; Wang, H.; Zhang, P.; Xue, L.; Chen, J.; Cui, J. Folding fluorescent probes for self-reporting transesterification in dynamic polymer networks. *Materials Horizons* **2021**, *8*, 1481-1487.
(223) Salaeh, S.; Das, A.; Wießner, S.; Stapor, M. Vitrimer-like material based on a biorenewable elastomer crosslinked with a dimeric fatty acid. *European Polymer Journal* **2021**, *151*, 110452.
(224) Argyle, M. D.; Bartholomew, C. H. Heterogeneous catalyst deactivation and regeneration: a review. *Catalysts* **2015**, *5*, 145-269.
(225) Qiu, M.; Wu, S.; Tang, Z.; Guo, B. Exchangeable interfacial crosslinks towards mechanically robust elastomer/carbon nanotubes vitrimers. *Composites Science and Technology* **2018**, *165*, 24-30.
(226) Liu, W.; Schmidt, D. F.; Reynaud, E. Catalyst Selection, Creep, and Stress Relaxation in High-Performance Epoxy Vitrimers. *Industrial & Engineering Chemistry Research* **2017**, *56*, 2667-2672.
(227) Demongeot, A.; Groote, R.; Goossens, H.; Hoeks, T.; Tournilhac, F.; Leibler, L. Cross-Linking of Poly(butylene terephthalate) by Reactive Extrusion Using Zn(II) Epoxy-Vitrimer Chemistry. *Macromolecules* **2017**, *50*, 6117-6127.
(228) Long, R.; Qi, H. J.; Dunn, M. L. Modeling the mechanics of covalently adaptable polymer networks with temperature-dependent bond exchange reactions. *Soft Matter* **2013**, *9*, 4083-4096.

(229) Sinha Ray, S.; Bousmina, M. Biodegradable polymers and their layered silicate nanocomposites: In greening the 21st century materials world. *Progress in Materials Science* **2005**, *50*, 962-1079.

Australian National University

Statement of Contribution

This thesis is submitted as a Thesis by Compilation in accordance with https://policies.anu.edu.au/ppl/document/ANUP_003405

I declare that the research presented in this Thesis represents original work that I carried out during my candidature at the Australian National University, except for contributions to multi-author papers incorporated in the Thesis where my contributions are specified in this Statement of Contribution.

Title: Simple synthetic route to an enzyme-inspired transesterification catalyst

Authors: **Ashwani Kumar**, Mitchell D. Nothling, Heather M. Aitken, Zeyun Xiao, Matthew Lam, Craig A. Bell, Megan L. O'Mara and Luke A. Connal

Publication outlet (Journal): Catalysis Science & Technology

Current status of paper: Published (*Catal. Sci. Technol.* 2022, 12, 6655-6659.)

Contribution to paper: My contribution to the manuscript includes design of purification protocols, characterization, catalytic assays, and data analysis as well as preparing and revising manuscript and figures (overall 75%).

Senior author or collaborating authors endorsement:

ASHWANI KUMAR	Ashwani	2nd March 2023
Candidate – Print Name	Signature	Date

Endorsed

LUKE CONNAL		14th March 2023
Primary Supervisor – Print Name	Signature	Date
Mark Humphrey		15th March 2023
Delegated Authority – Print Name	Signature	Date

Chapter 2 Simple synthetic route to an enzyme-inspired transesterification catalyst

Kumar, A.; Nothling, M. D.; Aitken, H. M.; Xiao, Z.; Lam, M.; Bell, C. A.; O'Mara, M. L.; Connal, L. A. *Catal. Sci. Technol.,* **2022**, *12*, 6655-6659.

Preface

This chapter outlines the design and fabrication of an organocatalyst for the dynamic transesterification chemical reaction. This chapter was published in Oct 2022 edition of the journal *Catalysis Science & Technology*,[1] in which I am the first author. My contribution to the manuscript includes the design of purification protocols, characterization, catalytic assays, and data analysis, as well as preparing and revising the manuscript and figures (overall 75%). The published version of the manuscript is presented here. Dr. Mitchell D. Nothling conducted the synthesis and catalytic assays, while Dr. Heather M. Aitken did the molecular dynamics; both are former PhD students in the Connal lab. Dr. Zeyun Xiao assisted in project designing, Matthew Lam did the catalytic assay, and Craig A. Bell, collaborator at the University of Queensland, carried out the Dynamic Light Scattering (DLS) measurements.

Foreword

This thesis is focused on developing dynamic chemistry. Catalysis to promote dynamic chemistry is an important and fundamental approach. One of the most powerful classes of catalysts are enzymes. In this chapter, I focus on an enzyme inspired approach to create a transesterification catalyst. Catalysts play a significant role in thermosets based on dynamic transesterification chemical reaction. Several chemical and biological catalysts are used, with each having intrinsic benefits and drawbacks. Most of the catalysts are prepared using

complex, multistep, protecting group synthetic procedures and require extreme reaction conditions for activation. Considering all of these obstacles, in this chapter I designed a catalyst for the transesterification chemical reaction using a simple modular synthetic technique. The catalysts design was motivated by the natural lipase enzyme. Lipases are the enzymes with the widest range of biocatalytic applications.[2-7] The Lipase enzyme consists of the well-known serine-histidine-aspartate architecture, known as the catalytic triad. In this chapter, the transesterification ability of an organocatalyst termed as artificial catalytic triad (ACT) is investigated. The ACT was prepared by integrating three catalytic triad residues (histidine, serine, and aspartate) onto a surfactant-type molecule, analogous to the native chymotrypsin enzyme. The catalytic potential of the ACT was evaluated at room temperature using the model reaction of vinyl trifluoroacetate (VTFA) with methanol. The catalyst shows high catalytic efficiency, with rate acceleration (k_{cat}/k_{unc}) of 4.81 × 10^4-fold over the background reaction.

Introduction

The structure, mechanism and complexity of natural enzymes offers unique insight for the development of new synthetic catalysts. These blueprints have led to the development of new synthetic catalysts,[8] yet relatively few efforts have achieved organocatalysts which mimic the high efficiency of enzymes.[8] Led by the ground breaking work of Breslow,[9] Cram,[10, 11] Rebek[12] and their colleagues, artificial enzymes or enzyme mimics are a class of molecules that provide catalysis inspired by aspects of enzymes.

Hydrolases are an important family of industrially relevant enzymes that catalyse the degradation of a range of ester and amide molecules. Different hydrolase enzyme families with specific biochemical functions have been formulated by nature, including proteases,

lipases, nucleases, and amylases.[13] Many hydrolases facilitate catalysis with a similar catalytic active site to that of the well-researched serine protease, α-chymotrypsin. Lipases are an important biocatalyst due to their excellent biochemical and physiological properties, employed for kinetic resolution of racemic alcohols, esters, acids or amines,[14] desymmetrization of prochiral compounds,[15, 16] or in conjunction with the esterification or transesterification of polyfunctional compounds.[17-20] One of the most promising applications is the preparation of biodiesel through the transesterification reaction.[20] A small functional region, the active site, is at the centre of the lipase protein structure, which facilitates transesterification. The active site of the chymotrypsin- is comprised of hydrophobic pocket encompassing, histidine, aspartate and serine residues known as the 'catalytic triad'.[21, 22] H-bonding interactions between nearby complimentary residues and substrate intermediates, during catalysis, result in a decrease in the activation energy of the catalytic system.[23, 24] The precisely designed combination of specific chemical interactions between the three residues in the enzyme results in unparalleled rate enhancement.[25] The incorporation of similar chemical functionalities as this active site is a major goal for researchers to develop simple, small molecule models for enzyme mimics. Recently, we have developed new techniques to mimic this active site, creating solid supported and micellar catalysts for the hydrolysis of ester bonds.[26-28]

Transesterification refers to the class of chemical reaction in which an ester is converted into another *via* alkoxy exchange. In industrial environments, this is achieved by heating a mixture of anhydrous esters and alcohols to very high temperatures or by using alkali alkylates or alkali metals or at lower temperatures. Lipases have shown to be active in transesterification reactions.[20, 29-33] However, there are pitfalls to using biocatalysts, including expensive reagents

and the instability of enzymes in organic solvents. Organocatalysts for transesterification between vinyl trifluoroacetate (VTFA) and methanol, have been reported.[34-36] However the downfalls in these approaches are the multistep low yielding protecting group chemistry to the final catalyst. At least two stages of a protection/deprotection process involve the expenditure of excessive chemicals and increases waste disposal, often leading to a reduction in the total yield. A highly efficient strategy that is industrially practical must be economical and high yielding. It should be feasible to achieve these paths by applying high yielding simple modular protection free chemistry. Herein, our approach for organocatalyst construction is simple high yielding modular synthetic procedure without any protecting groups. We have developed a highly efficient (k_{cat}/K_m) catalyst with significant rate acceleration through an artificial catalytic triad (ACT) comprised of a hydroxyl to act as a nucleophile, imidazole residue as a base, carboxylate group as an acid and the C-8 alkyl chain to address solubility in the non-aqueous environment, leading to transition state stabilization for transesterification reactions between VTFA and methanol. To recreate the architecture of enzymes, we engineered the three members of the triad onto a single molecule, culminating in a surfactant type-molecule with a functional catalytic triad headgroup that assemble into a cluster in organic solvent. In addition, motivated by the native enzyme hydrophobic binding pocket, these ACT surfactant clusters are important in fostering the ACT in catalysis by binding the substrate through H-bonding between the functional head group of ACT surfactants.

We demonstrate, with experiment and computation the efficacy of this surfactant enzyme mimic to catalyse the transesterification of VTFA with methanol. Furthermore, the unique activity of the catalytic triad highlights the interdependence of three functional groups, analogous to native enzymes.

Results and Discussion

We developed, a simple synthetic strategy to afford an organocatalyst synthesis *via* two-step reductive amination without the need for protecting groups resulting in a surfactant molecule, with an ACT as a head group (**Figure 2.1a and Scheme S2.1**).[27] This simple synthesis leads to a trifunctional bioinspired molecule (ACT), with each of the three catalytic triad groups arranged in close vicinity on a single molecule. This highly functional molecule has a OH- nucleophile from the serine, an imidazole as a base, a carboxylic acid and a C-8 alkyl chain to improve the solubility in a non-aqueous environment (**Figure 2.1a**). Dyad compounds as control structures were also prepared (Imz-COOH and OH-COOH), which lack one of the triad groups and were examined to understand the role of each catalytic group.

Next, the catalyst was then evaluated for transesterification of VTFA with methanol (**Figure 2.1c**). Transesterification reaction is seamlessly carried out by native lipases and has mechanistic resemblances to natural reactions of esterolysis and proteolysis.[37-40] Encouraged by the favourable findings obtained by Ema *et al.*, VTFA was selected as a desirable substrate for this study.[36] Surprisingly, with a low loading of ACT surfactant (5 mol%) with VTFA in dry *d*-chloroform/methanol, the acyl transfer reaction was too rapid to be detected using ^{1}H-NMR, with complete conversion in less than 3 minutes. We then investigated lower ACT loading (1 mol%) and managed to track the advancement of reaction through emergence of a methyl proton peak corresponding to product methyl trifluoroacetate (δ = 3.91 ppm) with the concomitant decrease of vinyl proton peak (δ = 7.19, 5.16, 4.87 ppm) (**Figure 2.2a**). The reactions were conducted in triplicate showing exemplary reproducibility and the computed relative standard error for velocity measurements were consistently lower than 4% for all

catalyst loadings after 3 minutes of reaction time. The transformation of VTFA to methyl

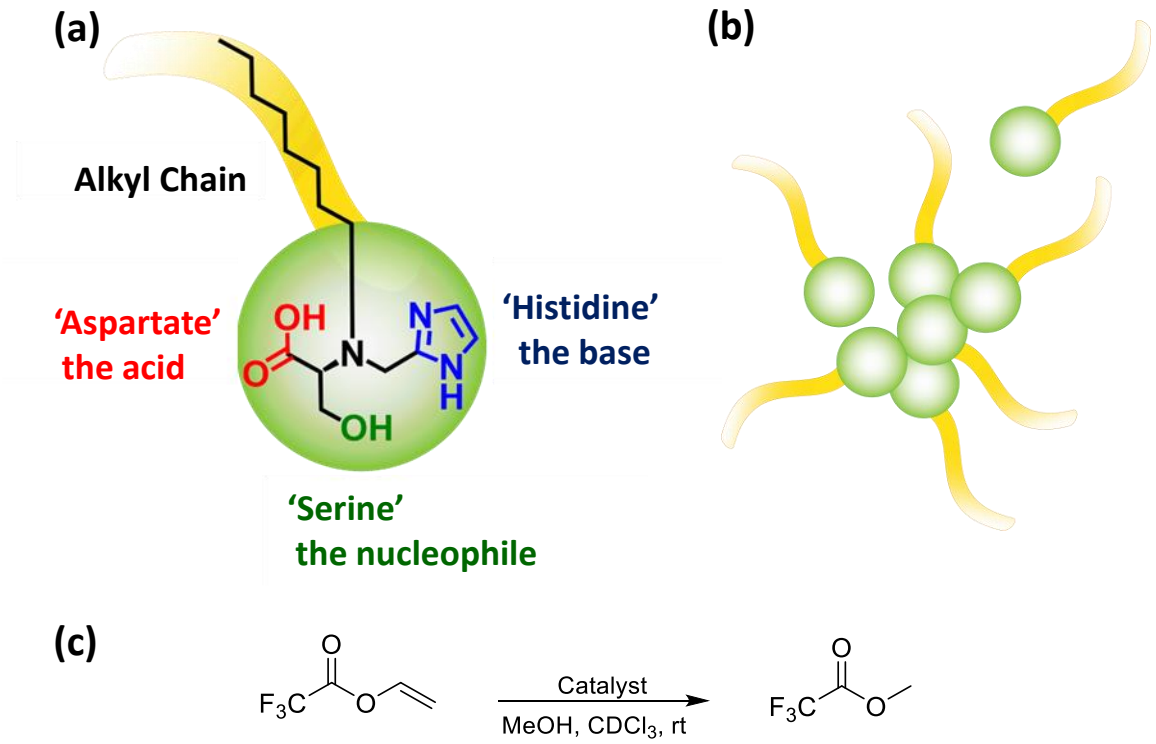

***Figure 2.1**: Native enzyme inspired catalyst, (a) model of our ACT surfactant highlighting the tri-functional headgroup, (b) complex of ACT surfactant molecules formed through H-bonding between all three functional groups (carboxylic acid, hydroxyl, and imidazole) of the ACT, (c) model transesterification reaction used to assess the ACT surfactant.*

trifluoroacetate catalysed by the ACT surfactant was complete in 1 hour at the conditions studied, with ^{19}F NMR confirming an approximate stoichiometric conversion to the ester product with a peak shift (**Figure S2.6**). Trace generation of trifluoroacetic acid (TFA) is noticed with longer reaction duration, owing to hydrolysis by residual water present in organic solvent. Compared to the transesterification reaction, the competitive hydrolysis reaction is unfavourable, thus relatively little TFA for the early reaction time is observed and becomes more pronounced at subsequent time periods (up to 10% mol after 12 hours).

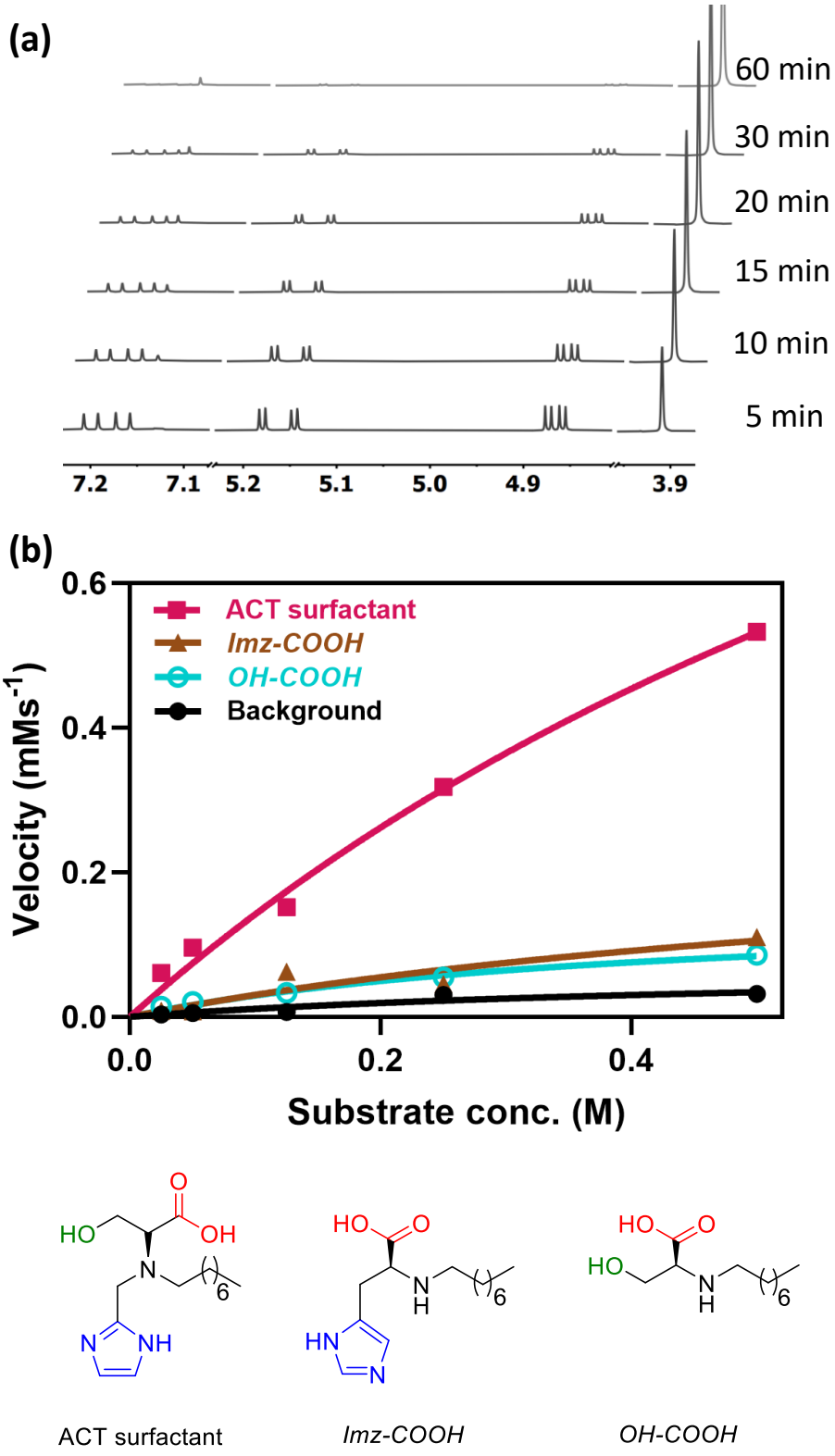

***Figure 2.2**: ACT surfactant catalysed transesterification of VTFA with methanol, (a) 400 MHz ^{1}H NMR spectra of a mixture of ACT surfactant (1 mol%), VTFA (0.05 M) and methanol (2 M)*

in d-chloroform. A reduction in the vinyl proton peaks associated with VTFA coincides with the appearance of a methyl proton peak associated with methyl trifluoroacetate (the displayed intensity of the 4.85 – 5.20 ppm region has been amplified 3-fold to allow a clearer representation of the vinyl peaks). (b) Michaelis-Menten plot for the initial 'burst' phase reaction rates (after 3 minutes) of the catalysed (■) and uncatalyzed (●) reactions. k_{cat} *= 3.302* s^{-1}*,* k_{uncat} *= 6.86 x* 10^{-5} s^{-1}*. (ACT loading 0.5 mM, reaction velocity taken as the tangent to the product concentration vs. time profile after 3 minutes mixing time).*

To assess the reaction kinetics, different catalyst loadings were investigated (0.1 – 2 mol%, [VTFA] = 0.025 – 0.5 M), and the initial reaction velocities were compared to the uncatalyzed system. As an example, representative kinetic profiles of ACT surfactant using ^{1}H NMR and the corresponding fits to obtain initial velocity were shown in (**Figures S2.7—S2.11**). We used short durations of 5 and 10 min to capture the initial rate of the reaction during the burst phase (**Figure S2.7—S2.11**). The very small negative value (close to zero) of the y intercept observed in the **Figure S2.7—S2.9 and Figure S2.11** is a result of the extremely rapid nature of the reaction. When the reaction velocities were fitted with a Michaelis-Menten function, the ACT surfactant has a remarkable turnover number (k_{cat}) of 3.3 s^{-1}. These results show a high turnover number for a small enzyme-mimic molecule catalysing a transesterification reaction. Background transesterification lacking catalyst was minimal during the time intervals investigated, with a reaction rate k_{uncat} of 6.86 x 10^{-5} s computed for the first order, uncatalyzed process. The rate acceleration ascribed to ACT surfactant is thus ~48,000-fold that of the uncatalyzed reaction with a high turnover of 3.3 s^{-1}. We then investigated the effect of removing a functional group from the artificial triad. The dyad control structures Imz-COOH and OH-COOH showed inappreciable acceleration under the same reaction conditions (**Figure**

2.2b and Table S2.1). These results highlight the necessity of all three ACT surfactant functional groups to maximise catalysis. Furthermore, the crystal structure of the ACT surfactant shows the distance between the carboxyl (O) and imidazolyl (N) of the ACT was measured at 2.72 Å, which is relatively short and is approaching the separation of these groups in the native enzyme (2.64 Å).[27, 41] In this way, the catalyst mimics both synthetic and natural enzymes.[42-45]

Molecular dynamics (MD) simulations were used to study the self-assembly of the ACT surfactant in chloroform as we suspected that hydrogen bonding of the catalytic head groups along with the non-polar tail may cause inverse micellar complexation, to form a catalytic pocket. We further suspected that the additional methanol used for solubility of the ACT would influence self-assembly, therefore a pre-equilibrated 90/10 chloroform/methanol explicit solvent environment was used. Over the course of all three 500 ns replicate simulations, clusters between 2 and – 6 ACT-surfactant molecules in size were observed (**Figure 2.3**). Analysis was performed on data collected every 0.1 ns over the course of all three 500 ns replicates. On average 11 clusters were present throughout the simulation with an average size of 3 molecules, calculated by computing the size distribution of molecular clusters with a cut-off of 3.5 nm (the end-to-end distance of a single linear chained ACT surfactant molecule). These complexes were governed by interactions between head groups of the catalyst molecules. To further characterise these complexes, we analysed the number of hydrogen bonds formed by the ACT surfactant and methanol, defined as the number of contacts between hydrogen bond donors and acceptors that were within 3.5 Å and an angular cut-off of 30°. These ACT surfactant clusters were observed to be strengthened by complexation with MeOH (**Figure 2.3b**). Approximately 19% of all MeOH molecules in solution

exhibited H-bonding contacts over the course of the 500 ns trajectory. Similar to native enzymes, the ACT surfactant catalyst form cluster through H-bonding and hydrophobic interactions, to enable complexation of the VTFA molecule inside a catalytic pocket (**Figure 2.3a (inset)**). MD revealed that H bonding interactions adhere ACT surfactants in cluster fashion. Furthermore, the aggregation behavior was investigated using DLS and ^{1}H NMR.[46] According to DLS, no micelles were formed, however clusters of a few ACT surfactants could have formed as indicated by the MD simulations. The apparent hydrodynamic diameters (d_{app}) of clusters were less than 1 nm (**Figure S2.12—S2.14**). ^{1}H NMR measurements of ACT surfactants in methanol/chloroform solution were carried out by varying the methanol content (**Figure S2.15**). The results show that signal of H from imidazole shifts to an upfield position from 8.01 to 7.91 ppm upon increase in methanol content from 8 to 24%. This peak shift indicates an increase in electron density on imidazole protons which could be attributed to ACT surfactant-methanol interactions when methanol content increases.

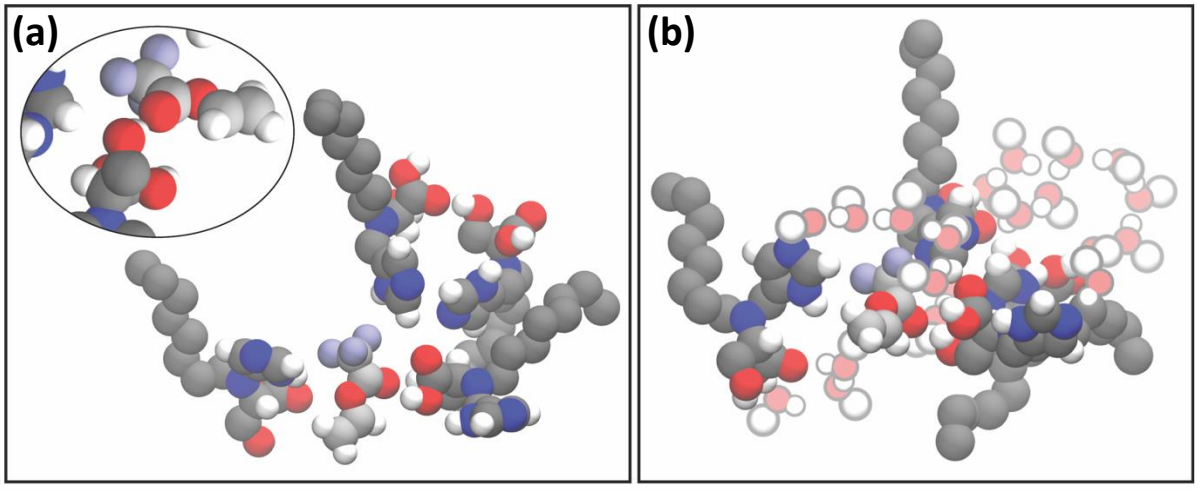

***Figure 2.3**: Hydrogen bonding both between the catalytic head groups, and between the headgroups and methanol stabilize cluster formation and complexation with VTFA. MD of catalysis, (a) complex with the substrate, inset highlights an inter-molecular hydroxyl-carbonyl*

hydrogen bond between VTFA and serine moiety of ACT surfactant. (b) the same complex shown in (a) with methanol residues within 5 Å of the complex.

Conclusion

In summary, we report a modular, protection group free synthetic approach *via* a two-step reductive amination to afford a bioinspired trifunctional organocatalyst. The catalyst forms cluster in organic solvents and facilitates the transesterification of a model VTFA ester substrate. The catalyst shows ~48,000-fold acceleration over the background reaction using methanol at room temperature. Michaelis—Menten fit to the reaction profiles gives a high turnover number (k_{cat}) of 3.3 s^{-1} for the ACT surfactant. Dyad control structures, Imz-COOH and OH-COOH reveals the importance of all three functional groups in accelerating the reaction. Moreover, MD simulations further support the harmony between the three functional head groups, which highlights the resemblance of the ACT surfactant to a native enzymatic reaction.

Supporting Information

Experimental

All commercially obtained solvents and reagents were used without further purification. L-serine(99%), sodium hydroxide(97%), anhydrous methanol(99.8%), 1H-imidazole-2-carbaldehyde(97%), Sodium borohydride(99%), glacial acetic acid(99%), *n*-octan-1-ol(99%), dichloromethane(99.8%), pyridinium dichromate(98%), diethyl ether(99%), hexane, ethyl acetate(99.5%), Sodium triacetoxyborohydride(97%), acetonitrile(99.9%), *L*-histidine(99%), hydrochloric acid 37% and 1-Octanal(99%) were all purchased from the Sigma Aldrich. Analytical thin-layer chromatography (TLC) was carried out on Merck silica gel 60 F254 glass plates and flash chromatography (FC) was performed on Merck silica gel 60 (70 - 230 mesh).

Visualization was achieved using short-wave UV light and/or $KMnO_4$ staining solution, followed by mild heating. Surfactants were purified by preparative reverse-phase high performance liquid chromatography (RP-HPLC) on a Biotage SP-1 HPFC Flash Purification System using a reverse-phase Biotage SNAP Cartridge (KP-C18-HS, 60 g).

^{1}H, ^{13}C and ^{19}F solution-state NMR were recorded on a Varian Unity Inova 500 (500 MHz for ^{1}H and 125 MHz for ^{13}C) or a Varian Unity Inova AS600 (600 MHz for ^{1}H and 150 MHz for ^{13}C) or a Varian INOVA 400 (400 MHz for ^{1}H and 376 MHz for ^{19}F) spectrometers. Chemical shifts δ are reported relative to the resonance signal of ^{1}H or ^{13}C cores of tetramethylsilane and in ppm. The ^{1}H spectra were calibrated by setting the solvent peaks, caused by remaining traces of protons, to values known from the literature ($\delta CHCl_3$ = 7.26 ppm, δCD_3OH = 4.87 ppm, δD_2O = 4.79 ppm). The ^{13}C spectra were calibrated by setting the Deuterium coupled solvent signal to values known from the literature ($\delta CDCl_3$ = 77.16 ppm, δCD_3OD = 49.00 ppm). The coupling constants J are reported in Hz.

Single Crystal X-ray Diffraction of the ACT surfactant see *Nothling et al.*[27]

Modular synthesis

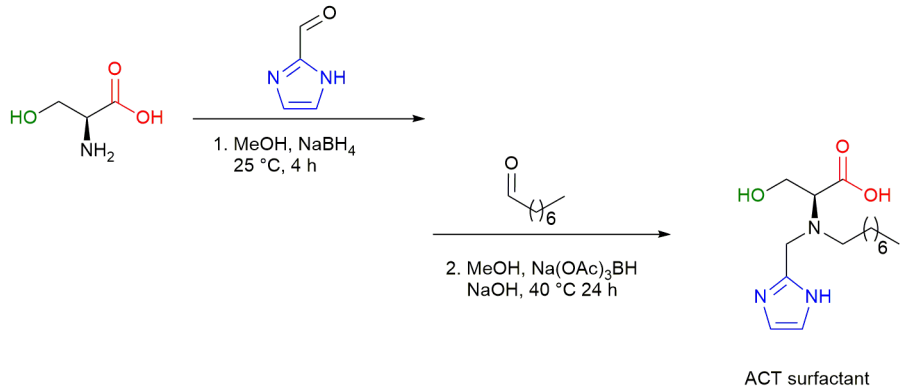

***Scheme S2.1**: Modular synthesis of ACT surfactant.*

Reductive amination of L-serine with 1H-imidazole-2-carbaldehyde (Preparation of ACT molecule)[27]: To a solution of L-serine (1.05 g, 10 mmol, 1.00 eq) and sodium hydroxide (420

mg, 10.5 mmol, 1.05 eq) in methanol ($c_{L\text{-serine}}$ ≈ 85 mM) was added 1*H*-imidazole-2-carbaldehyde (1.06 g, 11 mmol, 1.10 eq) while stirring. The resulting mixture was allowed to stir at 40°C for 30 minutes and thereafter cooled down to room temperature over 4 hours while stirring. Sodium borohydride (605.3 mg, 16 mmol, 1.60 eq) was gradually added and the reaction mixture was stirred at room temperature for 30 min. Glacial acetic acid was added dropwise until the mixture achieved approximately a pH of 4 – 5 and the resultant suspension stirred at room temperature for another 10 minutes followed by filtration and washing with methanol yielded product as a precipitate (*L*-serine derivative were obtained as fine, white solid, yield >99%). ^{1}H-NMR (600 MHz, D_2O, 298 K): δ = 7.28 (*s*, 2H, aromatic); 4.35 (*d*, ^2J = 15.1 Hz, 1H, CHHN); 4.28 (*d*,^2J = 15.1 Hz, 1H, CHHN); 3.96 – 3.84 (*m*, 2H, CH_2OH); 3.56 (*dd*, ^3J = 5.3 Hz, ^3J = 4.1 Hz, 1H, $CHCO_2^-$). MS (ESI) calculated for $C_7H_{11}N_3O_3H^+$ ($[M+H]^+$): 186.09. Found: 186.09.

Preparation of *n*-octan-1-al from *n*-octan-1-ol[27]: To a solution of *n*-octan-1-ol[50] (1.3 g, 10 mmol, 1.0 eq.) in dichloromethane ($c_{alcohol}$ ≈ 65 mM) was added pyridinium dichromate (4.5 g, 12 mmol, 1.2 eq.) portion wise and the mixture was stirred at room temperature for 8 hours. The obtained suspension was filtered using filter paper and a short silica pad followed by multiple washing with diethyl ether. The solvents were removed under reduced pressure and the crude product was purified by flash chromatography (hexanes/ethyl acetate = 19:1) to yield a waxy colorless solid (819 mg, 64%). ^{1}H NMR (400 MHz, $CDCl_3$, 298 K): δ = 9.74 (t, *J* = 1.9 Hz, 1H, CHO), 2.40 (td, *J* = 7.4, 1.9 Hz, 2H, CH_2CHO), 1.60 (m, CH_2, 2H), 1.35 to 1.19 (m, CH_2, 8H), 0.86 (t, *J* = 6.8 Hz, 3H).

Reductive amination of ACT molecule with *n*-Octan-1-al (Preparation of ACT surfactant): The synthesis of ACT surfactant has been published.[27] To a solution of ACT molecule (1.00 eq) and

sodium hydroxide (1.05 eq.) in methanol ($c_{precursor}$ ≈ 100 mM) was added *n*-Octan-1-al (1.20 eq.) and sodium triacetoxyborohydride (1.40 eq.) and the resulting mixture was left for stirring at 40 °C for 2 hours. Every 2 hours, another two batch of *n*-Octan-1-al (2 × 1.20 eq.) and Sodium triacetoxyborohydride (2 × 1.40 eq.) were added to the solution, and after 4 hours, the mixture was allowed to stir at 40 °C for another 20 hours. The reaction was quenched with glacial acetic acid and the solvents were removed under reduced pressure followed by washing with the ethyl acetate and the resulting crude product was purified by RP-HPLC with an H_2O/acetonitrile gradient (19:1 → 1:19) to yield a pale-yellow solid (60%). ^{1}H-NMR (800 MHz, D_2O, 298 K): δ 7.22 (*s*, 2H, aromatic); 4.17 – 4.02 (*m*, 2H, ImCH_2N), 3.98 – 3.88 (*m*, 3H, CH_2OH), 3.56 (*dd*, ^3J = 5.9, ^3J = 2.0 Hz, 1H, $CHCO_2H$), 2.78 – 2.72 (*m*, 2H, NCH_2CH_2), 1.50 – 1.27 (*m*, 12H, CH_2), 0.98 (*t*, ^3J = 7.2 Hz, 3H, CH_3), (**Figure S2.1**). MS (ESI) calculated for $C_{15}H_{27}N_3O_3H^+$ ($[M+H]^+$): 298.21. Found: 298.24.

Preparation of *Imz-COOH* [(R)-3-(1H-imidazol-5-yl)-2-(octylamino)propanoic acid] control structure: *L*-histidine (620.8 mg, 4.0 mmol, 1.0 eq.) was dissolved in 20 mL of methanol at 50°C followed by addition of sodium hydroxide (168 mg, 4.2 mmol, 1.1 eq.) with stirring. 1-Octanal (620 mg, 4.8 mmol, 1.2 eq.) was then added, and the reaction was stirred overnight at room temperature. $NaBH_4$ (300 mg, 8.0 mmol, 2.0 eq.) was then added, and the reaction mixture was stirred for a further 1 hour at room temperature. Concentrated hydrochloric acid (32%, ~1.0 mL) was added to quench the reaction mixture, the suspension was filtered, and the solvent was removed in vacuo. The crude product was washed with ethyl acetate and a small amount of water and then purified *via* reverse-phase column chromatography (MeOH/H_2O 19:1→0:1) to yield target structure (639 mg, 2.4 mmol, 60%). ^{1}H NMR (400 MHz, MeOD): δ 8.69 (*s*, 1H, Im), 7.39 (*s*, 1H, Im), 3.89 (*s*, 1H, CHCOOH), 3.09 – 3.02 (*m*, 2H, CH_2NH), 1.73 – 1.68

(*m*, 2H, CH_2CH_2NH), 1.41 – 1.29 (*m*,12H, CH_2), 0.92 – 0.89 (*m*, 3H, CH_3), (**Figure S2.2**); ^{13}C NMR (400 MHz, Methanol-d_4): δ= 168.9, 134.1, 127.6, 117.9, 53.4, 31.4, 28.7, 26.1, 25.8, 24.4, 22.2, 13.0, (**Figure S2.3**). MS (ESI) was calculated for $C_{14}H_{25}N_3O_2H^+$ ($[M + H]^+$): 268.20. Found: 268.21.

Preparation of *OH-COOH* [(S)-3-hydroxy-2-(octylamino)propanoic acid] control structure: *L*-serine (210 mg, 2.0 mmol, 1.0 eq.) was dissolved in 15 mL of methanol at 50°C followed by addition of sodium hydroxide (88 mg, 1.4 mmol, 1.1 eq.) while stirring. 1-Octanal (310 mg, 2.4 mmol, 1.2 eq.) was then added, and the reaction was stirred overnight at room temperature. $NaBH_4$ (150 mg, 4.0 mmol, 2.0 eq.) was then added, and the reaction mixture was stirred for a further 1 hour at room temperature. Concentrated hydrochloric acid (32%, ~0.7 mL) was added to quench the reaction mixture, the suspension was filtered, and solvent was removed in vacuo. The crude product was washed with ethyl acetate and then purified *via* reverse-phase column chromatography (MeOH/H_2O 19:1→0:1) to yield target structure (239 mg, 1.1 mmol, 54%). ^1H NMR (400 MHz; MeOD, 298 K): δ = 4.03 (*dd*, ^2J = 12.4, ^3J = 3.6 Hz, 2H, CH_2OH), 3.98 (*dd*, ^2J = 12.1, ^3J = 4.8 Hz, 2H, CH_2OH), 3.84 (*dd*, ^3J = 3 Hz, 1H, $CHCH_2OH$), 3.08 – 3.04 (*m*, 2H, CH_2NH), 1.73 (*p*, ^3J = 7.6 Hz, 2H, $CH_2CH_2CH_2$), 1.41 – 1.30 (*m*, 10H, CH_2), 0.92 – 0.88 (*m*, 3H, CH_3), (**Figure S2.4**); ^{13}C NMR (400 MHz, Methanol-d_4): δ= 170.4, 63.6, 60.1, 47.7, 32.9, 30.2, 27.6, 27.1, 23.7, 14.4, (**Figure S2.5**). MS (ESI) was calculated for $C_{11}H_{23}NO_3H^+$ ($[M + H]^+$): 218.17. Found: 218.19.

Transesterification of VTFA and methanol in the presence of ACT surfactant catalyst: Pre-dried methanol and *d*-chloroform from Sigma were again dried by passing through a column of activated basic alumina, prior to addition of reactants. In 5 mL of dry methanol, ACT surfactant (9.2 mg) was dissolved to yield a catalyst solution (6.18 x 10^{-3} M). VTFA (Initial VTFA conc. = 0.025, 0.05, 0.125, 0.25, 0.5 M) was dissolved in dry *d*-chloroform (688.7 µL) and 64.7

µL of catalyst stock solution (catalysed runs) or dry methanol (blank runs) was added. The obtained mixture was immediately observed *via* 400 MHz ^{1}H NMR on a Varian INOVA spectrometer. The first spectrum was obtained at ~ 3 minutes, and subsequent spectra were taken every 4 minutes for up to 12 hours. Reaction progress (% conversion) was computed by comparing reduction of the vinyl proton peaks (δ = 7.19, 5.16, 4.87 ppm) with the appearance of a methyl proton peak associated with methyl trifluoroacetate (δ = 3.91 ppm) and aldehyde proton peak associated with acetaldehyde (δ = 9.71 ppm). Parallel reaction mixtures were subjected to 400 MHz ^{19}F NMR confirming the transesterification product methyl trifluoroacetate as major product for time periods up to 1.5 hours after mixing. The concentration of hydrolysis product trifluoroacetic acid was found to be rising over a longer length of time, possibly due to hydrolysis of the transesterification product (up to 10% mol after 12 hours).

Determination of Kinetic Parameters: Michaelis-Menten equation was used to measure k_{cat} and K_m for the catalytic activity of the catalysts. Dry *d*-chloroform and dry methanol were used in each kinetic experiment. A dried NMR tube was added with different initial VTFA conc. = 0.025, 0.05, 0.125, 0.25, 0.5 M and 64.7 µL of catalyst stock solution (0.5 mM catalyst loading) for catalysed runs or dry methanol for the background reaction in dry $CDCl_3$ at 23 °C. The progress of the reaction was monitored by ^{1}H NMR. Integration of the starting material and product signals was used to calculate the concentration of products. After 3 minutes of mixing time, the reaction velocity was measured as the tangent to the product concentration vs. time curve. All curve and Michaelis-Menten equation were fitted using the GraphPad prism software.

Preparation of ACT surfactant solutions for DLS/^{1}H NMR: Stock solutions of ACT surfactants/methanol were prepared by mass and volumetric dilution. Individual solutions were prepared from the stock solutions (80.9 µL), incorporating methanol (0, 20, 40, 60, 80, 100, 120, 140, 160 µL) and $CHCl_3$ (or $CDCl_3$ for ^{1}H NMR) with calibrated microsyringes. Therefore, each solution contains a different amount of methanol. The solutions were agitated in sonication bath to obtain clear transparent solutions with a single phase.

Dynamic Light Scattering Measurements: Particle sizing was measured by Dynamic Light Scattering (DLS) using a Zetasizer Nano ZS (Malvern Instruments) at 25 °C, using a forward scatter angle of 13° and Non-Invasive Back Scatter (NIBS) angle of 173°. The quartz cuvettes was cleaned with ethanol, then with doubly distilled water and dried with acetone; this step was critical for producing consistent and reproducible data.[47] The cuvettes was then washed twice with pure chloroform and then with the solution to be analysed before each sample was inserted into the cuvette. Before data acquisition, samples were equilibrated in the DLS instrument for 10 min at 25 °C, and where each replicate was measured 10 times to determine the average apparent diameter (d_{app}). DLS experiments were carried out at [ACT surfactant] = 0.5 mM. For each experiment, 1 mL cuvettes were filled with increasing volume of methanol = 0, 20 and 60 µL, catalyst stock volume of 80.9 µL and adding sufficient chloroform to make up the final volume. The DLS instrument was not able to measure at 40 µL and higher volumes of methanol (> 60 µL). In all DLS spectra, peak greater than 1 µm corresponds to dust while the peak around 100 nm is due to unknown contamination.

NMR

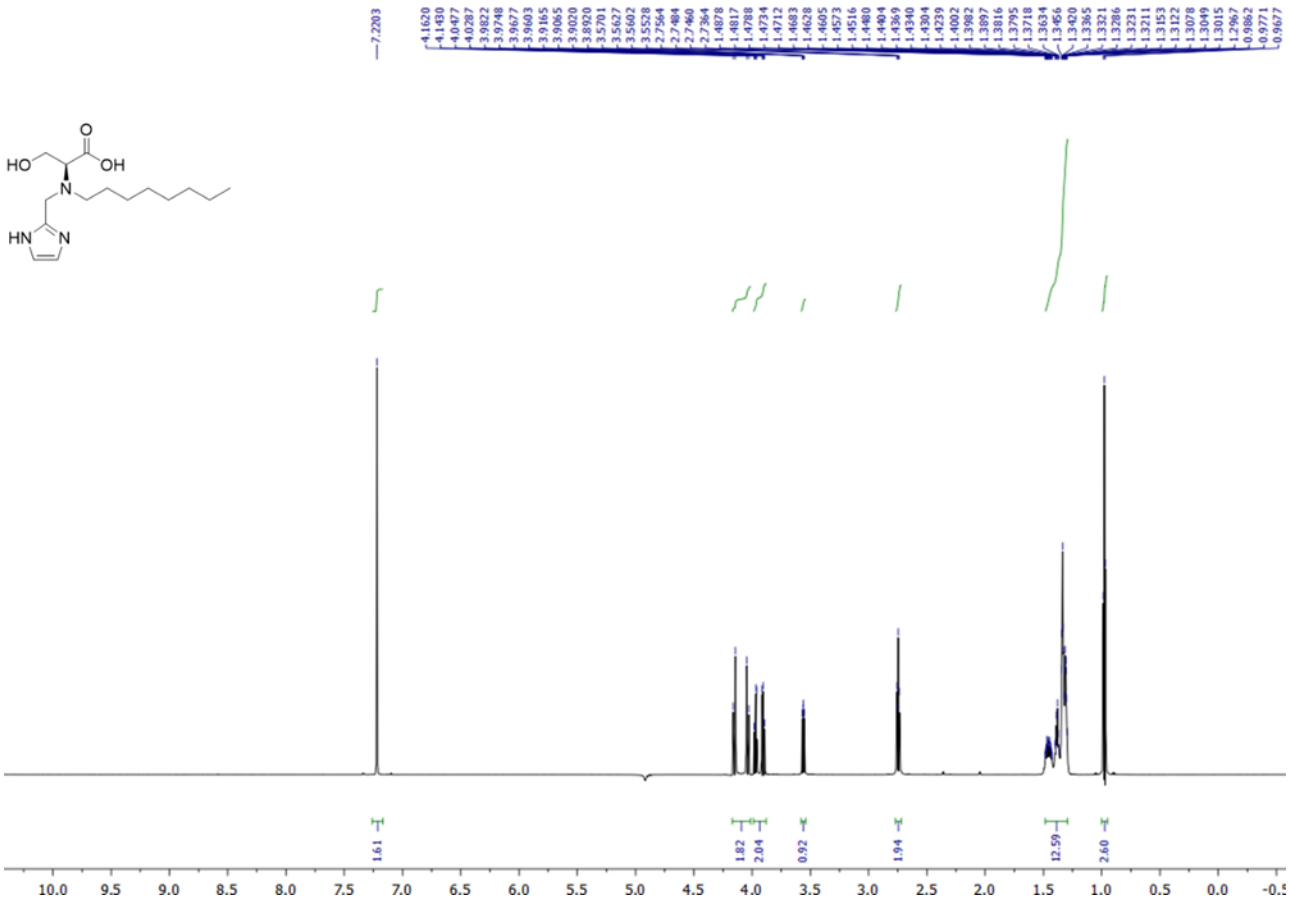

Figure S2.1: *^{1}H NMR of ACT surfactant using D_2O suppression.*

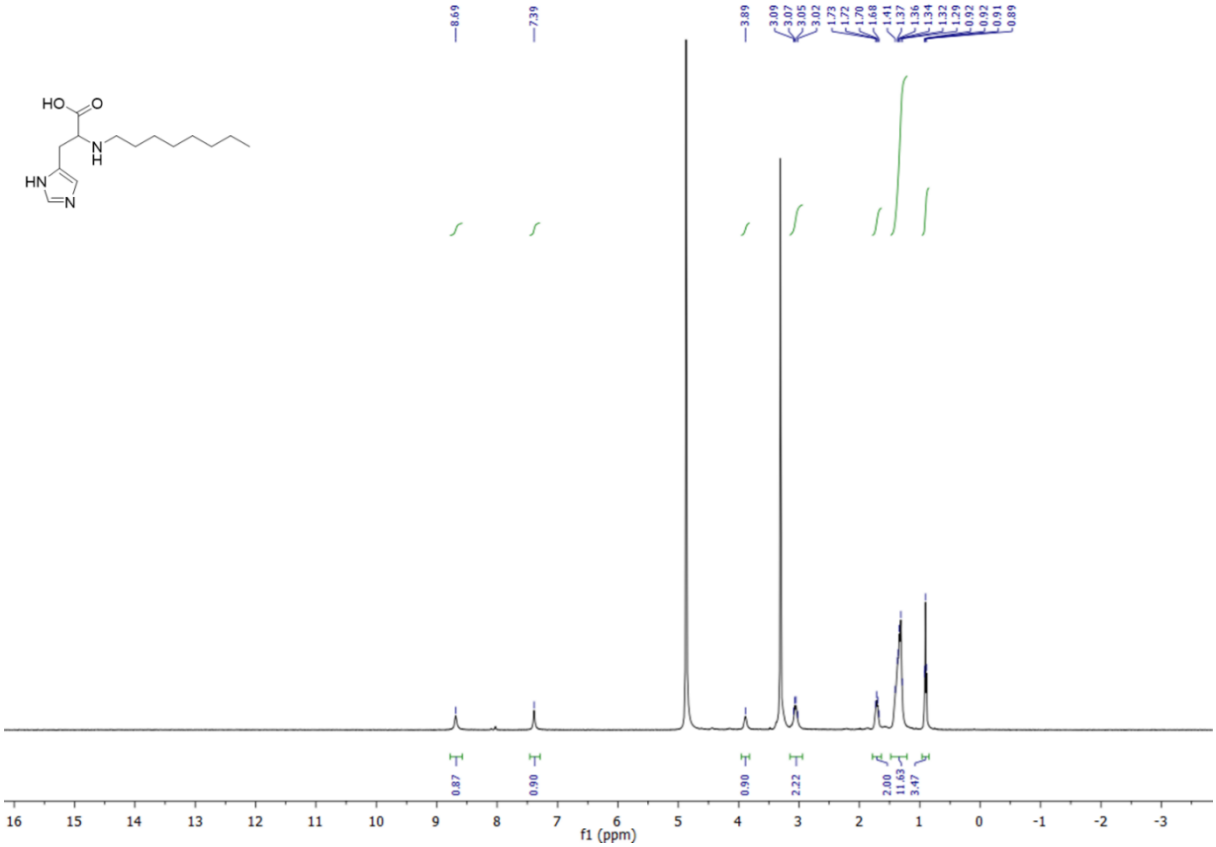

Figure S2.2: *^{1}H NMR of Imz-COOH in methanol-d_4.*

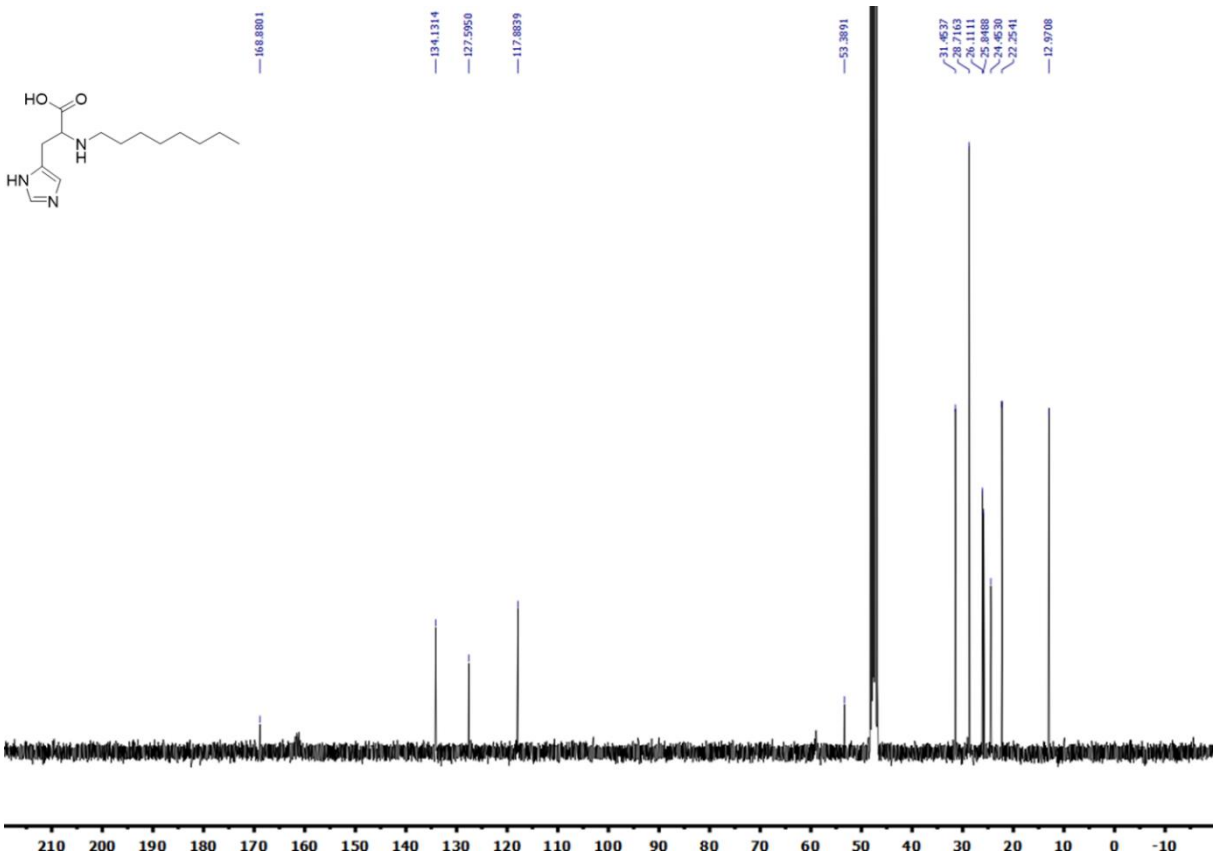

Figure S2.3: *^{13}C NMR of Imz-COOH in methanol-d_4.*

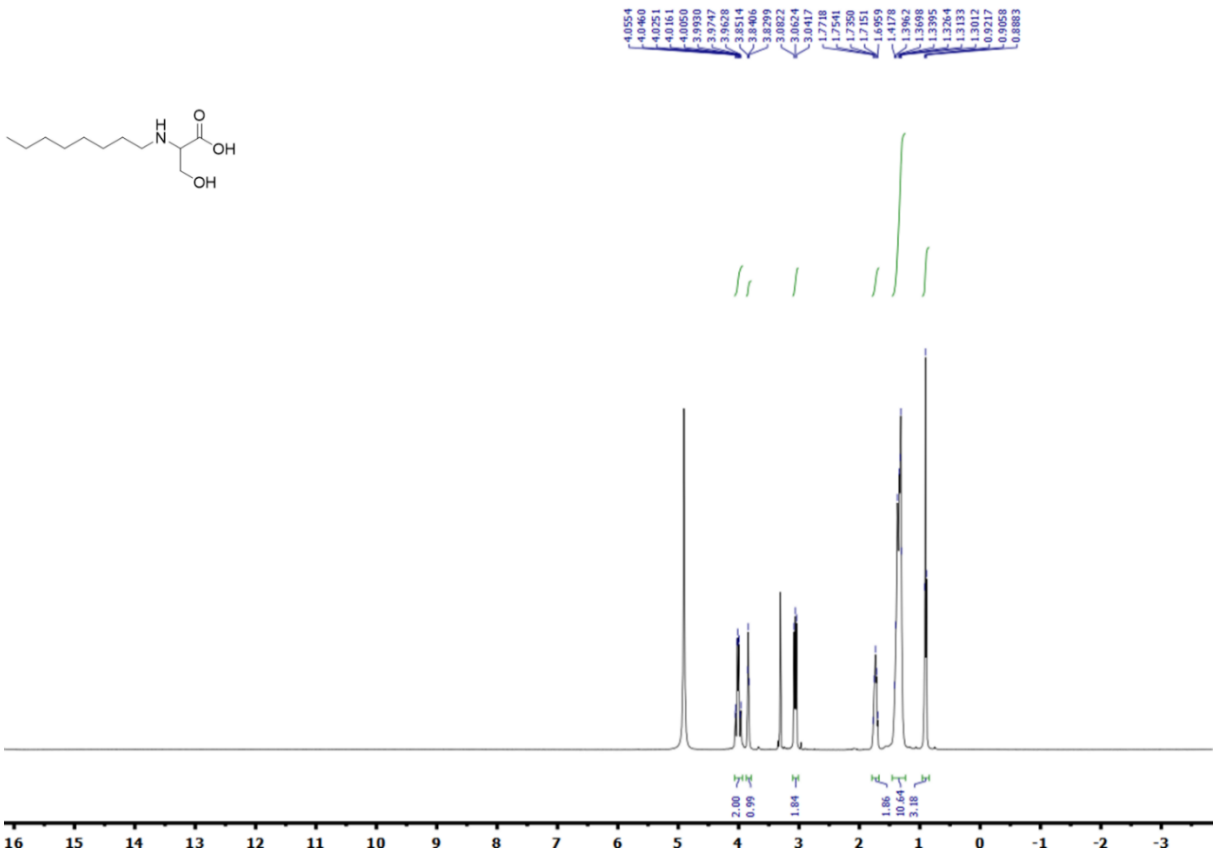

Figure S2.4: *^{1}H NMR of OH-COOH in methanol-d_4.*

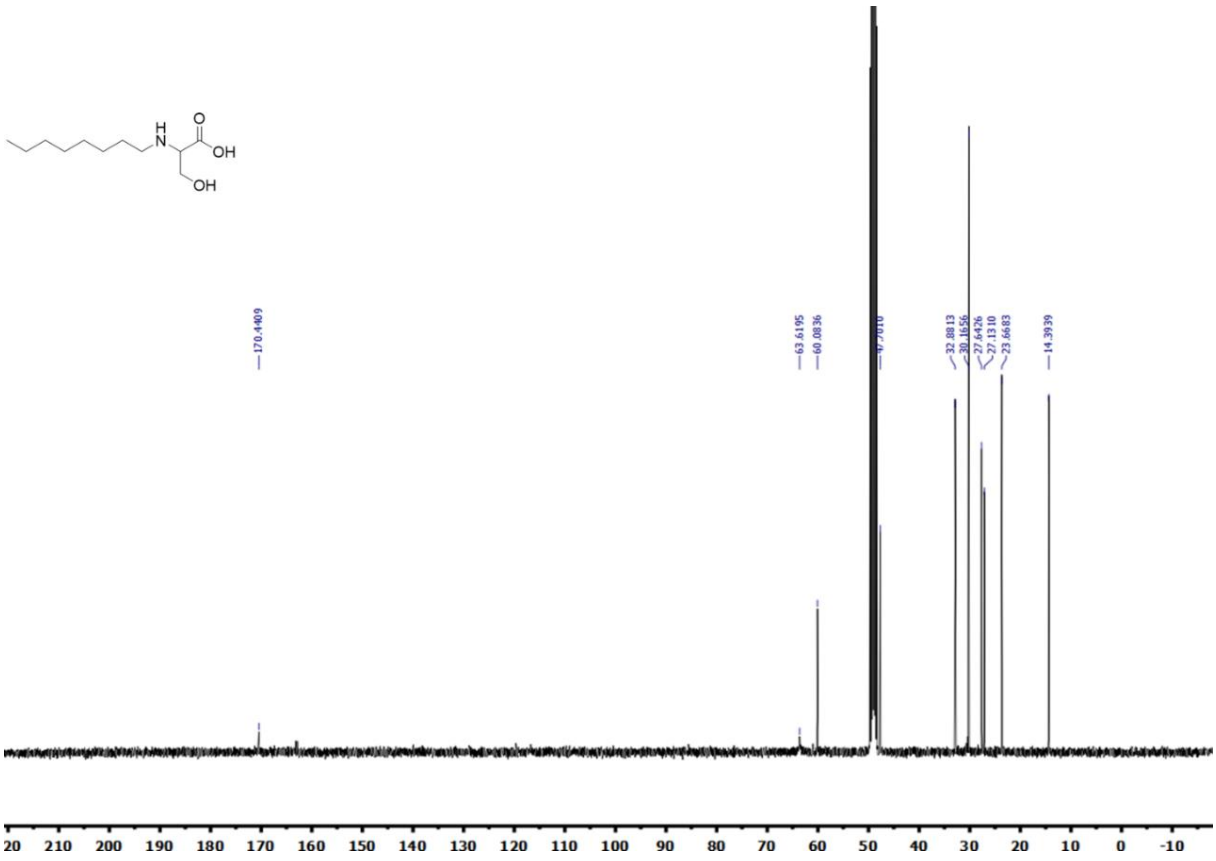

Figure S2.5: *^{13}C NMR of OH-COOH in methanol-d$_4$.*

^{19}F NMR

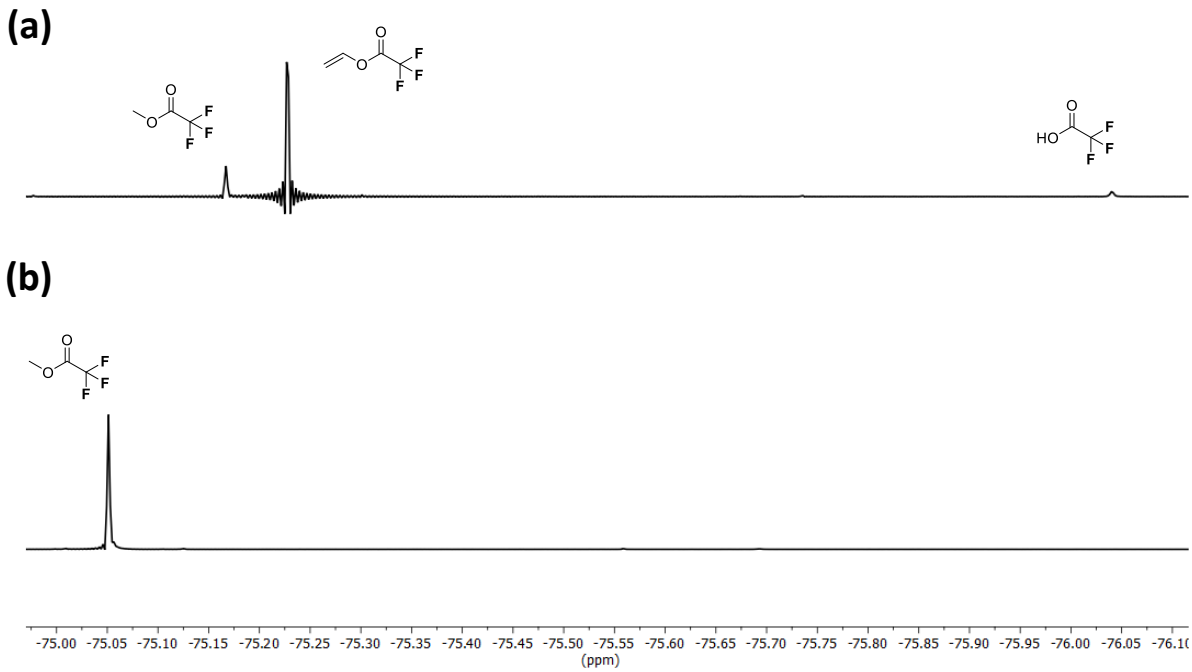

***Figure S2.6**: ^{19}F NMR of reaction mixture (1 mol% catalyst, 0.05 M VTFA, 2M MeOH, d-$CDCl_3$), (a) after 10 minutes of mixing, (b) after 1 h of mixing. The product peak shifted over a one-hour period. The appearance of a small peak due to the side hydrolysis reaction was observed (trifluoroacetic acid near -76.05 ppm).*

Michaelis-Menten kinetic parameters

Catalyst	k_{cat} and k_{unc} (s^{-1})	K_M (M)	k_{cat}/k_{unc}	k_{cat}/K_M ($s^{-1}M^{-1}$)
ACT surfactant	3.302	1.061	4.81×10^4	3.11
Imz-COOH	0.549	0.802	8.00×10^3	6.84×10^{-1}
OH-COOH	0.312	0.429	4.54×10^3	7.27×10^{-1}
Background	0.0000686			

Table S2.1: *Michaelis-Menten kinetic parameters of the ACT catalysts and the first-order rate constant for background transesterification.*

Molecular dynamics simulations of ACT surfactant

ACT surfactant in 10% MeOH/Chloroform solution

Method

All simulations were performed using GROMACS 2019.3[48] with the GROMOS 54a7 force field[49]. United atom parameters and co-ordinates for the solvents (chloroform (ATB ID 1307), methanol (ATB ID 15607)), VTFA (ATB ID 479693) and ACT surfactant (without charge, ATB ID 479692) were developed using the Automated Topology Builder (ATB) and are publicly available on the ATB website.[50] All simulations were performed in a 10 nm^3 box. Here, VTFA and ACT surfactant were added to a pre-equilibrated box of chloroform containing 10% methanol. All concentrations were determined relative to experimental ratios of components at 200 times the concentration used in experimental conditions to enable sampling. This is in accord with previous investigations of the behavior of ACT surfactant in a micellar solution.[27] Simulations were performed using an NPT ensemble with periodic boundary conditions. The temperature of all systems was set to 300 K, which was controlled using a v-rescale thermostat (τP = 0.1 ps). Isotropic pressure coupling was implemented using the Berendsen barostat (τP = 0.5 ps and isothermal compressibility = 4.5×10^{-5} bar). Long-range electrostatics were calculated using the particle-mesh Ewald method (1nm cutoff). All systems were minimized using a steepest descent for 10,000 steps and equilibrated for 2 fs to stabilise system density. The LINCS algorithm was used to constrain covalent bond lengths**.** Production simulations were run for 500 ns with a 2 fs timestep. For each system, replicate systems were prepared in triplicate, where each replicate system contained a unique random distribution of molecules

to remove bias. To initiate each system, random velocities were assigned. Using frames collected every 0.1 ns, data were analysed using inbuilt GROMACS 2019.3[48] analysis tools and the python package MDTraj[51]. Images of trajectory frames were produced using VMD.[52] Coordinates of the first and last frames of each trajectory may be found on github at https://github.com/OMaraLab/ACT-Chlor-MeOH/

Kinetic profile of ACT surfactant

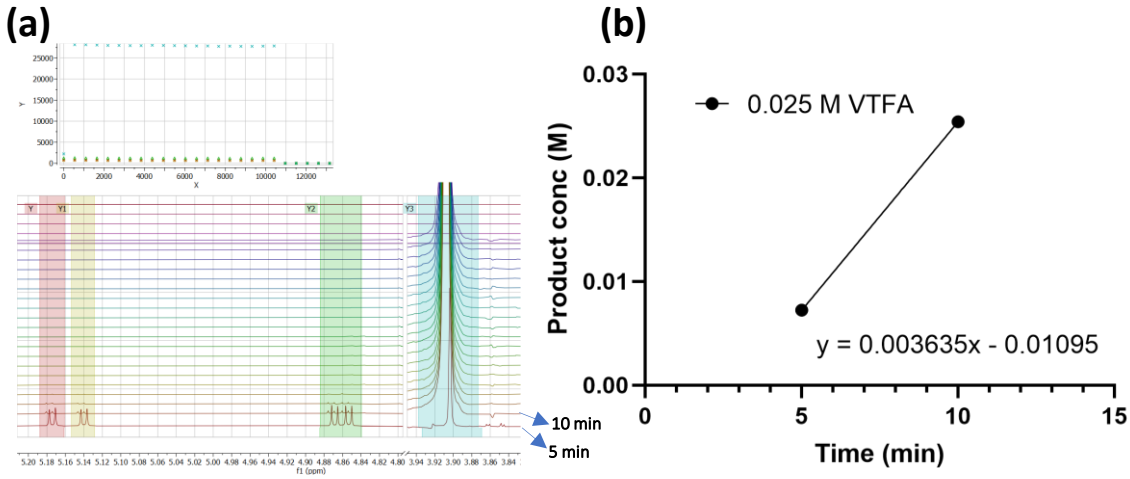

Figure S2.7: *Kinetic profile of ACT surfactant catalysed transesterification of 0.025 M VTFA with methanol, (a) ^{1}H NMR spectra of the reaction mixture of ACT surfactant (1 mol%), VTFA (0.025 M) and methanol (2 M) in d-chloroform with time. The first spectrum was acquired at 5 minutes, while subsequent spectra were acquired at interval of 5 minutes. Different coloured regions show the integral area (red, yellow and green corresponds to vinyl proton peaks while blue corresponds to methyl proton peaks of methyl trifluoroacetate), (b) Linear regression for initial velocity measurements taken at 5 and 10 minutes.*

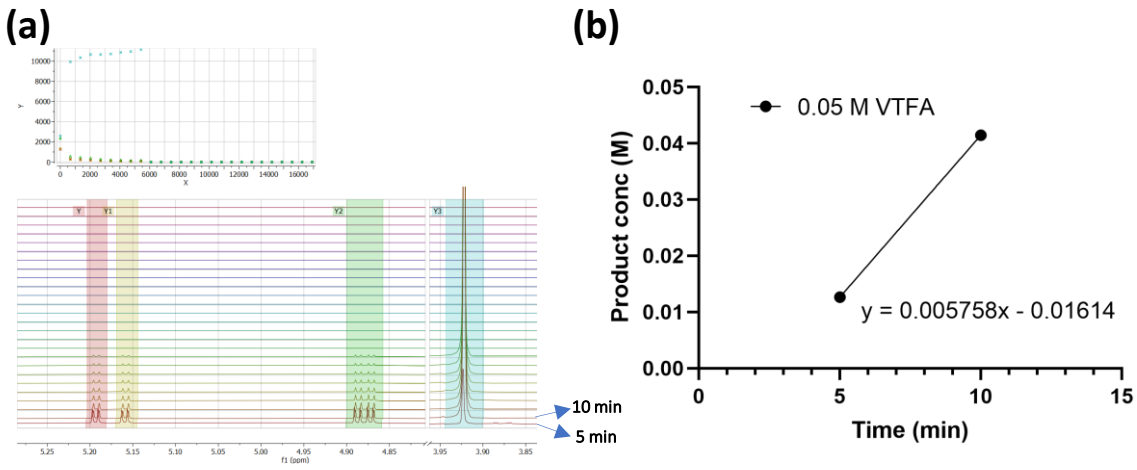

Figure S2.8: *Kinetic profile of ACT surfactant catalysed transesterification of 0.05 M VTFA with methanol, (a)* ^{1}*H NMR spectra of the reaction mixture of ACT surfactant (1 mol%), VTFA (0.05 M) and methanol (2 M) in d-chloroform with time. The first spectrum was acquired at 5 minutes, while subsequent spectra were acquired at interval of 5 minutes. Different coloured regions show the integral area (red, yellow and green corresponds to vinyl proton peaks while blue corresponds to methyl proton peaks of methyl trifluoroacetate), (b) Linear regression for initial velocity measurements taken at 5 and 10 minutes.*

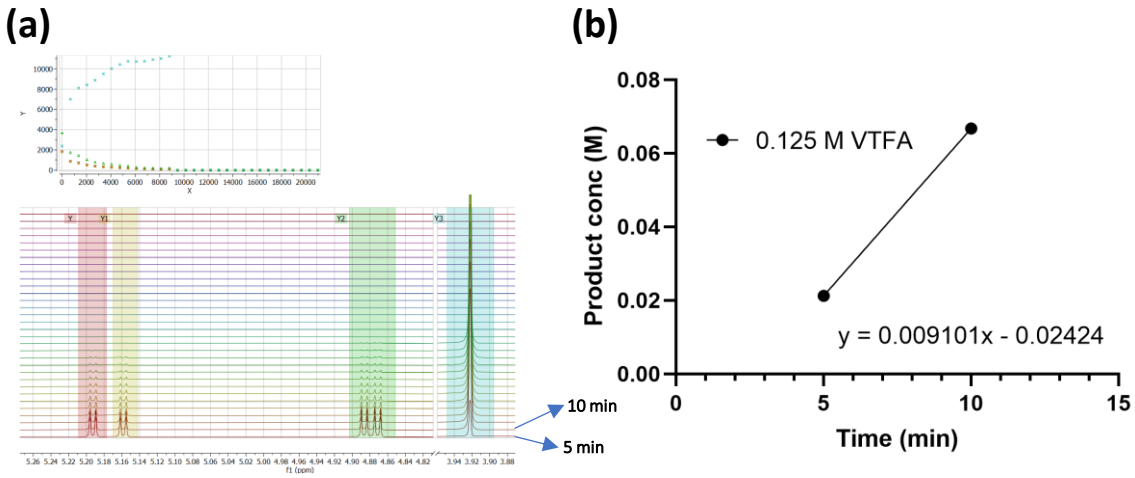

Figure S2.9: *Kinetic profile of ACT surfactant catalysed transesterification of 0.125 M VTFA with methanol, (a) ^{1}H NMR spectra of the reaction mixture of ACT surfactant (1 mol%), VTFA (0.125 M) and methanol (2 M) in d-chloroform with time. The first spectrum was acquired at 5 minutes, while subsequent spectra were acquired at interval of 5 minutes. Different coloured regions show the integral area (red, yellow and green corresponds to vinyl proton peaks while blue corresponds to methyl proton peaks of methyl trifluoroacetate), (b) Linear regression for initial velocity measurements taken at 5 and 10 minutes.*

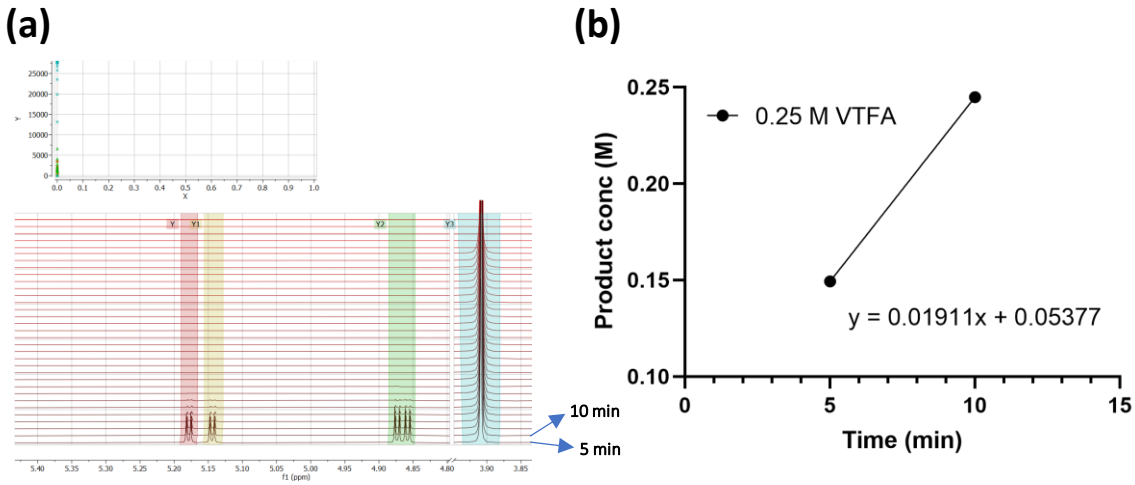

Figure S2.10: *Kinetic profile of ACT surfactant catalysed transesterification of 0.25 M VTFA with methanol, (a) ^{1}H NMR spectra of the reaction mixture of ACT surfactant (1 mol%), VTFA*

(0.25 M) and methanol (2 M) in d-chloroform with time. The first spectrum was acquired at 5 minutes, while subsequent spectra were acquired at interval of 5 minutes. Different coloured regions show the integral area (red, yellow and green corresponds to vinyl proton peaks while blue corresponds to methyl proton peaks of methyl trifluoroacetate), (b) Linear regression for initial velocity measurements taken at 5 and 10 minutes.

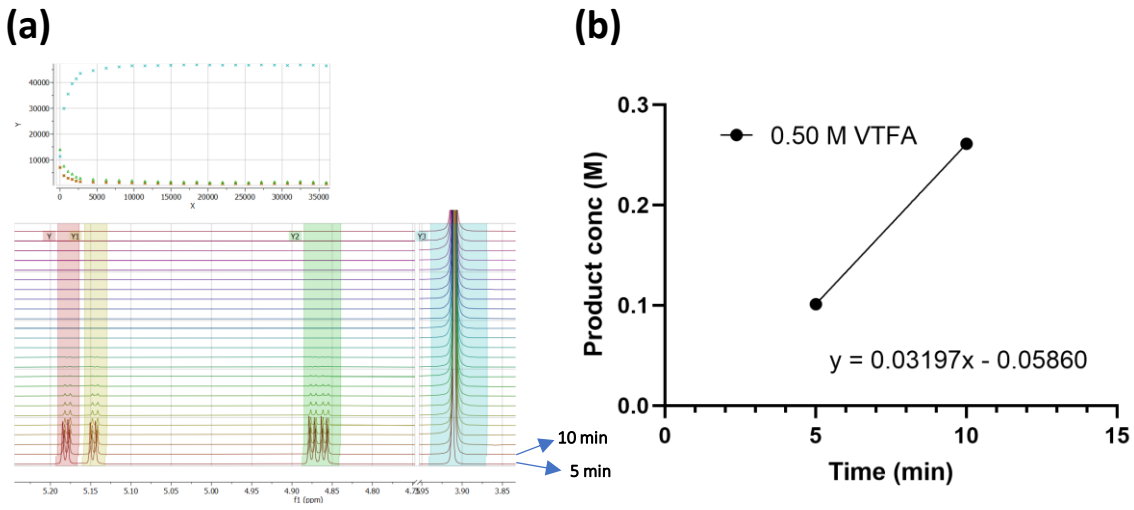

Figure S2.11: *Kinetic profile of ACT surfactant catalysed transesterification of 0.5 M VTFA with methanol, (a) ^{1}H NMR spectra of the reaction mixture of ACT surfactant (1 mol%), VTFA (0.5 M) and methanol (2 M) in d-chloroform with time. The first spectrum was acquired at 5 minutes, while subsequent spectra were acquired at interval of 5 minutes. Different coloured regions show the integral area (red, yellow and green corresponds to vinyl proton peaks while blue corresponds to methyl proton peaks of methyl trifluoroacetate), (b) Linear regression for initial velocity measurements taken at 5 and 10 minutes.*

DLS and ^{1}H NMR

Experiment 1

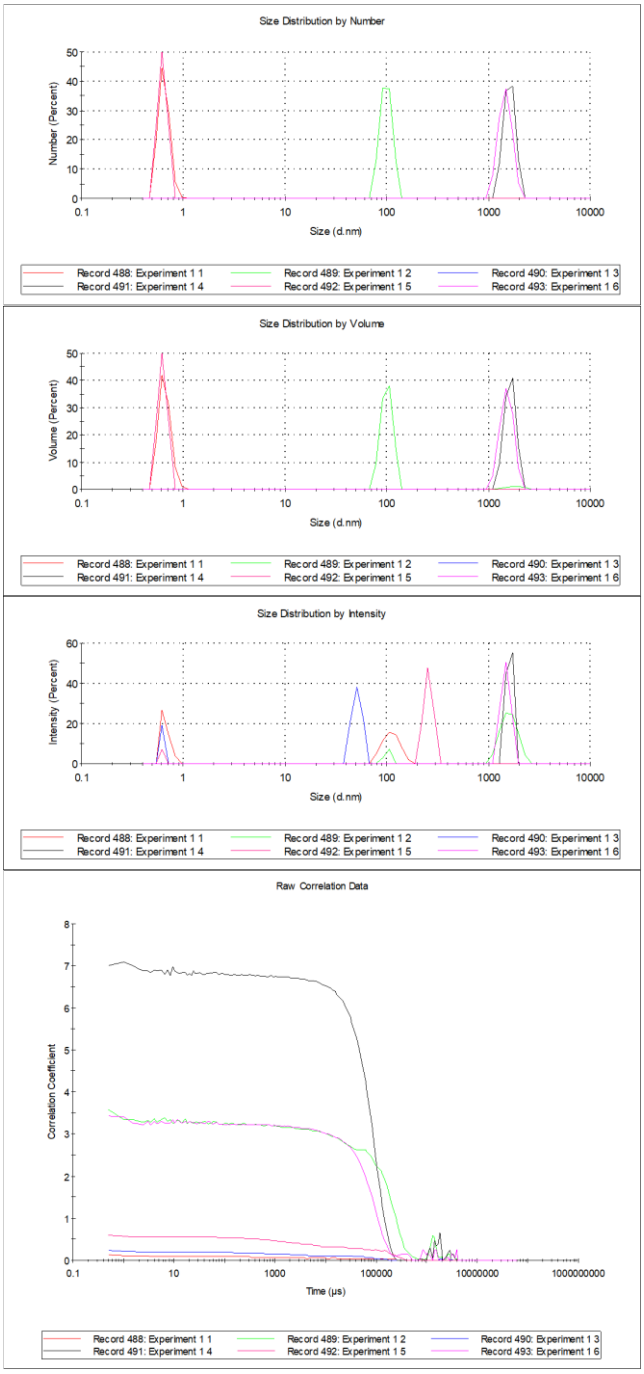

Figure S2.12: *DLS spectra and correlation coefficient of ACT surfactants at 25 °C containing 0 µL methanol, 80.9 µL ACT surfactant stock solution and adding sufficient chloroform to make up the final volume of 1 mL.*

Experiment 2

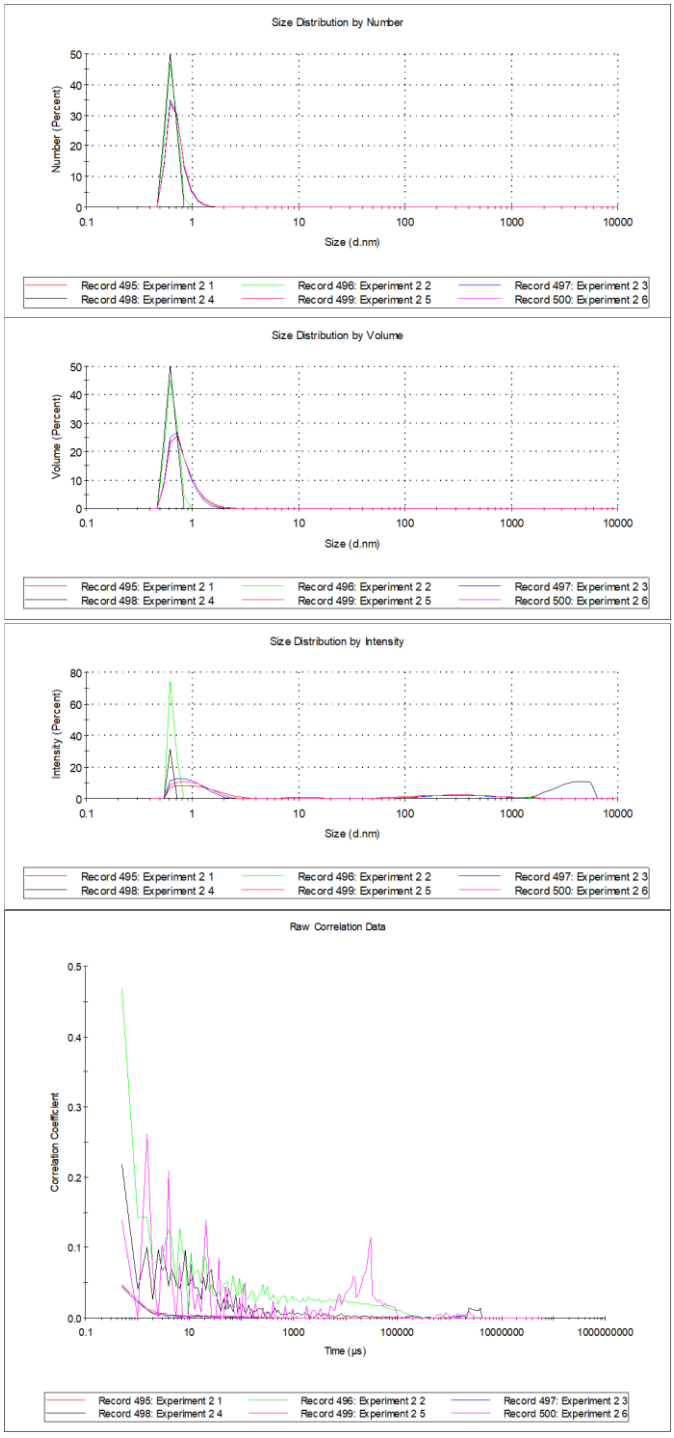

Figure S2.13: *DLS spectra and correlation coefficient of ACT surfactants at 25 °C containing 20 µL methanol, 80.9 µL ACT surfactant stock solution and adding sufficient chloroform to make up the final volume of 1 mL.*

Experiment 3

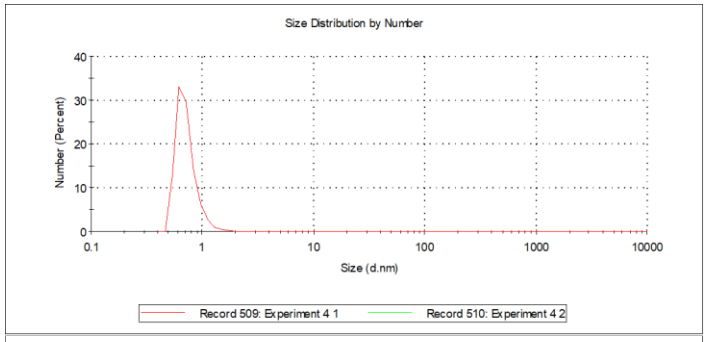

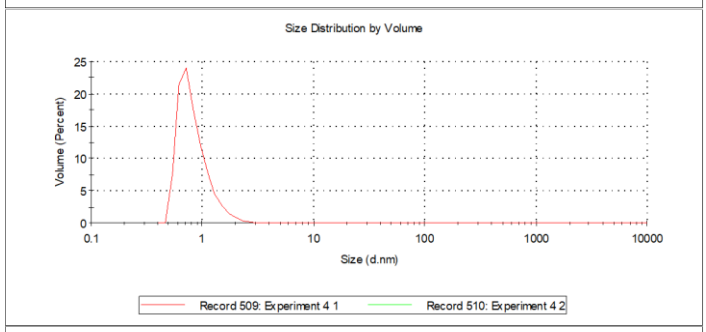

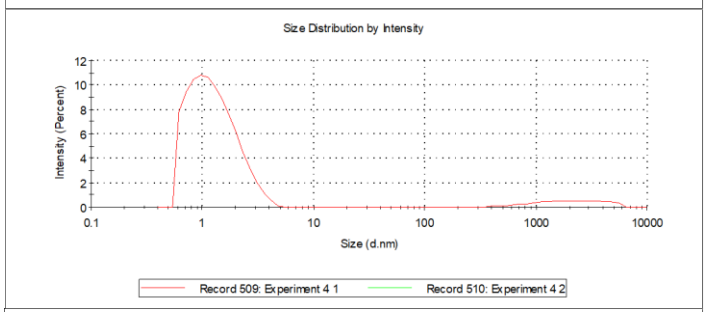

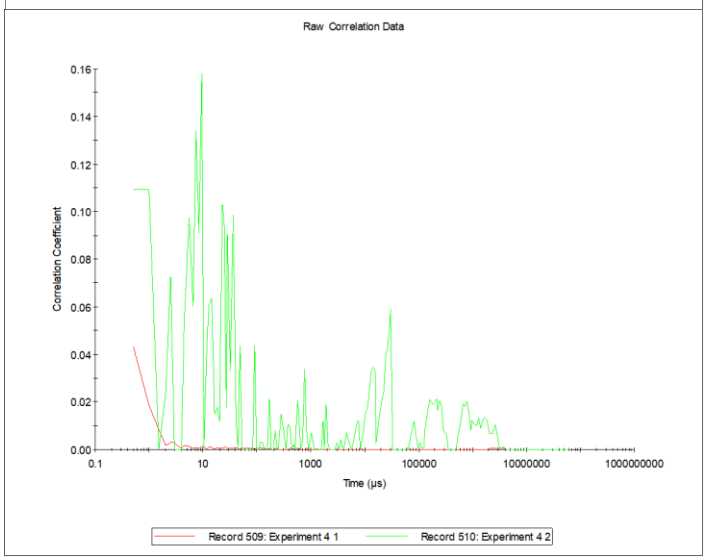

Figure S2.14: *DLS spectra and correlation coefficient of ACT surfactants at 25 °C containing 60 µL methanol, 80.9 µL ACT surfactant stock solution and adding sufficient chloroform to make up the final volume of 1 mL.*

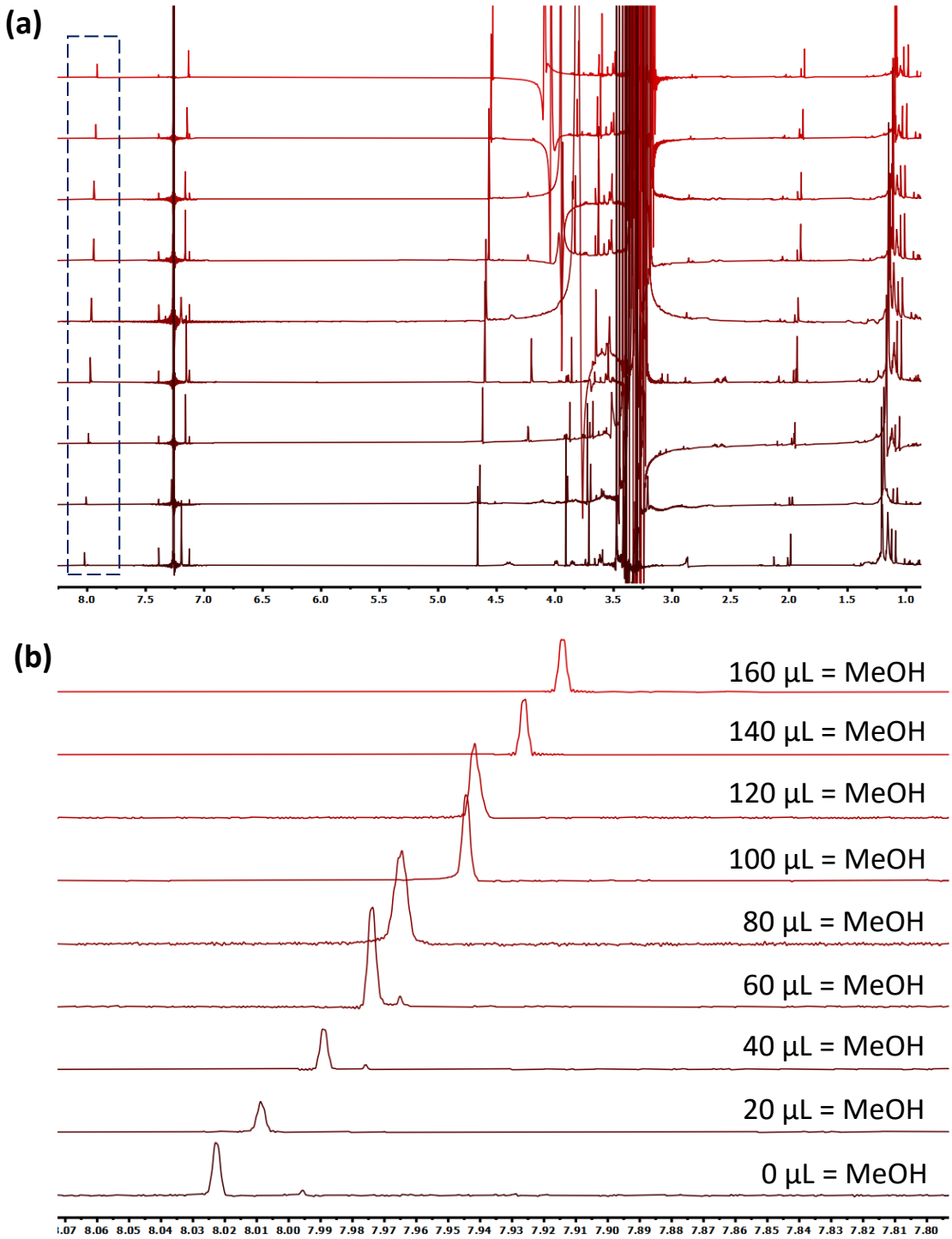

Figure S2.15: *^{1}H NMR spectra of ACT surfactants clusters in methanol/chloroform obtained by varying the methanol content at 25 °C, [ACT surfactant] = 0.5 mM, (a) the dotted blue line highlights the ^{1}H NMR signals from the imidazole proton, (b) ^{1}H NMR spectra in the region 7.80—8.06 ppm showing shifting of H in imidazole peak with increasing methanol content.*

References

(1) Kumar, A.; Nothling, M. D.; Aitken, H. M.; Xiao, Z.; Lam, M.; Bell, C. A.; O'Mara, M. L.; Connal, L. A. Simple synthetic route to an enzyme-inspired transesterification catalyst. *Catalysis Science & Technology* **2022**, *12*, 6655-6659.
(2) Drauz, K.; Waldmann, H. *Enzyme Catalysis in Organic Synthesis: A Comprehensive Handbook*; Wiley–VCH, 2002.
(3) Jaeger, K.-E.; Eggert, T. Lipases for biotechnology. *Current Opinion in Biotechnology* **2002**, *13*, 390-397.
(4) Reetz, M. T. Lipases as practical biocatalysts. *Current Opinion in Chemical Biology* **2002**, *6*, 145-150.
(5) Jaeger, K.-E.; Ransac, S.; Dijkstra, B. W.; Colson, C.; van Heuvel, M.; Misset, O. Bacterial lipases. *FEMS Microbiology Reviews* **1994**, *15*, 29-63.
(6) Schmid, R. D.; Verger, R. Lipases: Interfacial Enzymes with Attractive Applications. *Angewandte Chemie International Edition* **1998**, *37*, 1608-1633.
(7) Kazlauskas, R. J.; Bornscheuer, U. T.; Rehm, H. J.; Reed, G.; Pühler, A.; Stadler, P. J. W.; (Eds.), D. R. K. *Biotechnology, Biotransformations with Lipases*; Wiley–VCH, 1998.
(8) Nothling, M. D.; Xiao, Z.; Bhaskaran, A.; Blyth, M. T.; Bennett, C. W.; Coote, M. L.; Connal, L. A. Synthetic Catalysts Inspired by Hydrolytic Enzymes. *ACS Catalysis* **2019**, *9*, 168-187.
(9) Breslow, R. Biomimetic Chemistry and Artificial Enzymes - Catalysis by Design. *Accounts of Chemical Research.* **1995**, *28*, 146-153.
(10) Cram, D. J.; Katz, H. E.; Dicker, I. B. Host Guest Complexation .31. A Transacylase Partial Mimic. *Journal of the American Chemical Society.* **1984**, *106*, 4987-5000.
(11) Cram, D. J.; Cram, J. M. *Container Molecules and Their Guests*; 1994.
(12) Lücking, U.; Tucci, F. C.; Rudkevich, D. M.; Rebek, J. Self-Folding Cavitands of Nanoscale Dimensions. *Journal of the American Chemical Society.* **2000**, *122*, 8880-8889.
(13) Brocklehurst, K.; Neuberger, A. *Hydrolytic Enzymes*; Elsevier Science, 1988.
(14) Toda, F. *Enantiomer separation: fundamentals and practical methods*; Springer, 2007.
(15) Nakamura, K.; Yamanaka, R.; Matsuda, T.; Harada, T. Recent developments in asymmetric reduction of ketones with biocatalysts. *Tetrahedron: Asymmetry* **2003**, *14*, 2659-2681.
(16) Patti, A.; Sanfilippo, C. Breaking Molecular Symmetry through Biocatalytic Reactions to Gain Access to Valuable Chiral Synthons. *Symmetry* **2020**, *12*, 1454.
(17) Ferrero, M.; Gotor, V. Chemoenzymatic Transformationsin Nucleoside Chemistry. *Monatshefte für Chemie.* **2000**, *131*, 585-616.
(18) Stergiou, P.-Y.; Foukis, A.; Filippou, M.; Koukouritaki, M.; Parapouli, M.; Theodorou, L. G.; Hatziloukas, E.; Afendra, A.; Pandey, A.; Papamichael, E. M. Advances in lipase-catalyzed esterification reactions. *Biotechnology Advances* **2013**, *31*, 1846-1859.

(19) Santaniello, E.; Casati, S.; Ciuffreda, P. Lipase-Catalyzed Deacylation by Alcoholysis: A Selective, Useful Transesterification Reaction. *Current Organic Chemistry* **2006**, *10*, 1095-1123.
(20) Amini, Z.; Ilham, Z.; Ong, H. C.; Mazaheri, H.; Chen, W.-H. State of the art and prospective of lipase-catalyzed transesterification reaction for biodiesel production. *Energy Conversion and Management* **2017**, *141*, 339-353.
(21) Polgár, L. Chapter 3 Structure and function of serine proteases. *New Comprehensive Biochemistry* **1987**, *16*, 159-200.
(22) Wieczorek, R.; Adamala, K.; Gasperi, T.; Polticelli, F.; Stano, P. Small and Random Peptides: An Unexplored Reservoir of Potentially Functional Primitive Organocatalysts. The Case of Seryl-Histidine. *Life-Basel* **2017**, *7*.
(23) Warshel, A.; Sussman, F. Toward computer-aided site-directed mutagenesis of enzymes. *Proceedings of the National Academy of Sciences* **1986**, *83*, 3806-3810.
(24) Fodor, K.; Harmat, V.; Neutze, R.; Szilágyi, L.; Gráf, L.; Katona, G. Enzyme:Substrate Hydrogen Bond Shortening during the Acylation Phase of Serine Protease Catalysis. *Biochemistry* **2006**, *45*, 2114-2121.
(25) Purich, D. *Enzyme Kinetics: Catalysis and Control*; Elsevier, 2010.
(26) Nothling, M. D.; Ganesan, A.; Condic-Jurkic, K.; Pressly, E.; Davalos, A.; Gotrik, M. R.; Xiao, Z.; Khoshdel, E.; Hawker, C. J.; O'Mara, M. L.; et al. Simple Design of an Enzyme-Inspired Supported Catalyst Based on a Catalytic Triad. *Chem* **2017**, *2*, 732-745.
(27) Nothling, M. D.; Xiao, Z.; Hill, N. S.; Blyth, M. T.; Bhaskaran, A.; Sani, M.-A.; Espinosa-Gomez, A.; Ngov, K.; White, J.; Buscher, T.; et al. A multifunctional surfactant catalyst inspired by hydrolases. *Science Advances* **2020**, *6*, eaaz0404.
(28) Bhaskaran, A.; Aitken, H. M.; Xiao, Z.; Blyth, M.; Nothling, M. D.; Kamdar, S.; O'Mara, M. L.; Connal, L. A. Enzyme inspired polymer functionalized with an artificial catalytic triad. *Polymer* **2021**, *225*, 123735.
(29) Zaks, A.; Klibanov, A. M. Enzyme-catalyzed processes in organic solvents. *Proceedings of the National Academy of Sciences* **1985**, *82*, 3192-3196.
(30) Goldberg, M. Esterification and transesterification: effect of the reaction on enzyme activity. *Trends in Biochemical Sciences* **1989**, *14*, 442.
(31) Gotor, V. Lipases and (R)-oxynitrilases: useful tools in organic synthesis. *Journal of Biotechnology* **2002**, *96*, 35-42.
(32) Lozano, P.; Daz, M.; De Diego, T.; Iborra, J. L. Ester synthesis from trimethylammonium alcohols in dry organic media catalyzed by immobilized Candida antarctica lipase B. *Biotechnology and Bioengineering* **2003**, *82*, 352-358.
(33) Breslow, R. Artificial Enzymes and Enzyme Models. In *Advances in Enzymology and Related Areas of Molecular Biology*, 1986; pp 1-60.
(34) Kheirabadi, M.; Çelebi-Ölçüm, N.; Parker, M. F. L.; Zhao, Q.; Kiss, G.; Houk, K. N.; Schafmeister, C. E. Spiroligozymes for Transesterifications: Design and Relationship of Structure to Activity. *Journal of the American Chemical Society* **2012**, *134*, 18345-18353.
(35) Zaramella, D.; Scrimin, P.; Prins, L. J. Self-Assembly of a Catalytic Multivalent Peptide–Nanoparticle Complex. *Journal of the American Chemical Society* **2012**, *134*, 8396-8399.
(36) Ema, T.; Tanida, D.; Matsukawa, T.; Sakai, T. Biomimetic trifunctional organocatalyst showing a great acceleration for the transesterification between vinyl ester and alcohol. *Chemical Communications* **2008**, 957-959.

(37) Yadav, G. D.; Trivedi, A. H. Kinetic modeling of immobilized-lipase catalyzed transesterification of n-octanol with vinyl acetate in non-aqueous media. *Enzyme Microb. Technol.* **2003**, *32*, 783-789.
(38) Singh, M.; Singh, S.; Singh, R. S.; Chisti, Y.; Banerjee, U. C. Transesterification of primary and secondary alcohols using Pseudomonas aeruginosa lipase. *Bioresource Technology* **2008**, *99*, 2116-2120.
(39) Mahapatra, P.; Kumari, A.; Kumar Garlapati, V.; Banerjee, R.; Nag, A. Enzymatic synthesis of fruit flavor esters by immobilized lipase from Rhizopus oligosporus optimized with response surface methodology. *Journal of Molecular Catalysis B: Enzymatic* **2009**, *60*, 57-63.
(40) Löfgren, J.; Görbe, T.; Oschmann, M.; Svedendahl Humble, M.; Bäckvall, J.-E. Transesterification of a Tertiary Alcohol by Engineered Candida antarctica Lipase A. *ChemBioChem* **2019**, *20* , 1438-1443.
(41) Tsukada, H.; Blow, D. M. Structure of α-chymotrypsin refined at 1.68 Å resolution. *Journal of Molecular Biology* **1985**, *184*, 703-711.
(42) D'Souza, V. T.; Bender, M. L. Miniature organic models of enzymes. *Accounts Chem Res* **1987**, *20*, 146-152.
(43) Breslow, R.; Nesnas, N. Burst kinetics and turnover in an esterase mimic. *Tetrahedron Letters* **1999**, *40*, 3335-3338.
(44) Wayman, K. A.; Sammakia, T. O-Nucleophilic Amino Alcohol Acyl-Transfer Catalysts: the Effect of Acidity of the Hydroxyl Group on the Activity of the Catalyst. *Organic Letters* **2003**, *5*, 4105-4108.
(45) Fersht, A. *Enzyme Structure and Mechanism*; W.H. Freeman, 1985.
(46) Dib, N.; Falcone, R. D.; Acuña, A.; García-Río, L. Characterization of Reverse Micelles Formulated with the Ionic-Liquid-like Surfactant Bmim-AOT and Comparison with the Traditional Na-AOT: Dynamic Light Scattering, 1H NMR Spectroscopy, and Hydrolysis Reaction of Carbonate as a Probe. *Langmuir* **2019**, *35*, 12744-12753.
(47) Sedgwick, M. A.; Trujillo, A. M.; Hendricks, N.; Levinger, N. E.; Crans, D. C. Coexisting Aggregates in Mixed Aerosol OT and Cholesterol Microemulsions. *Langmuir* **2011**, *27*, 948-954.
(48) M.J. Abraham, D. v. d. S., E. Lindahl, B. Hess, and the GROMACS development team. GROMACS User Manual 2019 ed.; 2019.
(49) Schmid, N.; Eichenberger, A. P.; Choutko, A.; Riniker, S.; Winger, M.; Mark, A. E.; van Gunsteren, W. F. Definition and testing of the GROMOS force-field versions 54A7 and 54B7. *European Biophysics Journal* **2011**, *40*, 843.
(50) Stroet, M.; Caron, B.; Visscher, K. M.; Geerke, D. P.; Malde, A. K.; Mark, A. E. Automated Topology Builder Version 3.0: Prediction of Solvation Free Enthalpies in Water and Hexane. *Journal of Chemical Theory and Computation* **2018**, *14*, 5834-5845.
(51) McGibbon, Robert T.; Beauchamp, Kyle A.; Harrigan, Matthew P.; Klein, C.; Swails, Jason M.; Hernández, Carlos X.; Schwantes, Christian R.; Wang, L.-P.; Lane, Thomas J.; Pande, Vijay S. MDTraj: A Modern Open Library for the Analysis of Molecular Dynamics Trajectories. *Biophysical Journal* **2015**, *109*, 1528-1532.
(52) Humphrey, W.; Dalke, A.; Schulten, K. VMD: Visual molecular dynamics. *Journal of Molecular Graphics* **1996**, *14*, 33-38.

Australian National University

Statement of Contribution

This thesis is submitted as a Thesis by Compilation in accordance with https://policies.anu.edu.au/ppl/document/ANUP_003405

I declare that the research presented in this Thesis represents original work that I carried out during my candidature at the Australian National University, except for contributions to multi-author papers incorporated in the Thesis where my contributions are specified in this Statement of Contribution.

Title: Dynamic Elastomers based on Bio-derived Crosslinker

Authors: **Ashwani Kumar**, Matthieu Gresil and Luke A. Connal

Publication outlet (Journal): Journal of Polymer Science

Current status of paper: Published (*J. Polym. Sci. 2023,* 1.)

Contribution to paper: My contribution to the manuscript includes project designing, synthesis, characterization, and data analysis as well as preparing and revising manuscript and figures (overall 95%).

Senior author or collaborating authors endorsement:

ASHWANI KUMAR	Ashwani	2nd March 2023
Candidate – Print Name	Signature	Date

Endorsed

LUKE CONNAL		14th March 2023
Primary Supervisor – Print Name	Signature	Date
Mark Humphrey		15th March 2023
Delegated Authority – Print Name	Signature	Date

Chapter 3 Dynamic Elastomers based on Bio-derived Crosslinker

Kumar, A.; Gresil, M.; Connal, L. A. *J. Polym. Sci.*, 2023, 1.

Preface

In this chapter, raspberry biomass was used in the construction of dynamic networks based on the oxime transesterification process. This chapter was published in Mar 2023 edition of the journal *Journal of Polymer Science*,[1] in which I am the first author. My contribution to the manuscript includes project designing, synthesis, characterization, and data analysis, as well as preparing and revising the manuscript and figures (overall 95%). The published version of the manuscript is presented here. Matthieu Gresil, a collaborator at Monash University, carried out the Dynamic Mechanical Analysis (DMA) measurements.

Foreword

This thesis is focused on the development of eco-friendly, recyclable thermosets based on dynamic chemistry. Most of the non-recyclable thermosets based on dynamic transesterification reactions are composed of monomers generated from petroleum sources. In this chapter, I address the non-recyclability of traditional thermosetting polymers obtained from fossil fuels. In this chapter, we use what we learned about transesterification in the previous chapter to investigate the catalyst free transesterification chemistry involved in thermoset development. Renewable feedstocks have the potential to serve as a viable alternative to thermosets derived from petroleum resources. Most of these thermosets rely on external catalysts for the activation of dynamic bonds. As described in the last chapter, I overcame the synthetic challenges associated with creating a catalyst to improve its

sustainability. Dynamic networks based on ester bonds, which need catalysts, is problematic since catalyst deactivation or leaching diminishes its efficacy over time and may impair reuse. A solution to this problem is the fabrication of thermosets that do not require the use of catalysts. This can be achieved by using a significant excess of exchanging functional groups or by employing exchange reactions that do not need a catalyst. In this chapter, I outline the development of a thermoset network that features catalyst-free bond exchange reactions in catalyst-dependent polyester networks by replacing oxime-esters with conventional ester linkages. Raspberry ketone was employed to construct building blocks for dynamic oxime chemistry, a readily available and renewable feedstock. The dynamic oxime transesterification exchange mechanism enables stress relaxation and the reprocessing of elastomers. In the future, these thermosets can be used to develop recyclable elastomer hydrogels.

Introduction

Plastic pollution is a serious threat to the environment. The anticipated rise in human population and global plastic consumption are likely to accelerate the growth of plastic pollution over the next few decades.[2] The worldwide effort to counteract these effects requires recycling or reusing of all plastics and careful consideration of renewable feedstocks.

One particularly useful and prevalent class of polymers are thermosets. Thermosetting polymers provide several useful engineering benefits over non-crosslinked thermoplastics. Due to their dense network structure, these polymers exhibit superior chemical resistance and have desirable mechanical and thermal properties.[3-6] However, these are rarely recyclable owing to their permanent crosslinking, which creates difficulties in downstream processing.[5, 7-10] The basic components of synthetic elastomers, such as , isoprene, chloroprene, and

butadiene, is obtained from petrochemical resources. The majority of thermoset elastomers waste is disposed of *via* incineration or landfill. If the thermoset bonds were dynamic then this would create opportunities in recycling and reuse of thermoset materials. Vitrimers are dynamic thermoset materials that were recently identified as a new type of polymer distinguished by a crosslinked network that can flow without depolymerization when heated to a specified temperature.[11-14] This behavior is attributed to the associative crosslink exchange processes, which is triggered by temperature without reduction in crosslink density, thereby preserving the crosslinked networks. Vitrimers can change their original network topology by breaking and immediately reforming a covalently crosslinked bond. The advancement of bio-derived dynamic vitrimers has gained considerable attention in an approach to alleviate some of the environmental concerns of the classical thermosets.[15-17]

There is a significant opportunity to create thermoset elastomers from sustainable feedstocks. Unlike the commercial success of polymers made from biomass, sustainable biobased elastomers are still in their infancy. Bio-based elastomers provide an opportunity to decrease carbon emissions and preserve natural resources. They can be developed using biobased monomers sourced from renewable resources or extracted directly from plants. The use of molecular biomass, such as cellulose, starch, and vegetable oil, has been extensively researched in the development of elastomers.[18-21] Natural rubber, commonly known as Hevea rubber, is the major bio-based elastomer on the market and has exceptional mechanical properties. Bio-based polyester elastomers derived from diethyl itaconate have excellent oil-resistance and can replace commercially available acrylate rubber.[22] Biobased chemically cross-linked elastomers having the same structure and qualities as traditional synthetic elastomers are being developed in order to facilitate their commercial acceptance. Red

raspberry (*Rubus idaeus*) is a popular fruit that is typically grown in the northern temperate regions. Raspberries, especially red raspberries, are rich in bioactive phytochemicals in addition to their flavour and nutritional value.[23] A greater proportion of red raspberry phytochemicals are phenolics, such as polyphenols and ellagitannins.[24] Among the phenolic compounds found in raspberries, 4(4-Hydroxyphenyl)-2-butanone, also known as frambinone or raspberry ketone is a distinctive component.[25] This is an underexplored feedstock chemical to build valuable materials.

Herein, we present a new elastomer material based on raspberry ketone (4-(4-Hydroxyphenyl)-2-butanone) as a key building block. Raspberry ketone was functionalised with styrene which upon further functionalization was converted to oximes **(*1*)** ((E)-4-(4-((4-vinylbenzyl)oxy)phenyl)butan-2-one oxime) and oxime ester **(*2*)** ((2E,2'E)-O,O'-succinylbis(4-(4-((4-vinylbenzyl)oxy)phenyl)-4-(4-((4-vinylbenzyl)oxy)phenyl)butan-2-one oxime)). The ***1*** supplies free hydroxyl group and ***2*** serves as the ester unit, thereby facilitating the catalyst free oxime transesterification exchange process involving oxime hydroxyl groups.[26] When compared to conventional dynamic thermoset based on ester bonds, these elastomers do not need a catalyst, which eliminates problems like leaching and toxicity. This work employs catalyst-free bond exchange reactions in catalyst-dependent polyester networks by replacing conventional ester linkages with oxime-esters. The resulting elastomers exhibits stress relaxation and reprocessability. This work focuses on the structural design and development of catalyst free biomass derived dynamic elastomers which offers new opportunities for utilisation in a variety of fields, including hydrogels, recyclable elastomers, and commodity plastics.

Results and Discussion

Synthesis and characterization of elastomers

A facile synthetic method was used to produce elastomers from raspberry ketone, succinyl chloride and PEGMA. Initially, a styrenic derivative of raspberry ketone was synthesised through reaction with 4-vinylbenzyl chloride (**Figure S3.1**). This raspberry ketone-styrene derivative (4-(4-((4-vinylbenzyl)oxy)phenyl)butan-2-one) was transformed into ***1*** by reacting the carbonyl group of raspberry ketone with the hydroxylamine. Moreover, raspberry ketone-styrene derivative was treated with succinyl chloride to prepare ***2*** containing ester unit. The elastomer networks were then prepared by free radical polymerisation of reaction mixture containing ***1***, ***2*** and PEGMA (**Figure 3.1a**). Initially, we synthesised polymers using components ***1*** and ***2*** only, but the resulting polymer was too brittle and inhomogeneous to characterise. We choose to use PEGMA to create improved properties with low T_g thus improving the network homogeneity and plasticity. The hydrophilicity of PEGMA would allow these thermosets to serve as potential hydrogels in future applications. Different compositions of elastomers were prepared by varying ***1*** composition (**Figure 3.1b**).

Fourier-transform infrared spectroscopy (FT-IR) was used to understand the chemical functionality of ***1***, ***2***, and elastomers. The OH stretching vibrations of ***1*** were observed at 3250 cm^{-1}. ***2*** and elastomers showed three characteristic stretching vibrations of esters. The vibrations at 1727 cm^{-1}, 1240 cm^{-1} and 1100 cm^{-1} corresponds to the C=O, C-C-O and O-C-C stretching vibrations of esters, respectively (**Figure 3.1c**).

(a)

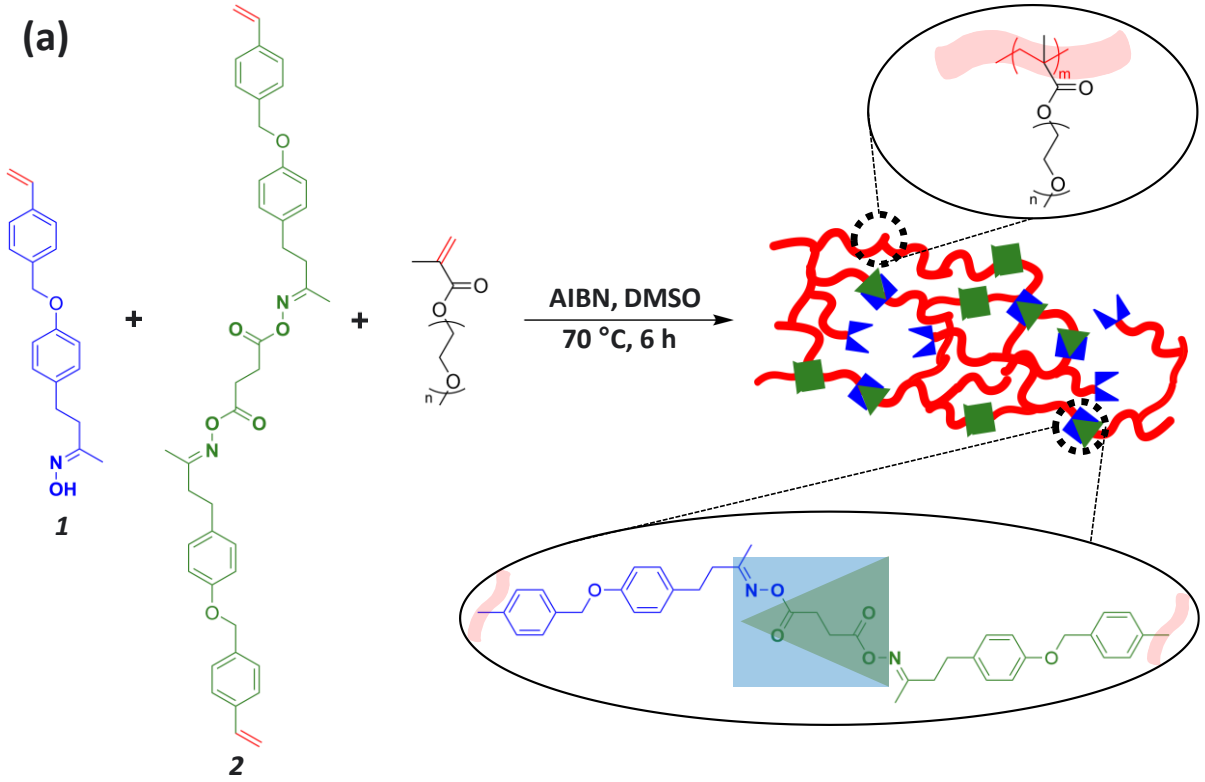

(b)

1 (Ratio)	*2 (Ratio)*	PEGMA (*Ratio*)	Sample
1	2	7	***V1***
2	2	7	***V2***
4	2	7	***V3***

(c)

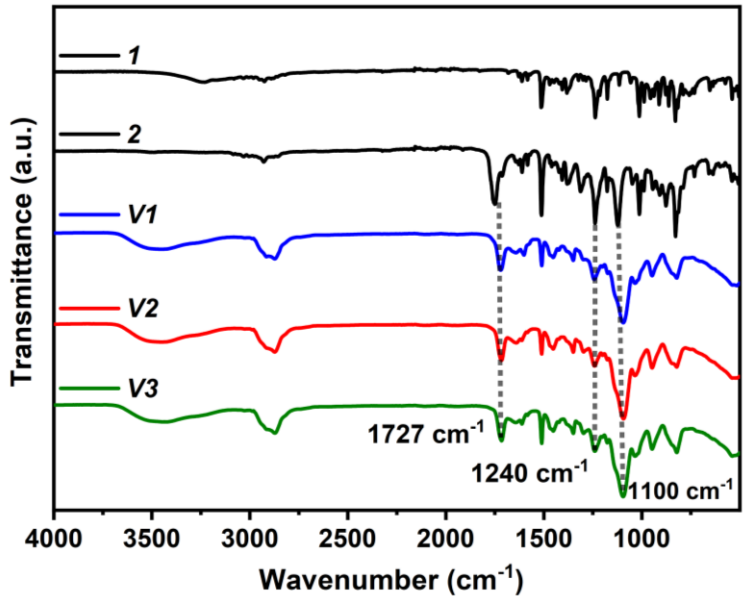

Figure 3.1: *Raspberry based elastomers, (a) synthetic route of elastomers, (b) various formulations of elastomers series prepared by varying molar ratios and (c) FT-IR spectra of* ***1****,*

***2** and elastomers. The elastomers are showing three characteristic peaks of esters at 1727 cm^{-1}, 1240 cm^{-1} and 1100 cm^{-1}.*

Thermal and Mechanical properties

The glass transition temperature (T_g) and thermal stability of elastomers were investigated using Differential Scanning Calorimetry (DSC) and Thermogravimetric Analysis (TGA), respectively. The DSC result indicates that the T_g of elastomers increases with increase in ***1*** composition, which rose from -55 °C to -40.2 °C, when composition increased from 10 to 40% (**Figure 3.2a**). This rise in T_g is due to the incorporation of bulky phenyl pendant groups to the backbone chain which restricts chain mobility.

TGA measurements were performed to understand the thermal decomposition of the elastomers. The initial weight loss around 189 °C is due to the evaporation of residual DMSO in elastomers (**Figure 3.2b**). The elastomers showed good thermal stability with 6—10% weight loss at 270 °C. Elastomers with higher ***1*** composition showed greater thermal stability at higher temperature. This increased thermal stability is attributed to the higher degree of crosslinking increased ***1*** composition.

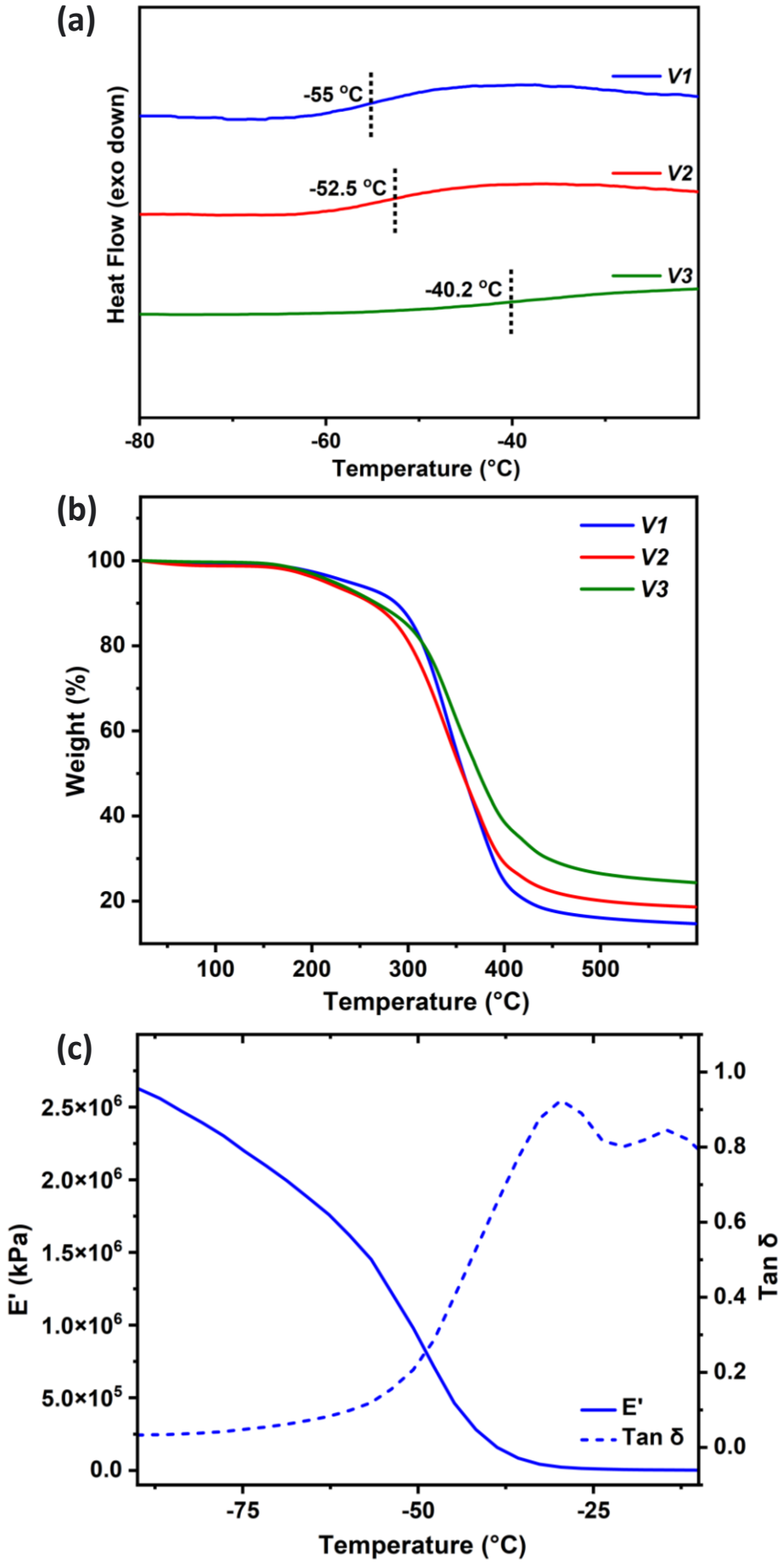
(a)
Heat Flow (exo down)
-55 °C
-52.5 °C
-40.2 °C
V1
V2
V3
-80
-60
-40
Temperature (°C)
(b)
Weight (%)
100
80
60
40
20
100
200
300
400
500
Temperature (°C)
V1
V2
V3
(c)
E' (kPa)
2.5×10^6
2.0×10^6
1.5×10^6
1.0×10^6
5.0×10^5
0.0
Tan δ
1.0
0.8
0.6
0.4
0.2
0.0
-75
-50
-25
Temperature (°C)
E'
Tan δ

Figure 3.2: *Thermal and thermomechanical properties of elastomers, (a) DSC thermogram of different elastomers were measured at a heating rate of 3 °C min^{-1}. T_g raises with higher content of **1** composition due to introduction of more bulkier phenyl pendant groups to the backbone which hindered chain motions, (b) TGA curve of elastomers, (c) temperature sweep measurement of E' of **V1** using single cantilever mode at 6.2 rads^{-1} angular frequency with a heating rate of 3 °C min^{-1} from -90 to 25 °C.*

Dynamic mechanical analysis (DMA) was used to understand the elastomers thermomechanical properties. DMA was performed on elastomers using single cantilever mode at 6.2 rads^{-1} angular frequency with a heating rate of 3 °C min^{-1} from -90 to 25 °C. The elastomers were very soft and fragile and only ***V1*** could withstand the forces of the DMA and obtain reproducible results. The storage modulus (E') of ***V1*** is 2.6 × 10^6 kPa at -90 °C and then this value suddenly decreases to 840 kPa in the rubbery state (**Figure 3.2c**).

To understand the degree of crosslinking and mechanical properties of the elastomers, swelling tests were performed in DMSO at room temperature. The swelling test showed that all the elastomers were insoluble but swollen after 24 h, yielding a gel fraction of 84.6 ± 8.7, 94.7 ± 9, and 100.6 ± 9.2 for ***V1***, ***V2***, and ***V3*** respectively (**Table 3.1**). This result suggests that, as the composition of ***1*** increases from ***V1*** to ***V3***, greater amount of ***1*** participate in the formation of permanent crosslink networks. This is consistent with the tensile testing of elastomers, which indicates that the tensile strength and Young's modulus of elastomers improves as the ***1*** content increases (**Table 3.1**).

Samples	T_g[a] (°C)	Gel fraction %[b]	Swell %[c]	Tensile Strength[d] (kPa)	Young's modulus[e] (kPa)
V1	-55	84.6 ± 8.7	171.1 ± 9	4.5 ± 2.4	0.5 ± 0.3
V2	-52.5	94.7 ± 9	161.6 ± 10	4.9 ± 2.7	0.6 ± 0.4
V3	-40.2	100.6 ± 9.2	96.3 ± 9.8	5.2 ± 3.0	1.9 ± 1.0

[a]Calculated from DSC. [b,c] Calculated using the following the equation:

$$Gel\ fraction\ \% = \frac{m_3}{m_1}\ , Swollen\ \% = \frac{m_2 - m_1}{m_1}$$

where, m_1 = initial mass of sample, m_2 = mass of swollen sample after soaking in DMSO for 24 h, m_3 = mass of dried sample after extraction of DMSO solvent.

[d,e]Calculated from the universal testing machine (Instron) at a loading rate of 3 mm min^{-1}. The mechanical properties were tested 3 times with a 10 N load cell at 48% humidity.

Table 3.1: *Gel fraction and mechanical properties of the elastomers.*

Stress Relaxation

In comparison to conventional elastomering polymer networks, the mechanical stress in dynamic covalent networks can be easily relaxed by the rearrangement of network topology using bond exchange mechanisms. The stress relaxation of elastomers was investigated at 160 °C using a rheometer. Upon heating, the oxime transesterification exchange reaction occurs between the residual oxime hydroxyl group of ***1*** with the ester group on ***2*** in elastomer network. The presence of ***1*** and ***2*** unit allow the relaxation of all 3 elastomers. ***V1*** showed fastest stress relaxation (**Figure 3.3a**). The rapid stress relaxation for ***V1*** has been attributed to the higher concentration of free exchangeable ***1***, which accelerates oxime transesterification exchange processes. While slower relaxation rates were observed for ***V2*** and ***V3*** compared to ***V1***. As ***V2*** and ***V3*** are more crosslinked compared to ***V1***, there are less free exchangeable ***1*** available for oxime transesterification exchange processes, resulting in slower relaxation. It is well known that polymers with a higher degree of crosslinking exhibit slower stress relaxation.[27-30] ***V3*** showed slightly faster stress relaxation compared to ***V2.*** Due

to high degree of crosslinking in ***V3***, some fractions of ***V3*** chains undergo chain scissioning because of the breakage of load-bearing chains when exposed to thermal stress, resulting in easy slipping. This chain slippage effect results faster stress relaxation of ***V3*** compared to ***V2***. The relaxation rate of ***V1*** increases from 120 to 160 °C, as temperature speeds up the oxime transesterification exchange process, which in turn accelerates the relaxation rate (**Figure 3.3b**).

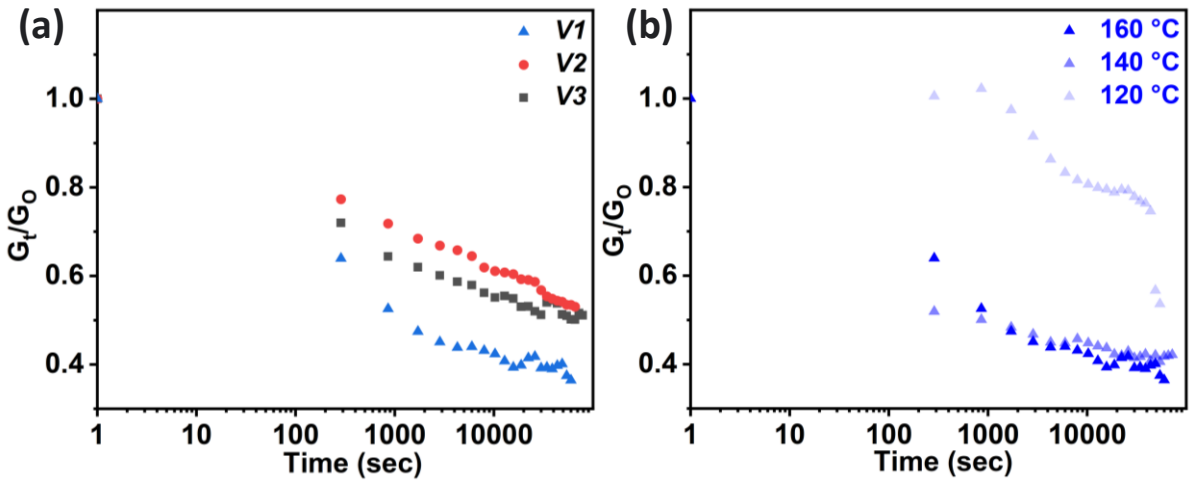

Figure 3.3: *Stress relaxation curves of elastomers, (a) stress relaxation curves at 160 °C. The stress relaxation rate increases with decrease in* ***1*** *content and (b) stress relaxation curves of* ***V1*** *at different temperatures. The increase in temperature accelerates the oxime transesterification exchange process, which in turn speeds up the stress relaxation rate.*

Tensile Testing and Reprocessing

We conducted uniaxial tensile tests to examine the mechanical properties of elastomers. Tensile tests were conducted at room temperature for elastomers with different ***1*** composition. The mechanical properties of elastomers improved as the ***1*** content increases, owing to the increasing degree of crosslinking from ***V1*** to ***V3*** (**Figure 3.4a**). On moving from

V1 to ***V3*** both the Youngs modulus (*E*) and tensile strength (σ) increased from 0.5 ± 0.3 kPa to 1.9 ± 1.0 kPa and 4.5 ± 2.4 to 5.2 ± 3.0 kPa respectively (**Table 3.1**).

The reprocessability of the elastomers was then investigated. The oxime transesterification exchange process allows reprocessing of elastomers. Small pieces were reprocessed in a hot press for 30 min at 160 °C and 8 × 10^3 kPa pressure. The elastomer pieces (using ***V3*** as an example) were completely recovered as a unified elastomer (**Figure 3.4b**). The mechanical properties of reprocessed elastomers were analysed and compared to virgin elastomers. The σ of the reprocessed ***V1***, ***V2*** and ***V3*** were recovered by 78.1 ± 10.9, 71.3 ± 12.6 and 68.1 ± 14.2% respectively (**Figure 3.4a, Table 3.1**). The recovery of σ decreases with increasing ***1*** composition were therefore expected since oxime transesterification exchange process is slower for elastomers with a higher degree of crosslinking. These results suggest that the mechanical properties of reprocessed elastomers varies significantly from those of virgin elastomers due to slow network topology rearrangements. The effects of reprocessing are likely to cause bulk inhomogeneities or degrade the polymer by random chain scissions in the polymer backbone, resulting in a decrease in the crosslinking units. FT-IR analysis was used to examine the chemical structure of elastomers before and after the reprocessing step. After reprocessing, there was no noticeable change in the FT-IR spectra, especially in regard to the three characteristic peaks of ester at 1727 cm^{-1}, 1240 cm^{-1} and 1100 cm^{-1}. This indicates that the chemical functionality was successfully preserved (**Figure 3.4c**).

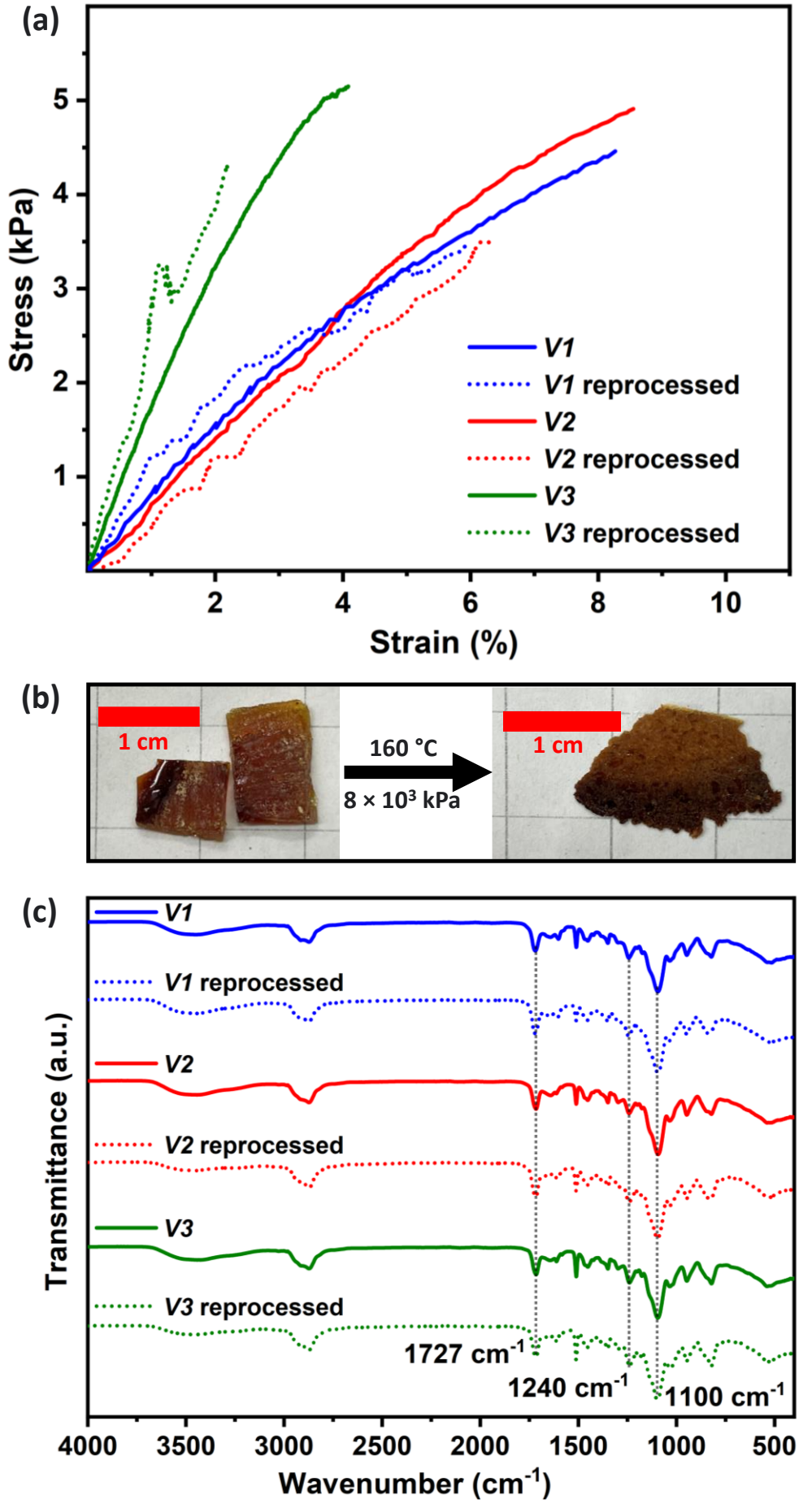
(a)
Stress (kPa)
Strain (%)
V1
V1 reprocessed
V2
V2 reprocessed
V3
V3 reprocessed
(b)
1 cm
160 °C
8 × 10³ kPa
1 cm
(c)
Transmittance (a.u.)
Wavenumber (cm⁻¹)
1727 cm⁻¹
1240 cm⁻¹
1100 cm⁻¹

Figure 3.4: *Reprocessing and stress-strain curves of elastomers, (a) stress-strain curves of virgin and reprocessed elastomers, (b) reprocessing of small pieces of* ***V3*** *by hot pressing at 160 °C for 30 min at a pressure of 8 × 10^3 kPa and (c) FT-IR spectra of virgin and reprocessed elastomers. The chemical functionality of the ester group was retained after reprocessing.*

Conclusion

This work reports the synthesis of soft elastomeric vitrimer type elastomers from plentiful and sustainable raspberry derived feedstocks. The degree of crosslinking increases upon increasing the amount of ***1***. When moving from ***V2*** to ***V3***, the degree of crosslinking increases more than ***V1*** to ***V2***. Increases in the crosslink density results in improved mechanical properties and thermal stability. The oxime transesterification exchange mechanism involving oxime hydroxyl groups is sensitive to temperature. Therefore, at a suitable temperature, the network topology of the elastomer can be reorganised *via* oxime transesterification bond exchange, enabling stress relaxation and reprocessability. The elastomers can be reprocessed in 30 min at 160 °C and 8 × 10^3 kPa pressure. After reprocessing, the elastomers original tensile strength can be recovered up to 78.1 ± 10.9%. We believe that the sustainability and simplicity of our approach may open new ways for the development of catalyst-free transesterification elastomers from renewable biomass.

Supporting Information

Experimental

All commercially obtained solvents and reagents were used without further purification. Raspberry ketone (4-(4-Hydroxyphenyl)-2-butanone), succinyl chloride 95%, 4-vinylbenzyl chloride, Poly(ethylene glycol) methyl ether methacrylate (PEGMA) M_n 500, 2,2'-Azobis(2-methylpropionitrile) (AIBN), sodium acetate and hydroxylamine hydrochloride were all purchased from the Sigma Aldrich.

^{1}H and ^{13}C solution-state NMR were recorded on a Bruker Ascend 400 MHz spectrometer (400 MHz for ^{1}H and 100 MHz for ^{13}C). Chemical shifts δ are reported relative to the resonance signal of ^{1}H or ^{13}C cores of tetramethylsilane and in ppm. The ^{1}H spectra were calibrated by setting the solvent peaks, caused by remaining traces of protons, to values known from the literature (δ $CHCl_3$ = 7.26 ppm). The ^{13}C spectra were calibrated by setting the deuterium coupled solvent signal to values known from the literature (δ $CDCl_3$ = 77.16 ppm). The coupling constants J are reported in Hz.

Fourier transform infrared spectroscopy (FTIR) was performed on a Perkin Elmer Spectrum 2, with a 0.5 cm^{-1} resolution, over 32 scans from 400 to 4000 cm^{-1}. All the measurements were performed at room temperature.

Low-resolution ESI mass spectra were recorded on a Micromass LC-ZMD single quadrupole liquid chromatograph mass spectrometer while high-resolution measurements were conducted on an LCT Premier time-of-flight instrument.

Differential scanning calorimetry (DSC) was performed using a TA Instruments Q20 at a heating rate of 3 °C min^{-1}. The sample (~10 mg) was placed in a closed aluminum crucible. The data was recorded between -80 °C and -20 °C.

Thermal gravimetric analysis (TGA) was performed on a TA Instruments TGA Q 500 under a N_2 atmosphere over a temperature range of 25 - 600 °C at a heating rate of 3 °C min^{-1}.

Dynamic mechanical analysis (DMA) was performed on a TA Instruments DMA 850-00552. Small films were cut into rectangular shape (17.5 × 6.3 × 2.6 mm) and measured using single cantilever mode at 6.2 $rads^{-1}$ angular frequency with a heating rate of 3 °C min^{-1} from -90 to -10 °C.

The Stress-relaxation tests were carried out on Anton Paar MCR 702 multidrive rheometer using a plate geometry (PP25) with a 25 mm diameter. The material was placed on the rheometer, and the upper geometry was lowered. After reaching the appropriate temperature (120 - 160 °C), the samples were equilibrated for 30 min and then a constant shear strain of 1.2% was applied, and the time dependent stress relaxation measurement was recorded.

Tensile tests were conducted on a universal testing machine (Instron) at a loading rate of 3 mm min^{-1}. The mechanical properties were tested 3 times with a 10 N load cell at 48% humidity.

Reprocessing experiment was performed on a PHI hydraulic press. The elastomer films were cut into small pieces and then placed into round steel mold (1 cm diameter) and subjected to a 20 min thermal equilibration at 160 °C. The elastomer films were then reprocessed at 160

°C for 30 min at a pressure of 8 MPa. The reprocessed elastomers were demolded after reaching room temperature.

Swelling test were conducted three times by soaking samples weighing m_1 in DMSO at room temperature for 24 h. Then, the DMSO and any sol fraction dissolved in the DMSO were carefully removed using a syringe. The samples were blotted to remove DMSO on the surface, and left drying under N_2 flow for 1 h, the swollen weight m_2 was determined. After that the samples were washed 3 times with methanol and then left for drying in oven at 120 °C for 90 min to ensure a complete removal of the residual solvent and got the mass of m_3. The gel fraction and swelling ratio were calculated using following equation:

$$Swollen\ \% = \frac{m_2 - m_1}{m_1}$$

$$Gel\ fraction\ \% = \frac{m_3}{m_1}$$

Synthesis of raspberry ketone-styrene (4-(4-((4-vinylbenzyl)oxy)phenyl)butan-2-one): In a round bottom flask raspberry ketone (4000 mg, 24.35 mmol, 1.00 eq) and K_2CO_3 (5049.80 mg, 36.53 mmol, 1.5 eq) in acetonitrile solvent were added and allowed to stir for 15 min. Then 4-vinylbenzyl chloride (5149.12 µl, 36.53 mmol, 1.5 eq) was added and stirred at 50 °C for 6 h and thereafter cooled down to room temperature followed by addition of excess of water. The reaction mixture was kept in the fridge overnight. The product was filtered and washed with cold MeCN/H_2O (15:85) solution. The resulting product was dried at 35–40 °C yielded product as a solid porous (76%) (**Figure S3.1**). ^{1}H-NMR (400 MHz, $CDCl_3$, 298 K): δ = 7.42 (d, 2H, *J* = 8.4 Hz); 7.38 (d, 2H, *J* = 8.4 Hz); 7.09 (d, 2H, *J* = 8.8 Hz); 6.89 (d, 2H, *J* = 8.8 Hz); 6.72 (dd, 1H, *J* = 17.6, 10.8 Hz); 5.76 (dd, 1H, *J* = 17.6, 1.2 Hz); 5.26 (dd, 1H, *J* = 10.8, 0.8 Hz); 5.03 (s, 2H);

2.84 (t, 2H, *J* = 6.8 Hz); 2.72 (t, 2H, *J* = 6.4 Hz); 2.13 (s, 3H) (**Figure S3.2**). ^{13}C NMR (100 MHz, $CDCl_3$, 298 K): δ = 208.3, 157.3, 137.4, 136.8, 136.6, 133.5, 129.4, 127.8, 126.5, 115.0, 114.2, 69.9, 45.6, 30.2, 29.0 (**Figure S3.3**). MS (ESI) was calculated for $C_{19}H_{20}O_2Na^+$ ([M + Na]$^+$): 303.1361 Found: 303.1362.

Synthesis of oxime ((E)-4-(4-((4-vinylbenzyl)oxy)phenyl)butan-2-one oxime) (*1*): In a 250 mL round bottom flask, raspberry ketone-styrene (4500 mg, 16.05 mmol, 1.00 eq) were first dissolved in THF. Then aqueous solution of $NH_2OH.HCl$ (1672.97 mg, 24.07 mmol, 1.5 eq) and NaOAc (3291.61 mg, 40.12 mmol, 2.5 eq) were charged to the round bottom flask. Then, ethanol was gently added until white solid precipitates appeared at room temperature. The product was filtered and washed with THF/H_2O (10:90) solution. The resulting product was dried at 35–40 °C yielded product (80%) (**Figure S3.1**).^{1}H NMR (400 MHz, $CDCl_3$, 298 K): δ = 7.42 (d, 2H, *J* = 8.6 Hz), 7.38 (d, 2H, *J* = 7.9 Hz), 7.12 (d, 1H, *J* = 3.1 Hz), 7.10 (d, 1H, *J* = 3.1 Hz), 6.91 (d, 1H, *J* = 2.7 Hz), 6.89 (d, 1H, *J* = 2.6 Hz), 6.72 (dd, 1H, *J* = 17.6, 10.9 Hz), 5.76 (d, 1H, *J* = 17.6 Hz), 5.25 (d, 1H, *J* = 10.9 Hz), 5.02 (s, 2H), 2.86 – 2.77 (m, 2H), 2.76 – 2.56 (m, 2H), 1.97 (s, 3H) (**Figure S3.4**). ^{13}C NMR (100 MHz, $CDCl_3$, 298 K): δ =158.5, 157.3, 137.4, 136.8, 136.6, 133.5, 129.4, 127.8, 126.5, 115.0, 114.2, 69.9, 38.0, 31.9, 13.8 (**Figure S3.5**). MS (ESI) was calculated for $C_{19}H_{21}NO_2Na^+$ ([M + Na]$^+$): 318.1470. Found: 318.1474.

Synthesis of oxime ester ((2E,2'E)-O,O'-succinylbis(4-(4-((4-vinylbenzyl)oxy)phenyl)-4-(4-((4-vinylbenzyl)oxy)phenyl)butan-2-one oxime)) (*2*): In a 100 mL round bottom flask, oxime (150 mg, 0.50 mmol, 1.00 eq) was first dissolved in minimum volume of 1,4-Dioxane, resulting a cloudy solution. Then K_2CO_3 (105.10 mg, 0.76 mmol, 1.5 eq) was added and stired for 15 min. The round bottom flask was purged with N_2 for 10 min, after that succinyl chloride (39.15 µl, 0.35 mmol, 0.7 eq) was added. The reaction mixture was stirred in oil bath at 50 °C for 1 h.

After 1 h excess water was added to the reaction mixture resulting formation of pale yellowish precipitates. The precipitates were filtered and washed 3 times with water. The resulting product was dried at 35-40 °C yielded pale yellow product (62%)(**Figure S3.1**).^{1}H NMR (400 MHz, $CDCl_3$, 298 K): δ = 7.42 (d, 4H, *J* = 8.3 Hz), 7.38 (d, 4H, *J* = 8.2 Hz), 7.14 – 7.07 (m, 4H), 6.93 – 6.87 (m, 4H), 6.72 (dd, 2H, *J* = 17.6, 10.9 Hz), 5.76 (dd, 2H, *J* = 17.6, 1.0 Hz), 5.26 (d, 2H, *J* = 10.9 Hz), 5.03 (s, 4H), 2.86 – 2.57 (m, 12H), 2.05 – 1.93 (m, 6H) (**Figure S3.6**). ^{13}C NMR (100 MHz, $CDCl_3$, 298 K): δ = 208.3, 170.1, 166.4, 157.4, 137.4, 136.7, 136.5, 129.4, 129.4, 127.8, 127.7, 126.5, 115.0, 114.2, 69.9, 45.5, 37.9, 33.0, 31.7, 29.0, 28.1, 20.6, 15.9 (**Figure S3.7**). MS (ESI) was calculated for $C_{42}H_{44}N_2O_6Na^+$ ([M + Na]$^+$): 695.3097 Found: 695.3098.

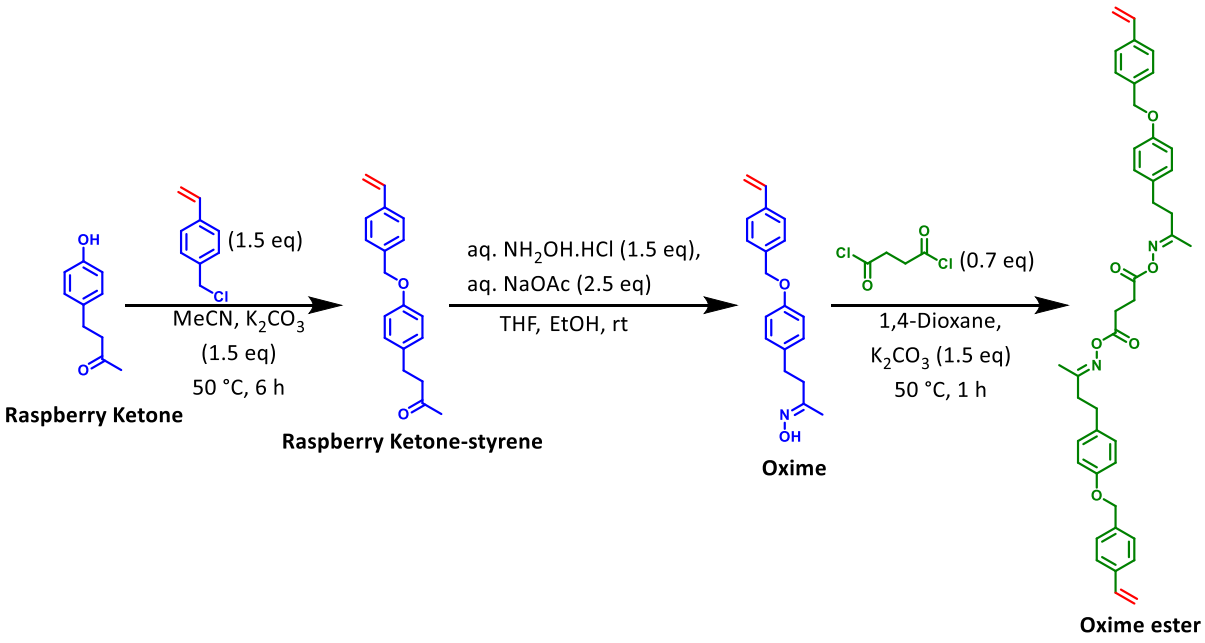

Figure S3.1: *Synthetic routes of raspberry ketone-styrene, oxime and oxime ester.*

Synthesis of thermoset elastomers: In 100 mL round bottom flask, ***1*** (219.61 mg, 0.74 mmol) and ***2*** (1000 mg, 1.48 mmol) were dissolved in minimuim amount of DMSO solvent. The solution was heated to a high temperature to dissolve completely. After that inhibitor free PEGMA (2602.25 mg, 5.20 mmol) was added. Then whole reaction mixture was transferred to

a reactangular mold (*ca.* 60 × 35 × 30 mm) followed by addition of AIBN (1.1 mol%). The reaction mixture was sealed and purged with the N_2 for 30 min and placed in preheated oil bath at 70 °C for 6 h. The elastomer films were dried at 90 °C for 7 days under reduced pressure, 120 °C for 2 days and 190 °C for 2 h. Similarly, ***V2*** and ***V3*** were prepared using same method by varying molar ratios of components.

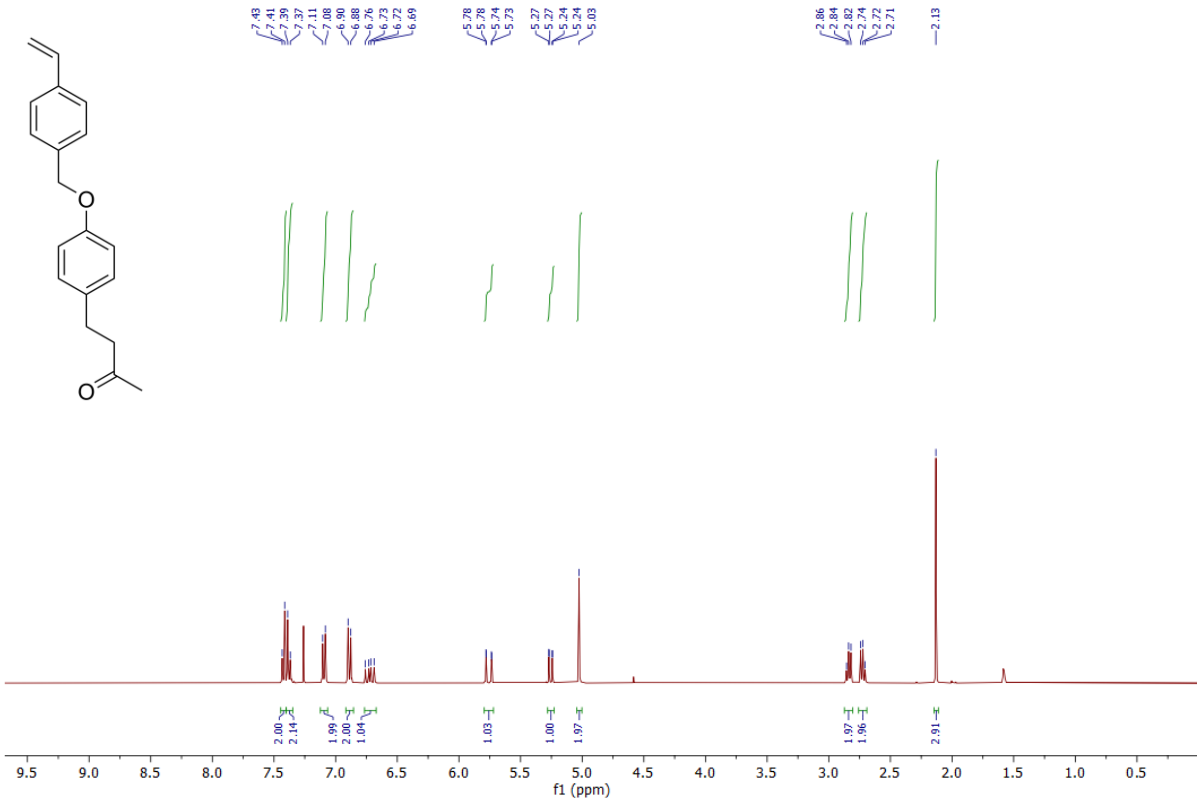

Figure S3.2: *^{1}H NMR of raspberry ketone-styrene in $CDCl_3$.*

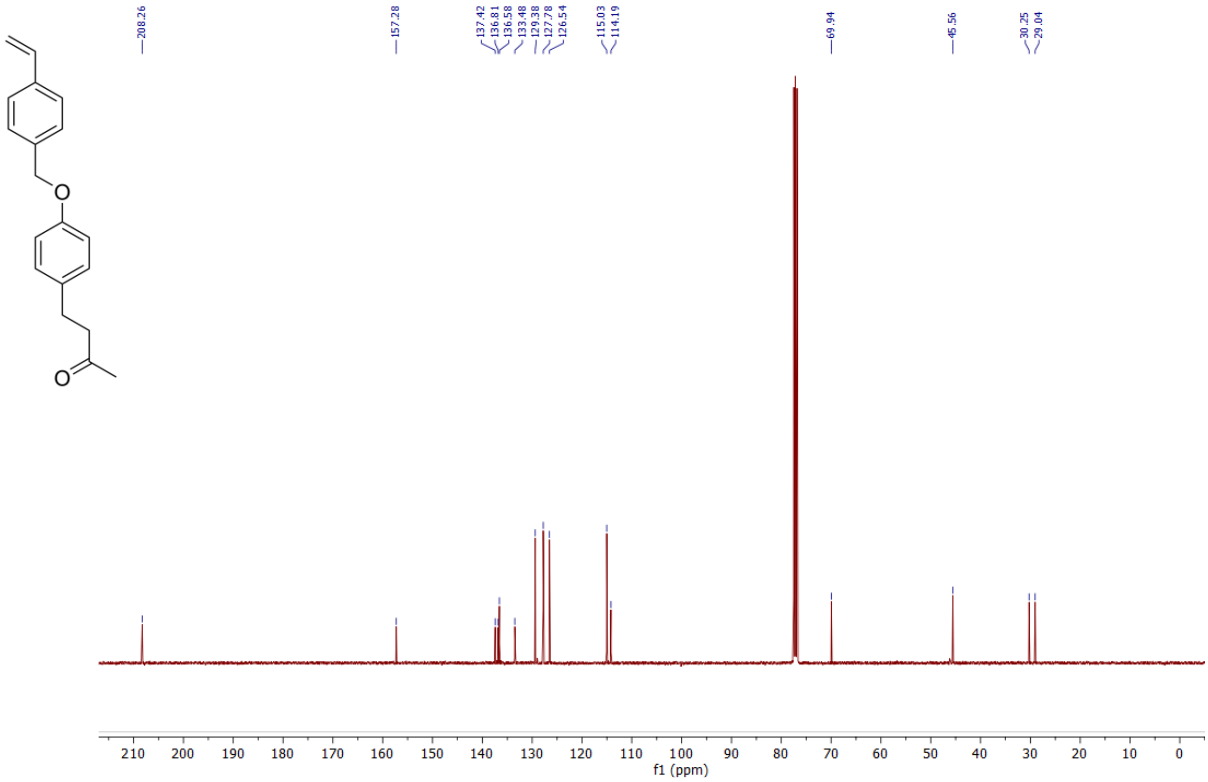

Figure S3.3: *^{13}C NMR of raspberry ketone-styrene in $CDCl_3$.*

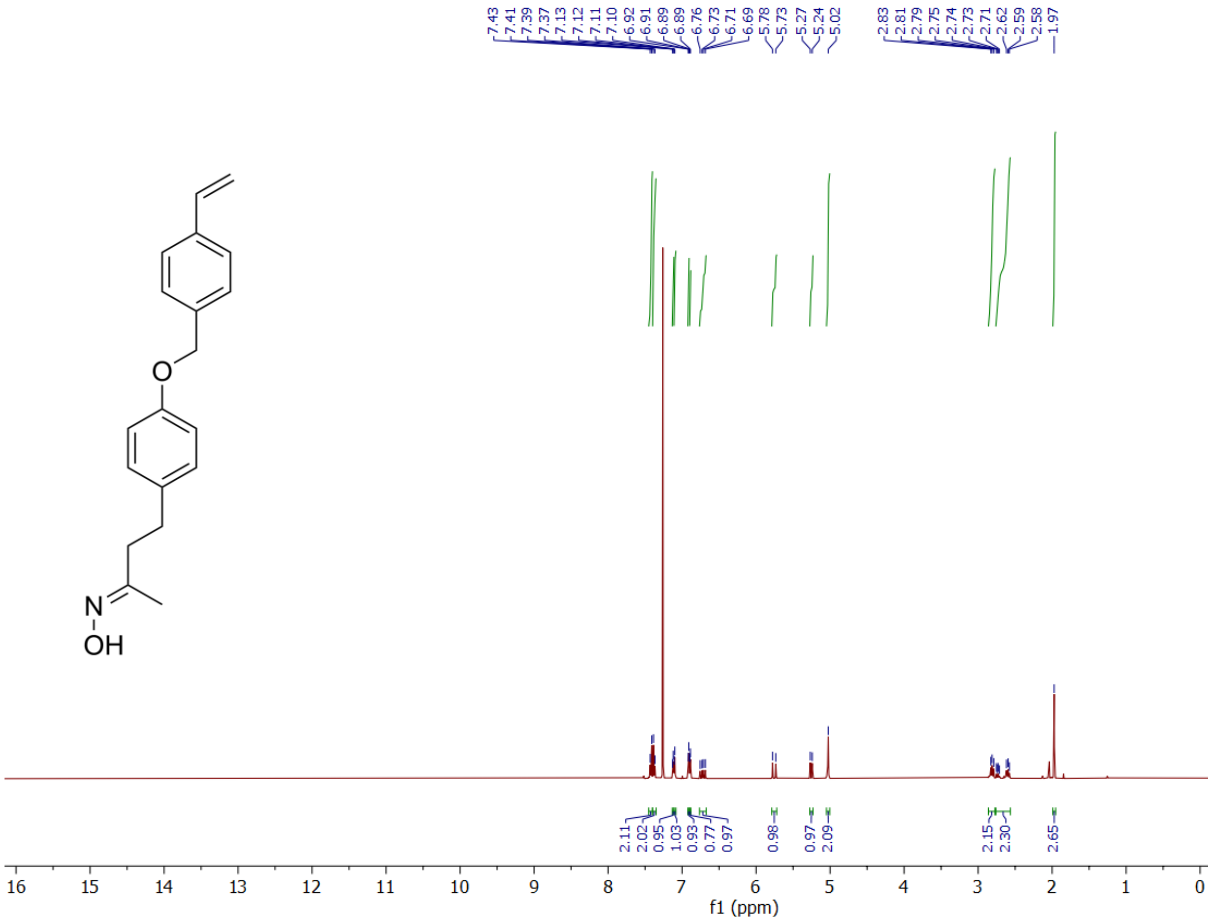

Figure S3.4: *^{1}H NMR of **1** in $CDCl_3$.*

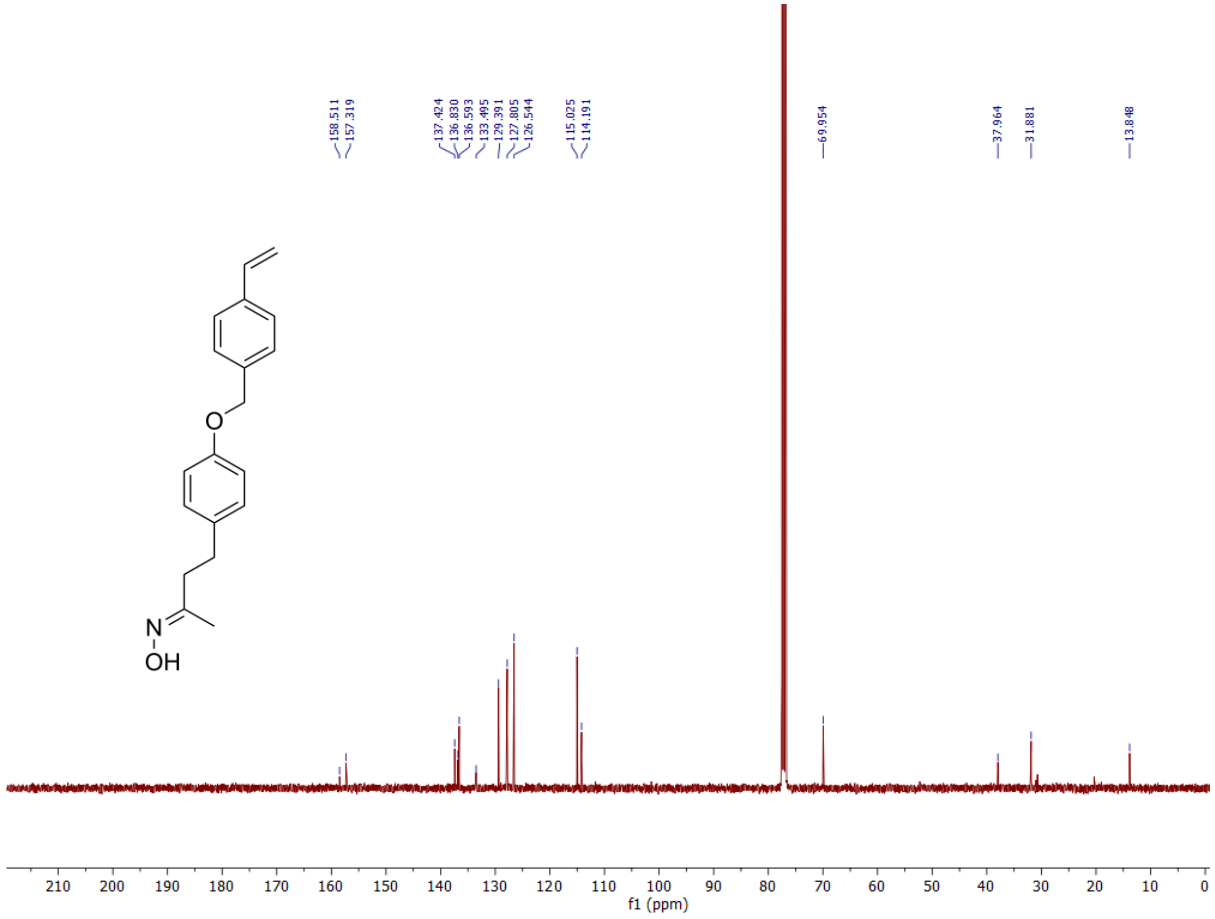

Figure S3.5: *^{13}C NMR of **1** in $CDCl_3$.*

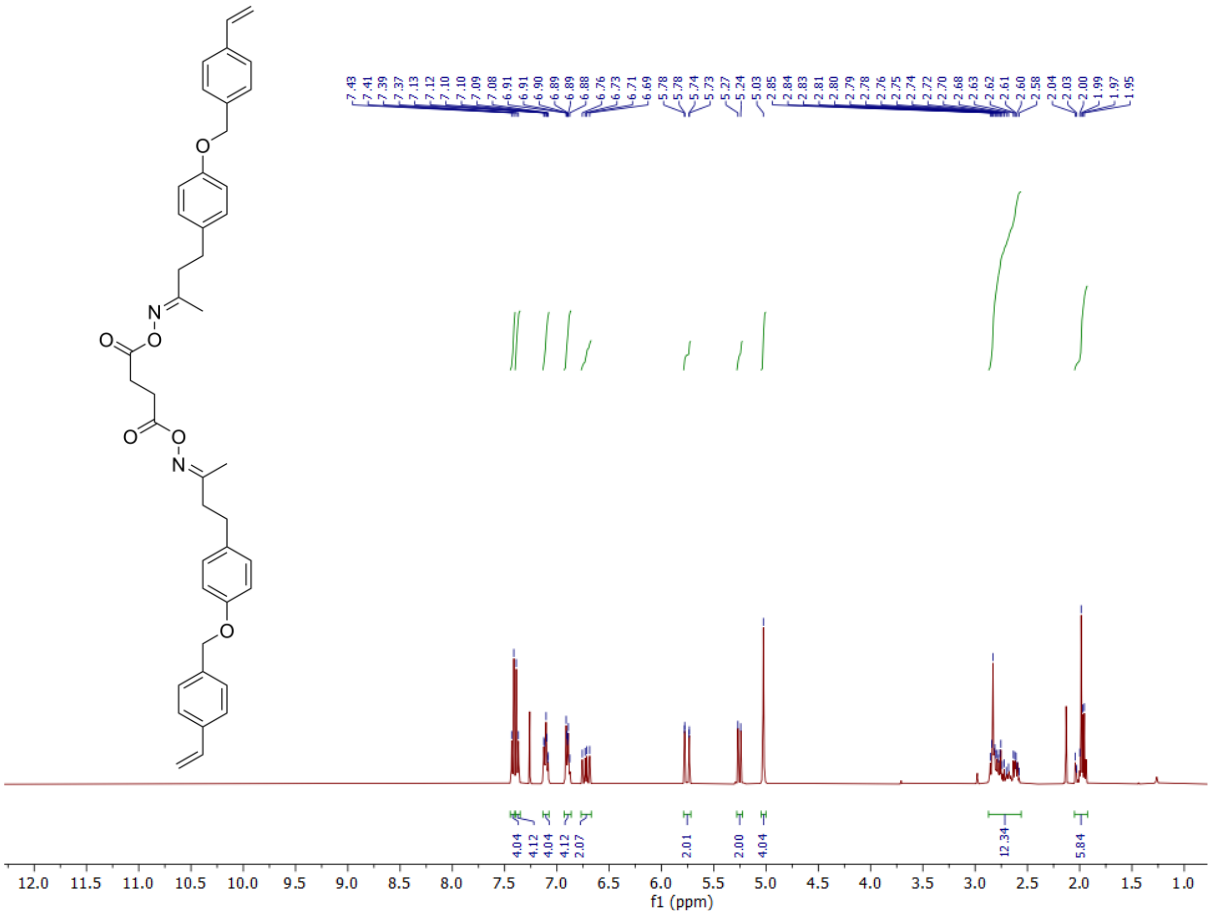

Figure S3.6: *^{1}H NMR of **2** in $CDCl_3$.*

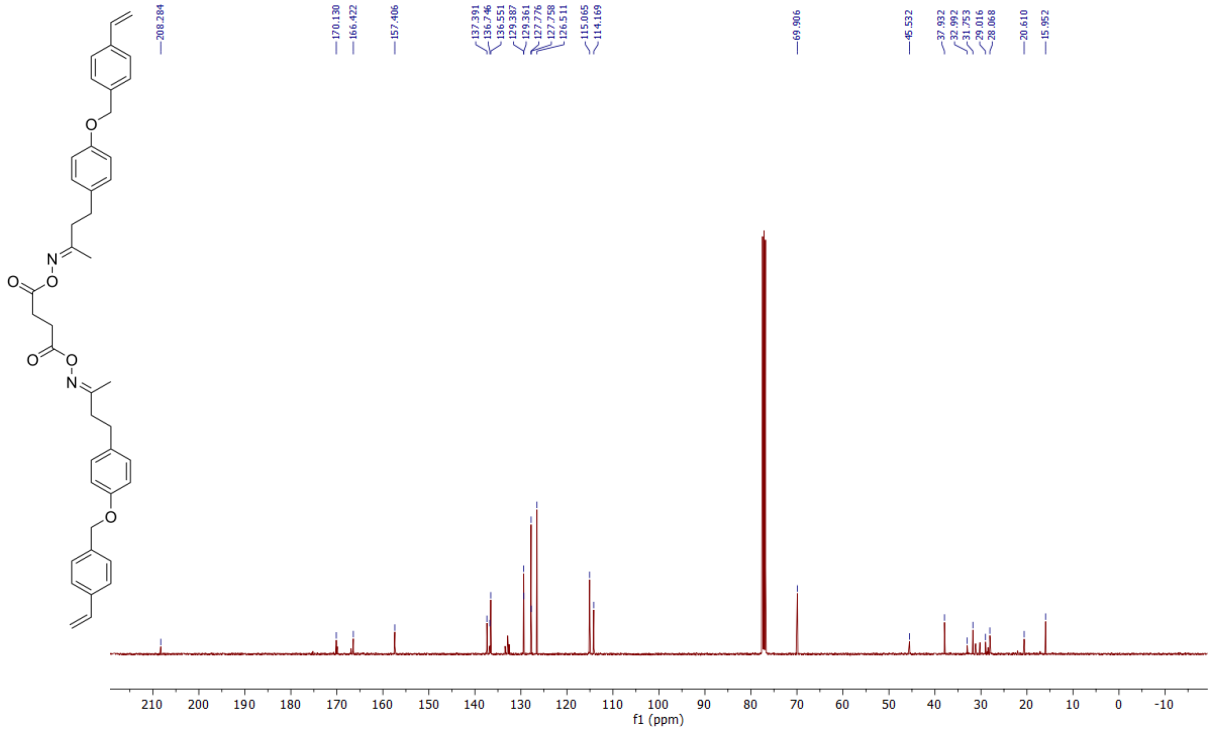

Figure S3.7: *^{13}C NMR of **2** in $CDCl_3$.*

References

(1) Kumar, A.; Gresil, M.; Connal, L. A. Dynamic elastomers based on bio-derived crosslinker. *Journal of Polymer Science* 2023, 1.
(2) Lau, W. W. Y.; Shiran, Y.; Bailey, R. M.; Cook, E.; Stuchtey, M. R.; Koskella, J.; Velis, C. A.; Godfrey, L.; Boucher, J.; Murphy, M. B.; et al. Evaluating scenarios toward zero plastic pollution. *Science* **2020**, *369*, 1455-1461.
(3) Ma, S.; Webster, D. C. Degradable thermosets based on labile bonds or linkages: A review. *Progress in Polymer Science* **2018**, *76*, 65-110.
(4) Raquez, J. M.; Deléglise, M.; Lacrampe, M. F.; Krawczak, P. Thermosetting (bio)materials derived from renewable resources: A critical review. *Progress in Polymer Science* **2010**, *35*, 487-509.
(5) Zhao, X.-L.; Liu, Y.-Y.; Weng, Y.; Li, Y.-D.; Zeng, J.-B. Sustainable Epoxy Vitrimers from Epoxidized Soybean Oil and Vanillin. *ACS Sustainable Chemistry & Engineering* **2020**, *8*, 15020-15029.
(6) Alabiso, W.; Schlögl, S. The Impact of Vitrimers on the Industry of the Future: Chemistry, Properties and Sustainable Forward-Looking Applications. *Polymers* **2020**, *12*, 1660.
(7) Häußler, M.; Eck, M.; Rothauer, D.; Mecking, S. Closed-loop recycling of polyethylene-like materials. *Nature* **2021**, *590*, 423-427.
(8) Hopewell, J.; Dvorak, R.; Kosior, E. Plastics recycling: challenges and opportunities. *Philosophical Transactions of the Royal Society B: Biological Sciences* **2009**, *364*, 2115-2126.

(9) Singh, N.; Hui, D.; Singh, R.; Ahuja, I. P. S.; Feo, L.; Fraternali, F. Recycling of plastic solid waste: A state of art review and future applications. *Composites Part B: Engineering* **2017**, *115*, 409-422.
(10) Rahimi, A.; García, J. M. Chemical recycling of waste plastics for new materials production. *Nature Reviews Chemistry* **2017**, *1*, 0046.
(11) Montarnal, D.; Capelot, M.; Tournilhac, F.; Leibler, L. Silica-Like Malleable Materials from Permanent Organic Networks. *Science* **2011**, *334*, 965-968.
(12) Capelot, M.; Unterlass, M. M.; Tournilhac, F.; Leibler, L. Catalytic Control of the Vitrimer Glass Transition. *ACS Macro Letters* **2012**, *1*, 789-792.
(13) Van Zee, N. J.; Nicolaÿ, R. Vitrimers: Permanently crosslinked polymers with dynamic network topology. *Progress in Polymer Science* **2020**, *104*, 101233.
(14) Capelot, M.; Montarnal, D.; Tournilhac, F.; Leibler, L. Metal-Catalyzed Transesterification for Healing and Assembling of Thermosets. *Journal of the American Chemical Society* **2012**, *134*, 7664-7667.
(15) Vidil, T.; Llevot, A. Fully Biobased Vitrimers: Future Direction toward Sustainable Cross-Linked Polymers. *Macromolecular Chemistry and Physics* **2022**, *223*, 2100494.
(16) Lucherelli, M. A.; Duval, A.; Avérous, L. Biobased vitrimers: Towards sustainable and adaptable performing polymer materials. *Progress in Polymer Science* **2022**, *127*, 101515.
(17) Kumar, A.; Connal, L. A. Bio-based Transesterification Vitrimers. *Macromolecular Rapid Communications* 2200892.
(18) Ohara, H. Biorefinery. *Applied Microbiology and Biotechnology* **2003**, *62*, 474-477.
(19) Sheldon, R. A. Green and sustainable manufacture of chemicals from biomass: state of the art. *Green Chemistry* **2014**, *16*, 950-963.
(20) Papageorgiou, G. Z.; Papageorgiou, D. G.; Tsanaktsis, V.; Bikiaris, D. N. Synthesis of the bio-based polyester poly(propylene 2,5-furan dicarboxylate). Comparison of thermal behavior and solid state structure with its terephthalate and naphthalate homologues. *Polymer* **2015**, *62*, 28-38.
(21) Montero de Espinosa, L.; Meier, M. A. R. Plant oils: The perfect renewable resource for polymer science. *European Polymer Journal* **2011**, *47*, 837-852.
(22) Yang, H.; Ji, H.; Zhou, X.; Lei, W.; Zhang, L.; Wang, R. Design, Preparation, and Evaluation of a Novel Elastomer with Bio-Based Diethyl Itaconate Aiming at High-Temperature Oil Resistance. *Polymers* **2019**, *11*, 1897.
(23) Basu, P.; Maier, C. In vitro antioxidant activities and polyphenol contents of seven commercially available fruits. *Pharmacognosy research* **2016**, *8*, 258.
(24) Liu, M.; Li, X. Q.; Weber, C.; Lee, C. Y.; Brown, J.; Liu, R. H. Antioxidant and antiproliferative activities of raspberries. *Journal of Agricultural and Food Chemistry* **2002**, *50*, 2926-2930.
(25) Borejsza-Wysocki, W.; Hrazdina, G. Biosynthesis of p-hydroxyphenylbutan-2-one in raspberry fruits and tissue cultures. *Phytochemistry* **1994**, *35*, 623-628.
(26) He, C.; Shi, S.; Wang, D.; Helms, B. A.; Russell, T. P. Poly(oxime–ester) Vitrimers with Catalyst-Free Bond Exchange. *Journal of the American Chemical Society* **2019**, *141*, 13753-13757.
(27) Lossada, F.; Jiao, D.; Yao, X.; Walther, A. Waterborne Methacrylate-Based Vitrimers. *ACS Macro Letters* **2020**, *9*, 70-76.
(28) Hayashi, M.; Sugimoto, K.; Takasu, A. Preparation of All Polyester-Based Semi-IPN Elastomers Containing Self-Associative or Non-Associative Guest Chains via Post-Blending Cross-Linking. *Macromolecular Materials and Engineering* **2019**, *304*, 1900147.

(29) Golkaram, M.; Fodor, C.; van Ruymbeke, E.; Loos, K. Linear Viscoelasticity of Weakly Hydrogen-Bonded Polymers near and below the Sol–Gel Transition. *Macromolecules* **2018**, *51*, 4910-4916.
(30) Chen, Q.; Liang, S.; Shiau, H.-s.; Colby, R. H. Linear Viscoelastic and Dielectric Properties of Phosphonium Siloxane Ionomers. *ACS Macro Letters* **2013**, *2*, 970-974.

Australian National University

Statement of Contribution

This thesis is submitted as a Thesis by Compilation in accordance with https://policies.anu.edu.au/ppl/document/ANUP_003405

I declare that the research presented in this Thesis represents original work that I carried out during my candidature at the Australian National University, except for contributions to multi-author papers incorporated in the Thesis where my contributions are specified in this Statement of Contribution.

Title: Upcycling waste: Fully biomass-derived and backyard compostable imine thermosets

Authors: **Ashwani Kumar**, Brett Pollard and Luke A. Connal

Publication outlet (Journal): In preparation

Current status of paper: In preparation

Contribution to paper: My contribution to the manuscript includes project designing, synthesis, characterization, and data analysis as well as preparing and revising manuscript and figures (overall 80%).

Senior author or collaborating authors endorsement:

ASHWANI KUMAR	Ashwani	2nd March 2023
Candidate – Print Name	Signature	Date

Endorsed

LUKE CONNAL		14th March 2023
Primary Supervisor – Print Name	Signature	Date

Mark Humphrey		15th March 2023
Delegated Authority – Print Name	Signature	Date

Chapter 4 Upcycling waste: Fully biomass-derived and backyard compostable imine thermosets

Kumar, A.; Brett, P.; Connal, L. A., ***in preparation*.**

Preface

In this chapter, abundant shrimp/crab and cellulose waste were harnessed as feedstocks to craft biodegradable imine thermosets. This chapter forms the basis of a manuscript that is ready to submit and in which I am the first author. My contribution to the manuscript includes project designing, synthesis, characterization, and data analysis, as well as preparing and revising the manuscript and figures (overall 80%). Brett Pollard, a PhD student in Connal lab, did the synthesis, characterization, and editing of the manuscript and figures.

Foreword

The overall goal of this thesis is to develop green, biodegradable, and dynamic thermosets using abundant biomass. A large number of currently accessible thermosets are produced from nonrenewable resources and are nonbiodegradable, causing environmental problems. In this chapter, I address the non-recyclability and non-biodegradability of conventional thermosetting polymers. In this chapter, I focus on upcycling cellulose and shrimp shell wastes to create biodegradable thermosets with dynamic properties. This chapter improves the sustainability of thermosets compared to the previous chapter by incorporating abundant cellulose and shrimp shells, together with a simple synthetic strategy and the ability to biodegrade at the end of their life. Moreover, the development of catalyst-free dynamic thermosets was further broadened in this chapter, building on the foundation laid in the previous chapter by the introduction of the catalyst-free transesterification process. Fully

biomass-derived dynamic imine thermosets are easily prepared by reacting chitosan with a novel levoglucosenone diketone (***1***) at room temperature. Thermosets exhibited remarkable thermal and mechanical properties. The dynamic nature of Schiff base allows thermosets to show stress relaxation behavior and reprocessability. These thermosets can be easily degraded in a home compost within 4–5 days. Altogether, the material has the potential to replace market-dominant thermoset plastics, which are ecologically harmful.

Introduction

Across every aspect of contemporary life, plastics have now become a necessary commodity owing to their incredible properties, low cost, light weight, transparency, and high stability.[1-3] The advancement of bio-derived polymers to address the environmental concerns of plastic reliance has gained significant attention. Biomass materials confers multiple advantages, both conserving resources and minimizing negative impact on the environment (in both their preparation and end-of-life).[4] Biomass feedstocks such as lignin,[5] rosin,[6] chitosan,[7] linseed oil,[8] and cellulose[9] have been employed to develop polymers with diverse features. Cellulose is the most abundant organic substance in the world.[10] Cellulose is utilised as a non-petroleum renewable feedstock for the production of valuable substrates such as 5-hydroxymethylfurfural (HMF)[11] and levoglucosenone (LGO).[12] LGO is a potential bio-renewable resource platform for the chemical industry.[13] LGO has an edge over other biomass platform molecules as it is readily prepared at a multi-ton scale *via* pyrolysis of industrial and urban waste cellulose sources, such as wastepaper, sawdust or wood chip. Among the numerous polysaccharides that can be produced from aquatic lifeforms, chitin is the most prevalent natural polymer following cellulose,[14] with roughly 100 billion tons of chitin bio-

synthesized annually. Chitosan is generally derived *via* alkaline deacetylation of chitin and has been extensively applied in the biomedical and pharmaceuticals because of its remarkable biocompatibility and biodegradability.[15, 16]

A particular environmentally unfriendly class of polymer are thermosets. Thermosets are generally immiscible and infusible. As they age or fail to operate, thermosets are typically burned or buried as landfill, which is an unsustainable end of life strategy resulting in environmental contamination. Development of crosslinking, reprocessing, self healing and re-forming crosslinked networks remains a challenge to allow sustainable production processes for thermosetting materials. One way to overcome these constraints is to incorporate the covalent adaptable networks (CANs) into thermosets framework.[17-21] CANs are reversibly dynamic polymeric materials with covalent crosslinks that can be driven by stimuli such as light, catalyst, temperature, or pH. Montarnal *et al.* have developed a novel class of CANs, coined vitrimers, which involve high temperature transesterification process using metal catalysts.[22] Since then, numerous chemistries have been investigated in the fields of vitrimers ranging from boronic ester exchange,[23, 24] disulfide exchange,[25, 26] imine chemistry,[27-29] olefin metathesis,[30] transalkylation,[31, 32] siloxane equilibrium[33] and vinylogous urethanes transamination.[34, 35] Tremendous efforts have been made to improve the sustainability of CANs, thermosets and vitrimers by adhering to green chemistry principles.[36-40]

The imine bond is a dynamic covalent bond that is formed by the condensation of amine and aldehyde. The imine reaction is based on three equilibrium process consisting of imine exchange, imine condensation/hydrolysis, and imine metathesis.[41] This reaction is intriguing not only because it enhances chitosan solubility (*via* breaking intermolecular hydrogen bonding)[42, 43] but also offers a versatile functional group offering novel routes for polymer

design, self-healing and 3D printing.[44-50] The reversible imine bond is also interesting thanks to its rapid exchange by changing pH,[51, 52] and temperature.[51]

There have been various reports on the preparation of biobased imine thermosets from vanillin,[51, 53-65] fructose,[66, 67] Priamine 1071,[66] soyabean oil,[56, 57, 64] chitin,[68] chitosan, [61, 69-71] cellulose,[72] Pripol 1040,[68] *etc*. However, the majority of these imine thermosets employed petroleum derived comonomers and required toxic solvents, with the products exhibiting low T_g and lacking high mechanical strength (**Table 4.2**). Furthermore, to the best of our knowledge there has been no previous reports of compostable imine thermosets. Therefore, the development of biobased compostable dynamic imine thermosets using principles of green chemistry with excellent thermal and mechanical properties remains a formidable obstacle we intend to address.

In this work, we incorporate the advantages of abundant shrimp/crab and cellulose waste as a feedstock to develop fully biomass-derived imine thermoset system with remarkable properties. A novel diketone-functionalised LGO derivative was condensed with amine groups on chitosan to develop a crosslinked polymeric system containing dynamic imine bonds. The thermosets were produced using a highly atom economical process at room temperature with dilute household vinegar, with water being the sole byproduct. The resulting imine thermoset exhibits high T_g, enhanced modulus, rapid stress relaxation as well as reprocessability. Furthermore, towards the end of their product life, these thermosets decompose completely in a household compost in 5 days. To the best of our knowledge, we report the first fully biomass-derived imine thermoset with the fastest degradation. From birth to grave, this biomass-derived thermoset meets 11 out of 12 green chemistry principles[36, 37] (**Table S4.1**). This work offers a new insight into the design and development of biodegradable thermoset.

Results and Discussion

Synthesis and characterization of imine thermosets

The preparation of imine thermosets from waste chitosan and LGO involved a simple synthetic strategy. First, levoglucosenone diketone (***1***) was prepared from an LGO-derived diol in a single step (**see ESI**). This modified LGO (***1***) was then condensed with the free amine groups bound to chitosan to afford a pale-yellow film (**Figure 4.1a and Figure 4.4d**).

Crosslinked imine thermosets were prepared by a rapid imine condensation process between ***1*** and chitosan at room temperature. We employed different molar ratios of polyamine to diketone to prepare different formulations (**Figure 4.1b**). The blended solution transitioned from near-colourless to pale yellow within 2–5 h at room temperature, visually indicating the progression of the imine reaction. FT-IR was employed to understand the chemical functionality of crosslinking bond between chitosan and ***1***. The band at 3000–3500 cm^{-1} was assigned to the stretching vibration of hydroxy (-OH) as well as the asymmetric and symmetric stretching of the amino (N-H) in the amino group, respectively.[61] These stretching vibrations were stronger in chitosan than in films containing ***1*** as well as chitosan (**Figure 4.1c**). This provided evidence for the free hydroxyl groups in the chitosan undergoing crosslinking reactions with ***1***.[61] In chitosan films, the band at 1590 cm^{-1} correlates to the deformation vibration of amino, however the intensity in the thermosets was reduced compared to pure chitosan. In the thermosets, the imine peak emerged at 1640 cm^{-1}.[61] We prepared a range of thermosets with controlled crosslink density: ***V1***, ***V2*** and ***V3*** (1.1×10^5, 1.6×10^5 and 2.1×10^5 $molm^{-3}$ respectively).

(a)

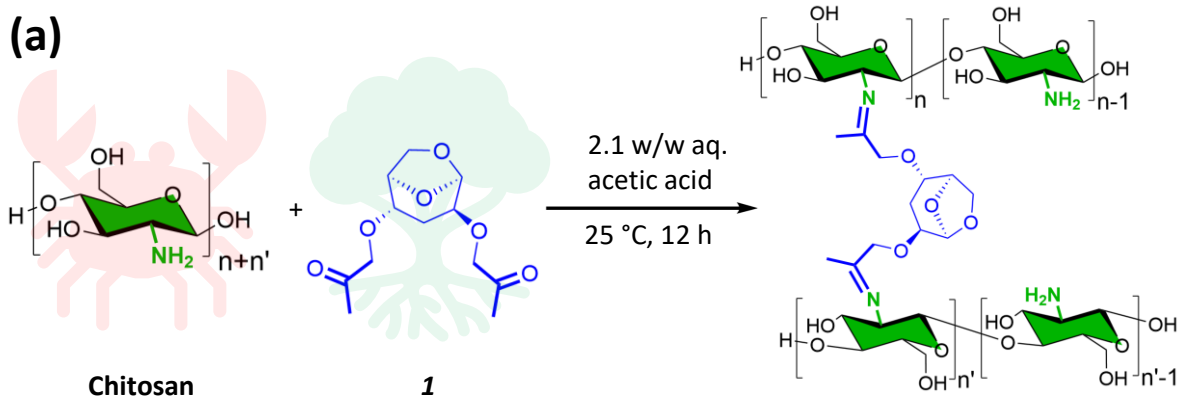

(b)

Entry	Chitosan (g)	*1* (g)	amine(mmol) : diketone(mmol)	Sample
1	0.50	-	-	**Chitosan**
2	0.50	0.0014	1 : 0.005	***V1***
3	0.50	0.014	1 : 0.05	***V2***
4	0.50	0.14	1 : 0.5	***V3***

(c)

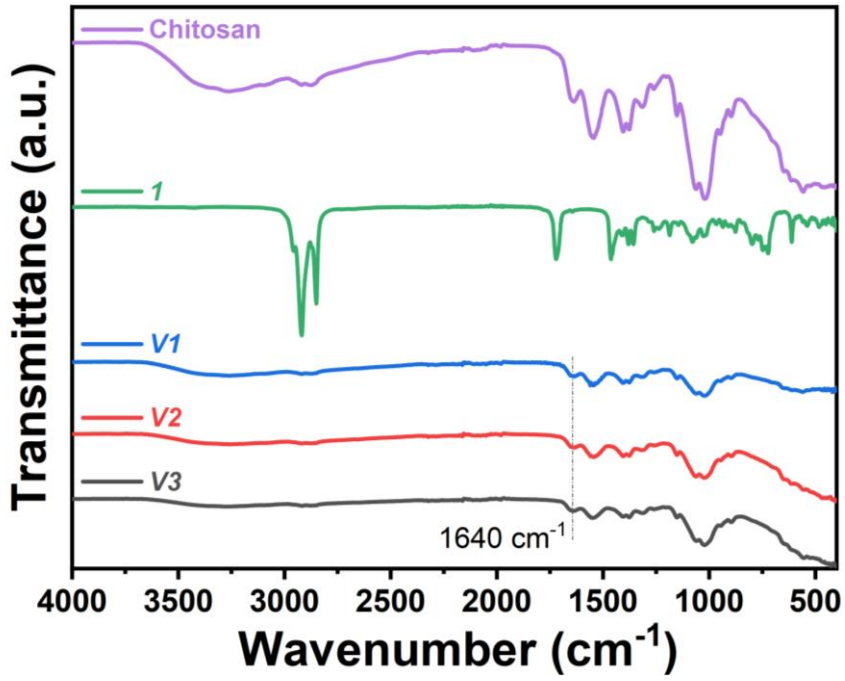

Figure 4.1: *Imine thermosets from chitosan and* ***1****, (a) synthetic route to prepare thermosets, (b) various formulations of thermoset series and (c) FT-IR spectra of chitosan,* ***1***

*(levoglucosenone diketone) and thermosets (**V1**, **V2**, **V3**). The thermosets are showing imine peaks at 1640 cm^{-1}.*[61]

Thermal and Mechanical properties

The thermal properties of imine thermosets were investigated using differential scanning calorimetry (DSC). The result indicates that the glass transition temperature (T_g) of imine films increases with a greater degree of crosslinking, rising from 171 to 176.1 °C (***V1***–***V3***) (**Figure 4.2a**). The thermal degradation behavior of imine thermosets was investigated by thermogravimetric analysis (TGA) and derivative thermogravimetric analysis (DTG). Comparing the DTG curves for first stage of weight loss, reveals that the DTG curve shapes of chitosan and thermosets are dissimilar. The first weight loss was recorded at a temperature (Td_1) of around 90–122 °C and is attributable to the evaporation of remaining water and acetic acid in the films (**Figure 4.2b**). It is well known that the hydration properties of these polysaccharides are affected by their primary and supramolecular structure.[73] Therefore, differences in the peak size and/or position associated with water loss are expected to represent molecular and physical changes resulting from the crosslinking. The thermoset films showed major weight loss occurring between 239–250 °C, compared to pure chitosan film, which decomposed at 252 °C. This major weight loss is possibly associated with a complex process including the dehydration of the saccharide rings, depolymerisation and decomposition of the acetylated and deacetylated units of the thermosets. The residual mass observed at 400 °C is black char. Generally, increasing the concentration of ***1*** led to higher decomposition temperature, because of the formation of new covalent bonds. However, in our work, the DTG curves reveals that the crosslinked thermosets begins to decompose at lower temperatures, suggesting that it is less thermally stable than the uncrosslinked chitosan.

Similar results have been previously observed.[61, 74-76] A plausible explanation for the decrease in thermal stability could be the formation of intra-crosslinking reactions between polysaccharides chains, which interferes with pre-existing attractive hydrogen bonds in those places where crosslinking happened.[76] As a result, the crosslinked thermoset structure become weaker, resulting a decrease in thermal stability.

To understand the dynamic mechanical properties of the thermosets, dynamic mechanical analysis (DMA) was conducted. DMA is a non-destructive technique for evaluating the properties of a material by the application of a dynamic load over time. DMA was performed on thermosets and the control chitosan film using tension mode at 1 Hz frequency with a heating rate of 3 °C min^{-1} from 22 to 220 °C. The storage modulus (E') of the thermosets (3.70–7.95 GPa) was higher than that of chitosan (3.62 GPa) at 25 °C, indicating that the thermosets prepared are stiffer than pristine chitosan (**Figure 4.2c**). The E' of the thermosets above T_g was higher than that of chitosan at the same temperature. As an example, at 195 °C, the E' of ***V3*** and chitosan were 2.5 GPa and 1.3 GPa, respectively. This result confirmed that the imine thermosets have a more rigid network topology compared to the chitosan control. The tan δ plot indicates that T_g of thermosets (177–181 °C) were higher than that of chitosan (172 °C) which is consistent with the DSC results (**Figure 4.2d**)**.** Additionally, the damping peak height of the thermosets were lower than that of chitosan during the transition zone, attributable to the fact that the thermosets were stiffer than chitosan, owing to the imine double bonds which reduce flexibility. The broad tan δ peak near 100 °C is a water-induced relaxation peak caused by desorption and successive evaporation of water molecules.[77] Moreover, we compared the dynamic mechanical properties of our crosslinked thermosets with those of commercial glutaraldehyde crosslinker and found that the E' values of our thermosets (3.70–

7.95 GPa) at room temperature is clearly superior to those of the glutaraldehyde system (*ca.* 400 MPa).[76]

One way to numerically understand the mechanical properties of the films is to calculate the crosslink density (v_e)[70, 78-81] (**see ESI**). The v_e increases with higher content of crosslinker ***1*** due to highly crosslinked networks, (**Table 4.1**). The v_e of ***V3*** was observed to be much higher than that of ***V2*** and ***V1***.

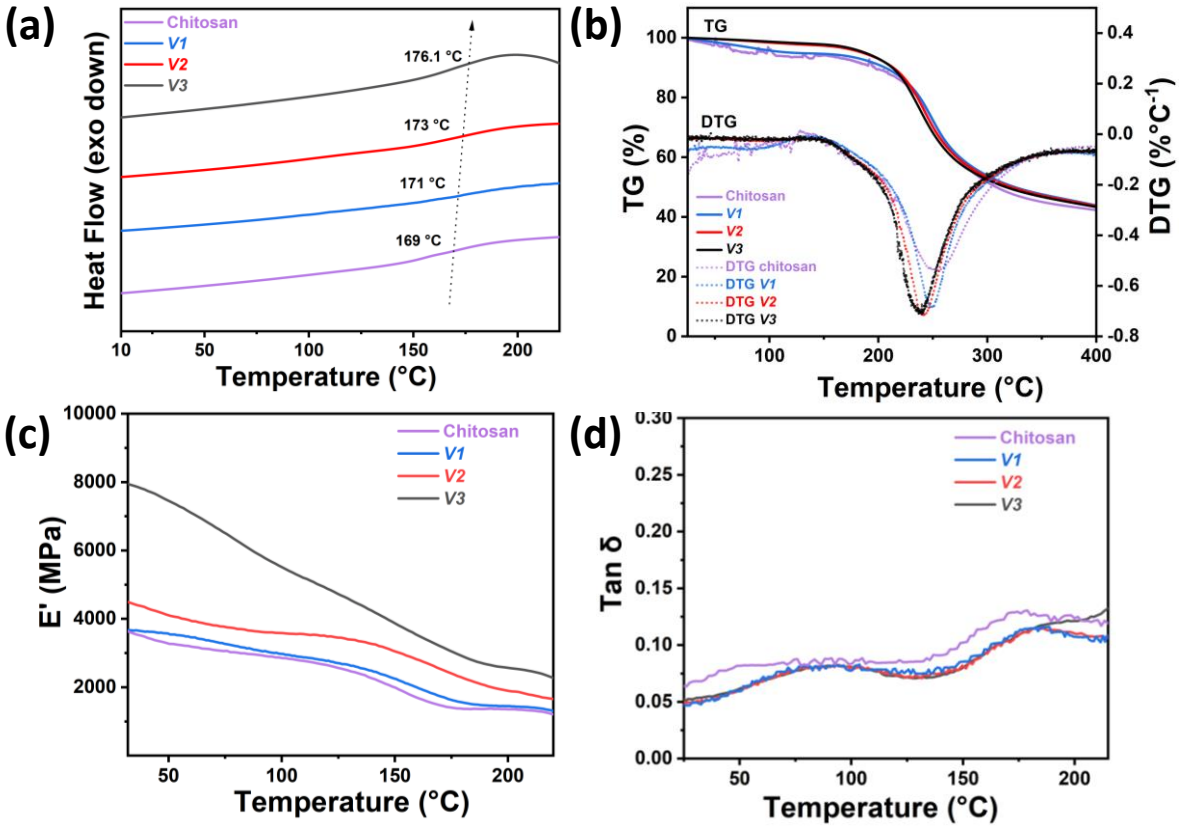

Figure 4.2: *Thermal properties of thermosets, (a) DSC thermograms of different crosslinked thermosets were measured at a heating rate of 3 °C min^{-1}. T_g raises with increase in crosslink density, (b) TGA and DTG curve of thermosets, (c) temperature sweep measurement of E' of different thermosets at 1 Hz frequency. The rigidity of thermosets raises as the v_e increases*

and (d) temperature sweep measurement of the tan δ across a range of temperatures of thermosets. All DMA tests were conducted in the tensile mode.

Samples	Crosslink density ($molm^{-3}$)	T_g (°C)	Storage Modulus at 25 °C (GPa)	Tensile Strength (MPa)	Young's modulus (MPa)	Elongation at break (%)
Chitosan	-	169	3.6	10.9 ± 2.1	2.1 ± 1.0	14.2 ± 2.4
V1	1.1×10^5	171	3.7	12.5 ± 3.5	2.2 ± 1.6	12.1 ± 3.0
V2	1.6×10^5	173	4.5	14.9 ± 3.2	3.7 ± 1.3	10.3 ± 3.0
V3	2.1×10^5	176.1	7.9	21.1 ± 3.1	5.3 ± 1.5	7.1 ± 3.2

T_g calculated from DSC.

Table 4.1: *Crosslinking density and mechanical properties of the thermosets.*

Stress Relaxation

Unlike in typical thermosetting polymer networks, the mechanical stress in dynamic covalent networks can be rapidly relieved by the reorganization of network topology induced by a bond exchange processes. The stress relaxation of thermosets and the chitosan control film were studied at 195 °C using a rheometer. Upon heating, the imine bond exchange reactions between the residual amine group exchanged with imine *via* a bond forming, bond-breaking reaction sequence. The chitosan control has no capacity for the exchange reaction. Consequently, no noticeable relaxation occurred within the time period. The existence of the Schiff base unit enabled all thermosets to undergo relaxation. ***V1*** had the slowest relaxation, attributed to its lower Schiff base content. With the increasing Schiff base content, the relaxation rate increased dramatically for ***V2*** and ***V3*** (**Figure 4.3a**). The rapid acceleration of relaxation rate was ascribed to the increased concentration of the exchangeable Schiff base units, hence increasing the probability of Schiff base exchange reactions. The influence of temperature on the stress relaxation of ***V3*** was investigated**.** The relaxation rate increased continuously with increasing temperature from 185 to 195 °C (**Figure 4.3b**). As may be

expected, increasing the temperature increases the rate of the Schiff base exchange reaction, resulting in accelerated relaxation.

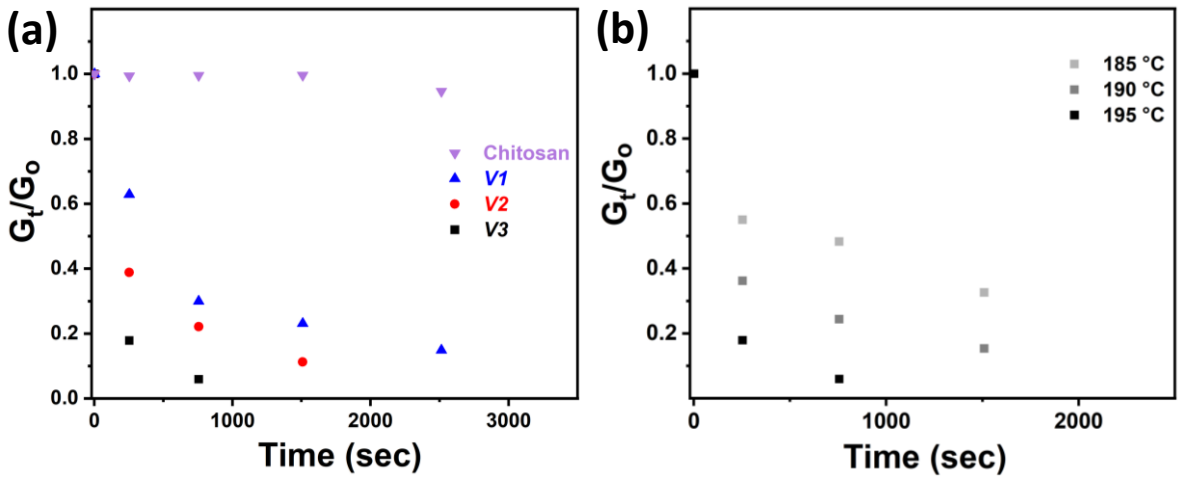

Figure 4.3: *Stress relaxation curves of thermosets, (a) stress relaxation curves at 195 °C. The stress relaxation rate increases with increases in Schiff base content and (b) stress relaxation curves of* ***V3*** *at different temperatures. The increase in temperature accelerates the Schiff base exchange process, which in turn speeds up the stress relaxation rate.*

Tensile Testing and Reprocessing

To investigate the mechanical properties of the imine thermoset films we employed uniaxial tensile testing. All of the crosslinked thermosets exhibited enhanced mechanical properties compared to the chitosan control, attributable to the increased network stiffness with increasing LGO derived crosslinker content (**Figure 4.4a**). Increasing from ***V1*** to ***V3*** the Young's modulus (*E*) and tensile strength (σ) increased from 2.2 ± 1.6 MPa to 5.3 ± 1.5 MPa and 12.5 ± 3.5 to 21.1 ± 3.1 MPa, respectively, while elongation at break (ε) of thermosets decreased from 12.1 ± 3.0% to 7.1 ± 3.2%, respectively (**Table 4.1**). Due to an increase in the amount of imine double bonds from ***V1*** to ***V3***, the network becomes stiffer and more rigid, resulting in increased *E* and σ but decreased ε. With a relatively low crosslinker (***1***) content, ***V1*** and ***V2***

behaved as soft plastic films with relatively high ε and low σ compared to ***V3***. To further investigate, we compared our thermosets mechanical properties to conventional epoxy thermosets.[82] Our thermosets offer comparable mechanical properties (Tensile strength: 21.1 ± 3.1) to conventional thermosets[82] (Tensile strength: 5.17 - 97.0 MPa).

We next investigated the reprocessability of the thermosets. Gratifyingly, the thermosets could be reprocessed thanks to the imine exchange process. Small pieces of films were reprocessed using a hot press at 180 °C for 30 min under 16 MPa pressure. The discrete film pieces (using ***V3*** as an example) were recovered as a single piece of integrated film (**Figure 4.4b**), and the mechanical properties of reprocessed thermosets were then compared with the pristine thermosets. The σ of the reprocessed ***V1***, ***V2*** and ***V3*** were recovered by 46.9%, 56.5% and 42% while ε was recovered by 46.2%, 75.7% and 97.5%, respectively (**Figure 4.4a**). When a higher pressure was applied for additional reprocessing, the reprocessed films became brittle and were crushed. In contrast to previously reported imine thermosets,[56, 66] which are soft and have a low T_g, the imine thermosets in this work have extremely rigid backbone structures and a high modulus in the rubbery state, which makes it challenging for fragmented thermosets to have a close contact and weld. The reprocessed chitosan (which lacked the Schiff base unit) showed poor mechanical properties (σ:7.6% and ε:28%) compared to the crosslinked thermosets. The chemical structures of thermosets before and after reprocessing were investigated using FT-IR. The material discoloured after reprocessing but there was no apparent change in the FT-IR spectra, particularly for the distinctive peak of C=N at 1640 cm^{-1}, showing that the chemical functionality was retained (**Figure 4.4c**).

Compostability

Cellulose and chitin are both biodegradable by enzymes found in a wide variety of species, including fungus, bacteria, archaea, rotifers, and algae.[83, 84] We investigated the breakdown of films in soil to determine their compostability under environmental conditions. Visual observation method was used to assess the degradation of films.[85] The thermosets were exposed to soil for a week; in two days, the films began to degrade, becoming increasingly brittle and shrinking (**Figure 4.4d**). In 4–5 days, all films were completely degraded. The soil moisture could readily penetrate into the film network, weakening the crosslinked network. The incredibly fast degradation of this material (within 5 days) is to the best of our knowledge, the fastest compostable imine thermoset to ever be reported.

Additionally, we compared the sustainability, thermal and mechanical properties of our thermosets to those produced by other biomass-derived systems as shown in **Table 4.2**. Our imine thermosets outperformed the competition in terms of sustainable synthesis, improved thermal and mechanical properties. Moreover, the green metrics for the thermosets were calculated (**see ESI**).

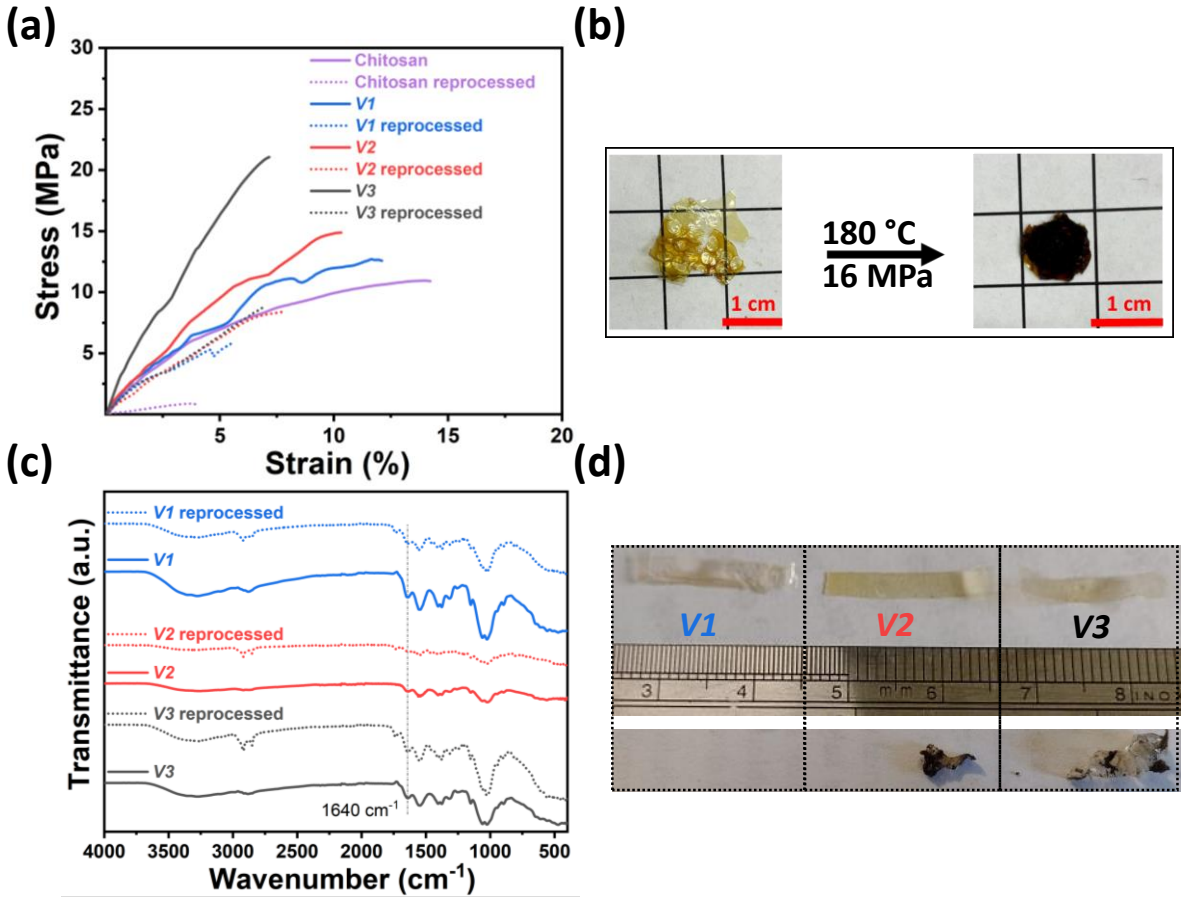

Figure 4.4: *Reprocessing and stress-strain curves of thermosets, (a) stress-strain curves of pristine and reprocessed thermosets, (b) reprocessing of small pieces* ***V3*** *by hot pressing at 180 °C for 30 min at a pressure of 16 MPa, (c) FT-IR spectra of pristine and reprocessed thermosets. The chemical functionality of the imine group was retained after reprocessing and (d) biodegradation of thermosets at home compost.* ***V1*** *was completely composted in 2 days while* ***V2*** *and* ***V3*** *was fully composted in 4–5 days.*

Biomass source	Solvent	T_g[a,b](°C)	Storage modulus at 25 °C (MPa)	Tensile strength (MPa)	Compostable	Ref.
Vanillin	DCM	56.5 ± 6.6–74.8 ± 0.9[b]	1500 ± 150–3300 ± 100	15 ± 2.9–22 ± 3.6	-	[53]
Vanillin	DCM	48-64[a]	1713–2341	47.43 ± 2.46–57.1 ± 6.01	-	[54]
Fructose and Priamine 1071	THF	-10[a]	~10	0.69 ± 0.03–0.73 ± 0.10	-	[66]

Vanillin	1-methoxy-2-propanol	14–139[a]	~10^3–10^4	2.2 ± 64	-	[55]
Vanillin and soybean oil	Ethanol	27.6[b]	~4–5.2	7.7 ± 1	-	[56]
Vanillin and soybean oil	Ethanol	40.5–75.7[b]	444–1582	0.63 ± 0.055–20.50 ± 0.23	-	[57]
Vanillin	-	172[b]	~4000	81 ± 1.2	-	[58]
Chitosan	Neat	188–205[a]	3704.76–3318.21	27–35	-	[70]
Vanillin	Chloroform	66-89[a]	320–1930	59.4–84.1	-	[59]
Vanillin	THF	57–69[a]	~1000	60.3 ± 4.3–77.1 ± 3.7	-	[60]
Fructose	THF	-50–16[a]	1.79–6.45	~0.2–1.1	-	[67]
Chitosan	Acetic and hydrochloric acid	70–80[a]	-	-	-	[69]
Chitosan and vanillin	Acetic acid	-	-	8.11 ± 0.83–10.18 ± 0.41	-	[61]
Vanillin	Chloroform	-	-	-	-	[62]
Vanillin	Chloroform	35 ± 3–45 ± 2[b]	353 ± 30–1220 ± 77	7.24 ± 0.23–16.68 ± 0.56	-	[51]
Chitin and Pripol 1040	1-ethyl-3-methylimidazolium acetate	19	-	4.99–6.25	-	[68]
Vanillin	Neat	71[b]	~2004	46	-	[63]
Cellulose	Ethanol	128[b]	~2500–4000	50–71	-	[72]
Vanillin and soybean oil	Neat	30–63.6[b]	~8–2129	6.8 ± 0.6–37.4 ± 4.1	-	[64]
Chitosan	Neat	124[b]	~3300	~25–47	-	[71]
Vanillin	DCM	121[b]	3560	65.0 ± 5.2	-	[65]
Chitosan and cellulose	**Dilute acetic acid**	**171–176.1[a]**	**3700–7900**	**12.5 ± 3.5–21.1 ± 3.1**	**Yes**	**This work**

a = T_g calculated from DSC. b = T_g calculated from DMA.

Table 4.2: *Comparison of imine thermosets.*

Conclusion

In conclusion, fully biomass-derived and compostable imine thermosets were prepared by employing widely abundant shrimp and cellulose waste materials. The imine thermosets showed a range of mechanical properties varying from soft to rigid, which can be modified by varying the amount of LGO-derived crosslinker. Furthermore, the thermosets showed enhanced modulus and high T_g. The imine thermosets exhibited good thermal stability with onset degradation temperatures of *ca.* 200 °C. With the incorporation of dynamic imine covalent bonds into the thermosets, the resulting biomass-derived thermosets exhibit rapid

stress relaxation and reprocessing functionality. At the end of material lifecycle, the thermosets can be decomposed in 4–5 days in a home compost. The fully biomass-derived imine thermosets have tremendous feasibility and promise as a sustainable alternative to typical thermosets because of their reprocessability, tuneable mechanical properties, rapid stress relaxation and biodegradability.

Supporting Information

Experimental

All commercially obtained solvents and reagents were used without further purification. Chitosan (M_w = 310000–375000 Da, degree of deacetylation > 75%), chloroacetone (95%), hexane, ethyl acetate and acetonitrile (99.9%) were all purchased from the Sigma Aldrich. Essentials White Vinegar 2 L was purchased from Woolworths supermarket Australia. Levoglucosenone (74.44%) was kindly supplied by Circa™ and was vacuum distilled before use. Analytical thin-layer chromatography (TLC) was carried out on Merck silica gel 60 F254 glass plates and flash chromatography (FC) was performed on Merck silica gel 60 (70–230 mesh). Visualization was achieved using short-wave UV light and/or $KMnO_4$ staining solution, followed by mild heating.

^1H and ^{13}C solution-state NMR were recorded on a Bruker Ascend 400 MHz spectrometer (400 MHz for ^1H and 100 MHz for ^{13}C). Chemical shifts δ are reported relative to the resonance signal of ^1H or ^{13}C cores of tetramethylsilane and in ppm. The ^1H spectra were calibrated by setting the solvent peaks, caused by remaining traces of protons, to values known from the literature (δ $CHCl_3$ = 7.26 ppm). The ^{13}C spectra were calibrated by setting the deuterium coupled solvent signal to values known from the literature (δ $CDCl_3$ = 77.16 ppm). The coupling constants J are reported in Hz.

The characterizations were performed after heating the thermoset films at 130 °C for 2 h.

Fourier transform infrared spectroscopy (FTIR) was performed on a Perkin Elmer Spectrum 2, with a 0.5 cm^{-1} resolution, over 32 scans from 400 to 4000 cm^{-1}. All the measurements were performed at room temperature.

Low-resolution ESI mass spectra were recorded on a Micromass LC-ZMD single quadrupole liquid chromatograph mass spectrometer while high-resolution measurements were conducted on an LCT Premier time-of-flight instrument.

Differential scanning calorimetry (DSC) was performed using a TA Instruments Q20 at a heating rate of 3 °C min^{-1}. The sample (∼10 mg) was ramped once till 120 °C to remove any remaining water and acetic acid and cooled slowly at room temperature. The data was recorded between 10 °C and 220 °C.

Thermal gravimetric analysis (TGA) was performed on a TA Instruments TGA Q 500 under a N_2 atmosphere over a temperature range of 25–460 °C at a heating rate of 3 °C min^{-1}.

Dynamic mechanical analysis (DMA) was performed on a Netzsch DMA242E Artemis. Small films were cut into rectangular shape to fit the tensile holder. Temperature sweep measurement were performed at 1 Hz from room temperature to 220 °C with a heating rate of 3 °C min^{-1}.

Stress-relaxation tests were carried out on Anton Paar MCR 702 multidrive rheometer using a plate geometry (PP25) with a 25 mm diameter. The material was placed on the rheometer, and the upper geometry was lowered. After reaching the appropriate temperature (185–195 °C), the samples were equilibrated for 30 min and then a constant shear strain of 2.1% was applied, and the time dependent stress relaxation measurement was recorded.

Tensile tests were conducted on a universal testing machine (Instron) at a loading rate of 3 mm min^{-1}. The mechanical properties were tested at least 3 times with a 5 kN load cell at 47 % humidity.

Optical rotations were recorded in $CHCl_3$ at 20 °C on a Perkin Elmer Model 343 Polarimeter.

Reprocessing experiment was performed on a PHI hydraulic press. The thermoset films were cut into small pieces and then placed into round steel mold (1 cm diameter) and subjected to a 20 min thermal equilibration at 180 °C. The thermosetting films were then reprocessed at 180 °C for 30 min at a pressure of 16 MPa. The reprocessed thermosets were demolded after reaching room temperature.

Compostability assessment were performed using typical household garden soil (Canberra, Australia) collected into glass scintillation vials (20 cm^3 in volume) so that the rapidly decomposing material could be isolated and investigated. Polymer samples (25 mm × 5 mm × 2 mm, length × width × thickness) were loaded into the soil without mechanical packing or agitation. The sample vials were then left uncapped (aerobic conditions) and partially buried in the garden and investigated at 24 h intervals. The visible changes in films were used to describe degradation which include roughening of the surface, formation of holes or cracks, de-fragmentation, changes in color, or formation of bio-films in the surface.[85]

Preparation of hydroxy-levoglucosenone ((1R,2S,5R)-2-hydroxy-6,8-dioxabicyclo[3.2.1]octan-4-one): A magnetically stirred solution of freshly vacuum distilled levoglucosenone (3.00 g, 23.79 mmol) in water (250 mL) maintained at 22 °C was treated with triethylamine (0.26 mL, 1.87 mmol). After 1 h the reaction mixture was concentrated under reduced pressure and the ensuing residue subjected to flash chromatography (silica, 1:10 v/v

ethyl acetate/40–60 petroleum ether → ethyl acetate gradient elution) and concentration of the relevant fractions (R_f = 0.2 in 1:10 ethyl acetate/petroleum ether) under reduced pressure afforded (1*R*,2*S*,5*R*)-2-hydroxy-6,8-dioxabicyclo[3.2.1]octan-4-one (2.60 g, 76%) as a clear, light-yellow oil that was identical, in all respects, with material obtained earlier (**Scheme S4.1**).[86] Potassium carbonate may be substituted for triethylamine as the catalyst.[87]

Reduction of hydroxy-levoglucosenone ((1R,2S,4S,5R)-6,8-dioxabicyclo[3.2.1]octane-2,4-diol): A magnetically stirred solution of (1*R*,2*S*,5*R*)-2-hydroxy-6,8-dioxabicyclo[3.2.1]octan-4-one obtained as described above (1.50 g, 10.41 mmol) in methanol (25.0 mL) chilled to 0 °C was treated portion-wise with 1.1 eq. $NaBH_4$ (440 mg, 11.63 mmol). After 4 h, the reaction mixture was concentrated *in vacuo* and adsorbed onto silica, and the residue obtained subjected to flash column chromatography (silica, 5% *v/v* MeOH in CH_2Cl_2). Concentration of the relevant fractions (R_f = 0.3 in 5% *v/v* MeOH in CH_2Cl_2) afforded (LGO-derived diol) (1*R*,2*S*,4*S*,5*R*)-6,8-dioxabicyclo[3.2.1]octane-2,4-diol as a clear, yellow oil (1.05 g, 69%) that was identical, in all respects, with material obtained earlier (**Scheme S4.1**).[88]

Alternatively, LGO-derived diol ((1R,2S,4S,5R)-6,8-dioxabicyclo[3.2.1]octane-2,4-diol) can be directly prepared from levoglucosenone using sustainable one pot synthesis.[89]

Preparation of levoglucosenone diketone (*1*) (1,1'-(((1R,2S,4S,5R)-6,8-dioxabicyclo[3.2.1]octane-2,4-diyl)bis(oxy))bis(propan-2-one): In 50 mL round bottom flask with magnetic stirring bar, was charged with K_2CO_3 (463 mg, 3.34 mmol, 5 eq), and NaI (80 mg, 0.53 mmol, 0.8 eq). The flask was evacuated and backfilled with nitrogen. Then (1*R*,2*S*,4*S*,5*R*)-6,8-dioxabicyclo[3.2.1]octane-2,4-diol (98 mg, 0.66 mmol, 1 eq) dissolved in DMSO and chloroacetone (127 µL, 1.60 mmol, 2.4 eq) was added and the resulting mixture

was allowed to stir at 50 °C for 90 min and thereafter cooled down to room temperature followed by filtration and purification with HPLC column (Phenomenex Luna 5u C18(2) 100A 250 x 10.00 mm, 5 micron, 30 °C) (20: 80 MeCN/H_2O) yielded ***1*** (34 mg, 35%) (**Scheme S4.1**). $[\alpha]_D$ = 0.23 (*c* = 1.32, MeOH), ^{1}H NMR (400 MHz, $CDCl_3$, 298 K): δ 3.49 (s, 2H), 3.11 (t, *J* = 5.6 Hz, 1H), 2.73 (d, *J* = 5.6 Hz, 2H), 2.36 (s, 3H), 2.26 (s, 6H), 2.17 (s, 2H), 1.83 (s, 1H), 1.25 (s, 1H) (**Figure S4.1**). ^{13}C NMR (100 MHz, $CDCl_3$, 298 K) δ = 204.9, 202.0, 64.8, 63.1, 45.5, 44.6, 28.7, 27.9, 20.1 (**Figure S4.2**), IR ν_{max} 2918, 2850, 1719, 1462, 1407, 1381, 1355, 1259, 1236, 1183, 1143, 1077, 1058, 1025, 965, 935, 907, 875, 797, 770, 748, 722, 611, 560, 537, 481, 446 cm^{-1}; MS (ESI, +ve) *m/z* 319 $(M+ISOPROP+H)^+$; HRMS (ESI, +ve) calcd for $C_{15}H_{27}O_7$ $(M+ISOPROP+H)^+$ 319.1756, found 319.1733.

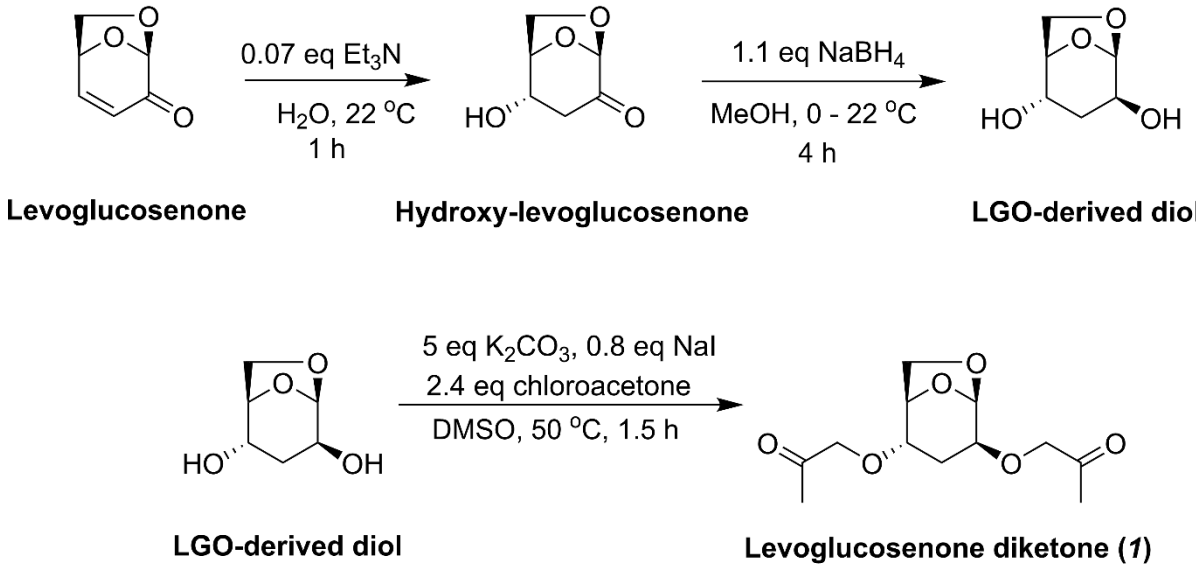

Scheme S4.1: *Synthetic route of monomer.*

Preparation of thermosets: Chitosan (0.50 g) was dissolved in 20 mL of 2.1% (*w*/*w*) dilute household white vinegar at room temperature while stirring for 0.5 h. A stock solution of ***1*** in 100% ethanol was prepared with concentration 1.4 gL^{-1}. Then, the thermosets were prepared by mixing solution ***1*** and the chitosan solution with continuous stirring at room temperature.

After stirring overnight at room temperature, equal volumes of thermoset solution were distributed into rectangular silicone moulds (7.5 cm × 1.8 cm × 1.4 cm) and left at room temperature until completely dried. Similarly, ***V2*** and ***V3*** were prepared using same method by varying the amount of crosslinker ***1*** added.

Calculation of crosslink density (v_e)

Crosslink density ($\boldsymbol{v_e}$) was calculated using the following equation:[70, 78-81]

$$\boldsymbol{v_e = \frac{E_r}{3RT_r}}$$

where, E_r is the storage modulus at temperature T_r, T_r is the absolute temperature in the rubbery region (T_g + 18 °C) and R is the universal gas constant (8.314 J mol^{-1} K^{-1}).

Green chemistry attributes

The LGO-derived diol can be directly prepared from levoglucosenone using sustainable one pot synthesis.[89] For green chemistry attributes, only the thermoset cross-linking step was assessed. We predict that with additional work the preparation of the waste-derived levoglucosenone diketone can be extensively optimised with respect to greenness. Further, the primary objective of this study was to determine the effectiveness of this waste-derived diketone in the preparation of a chitosan-based thermoset. We predict that a variety of levoglucosenone-derived diketone analogues with varying alkyl chain lengths and functionalities could be incorporated in the future to generate yet more favourable materials with tuneable properties.

Justification of principles of green chemistry

Principles of green chemistry	Justification of principles
(1) Prevention of waste	No toxic waste produced during polymer synthesis; water is the only byproduct; mechanical recycling of polymers; polymer biodegrades at the end of product life; and E-factor 0.011–0.015.
(2) Atom economy	>94% atom economy during polymer synthesis; water is the only byproduct.
(3) Less hazardous chemical syntheses	Diluted household vinegar was used in polymer synthesis; water is the only byproduct.
(4) Designing safer chemicals	Chitosan is non-toxic.
(5) Safer solvents and auxiliaries	Green/benign solvents[90] – water, ethanol, ethyl acetate, DMSO, dilute vinegar, and acetonitrile – are used for polymer synthesis.
(6) Design for energy efficiency	The polymer was synthesised at room temperature and atmospheric pressure.
(7) Use of renewable feedstocks	Chitosan and levoglucosenone diketone are biomass chemicals derived from crabs/shrimp shells and cellulose respectively.
(8) Reduce derivatives	No protection/deprotection and blocking group chemistry were used. Minimum number of steps were used to prepare polymer. Three steps were required to functionalize biomass derived monomer, however only one step is required for polymer synthesis.
(9) Catalysis	Dilute acetic acid was used as a catalyst.
(10) Design for degradation	At the end of product life, polymer biodegrades in home compost.
(11) Inherently safer chemistry for accident prevention	Straightforward simple procedure carried out at room temperature and atmospheric pressure; no special care/air-sensitive reagents required.

Table S4.1*: Justification of principles of green chemistry.*[36, 37]

Green metrics calculations

The developed thermosets were evaluated to green chemistry metrics calculations to assess their environmental impact and sustainability.

(1) Environmental factor (E-factor): E-factor is a well-known Green chemistry parameter that measures the ratio of waste mass to product mass. It provides information on the quantity of waste produced by a chemical process. E-factor should be zero for a perfect Green chemical reaction. The higher the E-factor, the greater the quantity of waste produced, which have an adverse effect on the environment.

$$E - factor = (mass\ of\ waste)/(mass\ of\ product)$$

$$Mass\ of\ waste = Total\ mass\ of\ raw\ materials - Total\ mass\ of\ product$$

The E factor for thermosets were found to 0.011–0.015.

(2) Atom economy (AE): The AE of a chemical reaction describes the total number of atoms in the product from the reactants. It is a crucial factor in determining the efficiency of a chemical reaction. The perfect value of AE is 100%.

$$AE = Mol.wt.of\ product/\ \Sigma(Mol.wt.of\ stoichiometric\ reactants) \times 100$$

The AE value for the thermosets were found to 94.15%.

(3) Mass intensity (MI): MI is the ratio of overall mass of the process to the product mass. The process will be cheaper and more environment friendly with lower MI value.

$$MI = (Total\ mass\ in\ process)\ /\ (Mass\ of\ product)$$

The MI value of thermosets were 1.011–1.015.

(4) Reaction mass efficiency (RME): RMI is the ratio of product mass to the sum of total mass of stoichiometric reactants. A higher RME value is considered preferable for an optimal green chemical reaction.

$$RME\ (\%)\ =\ mass\ of\ product\ /\Sigma(mass\ of\ stoichiometric\ reactants)\ \times\ 100$$

RME value of thermosets were 98.437–98.900.

(5) Carbon economy (CE): CE measures the carbon content of the product relative to the carbon content of the reactant.

$$CE\ (\%)\ =\ [Total\ carbon\ in\ product]\ /\ [Total\ carbon\ in\ reactant]\ \times\ 100$$

CE for thermosets were determined to 100%, indicating that the carbon content of both the reactant and the product remains unchanged.

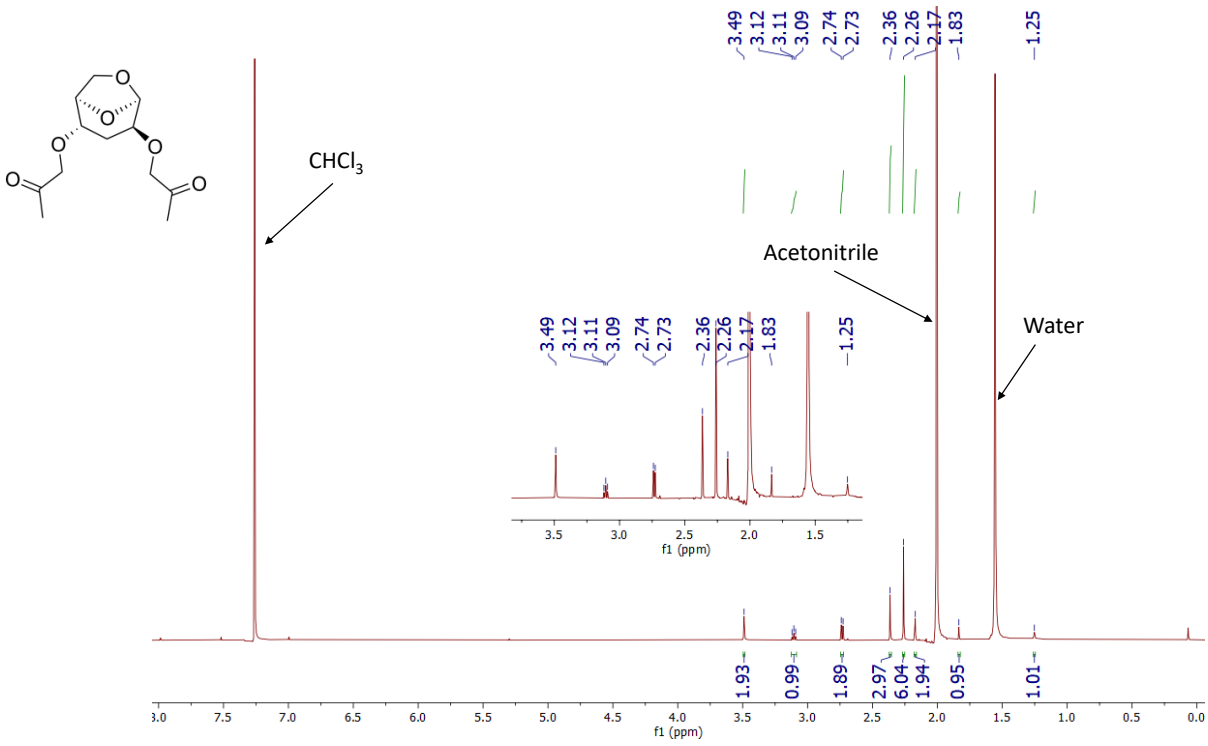

Figure S4.1: *^{1}H NMR spectrum of **1** in deuterated chloroform.*

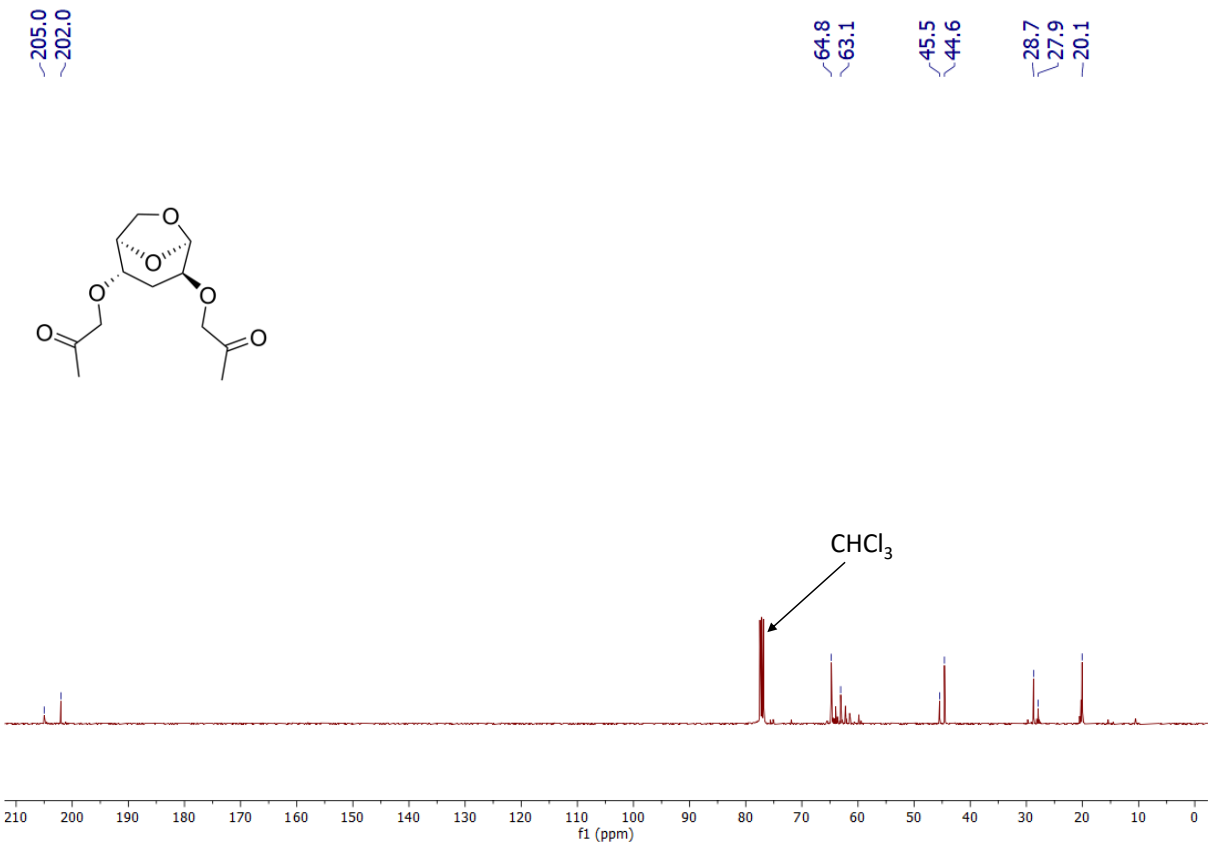

Figure S4.2: *^{13}C NMR spectrum of **1** in deuterated chloroform.*

References

(1) Tang, X.; Chen, E. Y. X. Toward Infinitely Recyclable Plastics Derived from Renewable Cyclic Esters. *Chem* **2019**, *5*, 284-312.
(2) Rorrer, N. A.; Nicholson, S.; Carpenter, A.; Biddy, M. J.; Grundl, N. J.; Beckham, G. T. Combining Reclaimed PET with Bio-based Monomers Enables Plastics Upcycling. *Joule* **2019**, *3*, 1006-1027.
(3) The future of plastic. *Nature Communications* **2018**, *9*, 2157.
(4) Zhu, Y.; Romain, C.; Williams, C. K. Sustainable polymers from renewable resources. *Nature* **2016**, *540*, 354-362.
(5) Yu, J.; Wang, J.; Wang, C.; Liu, Y.; Xu, Y.; Tang, C.; Chu, F. UV-Absorbent Lignin-Based Multi-Arm Star Thermoplastic Elastomers. *Macromolecular Rapid Communications* **2015**, *36*, 398-404.
(6) Wang, J.; Chen, Y. P.; Yao, K.; Wilbon, P. A.; Zhang, W.; Ren, L.; Zhou, J.; Nagarkatti, M.; Wang, C.; Chu, F.; et al. Robust antimicrobial compounds and polymers derived from natural resin acids. *Chemical Communications* **2012**, *48*, 916-918.
(7) Olivera, S.; Muralidhara, H. B.; Venkatesh, K.; Guna, V. K.; Gopalakrishna, K.; Kumar K, Y. Potential applications of cellulose and chitosan nanoparticles/composites in wastewater treatment: A review. *Carbohydrate Polymers* **2016**, *153*, 600-618.

(8) Supanchaiyamat, N.; Shuttleworth, P. S.; Hunt, A. J.; Clark, J. H.; Matharu, A. S. Thermosetting resin based on epoxidised linseed oil and bio-derived crosslinker. *Green Chemistry* **2012**, *14*, 1759-1765.
(9) Liu, Y.; Yao, K.; Chen, X.; Wang, J.; Wang, Z.; Ploehn, H. J.; Wang, C.; Chu, F.; Tang, C. Sustainable thermoplastic elastomers derived from renewable cellulose, rosin and fatty acids. *Polymer Chemistry* **2014**, *5*, 3170-3181.
(10) Van de Vyver, S.; Geboers, J.; Jacobs, P. A.; Sels, B. F. Recent Advances in the Catalytic Conversion of Cellulose. *ChemCatChem* **2011**, *3*, 82-94.
(11) Rout, P. K.; Nannaware, A. D.; Prakash, O.; Kalra, A.; Rajasekharan, R. Synthesis of hydroxymethylfurfural from cellulose using green processes: A promising biochemical and biofuel feedstock. *Chemical Engineering Science* **2016**, *142*, 318-346.
(12) Comba, M. B.; Tsai, Y.-h.; Sarotti, A. M.; Mangione, M. I.; Suárez, A. G.; Spanevello, R. A. Levoglucosenone and Its New Applications: Valorization of Cellulose Residues. *European Journal of Organic Chemistry* **2018**, 590-604.
(13) Kudo, S.; Goto, N.; Sperry, J.; Norinaga, K.; Hayashi, J.-i. Production of Levoglucosenone and Dihydrolevoglucosenone by Catalytic Reforming of Volatiles from Cellulose Pyrolysis Using Supported Ionic Liquid Phase. *ACS Sustainable Chemistry & Engineering* **2017**, *5*, 1132-1140.
(14) Silva, T. H.; Alves, A.; Ferreira, B. M.; Oliveira, J. M.; Reys, L. L.; Ferreira, R. J. F.; Sousa, R. A.; Silva, S. S.; Mano, J. F.; Reis, R. L. Materials of marine origin: a review on polymers and ceramics of biomedical interest. *International Materials Reviews* **2012**, *57*, 276-306.
(15) Francis Suh, J. K.; Matthew, H. W. T. Application of chitosan-based polysaccharide biomaterials in cartilage tissue engineering: a review. *Biomaterials* **2000**, *21*, 2589-2598.
(16) Rao, S. B.; Sharma, C. P. Use of chitosan as a biomaterial: Studies on its safety and hemostatic potential. *Journal of Biomedical Materials Research* **1997**, *34*, 21-28.
(17) Kloxin, C. J.; Scott, T. F.; Adzima, B. J.; Bowman, C. N. Covalent adaptable networks (CANs): a unique paradigm in cross-linked polymers. *Macromolecules* **2010**, *43*, 2643-2653.
(18) Bowman, C.; Du Prez, F.; Kalow, J. Introduction to chemistry for covalent adaptable networks. *Polymer Chemistry* **2020**, *11*, 5295-5296.
(19) Kloxin, C. J.; Bowman, C. N. Covalent adaptable networks: smart, reconfigurable and responsive network systems. *Chemical Society Reviews* **2013**, *42*, 7161-7173.
(20) Majumdar, S.; Zhang, H.; Soleimani, M.; Van Benthem, R. A.; Heuts, J. P.; Sijbesma, R. P. Phosphate triester dynamic covalent networks. *ACS Macro Letters* **2020**, *9*, 1753-1758.
(21) Bin Rusayyis, M.; Torkelson, J. M. Recyclable polymethacrylate networks containing dynamic dialkylamino disulfide linkages and exhibiting full property recovery. *Macromolecules* **2020**, *53*, 8367-8373.
(22) Montarnal, D.; Capelot, M.; Tournilhac, F.; Leibler, L. Silica-Like Malleable Materials from Permanent Organic Networks. *Science* **2011**, *334*, 965-968.
(23) Röttger, M.; Domenech, T.; Weegen, R. v. d.; Breuillac, A.; Nicolaÿ, R.; Leibler, L. High-performance vitrimers from commodity thermoplastics through dioxaborolane metathesis. *Science* **2017**, *356*, 62-65.
(24) Chen, Y.; Tang, Z.; Zhang, X.; Liu, Y.; Wu, S.; Guo, B. Covalently Cross-Linked Elastomers with Self-Healing and Malleable Abilities Enabled by Boronic Ester Bonds. *ACS Applied Materials & Interfaces* **2018**, *10*, 24224-24231.

(25) Xiang, H. P.; Qian, H. J.; Lu, Z. Y.; Rong, M. Z.; Zhang, M. Q. Crack healing and reclaiming of vulcanized rubber by triggering the rearrangement of inherent sulfur crosslinked networks. *Green Chemistry* **2015**, *17*, 4315-4325.
(26) Kim, S.-M.; Jeon, H.; Shin, S.-H.; Park, S.-A.; Jegal, J.; Hwang, S. Y.; Oh, D. X.; Park, J. Superior Toughness and Fast Self-Healing at Room Temperature Engineered by Transparent Elastomers. *Advanced Materials* **2018**, *30*, 1705145.
(27) Taynton, P.; Yu, K.; Shoemaker, R. K.; Jin, Y.; Qi, H. J.; Zhang, W. Heat- or Water-Driven Malleability in a Highly Recyclable Covalent Network Polymer. *Advanced Materials* **2014**, *26*, 3938-3942.
(28) Lei, X.; Jin, Y.; Sun, H.; Zhang, W. Rehealable imide–imine hybrid polymers with full recyclability. *Journal of Materials Chemistry A* **2017**, *5*, 21140-21145.
(29) Zhang, H.; Wang, D.; Liu, W.; Li, P.; Liu, J.; Liu, C.; Zhang, J.; Zhao, N.; Xu, J. Recyclable polybutadiene elastomer based on dynamic imine bond. *Journal of Polymer Science Part A: Polymer Chemistry* **2017**, *55*, 2011-2018.
(30) Lu, Y.-X.; Guan, Z. Olefin Metathesis for Effective Polymer Healing via Dynamic Exchange of Strong Carbon–Carbon Double Bonds. *Journal of the American Chemical Society* **2012**, *134*, 14226-14231.
(31) Hendriks, B.; Waelkens, J.; Winne, J. M.; Du Prez, F. E. Poly(thioether) Vitrimers via Transalkylation of Trialkylsulfonium Salts. *ACS Macro Letters* **2017**, *6*, 930-934.
(32) Obadia, M. M.; Mudraboyina, B. P.; Serghei, A.; Montarnal, D.; Drockenmuller, E. Reprocessing and Recycling of Highly Cross-Linked Ion-Conducting Networks through Transalkylation Exchanges of C–N Bonds. *Journal of the American Chemical Society* **2015**, *137*, 6078-6083.
(33) Wu, X.; Yang, X.; Yu, R.; Zhao, X.-J.; Zhang, Y.; Huang, W. A facile access to stiff epoxy vitrimers with excellent mechanical properties via siloxane equilibration. *Journal of Materials Chemistry A* **2018**, *6*, 10184-10188.
(34) Guerre, M.; Taplan, C.; Nicolaÿ, R.; Winne, J. M.; Du Prez, F. E. Fluorinated Vitrimer Elastomers with a Dual Temperature Response. *Journal of the American Chemical Society* **2018**, *140*, 13272-13284.
(35) Denissen, W.; Rivero, G.; Nicolaÿ, R.; Leibler, L.; Winne, J. M.; Du Prez, F. E. Vinylogous Urethane Vitrimers. *Advanced Functional Materials* **2015**, *25*, 2451-2457.
(36) Zimmerman, J. B.; Anastas, P. T.; Erythropel, H. C.; Leitner, W. Designing for a green chemistry future. *Science* **2020**, *367*, 397-400.
(37) Anastas, P. T.; Warner, J. C. *Green chemistry: theory and practice*; Oxford University Press, Oxford [England], 1998.
(38) Vidil, T.; Llevot, A. Fully Biobased Vitrimers: Future Direction toward Sustainable Cross-Linked Polymers. *Macromolecular Chemistry and Physics* **2022**, *223*, 2100494.
(39) Lucherelli, M. A.; Duval, A.; Avérous, L. Biobased vitrimers: Towards sustainable and adaptable performing polymer materials. *Progress in Polymer Science* **2022**, *127*, 101515.
(40) Kumar, A.; Connal, L. A. Bio-based Transesterification Vitrimers. *Macromolecular Rapid Communications* 2200892.
(41) Belowich, M. E.; Stoddart, J. F. Dynamic imine chemistry. *Chemical Society Reviews* **2012**, *41*, 2003-2024.
(42) Ying, G.-q.; Xiong, W.-y.; Wang, H.; Sun, Y.; Liu, H.-z. Preparation, water solubility and antioxidant activity of branched-chain chitosan derivatives. *Carbohydrate Polymers* **2011**, *83*, 1787-1796.

(43) Nishimura, S.; Kohgo, O.; Kurita, K.; Kuzuhara, H. Chemospecific manipulations of a rigid polysaccharide: syntheses of novel chitosan derivatives with excellent solubility in common organic solvents by regioselective chemical modifications. *Macromolecules* **1991**, *24*, 4745-4748.
(44) Shi, B.; Shen, Z.; Zhang, H.; Bi, J.; Dai, S. Exploring N-Imidazolyl-O-Carboxymethyl Chitosan for High Performance Gene Delivery. *Biomacromolecules* **2012**, *13*, 146-153.
(45) Nadgorny, M.; Xiao, Z.; Connal, L. A. 2D and 3D-printing of self-healing gels: design and extrusion of self-rolling objects. *Molecular Systems Design & Engineering* **2017**, *2*, 283-292.
(46) Nadgorny, M.; Collins, J.; Xiao, Z.; Scales, P. J.; Connal, L. A. 3D-printing of dynamic self-healing cryogels with tuneable properties. *Polymer Chemistry* **2018**, *9*, 1684-1692.
(47) Brisson, E. R. L.; Xiao, Z.; Franks, G. V.; Connal, L. A. Versatile Synthesis of Amino Acid Functional Polymers without Protection Group Chemistry. *Biomacromolecules* **2017**, *18*, 272-280.
(48) Diggle, B.; Jiang, Z.; Li, R. W.; Connal, L. A. Self-Healing Polymer Network with High Strength, Tunable Properties, and Biocompatibility. *Chemistry of Materials* **2021**, *33*, 3712-3720.
(49) Collins, J.; Xiao, Z.; Connal, L. A. Tunable degradation of polyethylene glycol-like polymers based on imine and oxime bonds. *Journal of Polymer Science Part A: Polymer Chemistry* **2017**, *55*, 3826-3831.
(50) Brisson, E. R. L.; Xiao, Z.; Levin, L.; Franks, G. V.; Connal, L. A. Facile synthesis of histidine functional poly(N-isopropylacrylamide): zwitterionic and temperature responsive materials. *Polymer Chemistry* **2016**, *7*, 1945-1952.
(51) Guo, Z.; Liu, B.; Zhou, L.; Wang, L.; Majeed, K.; Zhang, B.; Zhou, F.; Zhang, Q. Preparation of environmentally friendly bio-based vitrimers from vanillin derivatives by introducing two types of dynamic covalent CN and S–S bonds. *Polymer* **2020**, *197*, 122483.
(52) Tao, Y.; Liu, S.; Zhang, Y.; Chi, Z.; Xu, J. A pH-responsive polymer based on dynamic imine bonds as a drug delivery material with pseudo target release behavior. *Polymer Chemistry* **2018**, *9*, 878-884.
(53) Xu, Y.; Odelius, K.; Hakkarainen, M. Photocurable, Thermally Reprocessable, and Chemically Recyclable Vanillin-Based Imine Thermosets. *ACS Sustainable Chemistry & Engineering* **2020**, *8*, 17272-17279.
(54) Geng, H.; Wang, Y.; Yu, Q.; Gu, S.; Zhou, Y.; Xu, W.; Zhang, X.; Ye, D. Vanillin-Based Polyschiff Vitrimers: Reprocessability and Chemical Recyclability. *ACS Sustainable Chemistry & Engineering* **2018**, *6*, 15463-15470.
(55) Mo, R.; Song, L.; Hu, J.; Sheng, X.; Zhang, X. An acid-degradable biobased epoxy-imine adaptable network polymer for the fabrication of responsive structural color film. *Polymer Chemistry* **2020**, *11*, 974-981.
(56) Liu, Y.-Y.; He, J.; Li, Y.-D.; Zhao, X.-L.; Zeng, J.-B. Biobased epoxy vitrimer from epoxidized soybean oil for reprocessable and recyclable carbon fiber reinforced composite. *Composites Communications* **2020**, *22*, 100445.
(57) Song, F.; Li, Z.; Jia, P.; Zhang, M.; Bo, C.; Feng, G.; Hu, L.; Zhou, Y. Tunable “soft and stiff”, self-healing, recyclable, thermadapt shape memory biomass polymers based on multiple hydrogen bonds and dynamic imine bonds. *Journal of Materials Chemistry A* **2019**, *7*, 13400-13410.

(58) Wang, S.; Ma, S.; Li, Q.; Xu, X.; Wang, B.; Yuan, W.; Zhou, S.; You, S.; Zhu, J. Facile in situ preparation of high-performance epoxy vitrimer from renewable resources and its application in nondestructive recyclable carbon fiber composite. *Green Chemistry* **2019**, *21*, 1484-1497.
(59) Tao, Y.; Fang, L.; Zhou, J.; Wang, C.; Sun, J.; Fang, Q. Gel–Sol Transition of Vanillin-Based Polyimine Vitrimers: Imparting Vitrimers with Extra Welding and Self-Healing Abilities. *ACS Applied Polymer Materials* **2020**, *2*, 295-303.
(60) Snyder, R. L.; Lidston, C. A. L.; De Hoe, G. X.; Parvulescu, M. J. S.; Hillmyer, M. A.; Coates, G. W. Mechanically robust and reprocessable imine exchange networks from modular polyester pre-polymers. *Polymer Chemistry* **2020**, *11*, 5346-5355.
(61) Zhang, Z.-H.; Han, Z.; Zeng, X.-A.; Xiong, X.-Y.; Liu, Y.-J. Enhancing mechanical properties of chitosan films via modification with vanillin. *International Journal of Biological Macromolecules* **2015**, *81*, 638-643.
(62) Kan, K.; Akashi, M.; Ajiro, H. Polylactides Bearing Vanillin at Chain End Provided Dual Dynamic Interactions: Stereocomplex Formation and Nanostructure Control. *Macromolecular Chemistry and Physics* **2016**, *217*, 2679-2685.
(63) Zhao, S.; Abu-Omar, M. M. Recyclable and Malleable Epoxy Thermoset Bearing Aromatic Imine Bonds. *Macromolecules* **2018**, *51*, 9816-9824.
(64) Zhao, X.-L.; Liu, Y.-Y.; Weng, Y.; Li, Y.-D.; Zeng, J.-B. Sustainable Epoxy Vitrimers from Epoxidized Soybean Oil and Vanillin. *ACS Sustainable Chemistry & Engineering* **2020**, *8*, 15020-15029.
(65) Yu, Q.; Peng, X.; Wang, Y.; Geng, H.; Xu, A.; Zhang, X.; Xu, W.; Ye, D. Vanillin-based degradable epoxy vitrimers: Reprocessability and mechanical properties study. *European Polymer Journal* **2019**, *117*, 55-63.
(66) Dhers, S.; Vantomme, G.; Avérous, L. A fully bio-based polyimine vitrimer derived from fructose. *Green Chemistry* **2019**, *21*, 1596-1601.
(67) Hajj, R.; Duval, A.; Dhers, S.; Avérous, L. Network Design to Control Polyimine Vitrimer Properties: Physical Versus Chemical Approach. *Macromolecules* **2020**, *53*, 3796-3805.
(68) Chen, Z.; Wang, J.; Qi, H. J.; Wang, T.; Naguib, H. E. Green and Sustainable Layered Chitin–Vitrimer Composite with Enhanced Modulus, Reprocessability, and Smart Actuator Function. *ACS Sustainable Chemistry & Engineering* **2020**, *8*, 15168-15178.
(69) Abdel Aziz, M. S.; Salama, H. E.; Saad, G. R. Diglycidyl ether of bisphenol A/chitosan-graft-polyaniline composites with electromagnetic interference shielding properties: Synthesis, characterization, and curing kinetics. *Polymer Engineering & Science* **2019**, *59*, 372-381.
(70) Fusteș-Dămoc, I.; Măluțan, T.; Mija, A. High content chitosan-based materials with high performance properties. *International Journal of Biological Macromolecules* **2022**, *223*, 263-272.
(71) Lin, L.; Su, Z.; Zhang, H.; Zhou, G.; Zhou, H.; Ren, J.; Wang, X.; Liu, C.; Wang, X. Thermo-processable chitosan-based plastic substitute with self-adaptiveness and closed-loop recyclability. *Carbohydrate Polymers* **2022**, *291*, 119479.
(72) Su, Z.; Huang, S.; Wang, Y.; Ling, H.; Yang, X.; Jin, Y.; Wang, X.; Zhang, W. Robust, high-barrier, and fully recyclable cellulose-based plastic replacement enabled by a dynamic imine polymer. *Journal of Materials Chemistry A* **2020**, *8*, 14082-14090.
(73) Kittur, F. S.; Harish Prashanth, K. V.; Udaya Sankar, K.; Tharanathan, R. N. Characterization of chitin, chitosan and their carboxymethyl derivatives by differential scanning calorimetry. *Carbohydrate Polymers* **2002**, *49*, 185-193.

(74) Gliko-Kabir, I.; Penhasi, A.; Rubinstein, A. Characterization of crosslinked guar by thermal analysis. *Carbohydrate Research* **1999**, *316*, 6-13.
(75) Kim, J. H.; Lee, Y. M. Synthesis and properties of diethylaminoethyl chitosan. *Polymer* **1993**, *34*, 1952-1957.
(76) Neto, C. G. T.; Giacometti, J. A.; Job, A. E.; Ferreira, F. C.; Fonseca, J. L. C.; Pereira, M. R. Thermal Analysis of Chitosan Based Networks. *Carbohydrate Polymers* **2005**, *62*, 97-103.
(77) Pizzoli, M.; Ceccorulli, G.; Scandola, M. Molecular motions of chitosan in the solid state. *Carbohydrate Research* **1991**, *222*, 205-213.
(78) Zhang, L.; Rowan, S. J. Effect of Sterics and Degree of Cross-Linking on the Mechanical Properties of Dynamic Poly(alkylurea–urethane) Networks. *Macromolecules* **2017**, *50*, 5051-5060.
(79) He, C.; Shi, S.; Wang, D.; Helms, B. A.; Russell, T. P. Poly(oxime–ester) Vitrimers with Catalyst-Free Bond Exchange. *Journal of the American Chemical Society* **2019**, *141*, 13753-13757.
(80) Brutman, J. P.; Delgado, P. A.; Hillmyer, M. A. Polylactide Vitrimers. *ACS Macro Letters* **2014**, *3*, 607-610.
(81) Escamilla-García, M.; Calderón-Domínguez, G.; Chanona-Pérez, J. J.; Farrera-Rebollo, R. R.; Andraca-Adame, J. A.; Arzate-Vázquez, I.; Mendez-Mendez, J. V.; Moreno-Ruiz, L. A. Physical and structural characterisation of zein and chitosan edible films using nanotechnology tools. *International Journal of Biological Macromolecules* **2013**, *61*, 196-203.
(82) *Overview of materials for Epoxy Cure Resin*. **2023**.(accessed 2023 Feb 2023).
(83) Béguin, P.; Aubert, J.-P. The biological degradation of cellulose. *FEMS Microbiology Reviews* **1994**, *13*, 25-58.(acccessed 5/6/2022).
(84) Beier, S.; Bertilsson, S. Bacterial chitin degradation—mechanisms and ecophysiological strategies. *Frontiers in Microbiology* **2013**, *4*, Review.
(85) Vaverková, M.; Kotovicová, J.; Adamcová, D. Testing the biodegradability and biodegradation rates of degradable/biodegradable plastics within simulated environment. *Infrastruktura i Ekologia Terenów Wiejskich* **2011**, (12).
(86) Liu, X.; Pollard, B.; Banwell, M. G.; Yu, L.-J.; Coote, M. L.; Gardiner, M. G.; van Vugt-Lussenburg, B. M. A.; van der Burg, B.; Grasset, F. L.; Campillo, E.; et al. Simple and modestly scalable synthesis of isoCyrene from levoglucosenone and its comparison to the bio-derived and polar aprotic solvent Cyrene®. *Australian Journal of Chemistry* **2022**, *75*, 331-344.
(87) Diot-Néant, F.; Mouterde, L.; Fadlallah, S.; Miller, S. A.; Allais, F. Sustainable Synthesis and Polycondensation of Levoglucosenone-Cyrene-Based Bicyclic Diol Monomer: Access to Renewable Polyesters. *ChemSusChem* **2020**, *13*, 2613-2620.
(88) Ma, X.; Liu, X.; Yates, P.; Raverty, W.; Banwell, M. G.; Ma, C.; Willis, A. C.; Carr, P. D. Manipulating the enone moiety of levoglucosenone: 1,3-Transposition reactions including ones leading to isolevoglucosenone. *Tetrahedron* **2018**, *74*, 5000-5011.
(89) Diot-Néant, F.; Mouterde, L. M. M.; Veith, C.; Couvreur, J.; Miller, S. A.; Allais, F. Sustainable One-Pot Synthesis and Polycondensation of a Levoglucosenone-Derived Cyclic Acetal Diol. *ACS Sustainable Chemistry & Engineering* **2022**, *10*, 10132-10143.
(90) Alfonsi, K.; Colberg, J.; Dunn, P. J.; Fevig, T.; Jennings, S.; Johnson, T. A.; Kleine, H. P.; Knight, C.; Nagy, M. A.; Perry, D. A.; et al. Green chemistry tools to influence a medicinal chemistry and research chemistry based organisation. *Green Chemistry* **2008**, *10*, 31-36.

Australian National University

Statement of Contribution

This thesis is submitted as a Thesis by Compilation in accordance with https://policies.anu.edu.au/ppl/document/ANUP_003405

I declare that the research presented in this Thesis represents original work that I carried out during my candidature at the Australian National University, except for contributions to multi-author papers incorporated in the Thesis where my contributions are specified in this Statement of Contribution.

Title: Pushing the Limits of Greenness: Fully Bio-Based & Compostable Dynamic Thermoset Composites

Authors: **Ashwani Kumar**,[†] Brett Pollard[†] and Luke A. Connal

Publication outlet (Patent): **Ashwani Kumar**, Brett Pollard, Luke A. Connal, "Bio-based Polymers". Australia Provisional Patent Application No. 2022903603 — 28th Nov 2022.

Publication outlet (Journal): Not Yet Submitted

Current status of paper: Not Yet Submitted

Contribution to paper: My contribution to the manuscript includes project designing, synthesis, characterization, and data analysis as well as preparing and revising manuscript and figures (overall 50%).

Senior author or collaborating authors endorsement:

ASHWANI KUMAR	Ashwani	2nd March 2023
Candidate – Print Name	Signature	Date

Endorsed

LUKE CONNAL		14th March 2023
Primary Supervisor – Print Name	Signature	Date

Mark Humphrey		15th March 2023
Delegated Authority – Print Name	Signature	Date

Chapter 5 Pushing the Limits of Greenness: Fully Bio-Based & Compostable Dynamic Thermoset Composites

Kumar, A.; Pollard, B.; Connal, L. A. "Bio-based Polymers". *Australia Provisional Patent Application No.* 2022903603 — 28th Nov 2022.

Preface

This work expands the boundaries of sustainability by integrating high-volume waste coffee grounds, vegetable oil, and algae. This work has been filed as a provisional patent and is almost ready for submission, in which I am the co-first author with Brett Pollard. My contribution to the manuscript includes project designing, synthesis, characterization, and data analysis, as well as preparing and revising the manuscript and figures (overall 50%). Brett Pollard, a PhD student in Connal lab, did the project designing, synthesis, characterization, data analysis, revising manuscript, and figures.

Foreword

This chapter culminates a number of goals of this thesis, here we have combined fully sustainable feedstocks with dynamic chemistry. In chapter 3, we learn the importance of a catalyst free dynamic transesterification exchange process, and in chapter 4, we learn about the upcycling of biomass waste into a degradable thermoset. In this chapter, I integrated my knowledge from chapters 3 and 4 to develop a fully biobased, biodegradable thermoset based on a catalyst-free transesterification exchange process. This chapter advances upcycling by embracing numerous substantial waste sources. The commercial and industrial sectors make very inefficient use of renewable feedstocks such as chia seed oil, brown algae, and spent coffee grounds. The objective of this chapter is to transform this biomass into a biodegradable,

green, dynamic thermoset composite with potential commercial applications. A fully green dynamic thermoset composite was developed using epoxidized chia seed oil, kelp-derived alginic acid, and spent coffee grounds at mild reaction temperatures (90–150 °C). The thermosets exhibit stress relaxation and reprocessability owing to the catalyst-free transesterification reaction of β-hydroxyester groups. Several prototypes, such as plant pots, thin film sheets, and beverage coolers, were made using the resulting suite of materials, which show potential application as industrial commodity materials. The thermoset composites can be readily composted at home under natural conditions in 4-5 months.

Introduction

Plastics are low-cost, lightweight, resilient, corrosion-resistant materials with excellent thermal and electrical insulating properties. As a result, plastic manufacturing has soared exponentially since 1950, reaching 380 Mt year^{-1} in 2015.[1] Most of the monomers required to manufacture plastics (such as ethylene and propylene) are generated from non-renewable petrochemical hydrocarbons. Thermosets, prepared through the irreversible curing of monomer resin, are remarkable materials because of their strongly crosslinked covalent networks which confer exceptional mechanical properties, dimensional stability, as well as heat and chemical resistance. Covalently crosslinked thermosets find many applications in coatings, dental materials, additive manufacturing and adhesives because of their ability to be cured on demand, as well as their stiffness.[2] Despite the benefits provided by the crosslinked networks, the thermosets' permanent, rigid three-dimensional structure prevents flow even at high temperatures, rendering the typical mechanical recycling of thermosets unfeasible.[3] As a consequence, the majority of thermosets are burned or disposed of in landfills come end

of life.[4] Incorporation of covalent adaptable network (CAN) into thermosets is an appealing solution for their lack of recyclability.[5] The CAN polymers and their associative mechanism maintain a constant crosslinking density and exhibit a glass-forming behavior at processing temperatures.[6] These types of associative exchange mechanism bearing CANs were termed "vitrimers" by Leibler and his colleagues.[7] This elegant modification of the traditional thermoset structure allows vitrimers to not only possess the same excellent mechanical and thermal stability as conventional thermosets, but also to display the same desired reprocessability as thermoplastics, thereby extending their service life.[8, 9] Within the last decade, several vitrimers based on various reversible processes, such as radical sulfur chemistry, olefin metathesis, imine exchange, vinylogous urethane exchange, borate exchange and transesterification have been reported.[3, 10]

A critical challenge in modern vitrimer research is finding sustainable replacements for monomers currently derived from petroleum. Recently the sustainability of CANs, thermosets, and vitrimers have consistently shown significant improvement.[11-15] Among various types of renewable raw resources, plant oils offer a number of benefits, such as their abundant availability on a global platform, and relatively rapid production, with a seasonal turnaround.[16-19] A significant benefit of employing vegetable oils as a monomer feedstock is the potential for functionalisation of their triglyceride alkenes. Oxidation of the alkenes into strained and reactive epoxide species, for example, offers energetically favourable routes to polymerisation *via* ring opening polymerisation or esterification, thereby avoiding the exceedingly toxic epichlorohydrin, an industry standard reagent for producing the diglycidyl ether of bisphenol A.

With this application in mind, the most notable variation in the seed oils of differing species is the composition of fatty acids, which influences the number of double bonds present per triglyceride molecule. One of the seed oils with the highest degree of double bonds present in the fatty acid chains is chia seed oil (*Salvia hispanica,* L.), a non-toxic plant oil which is produced by national farmers for commercial supply as a cosmetic product.[20] Given this excellent degree of unsaturation, the resultant epoxidized chia seed oil (ECO) provides opportunities for a relatively high degree of crosslinking when compared to more highly saturated seed oils. To the best of our knowledge, there has been just one previous report of ECO being employed in the polymer space, where it was used as a plasticizer with poly(lactic acid) analogous to the use of epoxidized soybean oil (ESBO) in poly(vinyl chloride).[21] Encouragingly, the report demonstrates that ECO admixtures are readily compostable under standard conditions.[21]

Epoxides are known to react with carboxylic acids to yield β-hydroxyester linkages, and various naturally occurring polycarboxylic acids can be employed as crosslinkers with epoxidized vegetable oil.[22] Alginic acid is a naturally occurring polysaccharide obtained from brown seaweeds such as kelp, gulfweed, *Ascophyllum* and macroalgae which contains a high percentage of carboxylic acid moieties (19-25%). Alginic acid is a linear copolymer mainly composed of *α*-1,4-linked L-glucuronic acid and *β*-1,4-linked D-mannuronic acid residues. The use of a polycarboxylic acid such as alginic acid as a crosslinking scaffold for ECO confers a crucial feature to the resultant networks: epoxy-acid interactions form β-hydroxyester linkages, which can undergo catalyst-free transesterification reactions at appropriate temperatures.[23]

For tailored mechanical properties, thermoset polymers are often coupled with reinforcements, *inter alia*, carbon or glass fibres, carbon nanotubes and graphene.[24] Being a renewable waste product, spent coffee grounds have garnered significant attention as a composite filler. For every 1 ton of green coffee industrially processed to prepare soluble coffee products, as an example, roughly 650 kg of spent coffee grounds are generated as a waste product.[25] While some attempts have been made to generate composites from spent coffee grounds waste,[26-30] to date, little of widespread practical application has been accomplished and so this represents a largely untapped resource.

Herein, we report our development of a completely eco-friendly dynamic thermoset composite material out of abundant renewable chia seed oil, alginic acid, and spent coffee grounds. The network contains β-hydroxyester linkages which can undergo catalyst-free transesterification exchange process, allowing them to exhibit thermally induced stress relaxation and reprocessing capabilities. The combination of green materials and processes generated an entirely green biomass-derived, biodegradable composite with tuneable properties such as stiffness, which has scope for production at industrial scale. Furthermore, we demonstrated a suite of potential applications such as the production of biodegradable plant pots, thin films, large scale sheets and a beverage cooler.

Results and Discussion

Synthesis and characterization of thermoset composites

Epoxidation confers two primary advantages: firstly, it produces highly reactive species, and secondly, can be installed using comparatively moderate reaction conditions.[31] The epoxidation of chia oil performed in this work was achieved inexpensively through oxidation of the triglyceride double bond with performic acid, generated *in situ* using hydrogen peroxide

and formic acid (**Scheme S5.1**). Similar attempts using an even greener (albeit more expensive) lipase B and hydrogen peroxide afforded a product that was in all ways identical to the peroxyacid ECO. The Fourier-transform infrared (FT-IR) spectrum of the resulting epoxidized chia seed oil (ECO) showed the disappearance of the characteristic stretching vibration peak of cis-olefinic double bonds at 3010 cm^{-1} present in virgin chia seed oil (**Figure 5.2c**). In comparison, the ECO FT-IR spectrum shows a new, low intensity absorption peak at 821 cm^{-1}, indicative of oxirane oxygen.[32] The ^{1}H NMR spectra of chia oil and ECO are shown in **Figure S5.1-5.2**, with relevant expansions shown in **Figure 5.1**. The signals at δ 5.59 – 5.25 (m) (shown in blue) are derived from olefinic protons of chia seed oil triglycerides, and signals at δ 3.13 – 2.94 (m) and 2.86 (ddd, J = 27.1, 11.9, 5.8 Hz) ppm correspond to the protons alpha to the alkenes (shown in orange). In the ^{1}H NMR spectrum of epoxidized chia seed oil, these signals are absent, and a broad new signal is observed at δ 3.24 – 3.12 (m) ppm, attributable to the oxirane-bound protons.[31] The peak integrals indicate the reaction proceeded to minimum 80% conversion with respect to the transformation of alkenes. Collectively, the FT-IR and ^{1}H NMR data confirm the successful transformation of the triglyceride-bound alkenes and incorporation of epoxide functionalities to the chia seed oil.

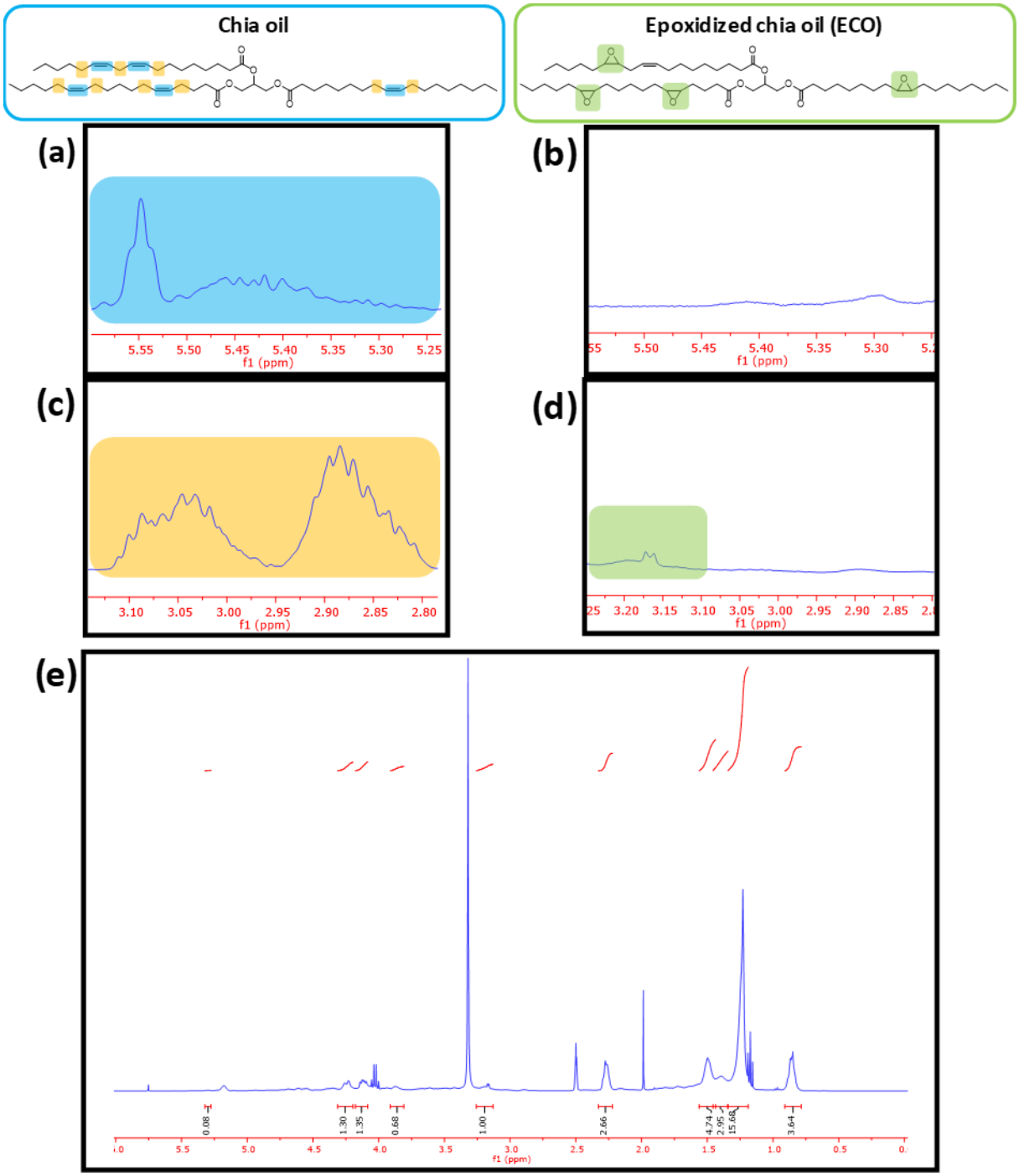

Figure 5.1: *Expansions of the primary regions of interest in the ^{1}H NMR spectra for virgin and epoxidized chia seed oil (left and right, respectively): (a) Proton signals δ 5.59 – 5.25 (m) (shown in blue) are derived from olefinic protons of virgin chia seed oil triglycerides, (b) ^{1}H NMR spectrum of epoxidized chia seed oil showing absence of olefinic protons, (c) signals at δ 3.13 – 2.94 (m) and 2.86 (ddd, J = 27.1, 11.9, 5.8 Hz) ppm corresponding to the protons at the*

alpha position of the alkenes (shown in orange) in virgin chia seed oil, and (d) new signals observed after epoxidation (δ 3.24 – 3.12 (m) ppm, shown in green) consistent with oxirane-bound protons, with the signals for protons alpha to the alkenes observed in (c) almost entirely absent, and, (e) full ^{1}H-NMR spectrum of epoxidized chia seed oil (ECO).

We used the sustainable and non-toxic cross-linking agent alginic acid (obtained from brown algae) to crosslink ECO. Wetting of the solid alginic acid with a small amount of water (mass ratio 1:4 water : alginic acid) facilitated stirring with the epoxidized oil, and the mixtures were incorporated until homogenous (*ca.* 60 s). The crosslinked networks containing β-hydroxyester groups were then constructed through the thermally induced chemical reaction (120 – 150 °C) between the epoxy groups of ECO and the carboxylic acid functionalities present in alginic acid (**Figure 5.2a**).

Soyabean oil, which bears a significantly lower iodine value than chia seed oil (**ESI**), is available at relatively low cost on an industrial scale. Soyabean oil (Alfa-Aesar) was epoxidized in an identical peroxyacid process to that employed for chia seed oil. Attempts to crosslink epoxidized soyabean oil with alginic acid invariably afforded a viscous, sticky and heterogenous brown sludge, indicating that a minimum iodine value oil is required to effect a satisfactory degree of crosslinking.

We then investigated if we could load spent coffee grounds into the polymer matrix. The thermoset composites were prepared by incorporating a varying weight percent of spent coffee grounds (**Figure 5.2b**) into the stirring step prior to heating. The thermosets showed carbonyl stretching vibration (C=O) of ester groups at 1743 cm^{-1}, overlapping with the ester peak of ECO (**Figure 5.2c**).

(a)

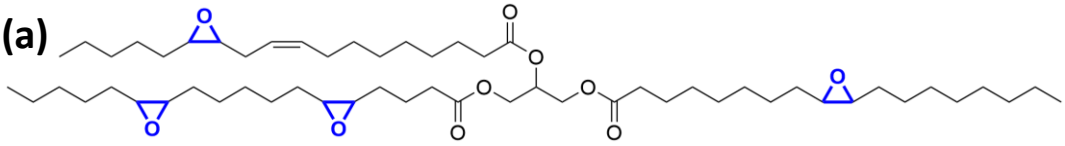

Epoxidized chia oil (ECO)

+

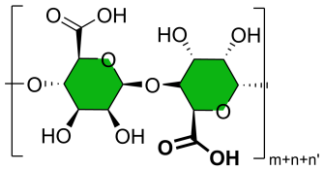

Alginic acid

1. 90 °C, 2 h
2. 150 °C, 24 h (curing step)

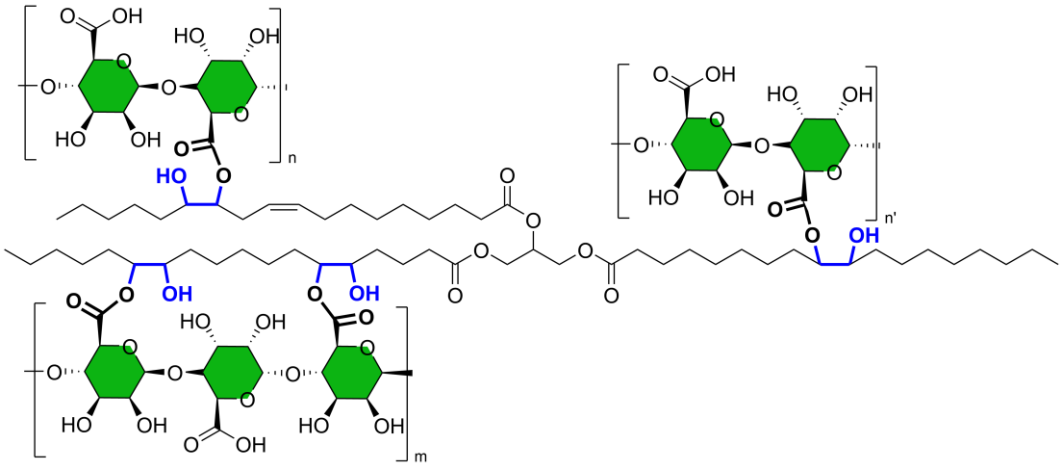

(b)

Spent coffee grounds (wt%)	Alginic acid (g)	ECO (g)	Water (g)	**Sample**
0	0.96	5	0.25	**0%**
10	0.96	5	0.25	**10%**
20	0.96	5	0.25	**20%**
30	0.96	5	0.25	**30%**

(c)

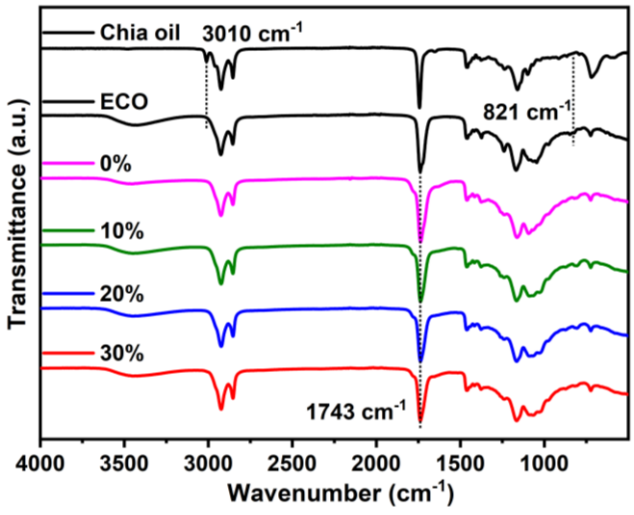

Figure 5.2: *Thermoset composites from epoxidized chia oil (ECO), alginic acid and spent coffee grounds, (a) synthetic route to prepare thermosets. The prepared thermoset networks contain β-hydroxyester groups, (b) various thermoset composite formulations prepared by varying spent coffee grounds content and (c) FT-IR spectra of chia seed oil, ECO, and thermoset composites.*

Thermal and Mechanical properties

The glass transition temperature (T_g) of the thermosets was investigated using differential scanning calorimetry (DSC). The results indicated that an increasing weight percentage of spent coffee grounds yielded a decrease in T_g from 1.4 to 0.3 °C (**0-30%**) (**Figure 5.3a**). This decrease in T_g from 0—30% is attributed to a reduction in the degree of crosslinking caused by spent coffee grounds physically disrupting the polymer network. The thermal stability of thermoset composites was investigated by thermogravimetric analysis (TGA). The initial weight loss (*ca.* Δw_1= 6%) at 150—230 °C is attributable to the thermal depolymerization of thermosets and hemicellulose[33] present in spent coffee grounds (**Figure 5.3b**). The most significant weight loss occurred between 270—430 °C. At this stage, the thermosets, and major constituents of spent coffee grounds i.e., cellulose and hemicellulose undergo decomposition, resulting in a 77% weight loss.[34, 35]

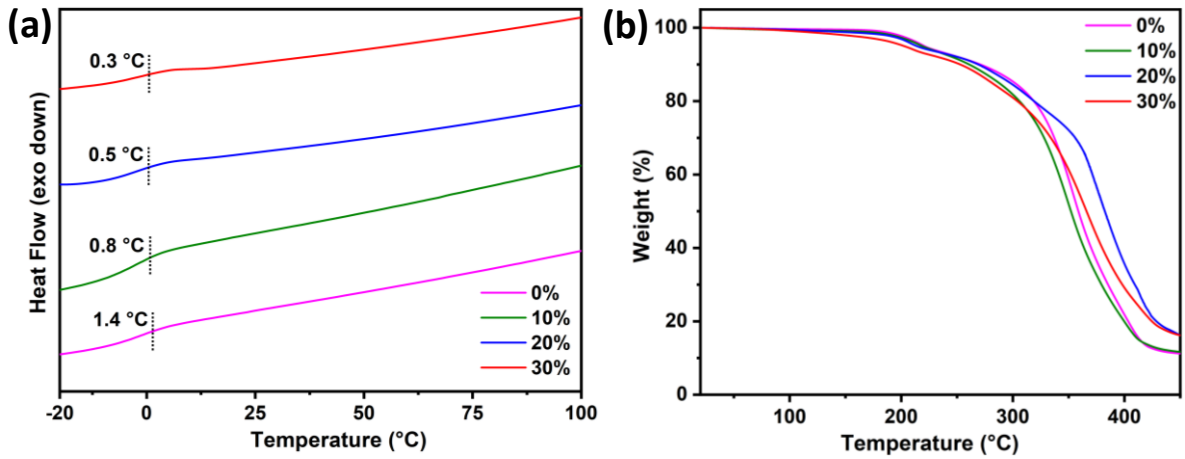

***Figure 5.3**: Thermal properties of thermoset composites, (a) DSC thermograms of thermoset composites were measured at a heating rate of 3 °C min^{-1}. T_g decreased with increasing percentage of spent coffee grounds owing to a lower crosslinking degree. (b) TGA curve of thermoset composites. All thermoset composites showed similar thermal stability.*

Swelling experiments were carried out in water at room temperature (22 °C) to better understand the hydrophilic nature of the polymer networks. The swelling test revealed that all thermoset composites were insoluble but swelled after 24 hours, with gel fractions of 98.7 ± 1.2, 97.9 ± 0.9, 96.8 ± 1.2, and 95.9 ± 1.3 for 0, 10, 20, and 30%, respectively (**Table 5.1**). The presence of hydrophilic groups in the polymer matrix, results swelling of all thermoset composites. These findings indicate that when the amount of spent coffee grounds increases from 0 to 30%, spent coffee grounds disrupts some polymer networks, resulting in a decrease in crosslinking units and an increase in the degree of swelling. This data aligned with the tensile testing of the thermoset composites, which showcased that the tensile strength and Young's moduli of composites increased with decreasing spent coffee grounds content (**Table 5.1**).

Table 5.1: *Gel fraction and mechanical properties of thermoset composites.*

Samples	T_g[a] (°C)	Gel fraction %[b]	Swell %[c]	Tensile strength[d] (kPa)	Young's modulus[e] (kPa)
0%	1.4	98.7 ± 1.2	3.8 ± 0.5	410.5 ± 7.3	46.8 ± 4.2
10%	0.8	97.9 ± 0.9	5.1 ± 0.7	215.3 ± 6.6	26.4 ± 3.9
20%	0.5	96.8 ± 1.2	6.3 ± 1.0	112.9 ± 5.9	13.6 ± 3.2
30%	0.3	95.9 ± 1.3	8.9 ± 1.4	33.1 ± 5.1	5.3 ± 2.9

[a]Calculated from DSC. [b,c] Calculated using the following the equation:

$$Gel\ fraction\ \% = \frac{m_3}{m_1}\ , Swollen\ \% = \frac{m_2 - m_1}{m_1}$$

where, m_1 = initial mass of sample, m_2 = mass of swollen sample after soaking in water for 24 h, m_3 = mass of dried sample after extraction of water solvent.

[d,e]Calculated from the universal testing machine (Instron) at a loading rate of 3 mm min^{-1}. The mechanical properties were tested 3 times with a 10 N and 5 kN load cell at 42% humidity.

The distribution of spent coffee grounds in the polymer matrix was evaluated by scanning electron microscopy (SEM). The SEM images of the cross-sectional cut of thermoset composite (30%) revealed a heterogeneous distribution of spent coffee grounds with aggregation in the polymer matrix (**Figure S5.3**). The addition of finely ground spent coffee particles results in a uniform distribution of filler particles in thermoset networks. However, larger spent coffee ground particles settle to the bottom of the thermoset due to the force of gravity.

Stress Relaxation

Unlike classical thermosets, the mechanical stress in dynamic covalent networks can be rapidly relieved by network topology rearrangement driven by bond exchange mechanisms. Stress relaxation experiments were conducted to investigate the dynamic properties of thermoset composites at 150 °C using a rheometer (**Figure 5.4a**). The presence of β-hydroxyester linkages in the networks permits a catalyst-free transesterification exchange process, which, gratifyingly, enabled these thermosets to exhibit stress relaxation. The

relaxation rate rapidly rose from 0 to 30% as the content of spent coffee grounds was increased, owing to a reduction in crosslinking degree and/or an increase in residual hydroxyl concentration. Previous reports have shown that the rate of stress relaxation increases as the concentration of hydroxyl functionalities increases, or, as the degree of crosslinking decreases.[36-40] The stress relaxation measurement of the 30 *wt*% spent coffee grounds composite was studied at different temperatures (**Figure 5.4b**). The relaxation rate increased with temperature in conjunction with the increase in the transesterification exchange process.

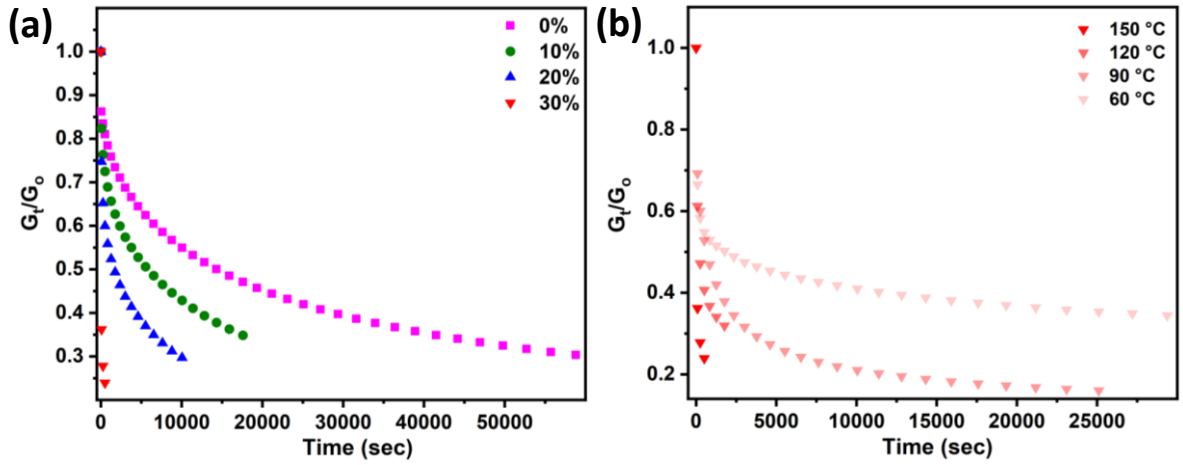

***Figure 5.4**: Stress relaxation measurements of thermoset composites (a) isothermal stress relaxation measurements at 150 °C. The stress relaxation rate increased with increasing spent coffee grounds content and (b) stress relaxation measurements of the 30% spent coffee grounds thermoset composite at a range of temperatures (60, 90, 120 and 150 °C). The relaxation rate increased with the temperature due to the rapid transesterification exchange process.*

Tensile Testing and Reprocessing

The mechanical properties of thermoset composites were examined using uniaxial tensile testing at room temperature (22 °C). Tunable mechanical properties were achieved by

incorporating different weight percentages of spent coffee grounds (**Figure 5.5a**). Comparing composites bearing 0 to 30 *wt*% coffee grounds indicated that both the tensile strength (σ) and Youngs modulus (*E*) decreased from 410.5 ± 7.3 kPa to 33.1 ± 5.1 kPa, and 46.8 ± 4.2 to 5.3 ± 2.9 kPa respectively **(Table 5.1)**. This is due to the spent coffee grounds physically disrupting the thermoset polymer networks, resulting in a decrease in the effective degree of crosslinking and hence mechanical strength of the material. Furthermore, as the content of spent coffee grounds exceeds 30 *wt*%, the resultant thermoset loses its integrity and becomes a highly viscous and sticky heterogeneous goo.

We next investigated the reprocessability of the thermoset composites. The availability of β-hydroxyester linkages enables a dynamic transesterification exchange process which confers reprocessability. Small pieces (5 mm x 5 mm x 3 mm) were reprocessed in a hot press for 0.5 h (150 °C, 8 MPa). The fragments of the thermoset (using 30 *wt*% composite as an example) were successfully reprocessed into a unified thermoset (**Figure 5.5b**). The mechanical properties of the reprocessed thermosets were then compared to the pristine thermosets. The σ of the reprocessed 0, 10, 20 and 30 *wt*% composites were recovered by 28.7 ± 7.1, 64.6 ± 6.8, 81.0 ± 6.0 and, 93.2 ± 5.8%, respectively. It is anticipated that the recovery of σ decreases with lower loading of spent coffee ground filler due to the slower transesterification exchange process in thermosets with a greater degree of crosslinking. The incomplete recovery of σ is presumably due to the deterioration of the crosslinking units caused by the elevated temperature during reprocessing. FT-IR analysis was used to evaluate the chemical structure of thermoset composites before and after the reprocessing step, which revealed no apparent change in the FT-IR spectra after reprocessing, particularly in the characteristic ester

peak observed at 1743 cm^{-1} (**Figure 5.5c**). This served to indicate that the chemical functionality was successfully preserved.

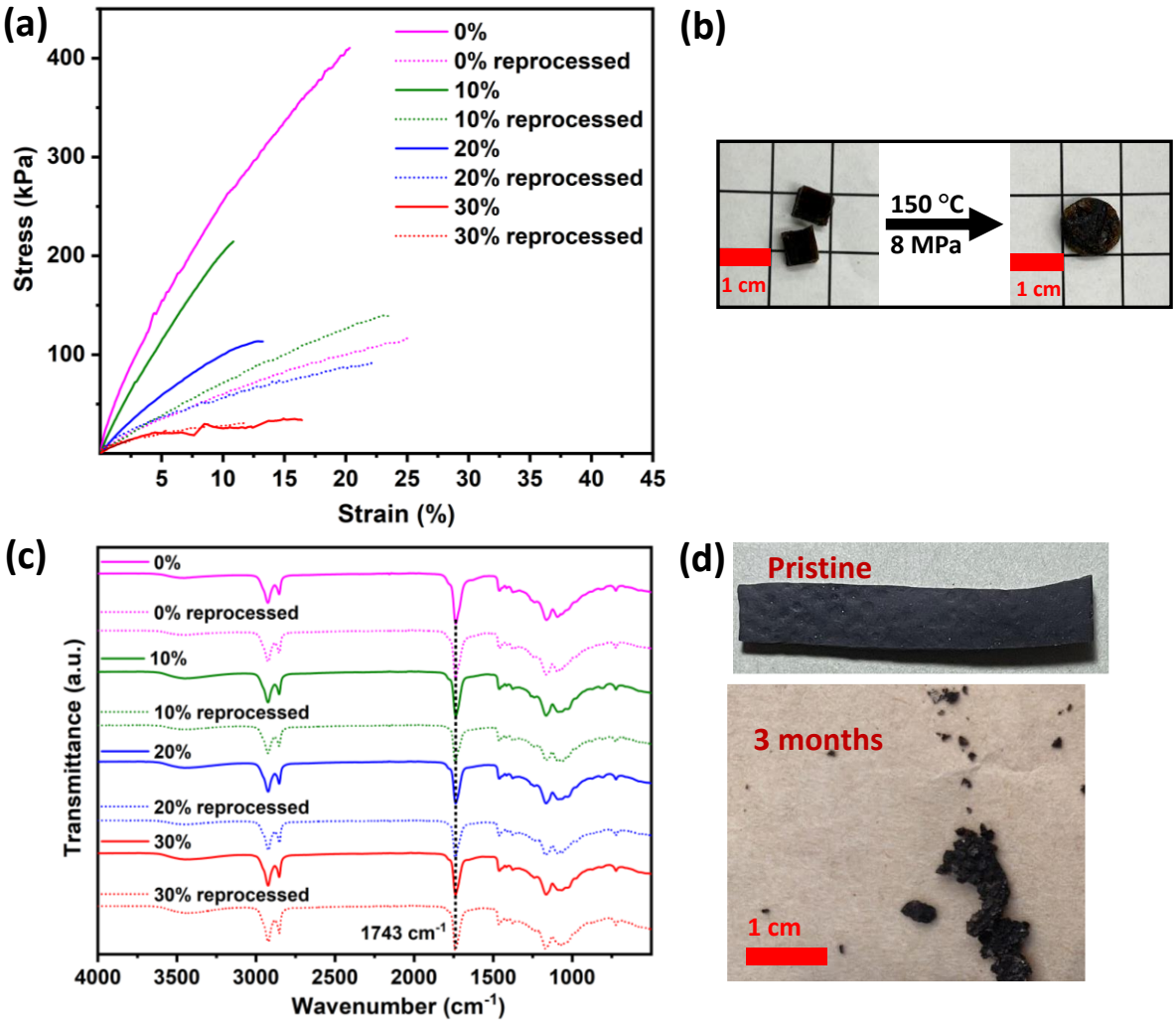

Figure 5.5: *Stress-strain curves and reprocessing of thermoset composites, (a) stress-strain curves of pristine and reprocessed thermoset composites. Both Young's moduli and tensile strength improved with decreasing wt% of spent coffee grounds, (b) reprocessing of small pieces of 30% thermoset composites by hot pressing at 150 °C for 0.5 h at a pressure of 8 MPa, (c) FT-IR spectra of pristine and reprocessed thermoset composites. The chemical functionality of the ester group was retained after reprocessing and, (d) biodegradation of 30 wt% thermoset composite. All thermosets were effectively composted within 4–5 months.*

Material Prototypes

We also employed these thermoset composites to fabricate a variety of prototype applications including plant pots, thin film sheets, and beverage coolers (**Figure 5.6**). These prototypes are mechanically robust, possess high-definition structures and have long shelf life. Moreover, we successfully demonstrated the large-scale preparation of thermoset sheets (210 mm × 300 mm × 5 mm, 350 g) in the laboratory (**Figure 5.6d**).

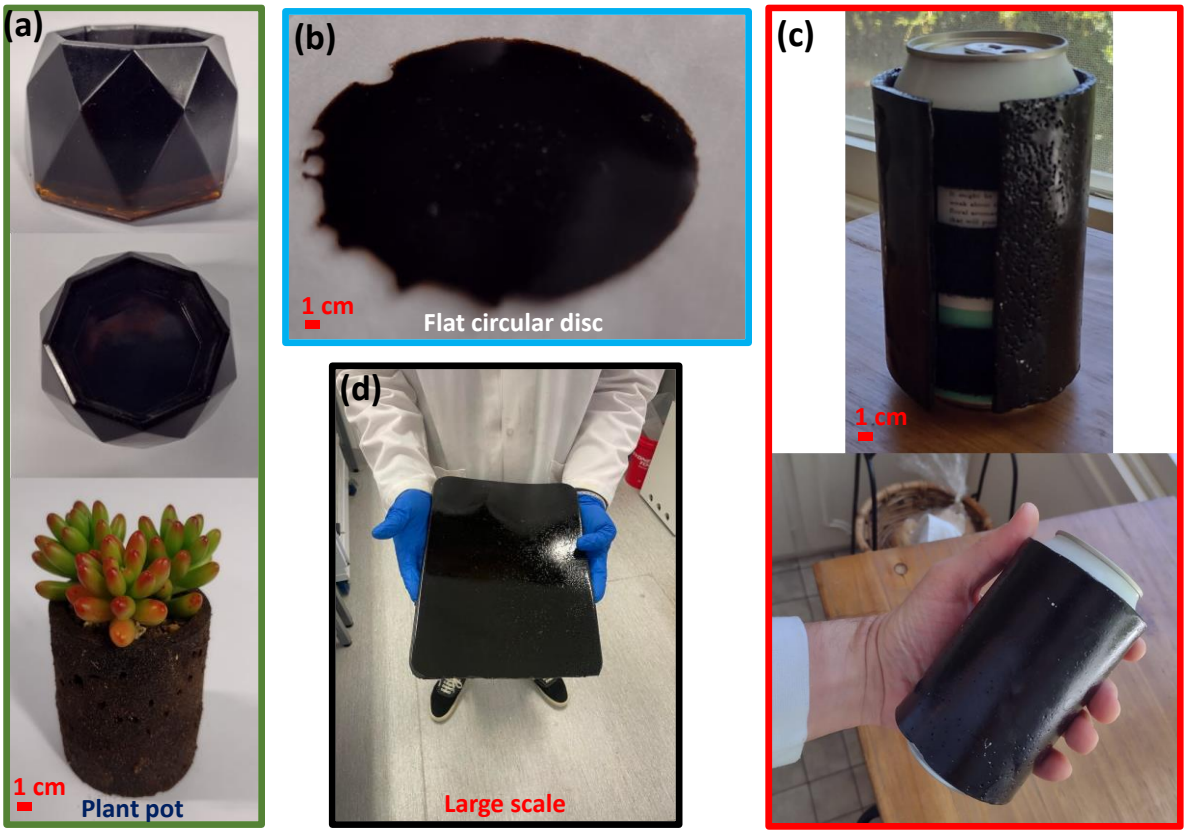

***Figure 5.6**: Range of prototypes prepared using thermoset composites, (a) different sets of plant pots showing high-definition vertices, (b) a thin flat circular disc approximately 1 mm thick, (c) beverage cooler sealed with hook-and-loop tape, and (d) large scale material development in laboratory (film mass = 350 g).*

Compostability

We then examined the compostability of our thermoset composites under environmental conditions. The thermoset composites were exposed to garden soil and compost over a period of 6 months, with the deterioration of the material determined by visual inspection.[41] Within 3 months, the materials disintegrated into small fragments (**Figure 5.5d**). After 4–5 months time the material had effectively degraded and could no longer be identified or isolated. We also investigated whether a pot made from the composite material was compatible with plant growth. We planted a small, ornamental succulent plant cutting in a plant pot cast from the composite thermoset, and it has been happily growing in an office environment for seven months (**Figure S5.4**).

Conclusion

Fully biomass derived, catalyst and solvent-free dynamic thermoset composites were prepared by incorporating the waste product spent coffee grounds into a novel thermoset, through cross-linking epoxidized chia seed oil and brown algae to yield a material that offers practical mechanical properties and sustainable end-of-life solutions. Alginic acid, which natively bears a 19-25% carboxylic acid content, was employed to open the strained oxirane rings of ECO and so form an exchangeable β-hydroxyester crosslinked network polymer. The inclusion of spent coffee grounds in the network allowed for tuneable mechanical properties through the physical disruption of otherwise rigid polymer networks. Due to the dynamic transesterification processes of β-hydroxyester groups in networks, the composite materials exhibited stress relaxation and were shown to be reprocessable. Furthermore, a variety of material prototypes were prepared using thermosets which are mechanically durable, have a high-definition structure, and possess a long shelf life. At the end of material lifecycle, the

thermosets can be decomposed in 4–5 months in a home compost, a feature which is critical to developing ecologically responsible plastic solutions. We anticipate that recyclable and compostable coffee composites derived from a plentiful natural resources will provide new, industrially viable and scalable alternative to traditional thermosets.

Supporting Information

Experimental

All commercially obtained solvents and reagents were used without further purification. Chia seed oil (100%) was purchased from Earthyard Australia. Soybean oil was purchased Alfa-Aesar. Hydrogen peroxide (30% *w*/*v*) and formic acid (98%) were purchased from Chemsupply. Alginic acid from brown algae (240 kDa, carboxyl group content 19-25%) was purchased from Sigma Aldrich. Spent coffee grounds were taken from local café shop knockbox and were screened to remove large particulate and were otherwise used as-is. Reverse osmosis (RO) water was used for wetting the solid ingredients.

^{1}H and ^{13}C solution-state NMR were recorded on a Bruker Ascend 400 MHz spectrometer (400 MHz for ^{1}H and 100 MHz for ^{13}C). Chemical shifts δ are reported relative to the resonance signal of ^{1}H or ^{13}C cores of tetramethylsilane and in ppm. The ^{1}H spectra were calibrated by setting the solvent peaks, caused by remaining traces of protons, to values known from the literature (δ $CHCl_3$ = 7.26 ppm). The coupling constants *J* are reported in Hz.

Fourier transform infrared spectroscopy (FT-IR) was performed on a Perkin Elmer Spectrum 2, with a 0.5 cm^{-1} resolution, over 32 scans from 500 to 4000 cm^{-1}. All the measurements were performed at room temperature (22 °C).

Differential scanning calorimetry (DSC) was performed using a TA Instruments Q20 at a heating rate of 3 °C min^{-1}. The data was recorded between -20 and 100 °C.

Thermal gravimetric analysis (TGA) was performed on a TA Instruments TGA Q 500 under a N_2 atmosphere over a temperature range of 25–460 °C at a heating rate of 3 °C min^{-1}.

Scanning electron microscopy (SEM) was performed on a Zeiss UltraPlus FESEM at 3 kV.

Stress-relaxation tests were carried out on Anton Paar MCR 702 multidrive rheometer using a plate geometry (PP25) with a 25 mm diameter. The material was placed on the rheometer, and the upper geometry was lowered. After reaching the appropriate temperature (60–150 °C), the samples were equilibrated for 30 min and then a constant shear strain of 2.1% was applied, with the time dependent stress relaxation measurement recorded.

Tensile tests were conducted on a universal testing machine (Instron) at a loading rate of 3 mm min^{-1}. The mechanical properties were tested at least 3 times with 10 and 5 kN load cells at 42% humidity.

The spent coffee grounds were screened using standard mesh sieves to obtain material with a particle size between 500-1000 μm.

Reprocessing experiment was performed on a PHI hydraulic press. The thermoset films were cut into small pieces and then placed into round steel mould (1 cm diameter) and subjected to a 20 min thermal equilibration at 150 °C. The thermosetting films were then reprocessed at 150 °C for 30 min at a pressure of 8 MPa. The reprocessed thermosets were demoulded after reaching room temperature.

Compostability assessment were performed using typical household garden soil (Canberra, Australia) and independently assessed by a local composting facility (Capital Scraps Composting, Canberra, Australia). Polymer samples (35 mm × 20 mm × 15 mm, *l* × *b* × *t*) were enclosed in a porous mesh bag and loaded 20 cm below the soil surface without mechanical packing or agitation so that the decomposing material could be isolated and investigated. The samples were then left for months and examined at weekly intervals. The visible changes in films were used to describe degradation which include roughening of the surface, formation of holes or cracks, fragmentation, changes in color, or formation of bio-films in the surface.[41] After 4–5 months time the material had effectively degraded.

Swelling tests were conducted three times by soaking samples weighing m_1 in water at room temperature for 24 h. Then, the water and any soluble fraction dissolved in the water was carefully removed using a syringe. The samples were blotted with lint-free wipes to remove water on the surface, dried under N_2 flow for 1 h, then the swollen weight m_2 was determined. Then, the samples were washed 3 times with methanol and then dried in oven at 110 °C for 120 min to ensure a complete removal of the residual solvent before recording m_3. The gel fraction and swelling ratio were calculated using following equations:

$$Swollen\ \% = \frac{m_2 - m_1}{m_1}$$

$$Gel\ fraction\ \% = \frac{m_3}{m_1}$$

Calculation of iodine value of oil

The iodine value of soyabean and chia seed oils were determined using a previously reported iodometric titration method.[42] Using this method, the iodine values of soyabean and chia seed oils were found to be 97 and 148, respectively.

Preparation of epoxidized oil

A magnetically stirred solution of seed oil (25 g) was maintained at 0 °C using an ice bath. Then, 22 mL of formic acid (98%) was added dropwise, with stirring, ensuring that the reaction mixture remained below 5 °C. After addition of the acid, 85 mL of hydrogen peroxide (30% *w/v*) was added to the reaction mixture dropwise. The reaction mixture was then removed from the ice bath and transferred to an oil bath, heating to 50 °C for 18 h. At this point, the mixture may become highly exothermic and potentially boil or overflow, and so adequate precautions (such as a splash guard and sufficiently large flask) were employed. After stirring the reaction mixture overnight, the mixture was allowed to cool to room temperature (22 °C) before being treated with 1.1 equivalents of saturated, aqueous sodium bicarbonate solution (53 g, 0.63 mol). Once gas evolution ceased, the mixture was extracted with ethyl acetate (3 × 50 mL), and the combined organic layers washed with water (3 × 50 mL), then, brine (3 × 50 mL). The organic layer was then dried using anhydrous sodium sulfate and gravity filtered before concentration under reduced pressure to afford epoxidized oil as a clear, mostly colorless and highly viscous oil (20 g, 80%).

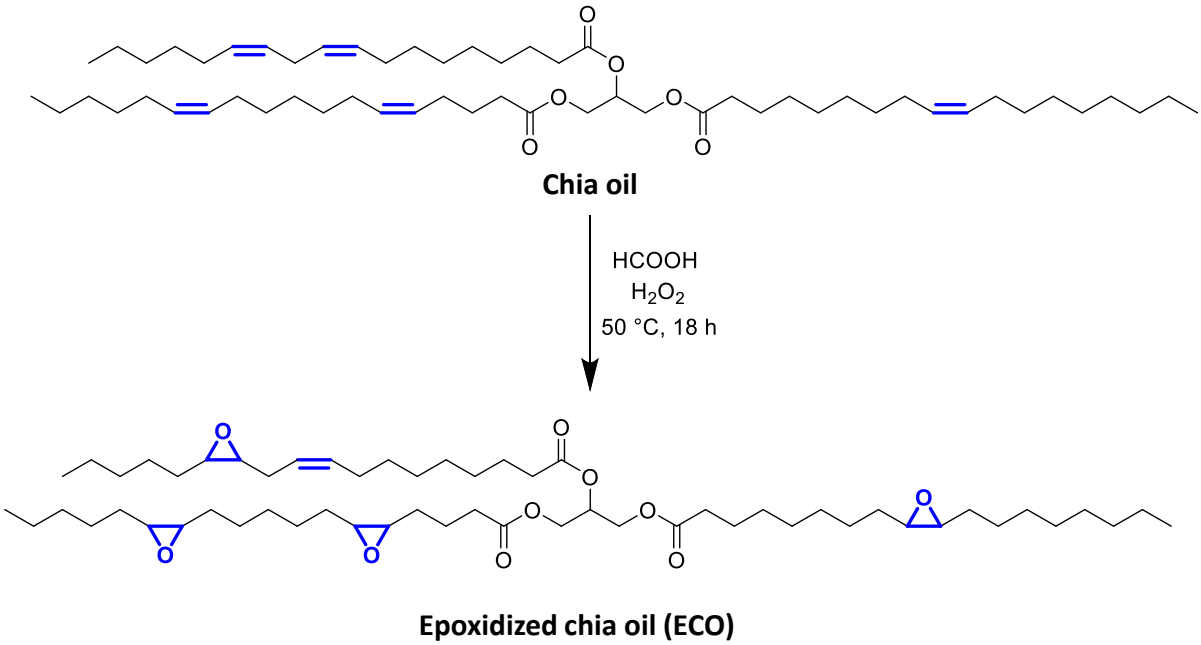

Scheme S5.1: *Synthesis of epoxidized chia oil (ECO).*

Preparation of thermoset composites

The dry ingredients (spent coffee grounds and alginic acid) were mixed separately before 0.25 g of water (RO) was added and the mixture were mechanically combined until homogeneous (*ca.* 45 s). Then, 5.00 g of epoxidized chia seed oil was added, and mixture was again manually stirred until homogenous (*ca.* 60 s). The reaction mixture was placed uncovered in a conventional oven at 90 °C for 2 h. After this time, the sample was again stirred to homogenise any solids which had separated, and the resulting viscous liquid was poured into silicone moulds (50 mm × 20 mm × 15 mm) before the temperature was increased to 150 °C. The films were then heated for 24 h (to ensure a complete thermoset reaction) before allowing to cool to room temperature, then, were extracted from the moulds. The prepared films were then cut into rectangular strips (45 mm × 8 mm × 5 mm) with exact measurements determined using digital callipers. Similarly, 0, 20 and 30% thermoset composites were prepared using the

same method by varying the amount of spent coffee grounds added to the mixture prior to heating.

Preparation of thermoset composite prototypes

Different silicone moulds were prepared using a commercially available two-part silicone. Then, we poured the homogenized thermoset mixtures (maintained at 90 °C) into the mould and heated to 150 °C for 24 h. After this time, the films were allowed to cool to room temperature (22 °C) before the cured films were separated from the moulds.

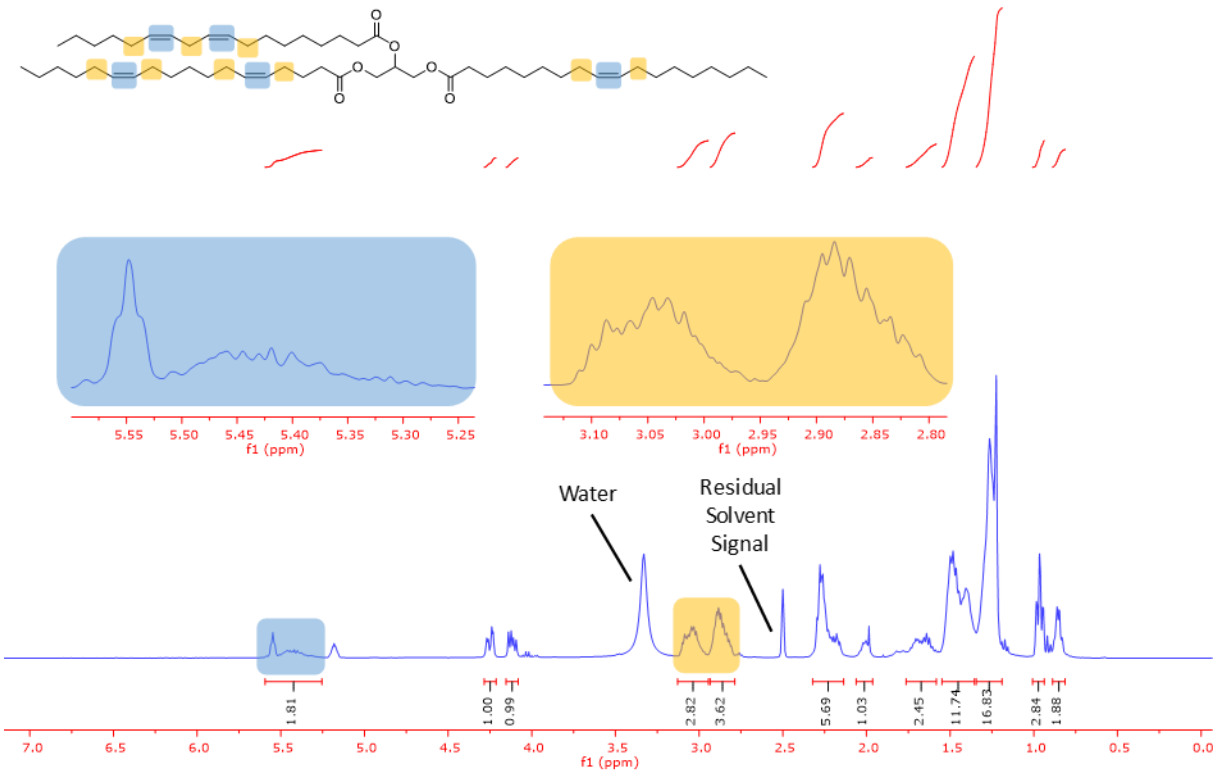

Figure S5.1: *^{1}H NMR spectrum for virgin chia seed oil, with expansion shown for alkene-associated proton signals: δ 5.59 – 5.25 (m) ppm (blue), and 3.13 – 2.94 (m), 2.86 (ddd), J = 27.1, 11.9, 5.8 Hz ppm (orange).*

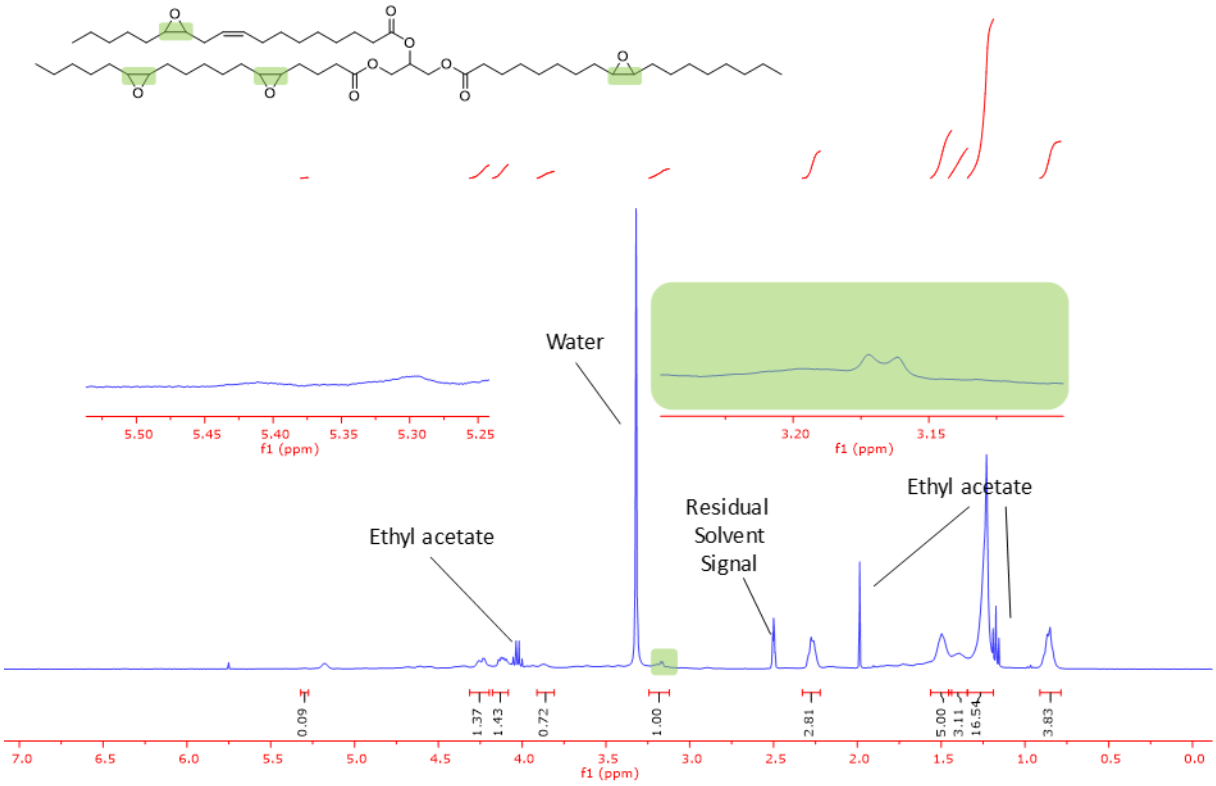

Figure S5.2: *^{1}H NMR spectrum for epoxidized chia seed oil, with alkene-associated signals present in* ***Figure S5.1*** *almost entirely absent, and the new oxirane-bound proton signals (δ 3.24 – 3.12 (m) ppm) shown in the expansion (green).*

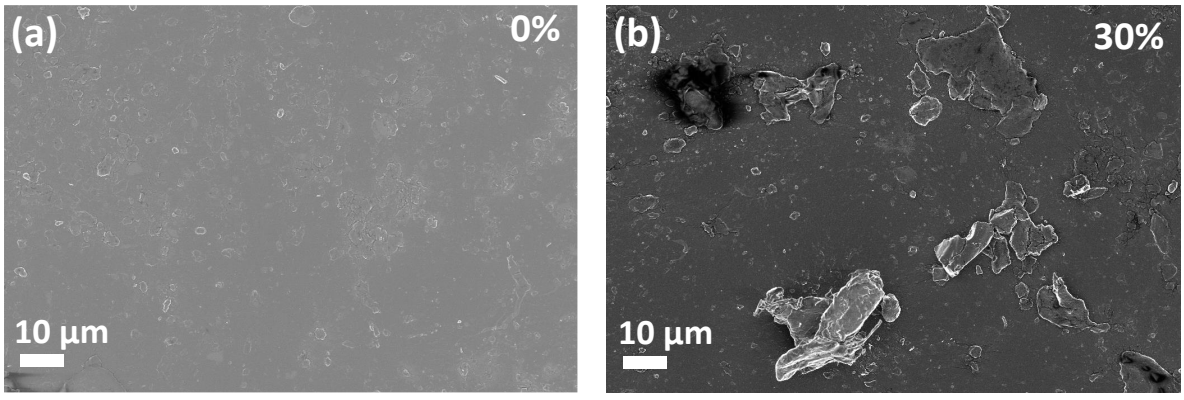

Figure S5.3: *SEM micrograph of thermoset composites, (a) SEM of 0% thermoset composite, (b) SEM of 30% thermoset composite. The spent coffee grounds are heterogeneously distributed throughout the polymer matrix with aggregation in 30% thermoset composite.*

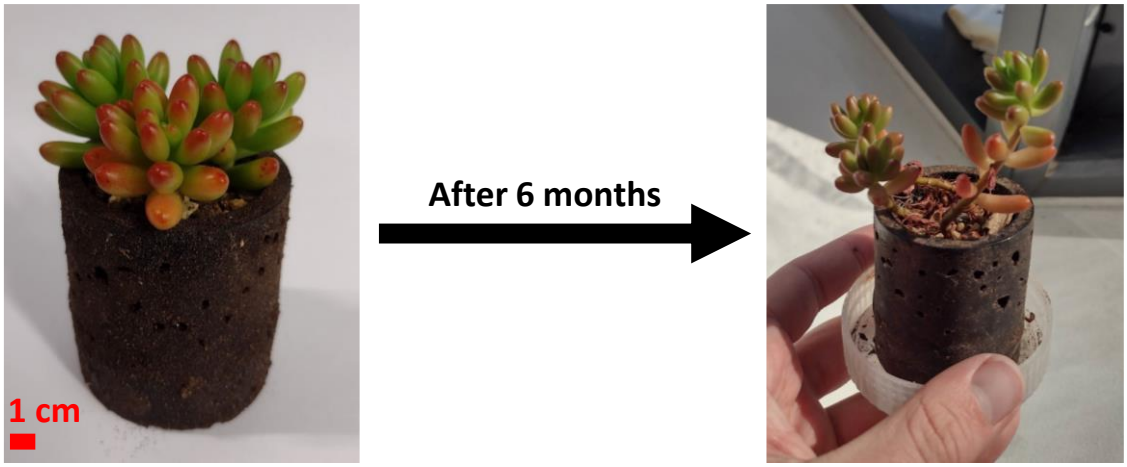

Figure S5.4: *Small plant growing in thermoset plant pot. To date, the plant continues to grow happily in our office.*

References

(1) Geyer, R.; Jambeck, J. R.; Law, K. L. Production, use, and fate of all plastics ever made. *Science Advances* **2017**, *3*, e1700782.
(2) Podgórski, M.; Fairbanks, B. D.; Kirkpatrick, B. E.; McBride, M.; Martinez, A.; Dobson, A.; Bongiardina, N. J.; Bowman, C. N. Toward Stimuli-Responsive Dynamic Thermosets through Continuous Development and Improvements in Covalent Adaptable Networks (CANs). *Advanced Materials* **2020**, *32*, 1906876.
(3) Fortman, D. J.; Brutman, J. P.; De Hoe, G. X.; Snyder, R. L.; Dichtel, W. R.; Hillmyer, M. A. Approaches to Sustainable and Continually Recyclable Cross-Linked Polymers. *ACS Sustainable Chemistry & Engineering* **2018**, *6*, 11145-11159.
(4) Hayashi, M. Implantation of Recyclability and Healability into Cross-Linked Commercial Polymers by Applying the Vitrimer Concept. *Polymers* **2020**, *12*, 1322.
(5) Kloxin, C. J.; Scott, T. F.; Adzima, B. J.; Bowman, C. N. Covalent Adaptable Networks (CANs): A Unique Paradigm in Cross-Linked Polymers. *Macromolecules* **2010**, *43*, 2643-2653.
(6) Denissen, W.; Winne, J. M.; Du Prez, F. E. Vitrimers: permanent organic networks with glass-like fluidity. *Chemical Science* **2016**, *7*, 30-38.
(7) Montarnal, D.; Capelot, M.; Tournilhac, F.; Leibler, L. Silica-Like Malleable Materials from Permanent Organic Networks. *Science* **2011**, *334*, 965-968.
(8) Imbernon, L.; Norvez, S. From landfilling to vitrimer chemistry in rubber life cycle. *European Polymer Journal* **2016**, *82*, 347-376.
(9) Zou, W.; Dong, J.; Luo, Y.; Zhao, Q.; Xie, T. Dynamic Covalent Polymer Networks: from Old Chemistry to Modern Day Innovations. *Advanced Materials* **2017**, *29*, 1606100.
(10) Krishnakumar, B.; Sanka, R. V. S. P.; Binder, W. H.; Parthasarthy, V.; Rana, S.; Karak, N. Vitrimers: Associative dynamic covalent adaptive networks in thermoset polymers. *Chemical Engineering Journal* **2020**, *385*, 123820.
(11) Zimmerman, J. B.; Anastas, P. T.; Erythropel, H. C.; Leitner, W. Designing for a green chemistry future. *Science* **2020**, *367*, 397-400.

(12) Anastas, P. T.; Warner, J. C. *Green chemistry: theory and practice*; Oxford University Press, Oxford [England], 1998.
(13) Vidil, T.; Llevot, A. Fully Biobased Vitrimers: Future Direction toward Sustainable Cross-Linked Polymers. *Macromolecular Chemistry and Physics* **2022**, *223*, 2100494.
(14) Lucherelli, M. A.; Duval, A.; Avérous, L. Biobased vitrimers: Towards sustainable and adaptable performing polymer materials. *Progress in Polymer Science* **2022**, *127*, 101515.
(15) Kumar, A.; Connal, L. A. Biobased Transesterification Vitrimers. *Macromolecular Rapid Communications* 2200892.
(16) Meier, M. A. R.; Metzger, J. O.; Schubert, U. S. Plant oil renewable resources as green alternatives in polymer science. *Chemical Society Reviews* **2007**, *36*, 1788-1802.
(17) Lligadas, G.; Ronda, J. C.; Galià, M.; Cádiz, V. Plant Oils as Platform Chemicals for Polyurethane Synthesis: Current State-of-the-Art. *Biomacromolecules* **2010**, *11*, 2825-2835.
(18) Montero de Espinosa, L.; Meier, M. A. R. Plant oils: The perfect renewable resource for polymer science. *European Polymer Journal* **2011**, *47*, 837-852.
(19) Biermann, U.; Bornscheuer, U.; Meier, M. A. R.; Metzger, J. O.; Schäfer, H. J. Oils and Fats as Renewable Raw Materials in Chemistry. *Angewandte Chemie International Edition* **2011**, *50*, 3854-3871.
(20) Jari, A.; Lidefelt, J.-O. *Handbook : Vegetable Oils and Fats*; Karlshamn: AarhusKarlshamn, 2007.
(21) Dominguez-Candela, I.; Ferri, J. M.; Cardona, S. C.; Lora, J.; Fombuena, V. Dual Plasticizer/Thermal Stabilizer Effect of Epoxidized Chia Seed Oil (Salvia hispanica L.) to Improve Ductility and Thermal Properties of Poly(Lactic Acid). *Polymers* **2021**, *13*, 1283.
(22) Sauer, M.; Porro, D.; Mattanovich, D.; Branduardi, P. Microbial production of organic acids: expanding the markets. *Trends in Biotechnology* **2008**, *26*, 100-108.
(23) Altuna, F. I.; Pettarin, V.; Williams, R. J. J. Self-healable polymer networks based on the cross-linking of epoxidised soybean oil by an aqueous citric acid solution. *Green Chemistry* **2013**, *15*, 3360-3366.
(24) Schenk, V.; Labastie, K.; Destarac, M.; Olivier, P.; Guerre, M. Vitrimer composites: current status and future challenges. *Materials Advances* **2022**, *3*, 8012-8029.
(25) Pfluger, R. A. Soluble coffee processing. *Solid Wastes Origin Collection Processing & Disposal. Cl Mantell* **1975**.
(26) Suaduang, N.; Ross, S.; Ross, G. M.; Pratumshat, S.; Mahasaranon, S. Effect of spent coffee grounds filler on the physical and mechanical properties of poly(lactic acid) bio-composite films. *Materials Today: Proceedings* **2019**, *17*, 2104-2110.
(27) Chang, Y.-C.; Chen, Y.; Ning, J.; Hao, C.; Rock, M.; Amer, M.; Feng, S.; Falahati, M.; Wang, L.-J.; Chen, R. K.; et al. No Such Thing as Trash: A 3D-Printable Polymer Composite Composed of Oil-Extracted Spent Coffee Grounds and Polylactic Acid with Enhanced Impact Toughness. *ACS Sustainable Chemistry & Engineering* **2019**, *7*, 15304-15310.
(28) Reis, K. C. d.; Pereira, L. C. C.; Melo, I. C. N. A. d.; Marconcini, J. M.; Trugilho, P. F.; Tonoli, G. H. D. Particles of Coffee Wastes as Reinforcement in Polyhydroxybutyrate (PHB) Based Composites. *Materials Research-ibero-american Journal of Materials* **2015**, *18*, 546-552.
(29) Kanai, N.; Honda, T.; Yoshihara, N.; Oyama, T.; Naito, A.; Ueda, K.; Kawamura, I. Structural characterization of cellulose nanofibers isolated from spent coffee grounds and their composite films with poly(vinyl alcohol): a new non-wood source. *Cellulose* **2020**, *27*, 5017-5028.

(30) Yoo, J.; Chang, S. J.; Wi, S.; Kim, S. Spent coffee grounds as supporting materials to produce bio-composite PCM with natural waxes. *Chemosphere* **2019**, *235*, 626-635.
(31) Meng, Y.; Chu, J.; Xue, J.; Liu, C.; Wang, Z.; Zhang, L. Design and synthesis of non-crystallizable, low-Tg polysiloxane elastomers with functional epoxy groups through anionic copolymerization and subsequent epoxidation. *RSC Advances* **2014**, *4*, 31249-31260.
(32) Dominguez-Candela, I.; Lerma-Canto, A.; Cardona, S. C.; Lora, J.; Fombuena, V. Physicochemical Characterization of Novel Epoxidized Vegetable Oil from Chia Seed Oil. *Materials* **2022**, *15*, 3250.
(33) García-García, D.; Carbonell, A.; Samper, M. D.; García-Sanoguera, D.; Balart, R. Green composites based on polypropylene matrix and hydrophobized spend coffee ground (SCG) powder. *Composites Part B: Engineering* **2015**, *78*, 256-265.
(34) Siriwong, C.; Boopasiri, S.; Jantarapibun, V.; Kongsook, B.; Pattanawanidchai, S.; Sae-Oui, P. Properties of natural rubber filled with untreated and treated spent coffee grounds. *Journal of Applied Polymer Science* **2018**, *135*, 46060.
(35) Essabir, H.; Bensalah, M. O.; Rodrigue, D.; Bouhfid, R.; Qaiss, A. e. k. Biocomposites based on Argan nut shell and a polymer matrix: Effect of filler content and coupling agent. *Carbohydrate Polymers* **2016**, *143*, 70-83.
(36) Lossada, F.; Jiao, D.; Yao, X.; Walther, A. Waterborne Methacrylate-Based Vitrimers. *ACS Macro Letters* **2020**, *9*, 70-76.
(37) Hayashi, M.; Sugimoto, K.; Takasu, A. Preparation of All Polyester-Based Semi-IPN Elastomers Containing Self-Associative or Non-Associative Guest Chains via Post-Blending Cross-Linking. *Macromolecular Materials and Engineering* **2019**, *304*, 1900147.
(38) Golkaram, M.; Fodor, C.; van Ruymbeke, E.; Loos, K. Linear Viscoelasticity of Weakly Hydrogen-Bonded Polymers near and below the Sol–Gel Transition. *Macromolecules* **2018**, *51*, 4910-4916.
(39) Chen, Q.; Liang, S.; Shiau, H.-s.; Colby, R. H. Linear Viscoelastic and Dielectric Properties of Phosphonium Siloxane Ionomers. *ACS Macro Letters* **2013**, *2*, 970-974.
(40) Capelot, M.; Montarnal, D.; Tournilhac, F.; Leibler, L. Metal-Catalyzed Transesterification for Healing and Assembling of Thermosets. *Journal of the American Chemical Society* **2012**, *134*, 7664-7667.
(41) Vaverková, M.; Kotovicová, J.; Adamcová, D. Testing the biodegradability and biodegradation rates of degradable/biodegradable plastics within simulated environment. *Infrastruktura i Ekologia Terenów Wiejskich* **2011**, 12.
(42) Simurdiak, M.; Olukoga, O.; Hedberg, K. Obtaining the Iodine Value of Various Oils via Bromination with Pyridinium Tribromide. *Journal of Chemical Education* **2016**, *93*, 322-325.

Chapter 6 Summary and Future Directions

Summary

In this thesis, I have outlined a new emerging family of thermosetting polymers that integrates the advantages of both dynamic chemical bonds and renewable feedstocks. The development of a new type of thermosetting polymer is required to address the present limitations of traditional thermosets, which include the utilisation of ecologically undesirable fossil fuels, potentially hazardous and expensive fabrication, lack of recyclability and circularity. The dynamic nature of transesterification and imine reactions have been recognized as a potential development route for the next generation of recyclable materials. Both transesterification and imine exchange processes led to the formation of non-toxic byproducts, and the versatile simple sustainable synthetic preparation pathway facilitates the fabrication of a vast array of functional monomers from biomass. In this thesis, **Chapter 2** outlined the development of a catalyst for the transesterification chemical reaction, **Chapter 3** described the development of dynamic thermoset elastomer based on oxime ester transesterification reaction using a crosslinker derived from raspberry biomass, and **Chapter 4—5** featured a biodegradable dynamic imine and transesterification thermosets from abundant biomass wastes.

In **Chapter 2**, a high-yielding, simple, modular synthetic approach devoid of protective groups was used to develop a highly efficient (k_{cat}/K_m) organocatalyst termed as artificial catalytic triad (ACT) for the transesterification reaction. The ACT was prepared using simple, modular, and protecting group free synthetic method from easily accessible starting materials with good to excellent yields. This ACT consists of three functional groups: hydroxyl as a nucleophile, imidazole as a base, and carboxylate groups as an acid. The rate acceleration

attributed to ACT surfactant is ~48000 fold over uncatalyzed reaction with a high turnover (k_{cat}) of 3.3 s^{-1}. Molecular dynamics simulations revealed a harmonious behavior between the three functional head groups, highlighting similarities between the ACT surfactant and natural enzymatic reaction. The application of simple modular and the exclusion of protecting groups in functional group placement provided an opportunity to develop an optimised path to transesterification catalyst.

Chapter 3 outlined the development of a crosslinker for thermoset elastomers. Similar to other dynamic covalent linkages, oxime bonds also exhibit dynamic properties. However, the use of oxime bonds, is still in its infancy as a tool for creating sustainable dynamic materials. This prompted the exploration into the use of raspberry biomass in the development of a novel, sustainable crosslinker thermosets based on oximes. Unlike conventional ester bonds, which required external catalyst, this thermoset network employed dynamic oxime and oxime ester which enable catalyst-free bond exchange processes. The network topology of the thermoset elastomers can be reorganised *via* oxime transesterification bond exchange, enabling stress relaxation and reprocessability. After reprocessing, the initial tensile strength of the elastomer can be regained up to 78.1 ± 10.9%. We anticipate that our sustainability approach and simplicity will pave the way for the development of catalyst-free transesterification elastomers.

Abundant shrimp and cellulose waste are sources of raw materials for the development of high-value products. In **Chapter 4**, we incorporate abundant shrimp/crab and cellulose waste as a feedstock to develop fully biomass-derived imine thermosets. I prepared crosslinked imine thermosets by condensing diketone-functionalised levoglucosenone (LGO) derivative with amine groups on chitosan, at room temperature, with water being the sole byproduct.

The dynamic imine thermoset possessed a high T_g, enhanced modulus, rapid stress relaxation, as well as reprocessability. Towards the end of the product life, these thermosets fully degrade in a home compost within 5 days. To the best of our knowledge, we reported the first fully biomass derived imine thermoset with the fastest degradation. This work contributes an innovative perspective on the design and development of biodegradable thermosets.

In **Chapter 5**, we developed a fully green thermoset composite material using abundant renewable chia seed oil, alginic acid, and spent coffee grounds. The mechanical properties of the thermoset composites can be modified by varying the amount of added spent coffee grounds. The thermoset network comprises of β-hydroxyester bonds that can undergo catalyst free transesterification exchange, enabling them to exhibit thermally induced stress relaxation and reprocessing properties. The tensile strength of the reprocessed thermosets can be recovered upto 93.2 ± 5.8%. Thermoset composites were employed to develop an array of prototype applications, including plant pots, thin film sheets, and beverage coolers. These prototypes are mechanically durable, feature high-definition structures, and have an extended shelf life. Additionally, we showed the large-scale production of thermoset sheets (210 mm × 300 mm × 5 mm, 350 g) in the laboratory. At the end of the material's lifespan, the thermosets can be degraded in a home compost in 4–5 months, a feature that is essential for the development of environmentally responsible plastic solutions. We expect that recyclable and biodegradable coffee composites made from abundant natural resources will offer an industrially feasible, scalable alternative to conventional thermosets.

Future Directions

We anticipate several applications of transesterification chemistry for the fabrication of materials in the future. In **Chapter 2**, I introduced an ACT catalyst that was synthesised using a simple modular procedure. This ACT catalyst has the potential to be investigated for the development of a variety of biobased thermosets.

The processing and performance of thermosets derived from biomass can be improved by using a variety of additive-based chemical processes. The development of biobased dynamic thermosets in combination with nanofillers such as graphene, carbon nanotubes, 2D layered materials, cellulose nanowhiskers, and nanoclays can be used to improve physical properties such as solvent absorption, thermal stability, barrier, flame resistance, and biodegradation rate. The inclusion of these nanoreinforcements is a very attractive strategy for creating innovative functional biomaterials with a broad range of applications. In the future, these novel and sustainable materials can be used in combination with a wide range of microfabrication processes, such as 3D/4D printing, and for demanding applications in the energy and healthcare sectors. Continuing with microfabrication, we can envision the coffee-based composites (**Chapters 5**) being refined into 3D printable material. The extrudability of coffee-based composites has recently been examined. Preliminary experiments revealed that coffee-based composites can be extruded, but it required more fine-tuning to be printable. In addition, it would be interesting to modify coffee-based composites using coffee husks, another significant waste derived from coffee beans, in order to increase the hydrophobicity of the composites for prospective commercial coffee cups.

Final Remark

In this thesis, I harnessed transesterification and imine chemical reactions to develop an array of fascinating materials. The dynamic nature of transesterification and imine bonds, coupled with renewable materials, attempted to address the practical limitations of conventional thermosets. This thesis has opened up new research avenues in the development of thermosetting polymers in the domains of sustainability, recyclability, and biodegradability. Although further research is required to prove these materials are effective under demanding circumstances, but their easy, flexible, and scalable production offers a lot of promise for the development of future thermosetting polymers.